THE WORK OF THE
RUTHERFORD LABORATORY
1971

Science Research Council

THE WORK OF THE RUTHERFORD LABORATORY IN 1971

Edited by

J R Smith and F M Telling

Contents

Director's Foreword

The year under review is dominated by two events outside the Rutherford Laboratory, which necessarily have had a considerable impact upon our programme. First of all, the decision to go ahead with the construction of the new accelerator at CERN has resulted in a reduction in the funds available for the Laboratory programme. At the start of 1972 we therefore carried out a detailed review of all aspects of our work and decided where the reductions should be made. In spite of the pruning, the work in the Laboratory is going ahead with considerable vigour, as I hope this report will illustrate.

Secondly, the Intersecting Storage Rings have come into successful operation at CERN and the Laboratory has built equipment for one of the first experiments to be accepted for it. The trend towards increasing use of CERN has therefore continued and about one-half of our high energy physics programme is now being carried out on the CERN accelerators. The Nimrod programme is, however, still very active and this year the number of protons accelerated was 35% higher than in 1970. Our 50 millionth beam pulse coincided with a visit to the Laboratory by members of the Royal Society and their distinguished guests as part of the celebrations to mark the centenary of Lord Rutherford's birth.

The computing power available to Laboratory users has been greatly increased with the installation and successful commissioning of the IBM 360/195 computer. Plans are now being considered for installing computer terminals in a number of University Departments linked directly to the IBM 360/195.

During the year the Science Research Council agreed to the formation of a Neutron Beam Research Unit at the Rutherford Laboratory, which will reinforce the support which is available for University research workers in this field and increase the scope of the Laboratory's activities.

G. H. Stafford

Divisional Organisation (December 1971)

HIGH ENERGY PHYSICS DIVISION

Experiments in fundamental particle physics and experiments on nuclear structure, in collaboration with University groups, at Nimrod and CERN. Nuclear Electronics. Photographic Services.

DIVISION HEAD & DEPUTY DIRECTOR: G. MANNING
DEPUTY DIVISION HEAD: J. J. THRESHER

NIMROD DIVISION

Operation and development of Nimrod (7 GeV Proton Synchrotron Accelerator). Accelerator design. Experimental area management. Design and installation of beam-lines. Superconducting beam-line elements. Liquid hydrogen targets. Bubble chamber operations and development.

DIVISION HEAD: D. A. GRAY
DEPUTY DIVISION HEAD: G. N. VENN

APPLIED PHYSICS DIVISION

Superconducting magnet studies. Rapid cycling vertex detector studies. Polarized targets. Radio-biological studies and radiation protection. Superconducting power supplies. High Flux Beam Reactor design study.

DIVISION HEAD: L. C. W. HOBBIS
ACTING DIVISION HEAD: D. B. THOMAS

NEUTRON BEAM RESEARCH UNIT

HEAD OF UNIT: L. C. W. HOBBIS

COMPUTING & AUTOMATION DIVISION

Operation and development of the Central Computer System and Satellite Computers. On-line applications including hardware and software for bubble and spark chamber film analysis. Theoretical High Energy Physics.

DIVISION HEAD: W. WALKINSHAW

ENGINEERING DIVISION

Design and manufacture of nuclear physics apparatus and applied research equipment. Engineering Science. Mechanical, Electrical and Building services. Chemical Technology. Safety services.

DIVISION HEAD & CHIEF ENGINEER: P. BOWLES

ADMINISTRATION DIVISION

Personnel, Finance and Accounts, Stores, Library, Transport, General and Specialised Administrative Support.

DIVISION HEAD & LABORATORY SECRETARY: J. M. VALENTINE

p

π⁻

Λ

K⁻
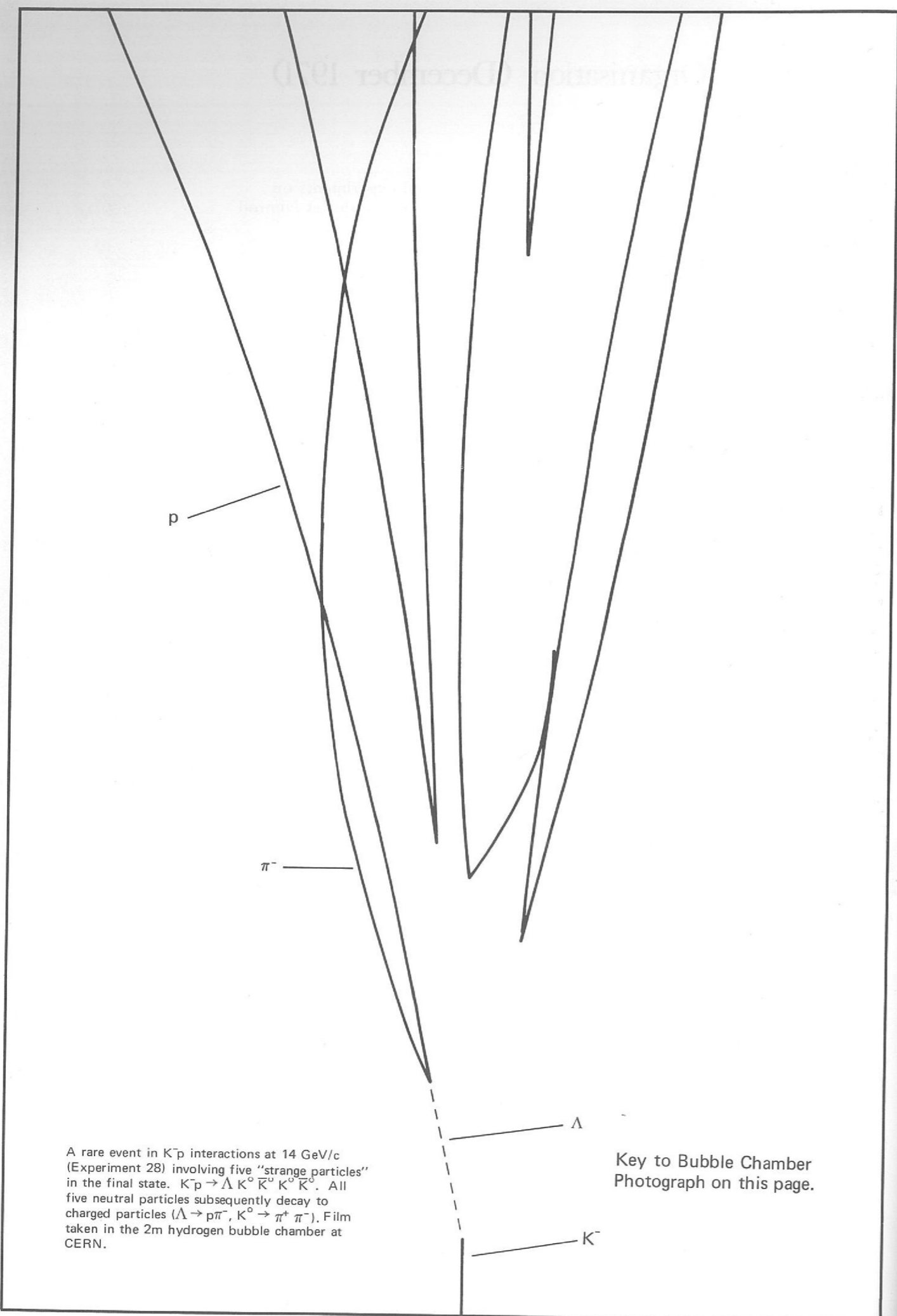
A rare event in K⁻p interactions at 14 GeV/c (Experiment 28) involving five "strange particles" in the final state. $K^-p \rightarrow \Lambda K^0 \bar{K}^0 K^0 \bar{K}^0$. All five neutral particles subsequently decay to charged particles ($\Lambda \rightarrow p\pi^-$, $K^0 \rightarrow \pi^+\pi^-$). Film taken in the 2m hydrogen bubble chamber at CERN.

Key to Bubble Chamber Photograph on this page.
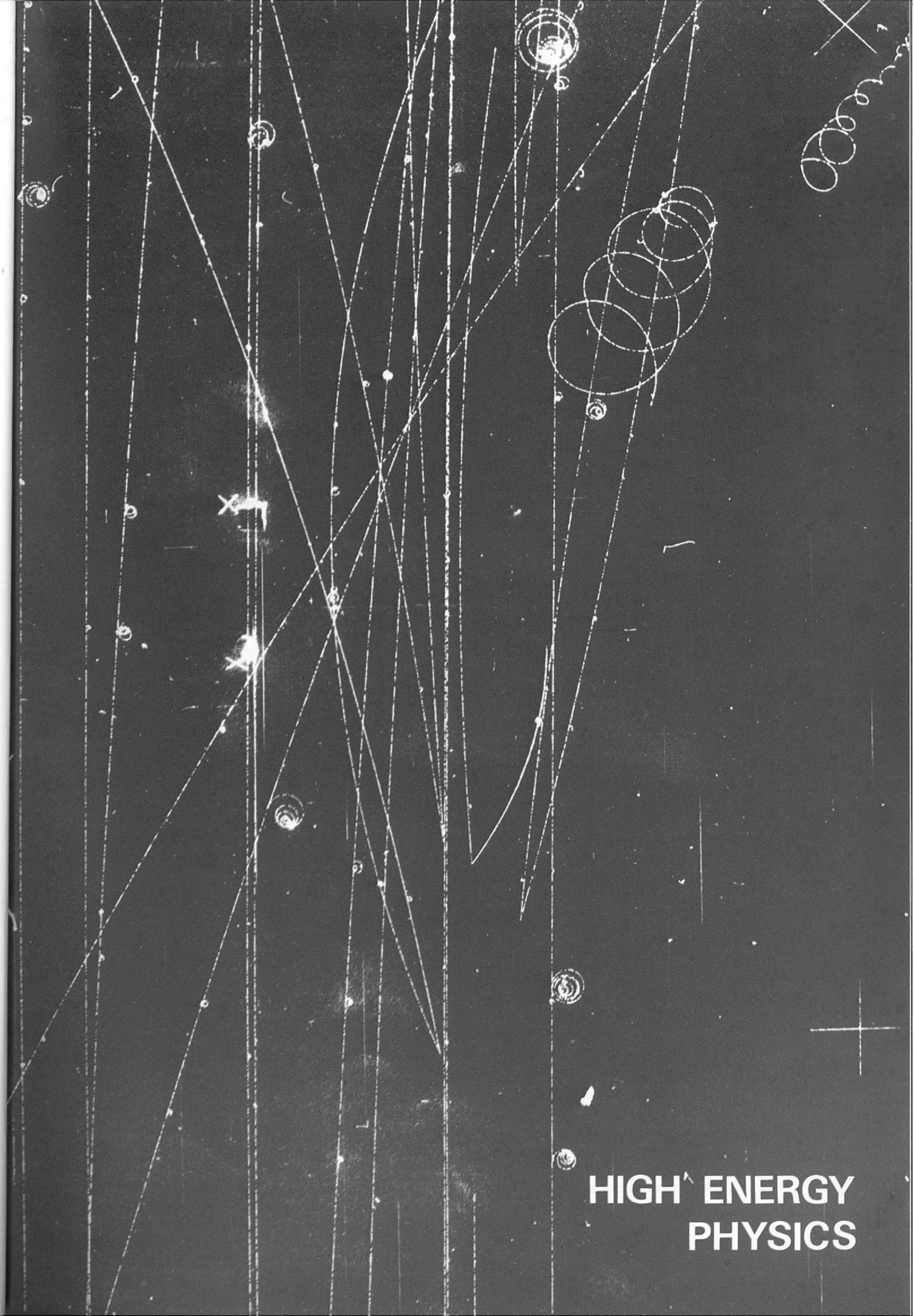
HIGH ENERGY
PHYSICS

High Energy Physics

There has been continuing high activity in the Fundamental Particle Physics research programme during 1971. Reports are given on 39 experiments compared to 31 experiments in 1970. There are 11 new experiments and the remainder are either experiments whose analysis has continued or which have moved to the data collection and analysis stage during the past year. Two of the new experiments use the bubble chamber technique (Experiments 38 and 39) and the remaining 9 use electronic techniques.

The involvement of Rutherford Laboratory groups at CERN has increased and new collaborations with institutions outside the UK have been arranged. Table 1 shows a list of Universities and Institutions who are participating in experimental work supported by the Rutherford Laboratory.

An important development in the facilities of the Laboratory has been the successful commissioning of Phase II of the secondary beams in Experimental Hall 3 so that two new beams ($\pi 9$ and N4) are now available from a second target station in the extracted proton beam (X3). There is provision for the installation of a third secondary beam at a future date. Figure 1 shows the layout of Hall 3 as of December 1971. It can be seen from the figure that X3 now supplies four secondary beams in Hall 3; the second target station is supplied by refocussing the proton beam after it has interacted in the first target. The proton flux available for refocussing is dependent on the length of this target and in practice, when the first station is operating under normal conditions, about 50% of the available proton flux reaches the second station. This flux is quite adequate for the experiments using this target station at present.

Experiments using Electronic Techniques

It is convenient to separate the experiments into two classes, those whose chief aim is the study of the strong interaction between particles and those which seek to gain information about the electromagnetic and the weak interactions. These are listed in Tables 2 and 3.

From these tables it is clear that a wide variety of work is in progress covering many aspects of particle physics. In this introduction to the reports themselves a review of one class of experiment, namely the study of the strong interaction between fundamental particles by means of measurements on two-body scattering processes, is given. This is a field in which the Laboratory has been active for several years and in which many important contributions are being made.

Table 1

Institutions Participating in the High Energy Physics and Nuclear Physics Programme

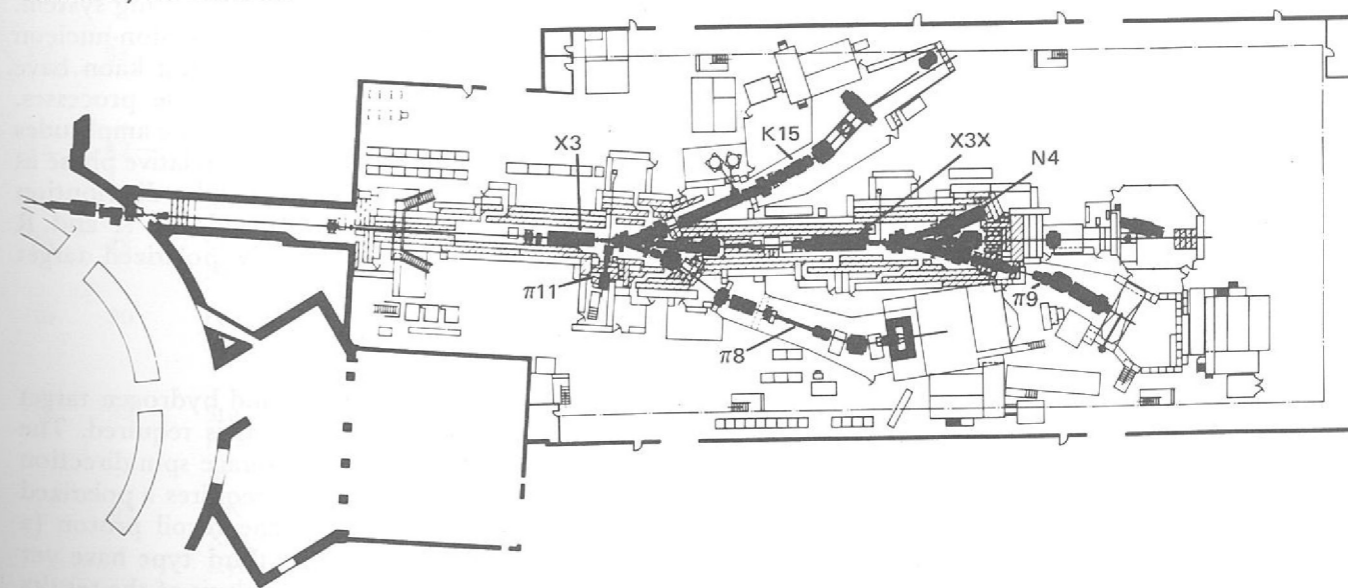| Counter Experiments	Bubble Chamber Experiments
AERE, Harwell	University of Bologna, Italy
AWRE, Aldermaston	University of Birmingham
Queen's University, Belfast	University of Brussels, Belgium
University of Bergen, Norway	University of Cambridge
University of Birmingham	CEN, Saclay, France
University of Bristol	CERN, Geneva, Switzerland
University of Cambridge	College de France
CERN, Geneva, Switzerland	Ecole Polytechnique, France
University of Chicago, USA	University of Durham
Daresbury Nuclear Physics Laboratory	University of Edinburgh
University of Genoa, Italy	University of Glasgow
University of Glasgow	Imperial College, London
Harvard University, USA	University of Liverpool
University of Liverpool	University of Oxford
King's College, London	University of Pisa, Italy
Imperial College, London	Rutherford High Energy Laboratory
University College, London	University of Strasbourg, France
Queen Mary College, London	Tufts University, USA
University College, London	University College, London
Westfield College, London	Westfield College, London
University of Mainz, Fed. Rep. Germany	
University of Manchester	
University of Oxford	
University of Paris-Sud, Orsay, France	
University of Pisa, Italy	
University Research Reactor, Risley	
University of Rome, Italy	
Rutherford High Energy Laboratory	
University of Southampton	
University of Surrey	
University of Stockholm, Sweden	
University of Sussex	
University of Warwick	

Figure 1. Beam lines in Experimental Hall 3 (January 1972).
X3 is the extracted proton beam.
X3X is the extension of X3 to a second target station.
(This figure and also one showing the layout of beam lines in Experimental Halls 1 and 2 is shown in larger scale on pages 222 and 223).

The strong interaction is believed to be responsible for the cohesion of the atomic nucleus and generates many new and interesting effects when it is studied in the Laboratory. The elucidation of the pattern of these phenomena and their inter-relationships is proving to be an exacting task. The main tool in this study is the scattering experiment — a tool which was first used by Geiger, Marsden and Rutherford to reveal the separate identity of the atomic nucleus. The simplest form of scattering process is the two-body reaction in which the incident beam particle and the target particle interact to produce only two outgoing, final state, particles. In a completely elastic process these final state particles will be identical with the beam and target particle but two-body processes in which the final state particles differ from those in the initial state are also quite common. Several examples of two-body reactions being studied by Rutherford Laboratory counter groups are shown in Table 4. From the experimental point of view, these reactions are very amenable to study using electronic detection techniques. They have this feature because conservation of energy and linear momentum impose a complete correlation on the directions and momenta of the outgoing particles. This can be used to identify the two-body events within the limits of accuracy of the experiment. A measurement of the directions of the two final state particles or the momentum and direction of one of them is sufficient to provide this identification. The equipment to detect these events usually consists of large arrays of scintillation counter hodoscopes or spark chambers surrounding a hydrogen or polarized proton spin target. The size of the detecting equipment makes possible a high data collection rate so that results of high statistical significance can be obtained in a short period of time. In order to handle this high rate of data collection, the detecting equipment is usually linked to a small computer which provides a buffer store for data received during each beam pulse from the accelerator. Between beam pulses, this data is written onto magnetic tape for subsequent analysis using the large computer of the Laboratory. This can often be the most time-consuming part of the experiment because, although the general plan for the analysis of the data is usually clear, it is the detailed programming to deal with problems which cannot usually be foreseen which involves a large expenditure of time and effort.

Any two-body reaction can be described completely in terms of mathematical functions called scattering amplitudes which are related to the experimentally measured quantities. It is the aim of each experiment to determine the behaviour of these amplitudes as a function of the total energy of the interacting system. The simplest reactions which can be studied experimentally are the pion-nucleon and kaon-nucleon scattering processes since, because the pion and kaon have zero spin, two amplitudes are sufficient to describe each of these processes. However three independent quantities must be measured because the amplitudes are, in general, complex quantities and we require to know their relative phase as well as their magnitude. These three measurements are the angular distribution (or differential cross-section, $d\sigma/d\Omega$), the polarization (P) and the A and R parameters which describe the spin rotation of an initially polarized target nucleon.

The measurement of $d\sigma/d\Omega$ can be made using a simple liquid hydrogen target since no information about the spin direction of the proton is required. The measurement of P requires a polarized target in which the average spin direction of the protons is known. The measurement of A and R also requires a polarized target and (for the elastic channels) a second scatter of the recoil proton (a "double scattering" experiment). No measurements of this third type have yet been made in the energy region accessible by Nimrod and the analysis of the results obtained from $d\sigma/d\Omega$ and P measurements must rely at present on theoretical constraints to make up for this deficiency in the experimental data.

Table 2

Strong Interaction Experiments using Electronic Techniques

Expt. No.	Proposal No.	Experiment	Team	Beam	Status (at Dec. 1971)
1	40, 63	$K^{\pm}p$ Differential Cross-Sections in the Momentum Range 0·45-0·90 GeV/c	Univ. of Birmingham Rutherford Lab.	K12	Analysis
2	30, 74	$K^{\pm}p$ Differential Cross-Sections in the Momentum Range 0·9-2·2 GeV/c (K^-) and 1·6-2·4 GeV/c (K^+)	Univ. College Rutherford Lab.	K8	Analysis
3	33, 92	Study of Hyperon Resonances Decaying into Neutral Final States	Univ. of Oxford	K10S	Analysis Data collection
4	55	Polarization Effects in π^+p Elastic Scattering	Univ. of Oxford Rutherford Lab.	K14A	Analysis
5	68	Wide Angle Elastic pp Scattering	Queen Mary College, Univ. of Bergen, AERE Rutherford Lab.	P71	Analysis
6	50, 99	An Investigation of Narrow Width Mesons produced in π^-p Interactions	Imperial College Univ. of Southampton	$\pi 7$	Analysis Setting up
7	67	Low Energy Pion-Nucleon Interactions	Univ. of Cambridge Rutherford Lab.	CERN	Analysis
8	43	K^+p Differential Cross-Sections in the Momentum Range 1-2 GeV/c	Univ. of Bristol Univ. of Southampton Rutherford Lab.	K15	Analysis
9	73	$K^{\pm}n$ Elastic and K^+ Charge Exchange Differential Cross-Sections	Univ. of Birmingham Rutherford Lab.	K12A	Data collection
10	75	$\bar{p}p$ Elastic Scattering and two-body Annihilation	Queen Mary College Univ. of Liverpool Daresbury Lab. Rutherford Lab.	CERN	Data collection
11	81, 101	Differential Cross-Sections and Polarization Effects in $\pi^-p \to \pi^0 n$ and $\pi^-p \to \eta^0 n$ from 0·6-3·5 GeV/c	Univ. of Glasgow Rutherford Lab.	$\pi 9$	Setting up
12	83	Differential Cross-Sections in $\pi^+p \to \pi^+p$ from 0·6-2·0 GeV/c	Univ. of Bristol Univ. of Southampton Rutherford Lab.	K15	Data collection
13	87	Differential Cross-Sections and Polarization Effects in $\pi^-p \to K^0\Lambda$ between Threshold and 1·5 GeV/c	Univ. of Cambridge Rutherford Lab.	K13C	Setting up
14	88	Study of Strangeness Zero Bosons using a Neutron Trigger	Univ. of Birmingham Westfield College	CERN	Setting up
15	90	Polarization Effects in $\pi^{\pm}p$ Backward Scattering at 6 GeV/c	CERN Univ. of Paris-Sud, Univ. of Oxford	CERN	Data collection
16	93	Study of the Mass Spectrum of X^0 in the Reaction $\pi^-p \to \Lambda^0 X^0$	Univ. of Rome CERN Rutherford Lab.	CERN	Data collection
17	98	π-N Scattering Lengths from Precise X-ray Energy Measurements on Pionic Hydrogen and Deuterium	Queen Mary College Univ. of Pisa Univ. of Mainz Daresbury Lab.	CERN	Setting up
18	100	A Study of the Reactions $\pi^+p \to \Sigma^+K^+$ and $K^-p \to \pi^-\Sigma^+$ at 10 GeV/c	Univ. of Birmingham Univ. of Stockholm Univ. of Genoa CERN Rutherford Lab.	CERN	Setting up

Table 3

Electromagnetic and Weak Interaction Experiments using Electronic Techniques

No.	Proposal No.	Experiment	Team	Beam	Status (at Dec. 1971)
19	31	Test of the $\Delta I = \frac{1}{2}$ Rule in the Decay $\Sigma^+ \to p\pi^\circ$	Westfield College Rutherford Lab.	K14	Analysis
20	45	Test of the $\Delta S = \Delta Q$ Rule for K° Leptonic Decays	Univ. of Cambridge Rutherford Lab.	K13	Analysis
21	70	Search for Charge Asymmetry in η Decay	Westfield College Rutherford Lab.	$\pi 8$	Analysis
22	76	A Search for the C-violating Decay $\eta \to \pi^\circ e^+ e^-$	Westfield College Rutherford Lab.	$\pi 8$	Analysis
23	72	ISR Search for the Intermediate Boson	Univ. of Bristol, Univ. of Cambridge, Univ. of Liverpool, Univ. College, Westfield College, Rutherford Lab.	CERN	Data collection
24	96	Muon-Proton Inelastic Scattering in the 100 GeV Region	Univ. of Oxford, Univ. of Chicago, Harvard Univ.	NAL	In preparation

A complete determination of the scattering amplitudes requires a programme of work spread over a period of several years. A set of measurements of any of the observable quantities by a group of physicists can take at least three years if the time for data analysis is included.

Until recently most of the research of the Laboratory has been directed towards pion-nucleon scattering, almost exclusively in the elastic channel, and about one quarter of the useful life of Nimrod has been devoted to this subject. This work has yielded rich dividends and the analysis of data obtained over the past few years has made it possible to map out the behaviour of the scattering amplitudes up to a total energy of 2 GeV. The data obtained at the Rutherford Laboratory accounts for well over 50% of the total world collection.

The behaviour of the amplitudes has proved very interesting and indicates the formation of many short lived states known as resonances, which are formed as intermediate states of the pion-nucleon system. The revealing of this amplitude behaviour has lead to the theoretical idea of duality which attempts to relate, with considerable success, the high and low energy behaviour of these amplitudes and therefore correlate, for example, data obtained at Nimrod and the CERN Proton Synchrotron.

In view of these developments several groups are making measurements of $d\sigma/d\Omega$ and P to greater precision than before, it being essential to test the new theories with improved experimental data. For example the measurements of $d\sigma/d\Omega$ in Experiment 12 and of P in Experiment 4 represent a degree of precision which is much greater than anything achieved previously. In addition work is beginning on a study of the $\pi^- p$ charge exchange reaction for which there are almost no good measurements of $d\sigma/d\Omega$ and none of P. This reaction is difficult to study because the final state particles carry no electric charge. However the measurements on this reaction, involving the same scattering amplitudes as in elastic scattering in a different combination, will bring new constraints to bear on the analysis of the data. Figure 2 gives some idea of the scale of this experiment. The neutrons are detected in a large matrix of 200 liquid scintillation counters. The two γ-rays from the decay of the neutral pion are detected in a network of counter hodoscopes in which the γ-rays are converted to an electron shower in a sheet of lead. This shower is then detected in three arrays of plastic scintillators. This arrangement detects scattered particles over almost 70% of the available solid angle. The polarized target, which will be used for the first time in this experiment, employs a separated function superconducting magnet in which the target is polarized under optimum conditions and then moved to a magnetic field region which gives optimum access for the scattered particle detectors.

Table 4

Two-Body Reactions being Studied by Electronic Techniques

| Reaction	Measurement and Experiment No.	
	Differential Cross-Section	Polarization
$\pi^+ p \to \pi^+ p$	7*, 12	4, 15†
$\pi^- p \to \pi^- p$	7*,	15†
$\pi^- p \to \pi^\circ n$	11, 18	11
$\pi^- p \to \eta^\circ n$	11	11
$\pi^- p \to \Lambda^\circ K^\circ$	13	
$\pi^+ p \to \Sigma^+ K^+$	19†	19†
$K^- p \to K^- p$	1, 2	
$K^- n \to K^- n$	9	
$K^- p \to \Lambda^\circ \pi^\circ$	3	3
$K^- p \to \pi^\circ \Sigma^\circ$	3	3
$K^- p \to \eta^\circ \Sigma^\circ$	3	3
$K^- p \to \pi^- \Sigma^+$	19†	19†
$K^+ p \to K^+ p$	1, 2, 8	
$K^+ n \to K^+ n$	9	
$K^+ n \to K^\circ p$	9	
$\bar{p} p \to \bar{p} p$	10†	
$\bar{p} p \to \pi^+ \pi^-$	10†	* CERN Synchrocyclotron
$\bar{p} p \to K^+ K^-$	10†	† CERN Proton Synchrotron
$p p \to p p$	5	

Many of the resonant states observed appear only as small effects in the analysis of the elastic scattering data. Work is therefore in preparation to carry out a similar programme for the inelastic two-body reactions. Experiment 13 is an example of this. It is most important to confirm that effects observed in the analysis of the elastic channel are in fact present also in an inelastic process. It is also possible that new resonant states will be observed which have not been detected in the elastic studies. An added attraction of this experiment is that measurement of the angular distribution of the decay products of the baryon (in this case the $\Lambda°$) makes it possible to measure P without the need of a polarized target. The latter is only required for A and R measurements and in this case the decay properties of the baryon obviate the need for a double scattering experiment.

Similar remarks can be made for the kaon-nucleon system as for the pion-nucleon case. However the work is less advanced, mainly because of the lower intensity of kaon beams, but excellent measurements are being made as Experiment 8 indicates. A most important difference between kaon and pion reactions is that the K⁻ and K⁺ have quite different strong interaction properties. Whereas for the K⁻+ nucleon system, similar resonant states have been observed as in the pion + nucleon system, for the K⁺ no resonances have been clearly seen. This absence of resonant states is a most important effect. It is related both to the ideas of duality, mentioned earlier, and also to the quark model. In this model the resonant states are regarded as excited states of a triplet combination of basic particles, known as quarks, and the observed states do in fact fit quite well into such a scheme. However resonant states formed in a K⁺+ nucleon interaction would require a combination of five quarks. The search for such states therefore constitutes an important test of this model.

The work on two-body strong interaction processes may be summarized by saying that we are now moving into an era in which the quark model and duality provide a theoretical framework into which the experimental data can be fitted. The requirements now, from the experimental point of view, are for several series of well planned and well executed experiments on the major processes (both elastic and inelastic) which will yield data which is either quite new, or of much greater accuracy than before. That is one of the aims of the research at the Nimrod accelerator at the present time.

Figure 2. Apparatus for Experiment 11. The polarized target is surrounded by scintillation counters to veto charged particles produced in the target: further out from the target an array of neutron detectors and a γ-ray hodoscope are being assembled.
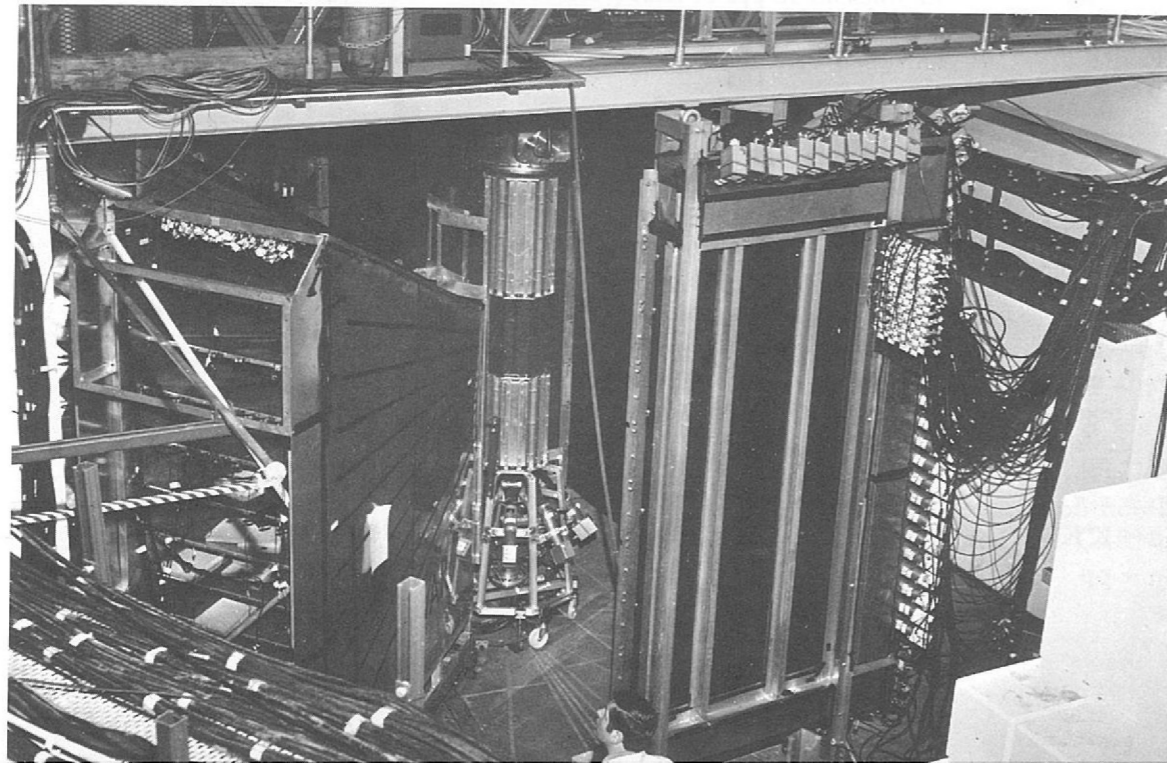
Experiment 1

The analysis of the data from this experiment to measure K⁻p and K⁺p elastic differential cross-sections is now almost complete and several results have been reported.

The K⁺p data at 13 momenta between 430 and 940 MeV/c have confirmed the existing idea that the low momentum angular distributions are almost structureless. They have established beyond doubt the repulsive nature of the nuclear scattering amplitude (see Figure 3) and show that the elastic cross-section is almost independent of energy below the inelastic threshold at 700 MeV/c, which contradicts some earlier counter measurements (Figure 4).

The improved accuracy of the data will allow the I = 1 KN phase shifts to be determined much more precisely. (I is the Iso-spin of the KN system.) This is important not only for K⁺p scattering but also for the analysis of K⁺n scattering (see Experiment 9) where a good knowledge of the I = 1 phase shifts is needed before the I = 0 phase shifts can be found. A good fit is obtained with the conventional, namely s-wave, type of solution, but other types of solution are being investigated.

The K⁻p data at 14 momenta between 590 and 940 MeV/c show considerable variation and encompass a region previously investigated in several other experiments using bubble chambers and spark chambers. The increased statistical accuracy will help in finding the properties of the several Y* resonances in this region.

K⁺p Differential Cross-Sections in the Momentum Range 0·45 to 0·90 GeV/c (ref. 1, 125, 126, 177)

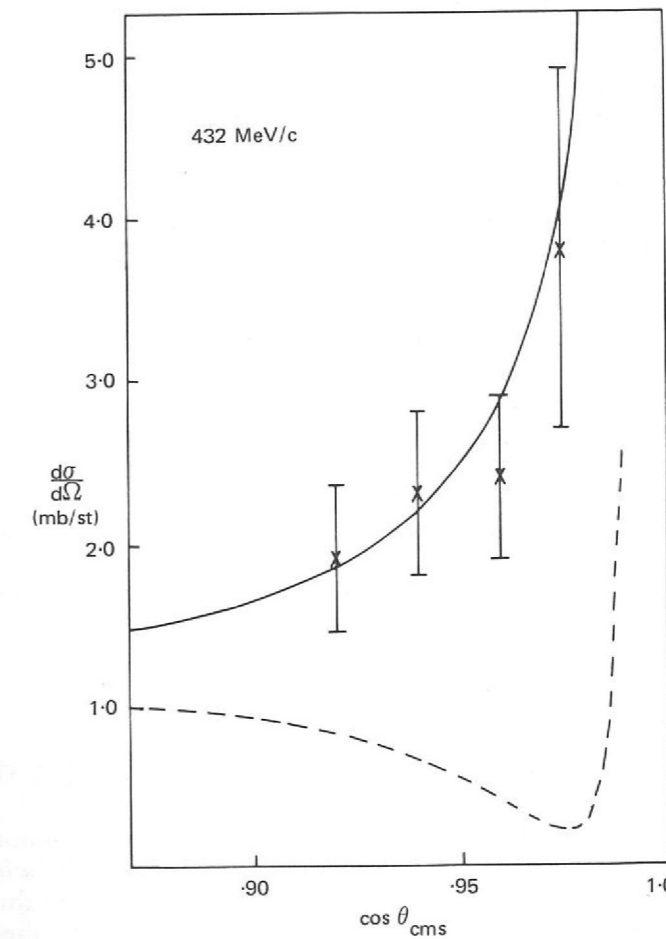Figure 3. Differential cross-sections in the Coulomb-nuclear interference region for K⁺p elastic scattering. The smooth curve is the prediction for a repulsive nuclear amplitude interfering constructively with the repulsive Coulomb amplitude. The dashed curve is the prediction for an attractive nuclear amplitude and is clearly a bad fit to the data. (Experiment 1).
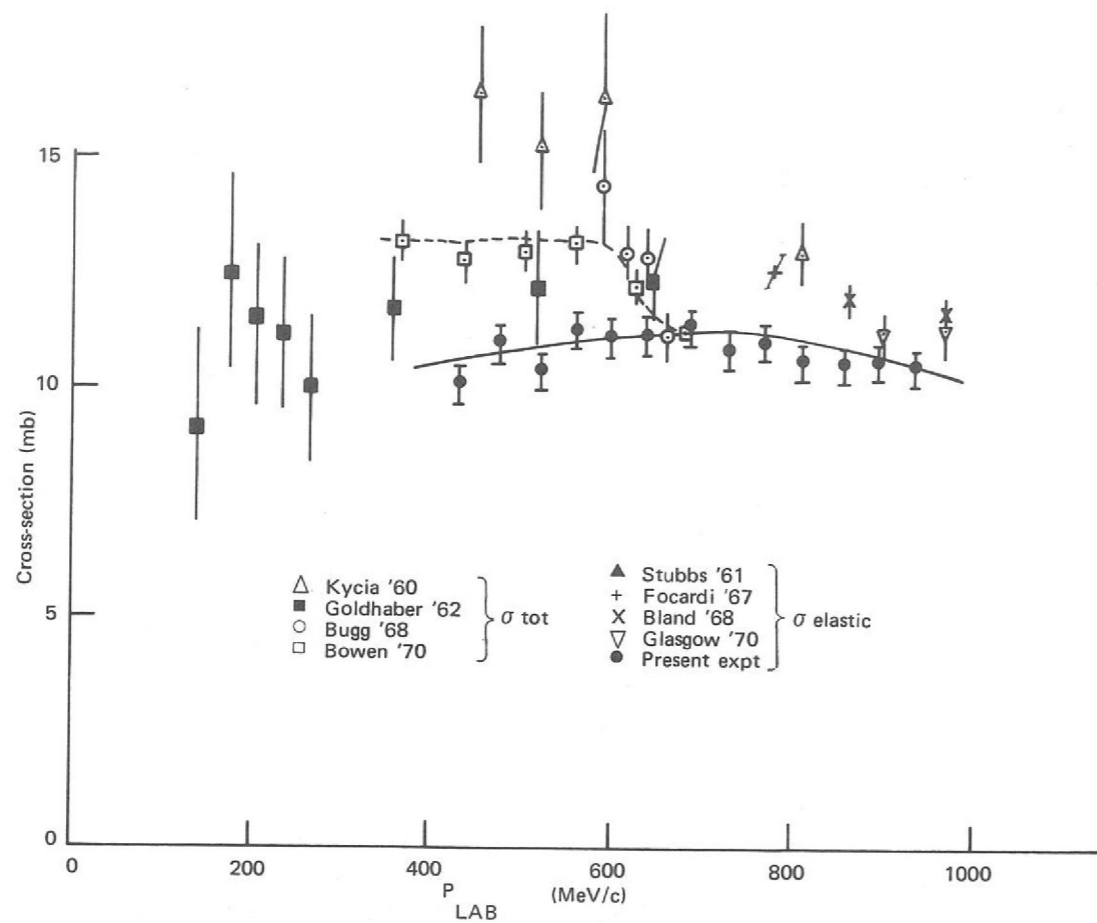
Figure 4. Measurements of the K⁺p elastic cross-section. (Experiment 1). The points labelled σtot are taken from measurements of the total cross-section in a momentum region where the inelastic cross-section is negligible. The data of Bugg et al and Bowen et al indicate a structure not seen in this experiment.

Experiment 2

**UNIVERSITY COLLEGE, LONDON
RUTHERFORD LABORATORY**

K±p Differential Cross-Sections in the Momentum Range 0·9 to 2·2 GeV/c (K⁻) and 1·6 to 2·4 GeV/c (K⁺)

Precise measurements of the differential cross-sections of K⁺p and K⁻p elastic scattering over a wide momentum range have been made in this experiment. The aim is to improve the classification of some of the hyperon resonances and look for evidence of the existence, or otherwise, of 'exotic' Z* resonances.

Data acquisition was completed in May 1970 and during the past year, further analysis of all the data has continued, in order to obtain reliable normalisations of the cross-sections and in order to provide a clearer understanding of an apparently anomalous behaviour of the K⁺p data at small angles and low momenta. As a result of this, the preliminary data will be slightly modified. This assessment is almost complete. An absolute normalisation has been achieved, yielding total elastic cross-sections which agree to better than 7% with existing data, where cross checks are possible. Final phase shift analyses of the K⁺ data and also π±p data (obtained during the course of the experiment) are being undertaken at present.

Experiment 3

UNIVERSITY OF OXFORD

Study of Hyperon Resonances Decaying into Neutral Final States (ref. 128, 169, 178, 180, 182)

Hyperon resonances with strangeness −1 are formed in K⁻p interactions in the low energy region. They exist for times of the order of 10^{-23} seconds before decaying into K̄N, as well as other final states such as $\Lambda°\pi°$ and $\Sigma\pi$ and can thus be studied by analysis of the formation of these states as a function of the incident K⁻ momentum.

This particular experiment is designed to study the final states $\Lambda\pi°$ and $\Sigma°\pi°$ which are pure isotopic spin states, I = 1 and I = 0 respectively. The unambiguous identification of these states and others like $\Lambda\pi°\pi°$, depends on high gamma ray detection efficiency, for it is essential to observe all the gamma rays from the decay of the neutral pions. The high efficiency is achieved by surrounding the liquid hydrogen target as completely as possible with steel plate spark chambers. In these the gamma rays have an individual probability of 98% of converting into a visible electron-positron shower. A scintillation counter system rejects those events which do not correspond to an 'all neutral' final state, from which a later Λ decay produces charged particles. These charged particles are detected in magnetostrictive wire chambers, which lie between the hydrogen target and the gamma chambers, and also in the gamma chambers.

Figure 5. Angular distributions in the momentum range of 685 to 805 MeV/c for the reaction K⁻p → $\Lambda\pi°$ from data collected in Experiment 3.
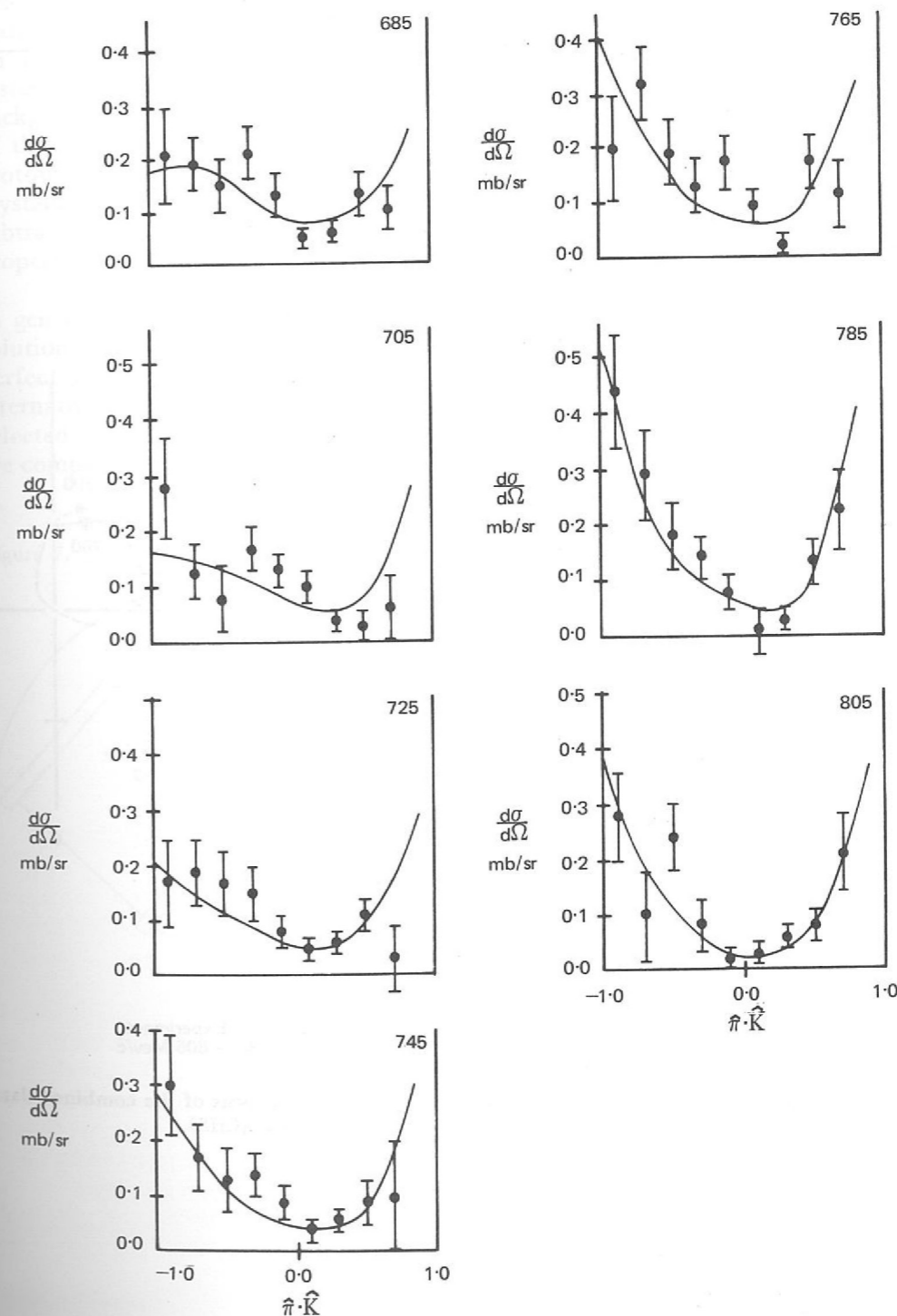
Data was initially taken at 16 values of K$^-$ momentum between 685 and 990 MeV/c, and a partial wave analysis of this is now approaching completion. Improvements to the apparatus have been made, and in particular a new set of low-mass magnetostrictive wire spark chambers have been added. Further data runs are now in progress and there will be new momentum points in the range 900 to 1100 MeV/c, each point with approximately five times as much data as before. Approximately 5000 $\Sigma^\circ \pi^\circ$ events should be obtained and a detailed study of $\Sigma^\circ \eta$ production near threshold will be made.
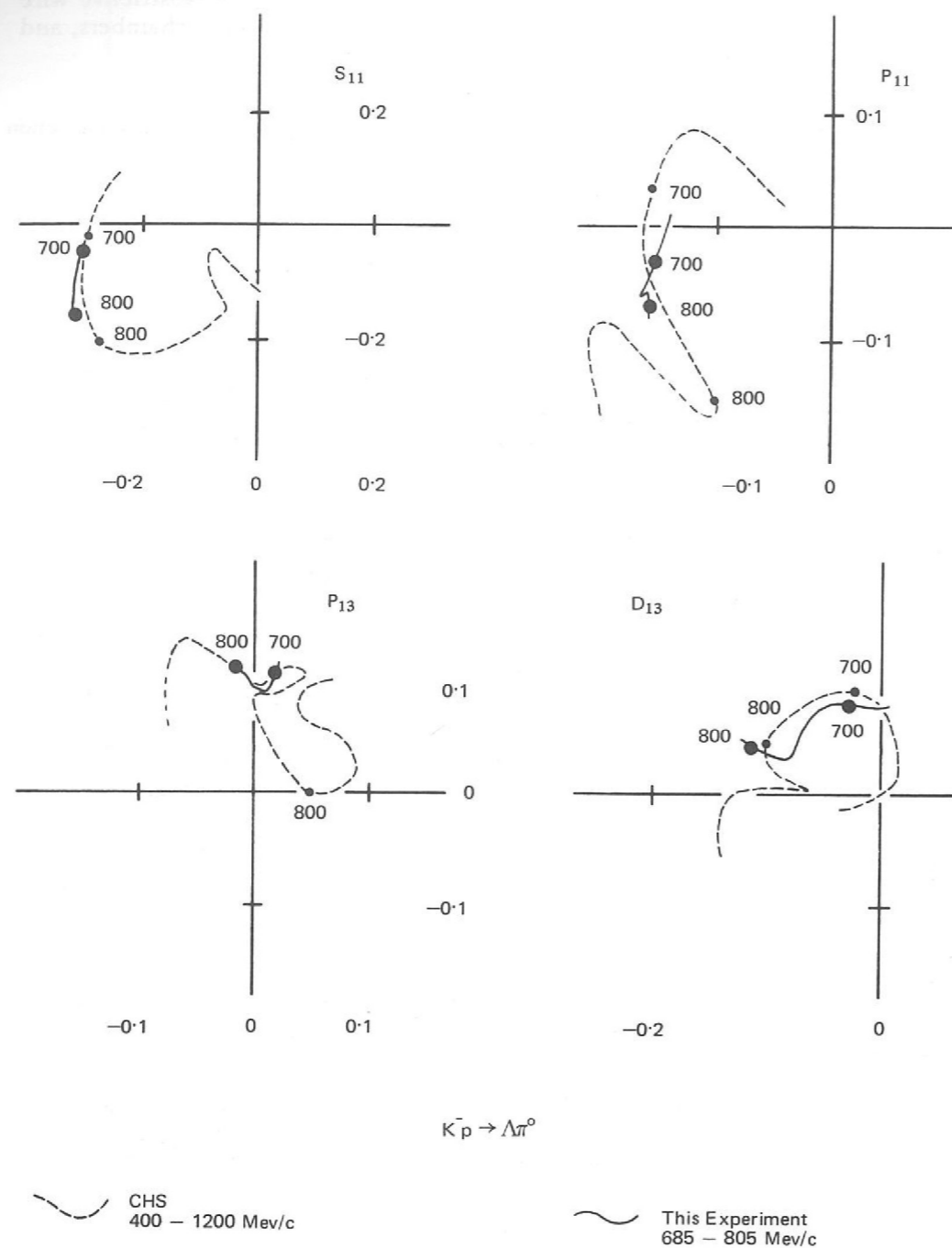

Figure 6. Partial wave amplitudes resulting from a phase shift analysis of the combined data from Experiment 3 and the CERN, Heidelberg, Saclay experiment (CHS).
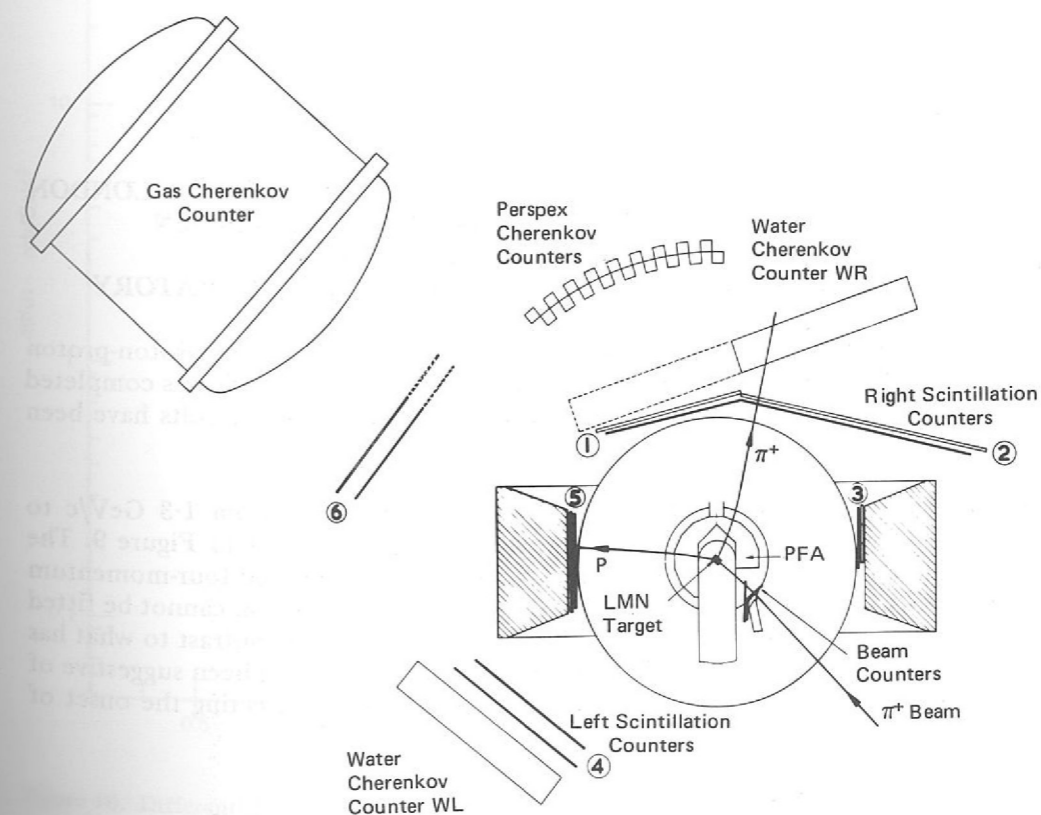
Experiment 4

The amplitude describing the scattering of a pion by a proton depends on the orientation of the proton spin with respect to the scattering plane. In order to investigate this spin dependence some scattering experiments are performed with a polarized target in which there is a net alignment or polarization of the proton spins. Measurements of the differential cross-section with the target polarization direction up and down with respect to a horizontal scattering plane will in general give different results. Changes in this asymmetry in the differential cross-section as a function of incident pion energy may indicate the formation of very short lived ($\sim 10^{-23}$ sec) intermediate states or resonances in the interaction process. Their properties are determined by the technique of phase shift analysis.

Polarization Effects in $\pi^+ p$ Elastic Scattering. (ref. 123, 133)

This experiment (see Figure 7) used a polarized target to measure the asymmetry described above for $\pi^+ p$ elastic scattering between 0·6 and 2·6 GeV/c in approximately 2% momentum steps. Because of the high statistical precision of the data (in some cases better than ± 1%), great care has been necessary to avoid any systematic error in the substraction of background. A considerable fraction of this background arises from quasi-elastic scattering on protons in the complex nuclei of the target (lanthanum magnesium nitrate crystals). These unpolarized bound protons outnumber the free polarized protons in the hydrogen of the water of crystallization by a factor of 15 to 1. In order to check the method of background subtraction some data was taken using a dummy target which had the same properties as the polarized target but contained no hydrogen.

In general, phase shift analyses at any particular energy give a large number of solutions all with comparable χ^2 probabilities. This is partly due to the less than perfect statistical quality of existing data. In an effort to eliminate some of the alternative solutions, twice the normal number of events were recorded at three selected momenta. Results at two of these momenta are shown in Figure 8, and are compared with the predictions of two recent phase shift analyses.

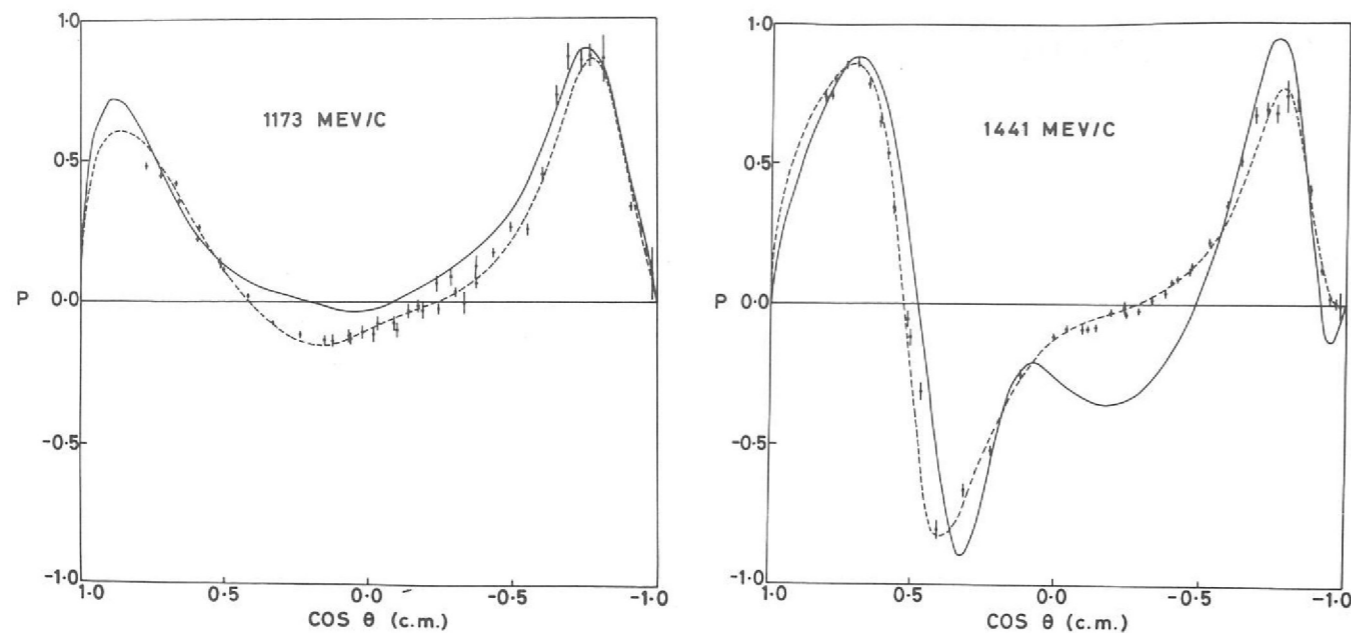Figure 7. Schematic diagram of apparatus used in Experiment 4.

Figure 8. Polarization data at two momenta from Experiment 4 compared with recent phase shift analysis predictions (smooth curves).
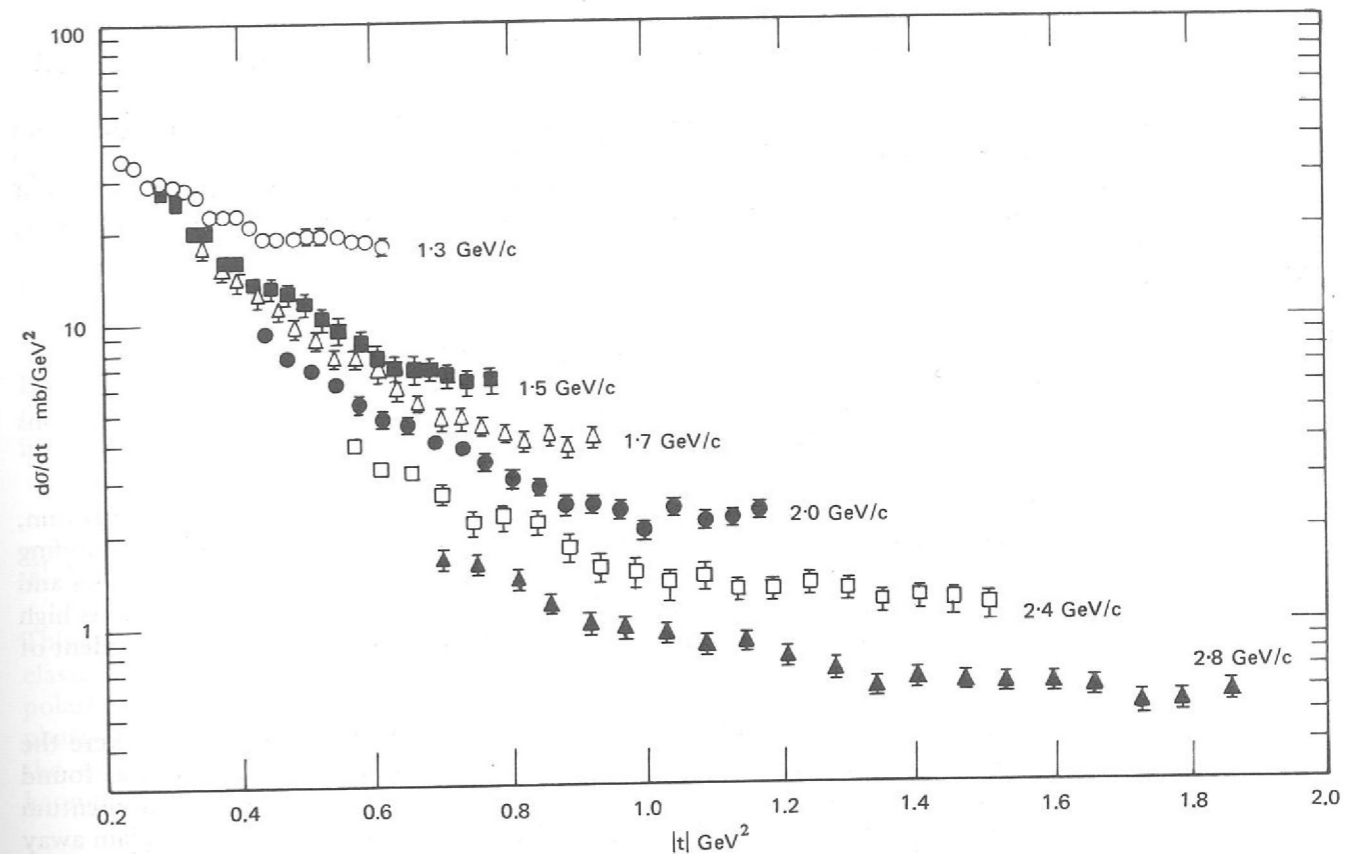
Figure 9. Typical distributions of $\frac{d\sigma}{dt}$ as a function of $|t|$ from data collected in Experiment 5.

QUEEN MARY COLLEGE, LONDON
UNIVERSITY OF BERGEN
AERE, HARWELL
RUTHERFORD LABORATORY

Experiment 5

Wide Angle
Elastic pp Scattering
(ref. 117)

This experiment measured the differential cross-sections for elastic proton-proton scattering at large centre-of-mass angles θ^*. The experimental work was completed in 1970. Analysis of this data was finalised in 1971 and the results have been published.

Differential cross-sections for $50° < \theta^* < 90°$ at 12 momenta from 1·3 GeV/c to 3·0 GeV/c have been obtained. A sample of these are shown in Figure 9. The cross-sections at $\theta^* = 90°$ are shown as a function of t (the squared four-momentum transfer) in Figure 10. It can be seen that the data in this region cannot be fitted by a set of straight lines of monotonically varying slopes, in contrast to what has been claimed at higher t values. The previous simple picture had been suggestive of scattering from different regions within the proton or as reflecting the onset of various production channels.

Figure 10. Differential cross-section, $\frac{d\sigma}{dt}$, as a function of $|t|$ for proton-proton scattering at $\theta^* = 90°$ (Experiment 5).

Experiment 6

IMPERIAL COLLEGE, LONDON
UNIVERSITY OF SOUTHAMPTON

An Investigation of Narrow Width Mesons Produced in π⁻p Interactions (ref. 21, 22, 129, 130, 131, 184, 189)

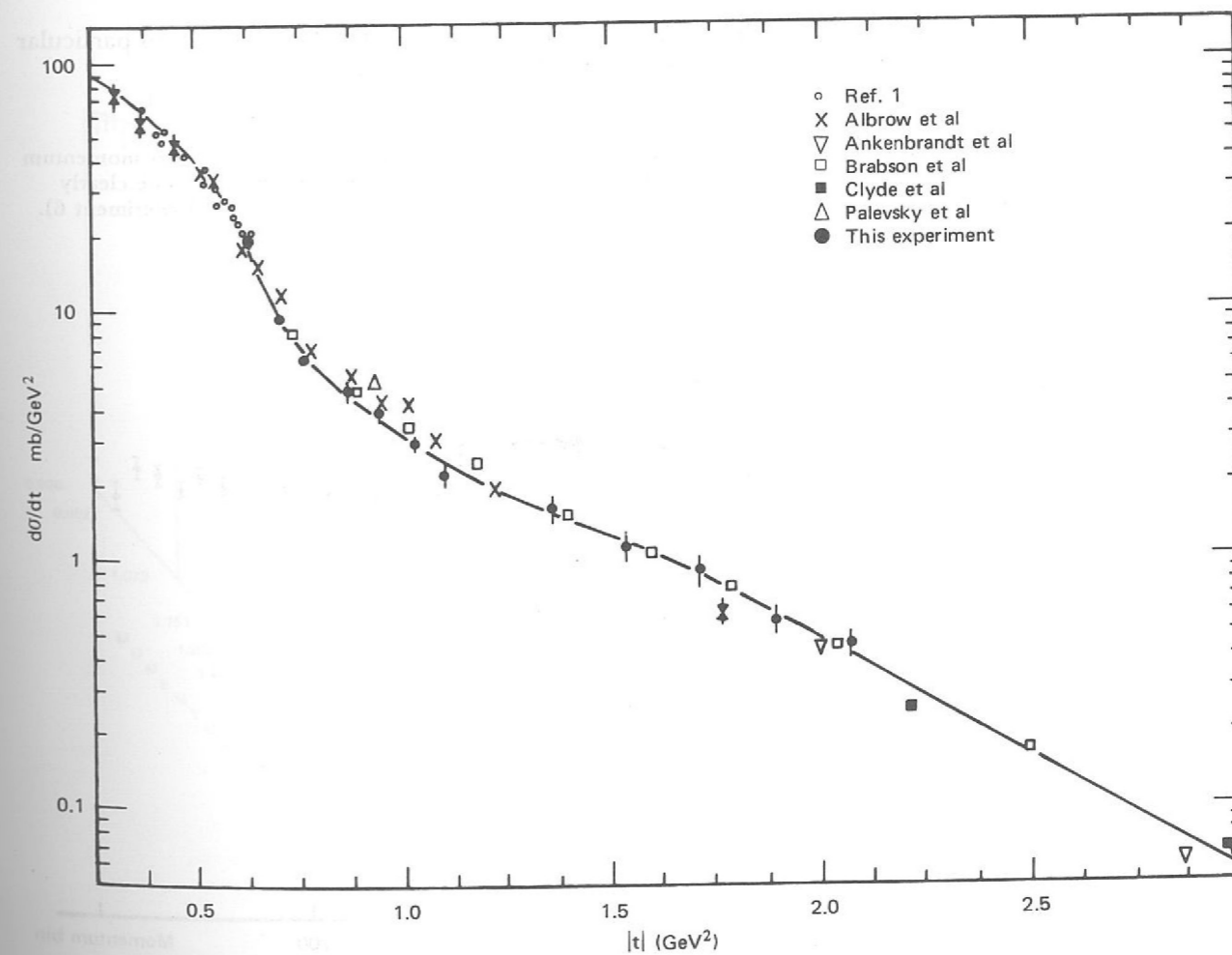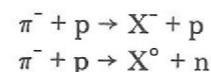This is a 'missing mass' type of experiment in which the yield of neutrons and protons from $\pi^- p$ interactions is studied as a function of the pion momentum and the nucleon time-of-flight. The measurement of the momentum and direction of the outgoing proton or neutron determines the mass of the 'missing meson' X, assuming interactions of the type

$$\pi^- + p \rightarrow X^- + p$$
$$\pi^- + p \rightarrow X^\circ + n$$

The general intention of the experiment is to search for and study narrow mesons in the mass range 500-2000 MeV/c² .

The equipment consists of a precisely controlled pion beam of variable momentum, a hydrogen target, six neutron counters near the forward direction and, surrounding the target, a set of 60 counters differentially sensitive to both charged particles and photons. Such a counter system defines common decay channels and permits high data acquisition rates. It has high mass resolution which is almost independent of the decay.

Most data were collected in the mass region around the A_2 meson and here the analysis into the 2π and 3π decay channels has been completed. It was found possible to examine the A_2 mass spectrum in three regions of four-momentum transfer, ranging from -0.9 to -0.2 (GeV/c)² . Evidence, difficult to explain away on statistical grounds, was found for a structure at low t in the channel $A_2^- \rightarrow \pi^- + $ neutrals.

It is planned to take further data with the same apparatus during 1972. In particular the η, ω and A_2 mesons will be carefully investigated.

Figure 11. Yield of neutrons into a fixed narrow time-of-flight gate as the beam momentum is varied in $\frac{1}{2}$% intervals ('bins') from 1373 to 1701 MeV/c. The X° and ϕ can be clearly identified on the basis of their masses. No decay selection has been used. (Experiment 6).

$$\pi^- p \rightarrow X + n$$

Yield in 3 ns cms Gate
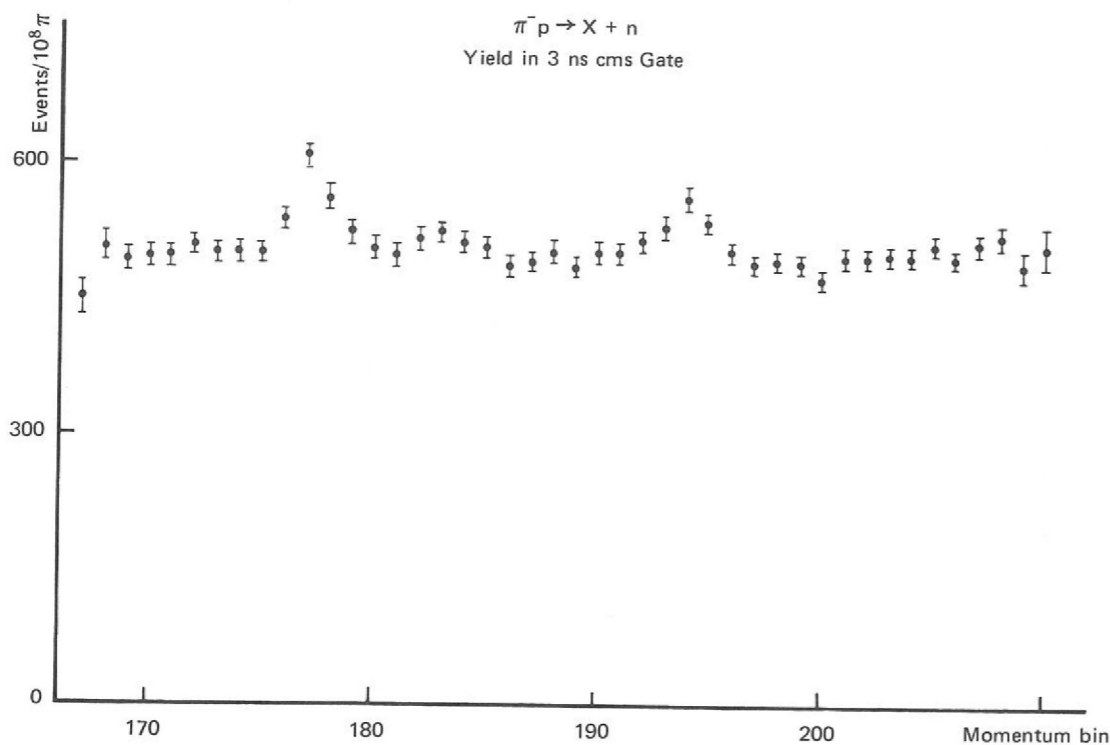
Experiment 7

UNIVERSITY OF CAMBRIDGE
QUEEN MARY COLLEGE, LONDON
RUTHERFORD LABORATORY

A knowledge of πN interactions in the region around the first N* resonance is fundamental to a general study of meson-nucleon physics at higher energies. Prior to this experiment the available data were sparse and relatively inaccurate, and warranted a comprehensive series of measurements of total cross-sections (at the $\frac{1}{2}$% level of accuracy) and angular distributions (at the 1% level of accuracy) over the energy region 80 to 300 MeV.

Low Energy Pion-Nucleon Interactions (ref. 25, 26, 159, 170)

Data collection was completed during the summer of 1970. The analysis and the theoretical implications of the results have been studied since then, and this work is now in its final phase.

Experiment 8

UNIVERSITY OF BRISTOL
RUTHERFORD LABORATORY

This experiment was designed to measure differential cross-sections for K^+p elastic scattering over a wide angular range. These measurements, combined with polarization measurements from other experiments, provide a basis for a detailed phase shift analysis of the K^+p interactions. This analysis will be used in studying the existence or otherwise of possible "exotic" Z* resonances in the positive kaon-nucleon system.

K^+p Differential Cross-Sections in the Range 0·9 to 2·0 GeV/c (ref. 171)

Figure 12. An isometric view of the differential cross sections in K^+p elastic scattering measured in Experiment 8.
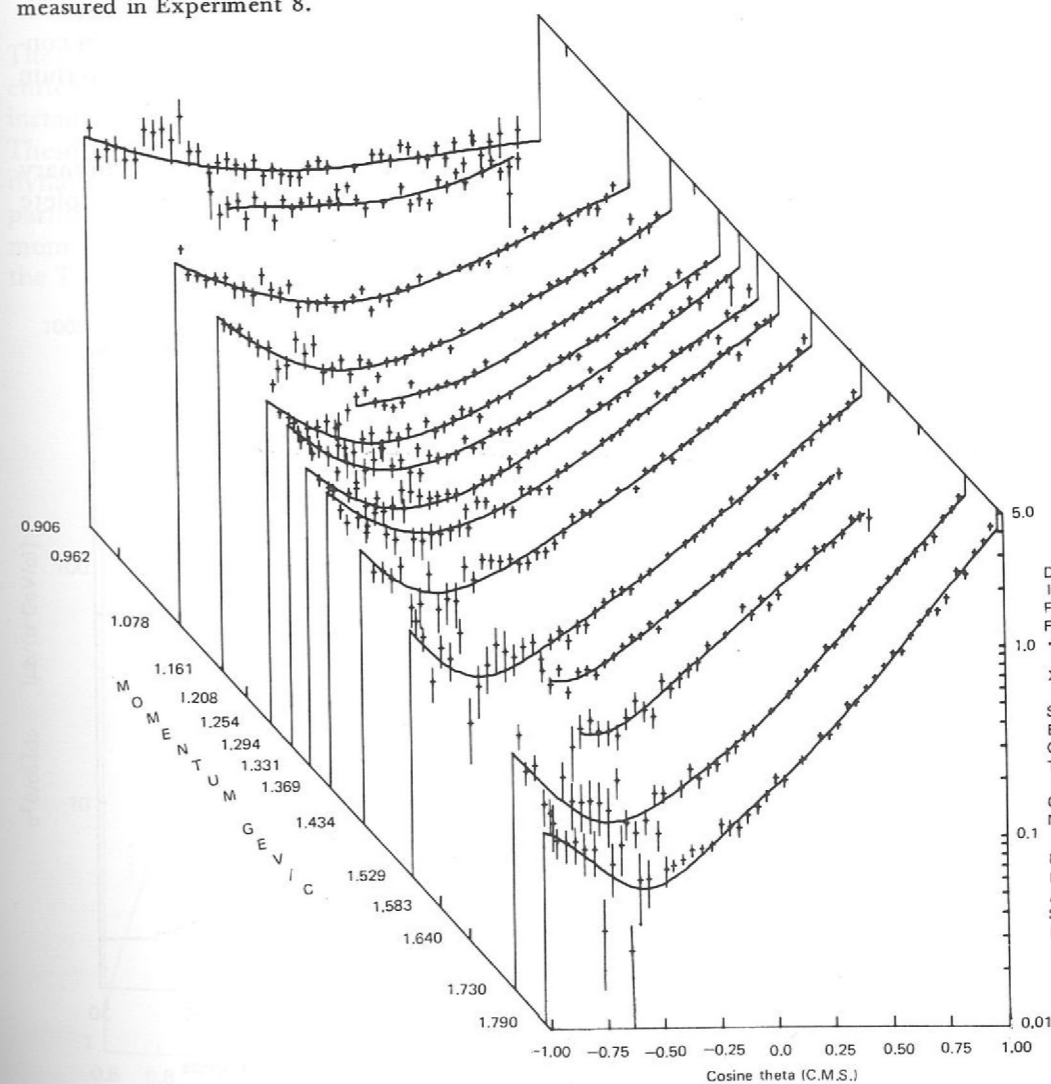
The measurements of the differential cross-sections are almost complete and the results are being finalised for publication. A total of about 250,000 elastic events were collected at 17 momenta in the momentum range 900 MeV/c to 1900 MeV/c during the year 1971. The angular range covered by the measurements is $-1.0 \leqslant \cos \theta^* < (0.90$ at low momentum to 0.97 at the highest momenta).

As soon as the final results of the measurements have been obtained they will be used in a comprehensive phase shift analysis. Comparison of preliminary results with published phase shift solutions indicates that the differential cross-sections from this experiment will enable a considerable number of them to be eliminated.

Experiment 9

UNIVERSITY OF BIRMINGHAM
RUTHERFORD LABORATORY

$K^{\pm}n$ Elastic and $K^{\pm}n$ Charge Exchange Differential Cross-Sections (ref. 90, 91, 92)

Data taking started early in 1971 on this sonic spark chamber experiment to measure $K^{\pm}n$ charge exchange and $K^{\pm}n$ elastic differential cross-sections using a liquid deuterium target. Several thousand good events have been recorded at each of 7 K^+ momenta between 430 and 940 MeV/c and 14 K^- momenta between 590 and 940 MeV/c. These represent a large addition to the meagre existing data. The K^+ data should clarify the still unsettled question of whether the large peak observed in the K^+n elastic cross-section at 0.75 GeV/c is an exotic I = 0 resonance (Z_0^*), while the K^- results will be useful for the further understanding of the Y^* resonances.

Elastically scattered kaons are identified by observing their decay in flight after their momentum has been measured in a large spectrometer magnet (M5). The time of flight of momentum analysed protons from charge exchange events is measured in a large counter array ($3.3 \times 1.5 \, m^2$). The correct time of flight in conjunction with the absence of a count in a counter almost surrounding the deuterium target uniquely identifies these events at all momenta.

The analysis of the large volume of data is proceeding satisfactorily and preliminary differential cross-section results look encouraging. Data taking is almost complete (December 1971).

Figure 13. Typical time of flight spectrum at 600 MeV/c. (Experiment 9).
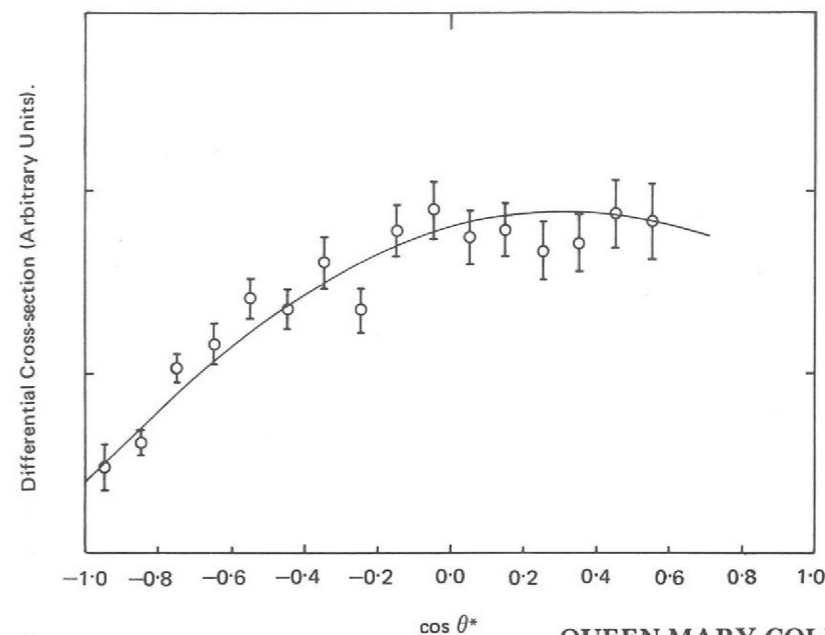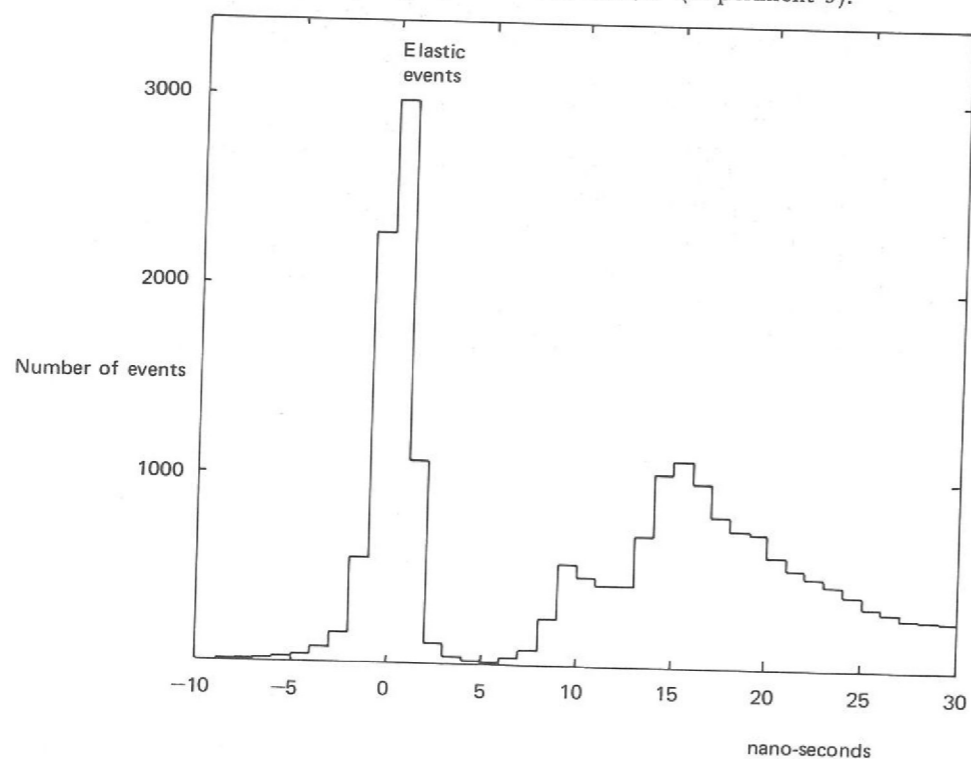
Figure 14. Charge exchange angular distribution at 600 Mev/c. (Experiment 9).

Experiment 10

QUEEN MARY COLLEGE, LONDON
UNIVERSITY OF LIVERPOOL
DARESBURY LABORATORY
RUTHERFORD LABORATORY

Antiproton-Proton Elastic Scattering and Two Body Annihilation

The proton-antiproton system has the same basic quantum numbers as the mesons of strangeness zero. Hence mesons with a mass greater than that of two nucleons may be formed in $\bar{p}p$ interactions. Such mesons are very short lived and are studied by their decay into various final states. The experiment is designed to investigate the reactions

$$\bar{p} + p \rightarrow \bar{p} + p$$
$$\bar{p} + p \rightarrow \pi^- + \pi^+$$
$$\bar{p} + p \rightarrow K^- + K^+$$

The Nimrod energy is too low to provide sufficient fluxes of antiprotons. A new enriched beam of antiprotons was designed for the CERN synchrotron. This was installed and tested during the early part of 1971 and the yields were measured. These are shown in Figure 15 and agree well with the predictions of a thermodynamic model. Antiproton selection is by time of flight. The beam provides particles up to a maximum momentum of 2.4 GeV/c. By varying the beam momentum, a mass range of 2.0 GeV/c² to 2.6 GeV/c² can be studied. This includes the T and U meson regions.
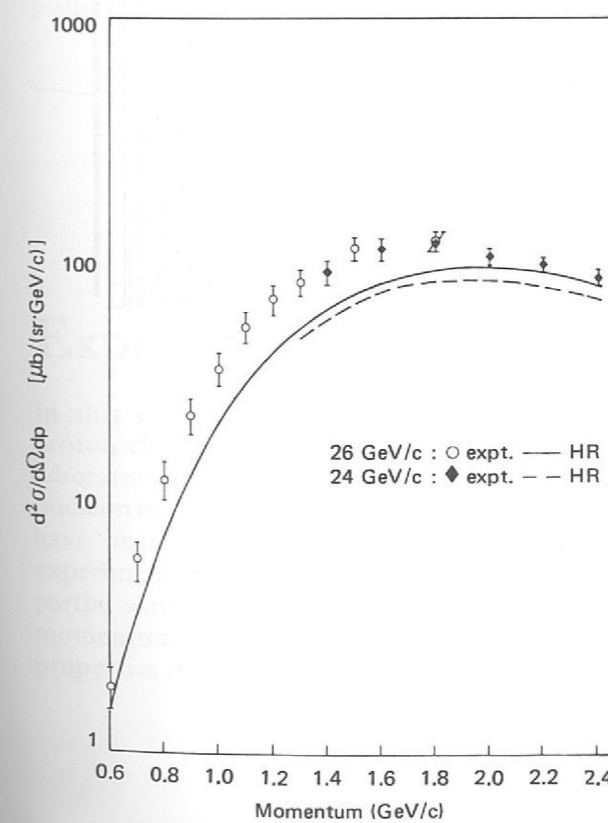
Figure 15. Antiproton yields in Experiment 10.

The apparatus was set up and tested during the first half of 1971 and the final item, a 130 ton spectrometer magnet belonging to CERN, was installed in June 1971. A plan view of the apparatus is shown in Figure 16. Counter hodoscopes and spark chambers define the positions of the incoming and outgoing particles from a liquid hydrogen target. The momentum of one outgoing particle is determined from its trajectory in the spectrometer magnet. Wire spark chambers with ferrite core read-out are used, the largest chambers having an active area of 2·69 m x 0·77 m. Information from the chambers is read into a PDP 9L computer which also provides an on-line monitor of the experiment and which writes all the information from each scattering event on to magnetic tape for subsequent off-line analysis. The entire apparatus apart from the beam chambers and counters can rotate about the hydrogen target, angular distributions at any particular momentum requiring two different positions of the rotating platform. Data is collected simultaneously for all three channels under investigation.

Data taking commenced in August 1971 and by November full angular distributions had been measured at 12 momenta between 1·0 GeV/c and 2·0 GeV/c. Running time has been allocated until Easter 1972 by which time data at some 20 momenta will have been taken with, for example, 2000 $\pi^+\pi^-$ events each. Preliminary analysis has begun at CERN and full scale analysis will be completed on computers at the Rutherford and Daresbury Laboratories.

Figure 16. Schematic diagram of the apparatus used in the $\bar{p}p$ scattering experiment (Experiment 10).
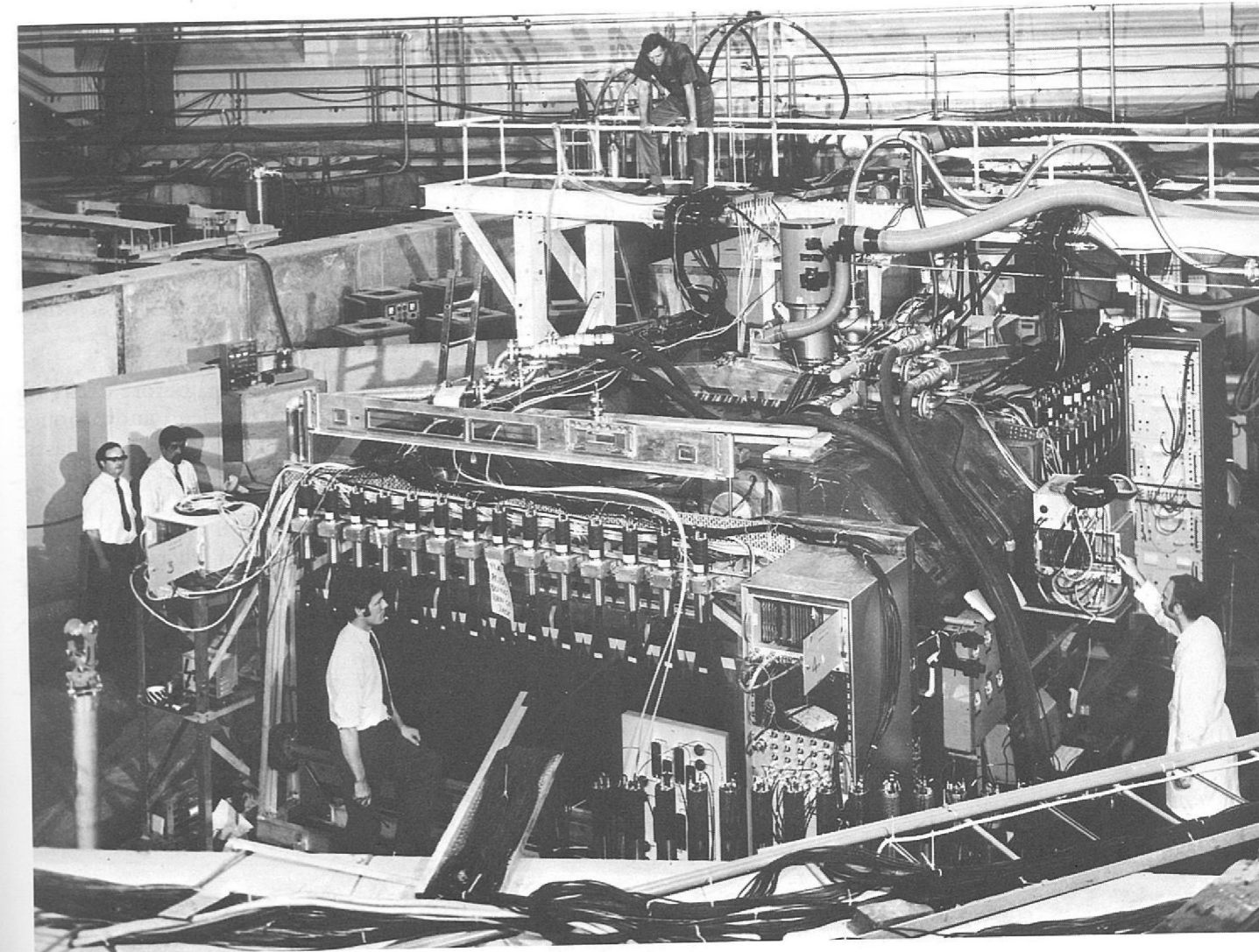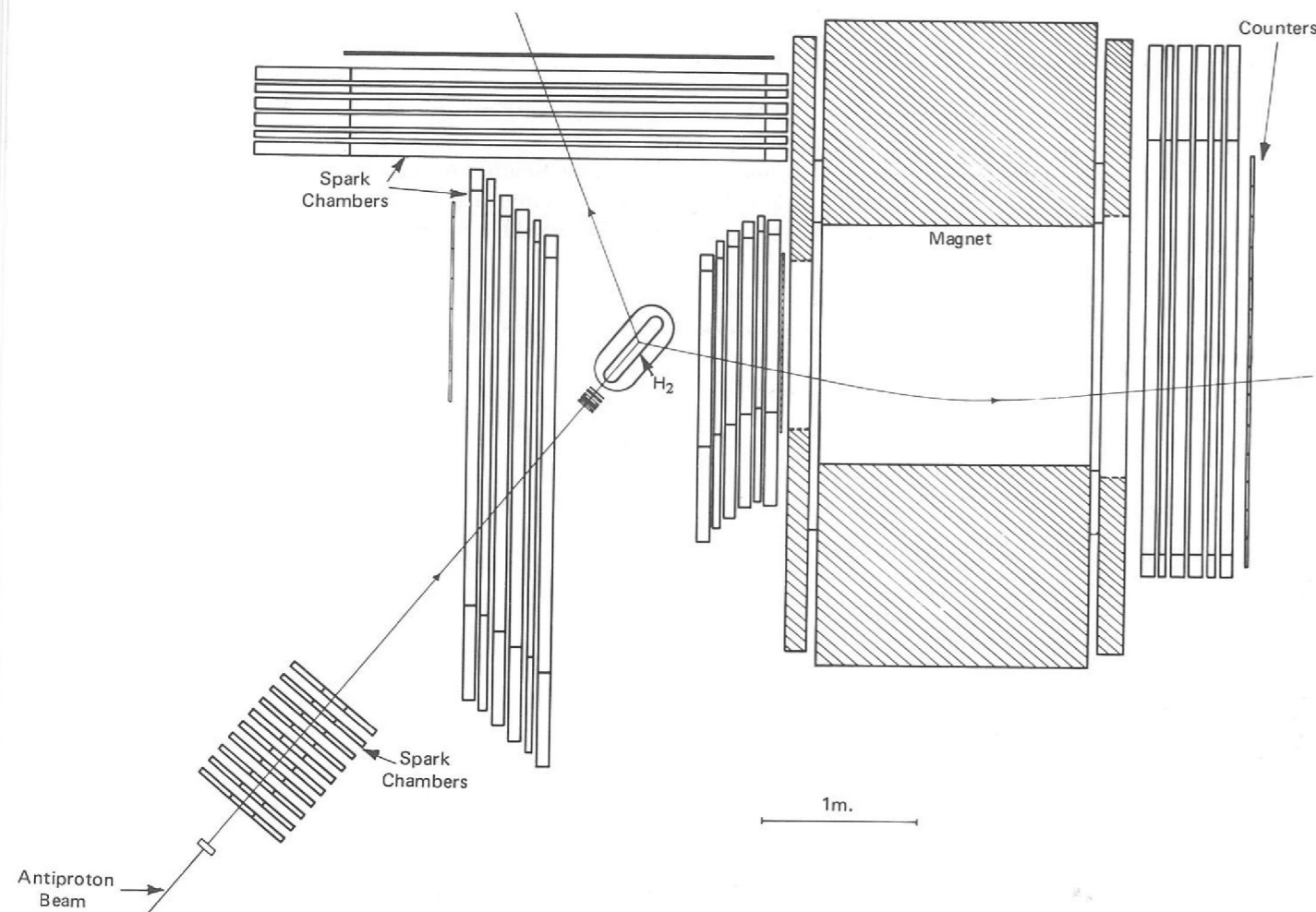
Figure 17. A view of the apparatus used in Experiment 10. Seen here are scintillation counter hodoscopes, core-read-out spark chambers and a bending magnet all mounted on a rotatable platform. (*CERN Photo*).

UNIVERSITY OF GLASGOW
UNIVERSITY OF WARWICK
RUTHERFORD LABORATORY

Experiment 11

In this experiment the differential cross-section and the asymmetry for pion-proton charge exchange scattering from a polarized target will be measured at 30 laboratory momenta between 600 and 4000 MeV/c. A large number of pion-nucleon resonances are known to be produced in this momentum range and others have been suggested by current theoretical models. One of the objects of the experiment is to provide new data to be incorporated into an analysis in terms of partial wave amplitudes. From the behaviour of these amplitudes as a function of momentum of the incident pion, it is possible to obtain information on the properties of any resonant states which may be formed in the scattering process.

Differential Cross-Sections and Polarization Effects in the Charge Exchange Reactions $\pi^-p \to \pi^\circ n$ and $\pi^-p \to \eta^\circ n$

The experimental arrangement is shown in Figure 18. The target consists of a mixture of glycerol and water in which the free protons are polarized by means of the "solid effect". The target assembly is of the new frozen spin type; it is described in detail on page 113. A very important feature of this new target is that it allows scattered particles to be detected over about 67% of the total possible solid angle.

The counter arrays surrounding the target are designed to take full advantage of the available solid angle. The neutron counters consist of cells, one metre in length, filled with liquid scintillator. The neutrons are detected in these counters when they suffer nuclear collisions which yield charged secondary particles. The scintillation light from the secondary particles is detected by photomultiplier tubes.

The π° and η° mesons travel only a minute distance ($< 10^{-4}$ cm) before decaying into two γ-rays. These γ-rays are converted by large sheets of lead and produce electron-positron showers. Each shower is detected in hodoscopes of plastic scintillation counters placed immediately behind the lead.

With this arrangement neutrons and γ-rays can be detected with sufficient angular resolution to distinguish charge exchange events from quasi charge exchange scattering off bound protons. Plastic scintillation counters placed around the target and in front of the counter arrays are used to reject charged particle backgrounds.

Figure 18. Schematic diagram of the apparatus in Experiment 11.

Plastic Scintillators
Lead Convertors
Anti Counters
Liquid Scintillators
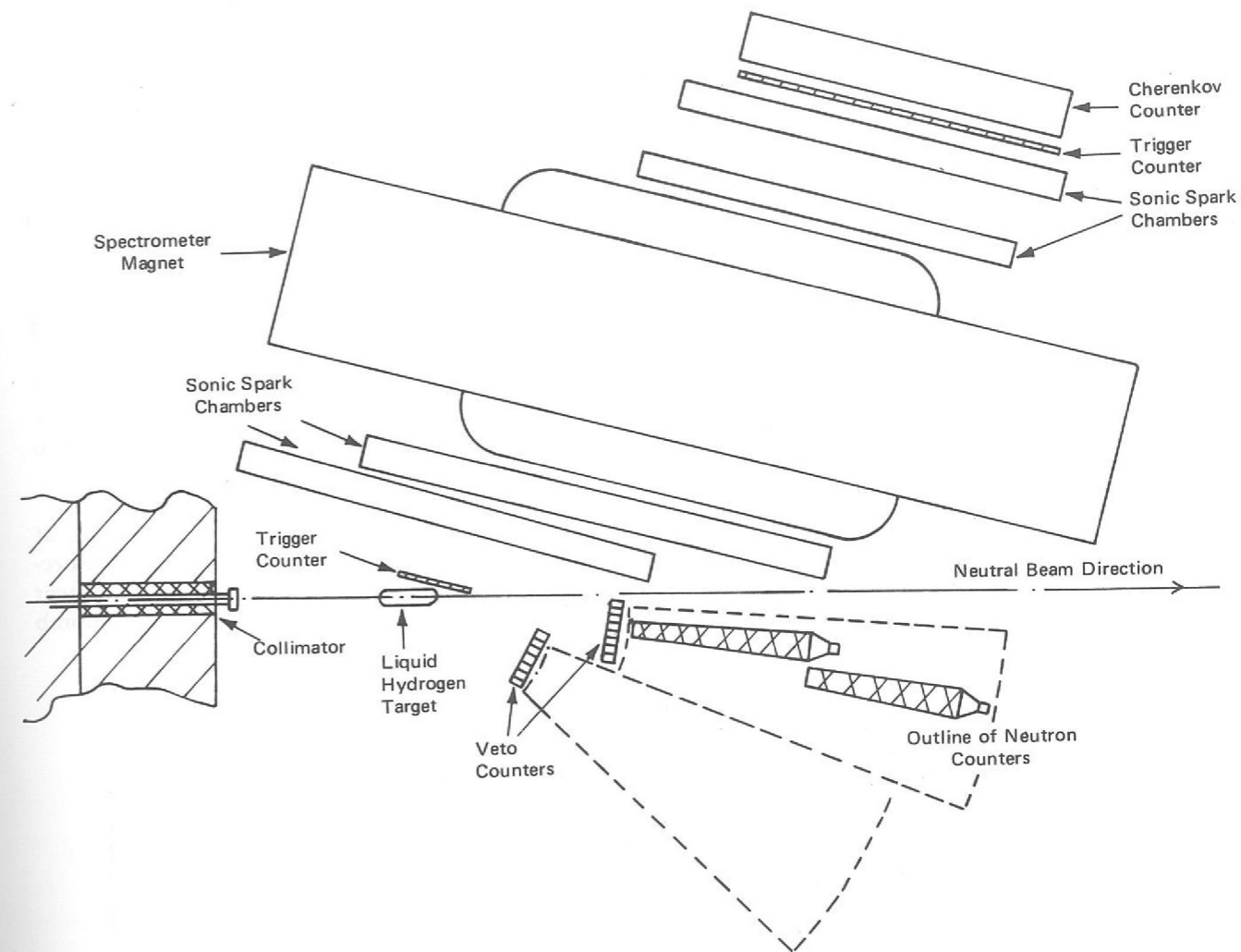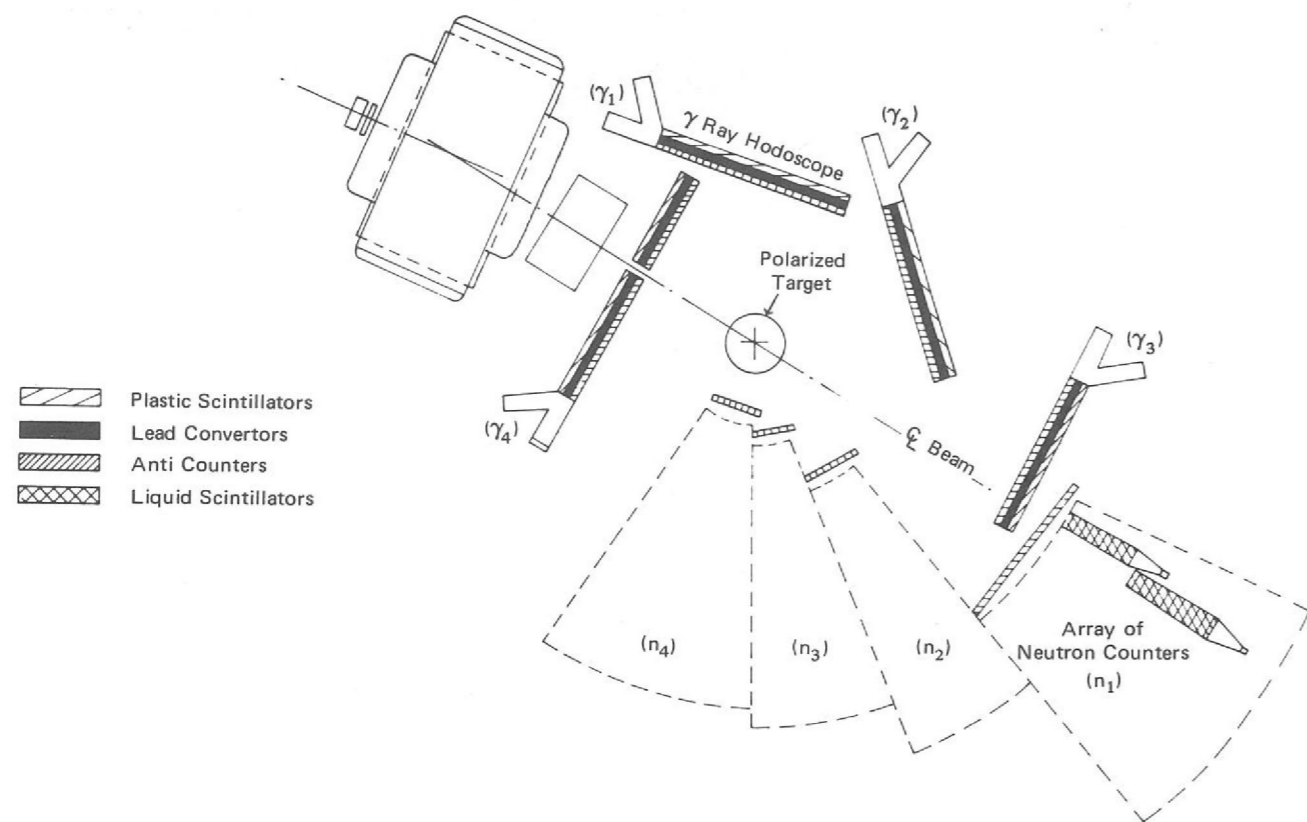
Figure 19. Arrangement for the calibration of neutron counters for Experiment 11 in the N4 neutral beam (Hall 3).

The measurement of the differential cross-section requires a precise knowledge of the detection efficiency of our apparatus. The efficiency calibration of the neutron counters will be done in a neutral beam derived from a target in the X3 extracted proton beam. The calibration apparatus is shown in Figure 19. The sonic spark chamber spectrometer to the left of the hydrogen target will be used to measure the momentum and angle of the scattered proton. This information is kinematically sufficient to determine the angle and energy of the scattered neutron. A comparison of the number of neutrons of known energy and direction with the number observed in the neutron array gives the detection efficiency as a function of angle and energy.

The γ-ray hodoscope will be calibrated using electrons present in the π9 beam. The forward-going photons produced from electron bremsstrahlung in a thin radiator will be "tagged" by measuring the momentum of the electron before and after the emission of the photon. This measurement determines the energy of the photon. Comparison of the number of photons tagged with the number observed in each γ-ray hodoscope then gives the γ-ray detection efficiency as a function of energy.

The apparatus is in the final commissioning stage. Test efficiency data and test charge exchange data have been recorded and are being analysed. Full scale data collection will commence in 1972.

Experiment 12

π⁺p Differential Cross-Sections in the Momentum Range 0·6 to 2·0 GeV/c

This experiment uses the same equipment as Experiment 8. Its aim is to systematically measure differential cross-sections in π^+p elastic scattering over the momentum range 0·6 GeV/c to about 2·0 GeV/c. These measurements will be of a higher statistical accuracy than any obtained before and will cover a wide angular range as in the case of the K⁺p elastic scattering measurements.

About 400,000 elastic events in the momentum range 800 MeV/c to 1600 MeV/c were collected at 16 different values of the central momentum in 12 days of 'good beam' time. The momentum bite is ± 2% which means that almost all the runs overlap in momentum. The accuracy of determination of the relative momenta for the incident pions before scattering is better than 0·4%. It will be possible to produce π^+p differential cross-section measurements at central momenta corresponding to those of the extensive polarization measurements done in this Laboratory.

Figures 20 and 21 show differential cross-sections for two momenta, one at 800 MeV/c and the other at 1451 MeV/c. It is interesting to note that the measurements extend very well into the forward region and in the case of the lower momentum the rise in the cross-section at small scattering angle is due to Coulomb scattering effects becoming important.

Figure 20. Differential cross-sections for π^+p elastic scattering at 800 MeV/c from analysed data of Experiment 12.
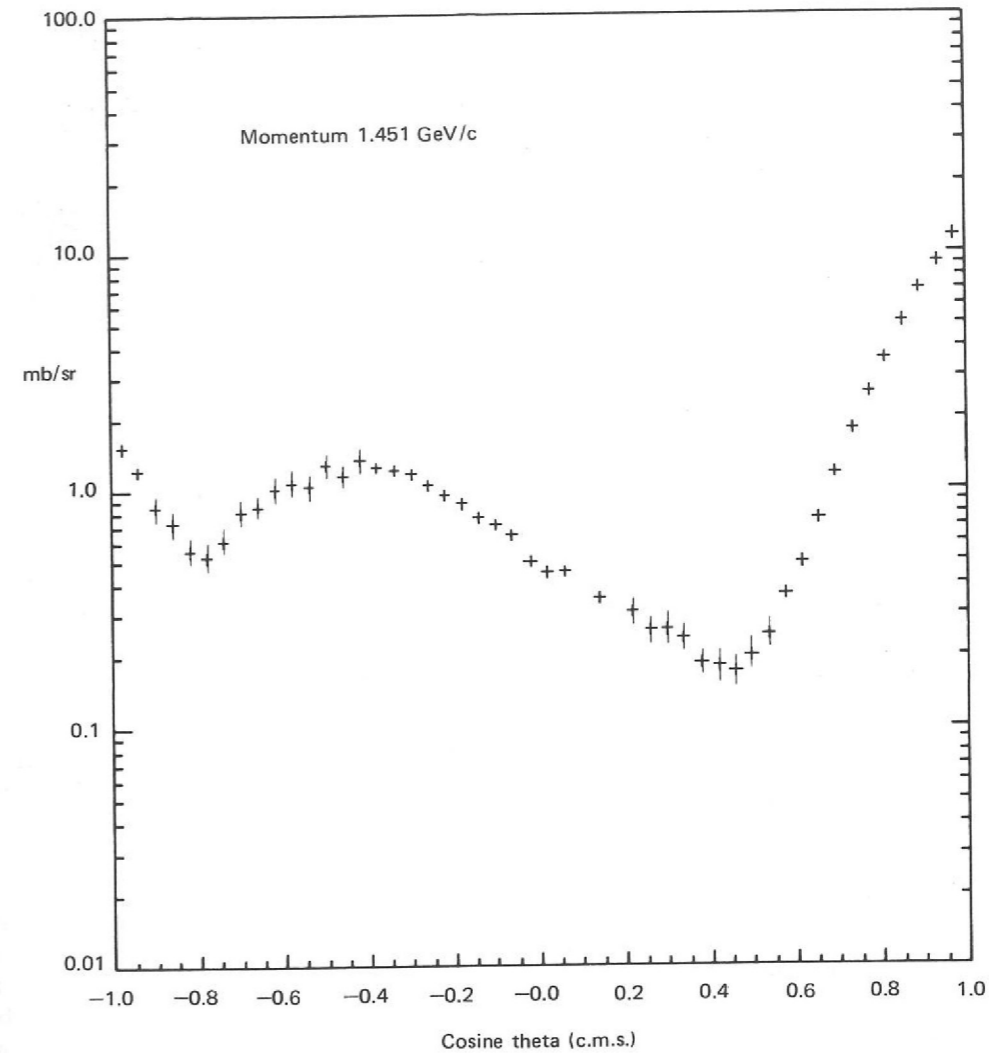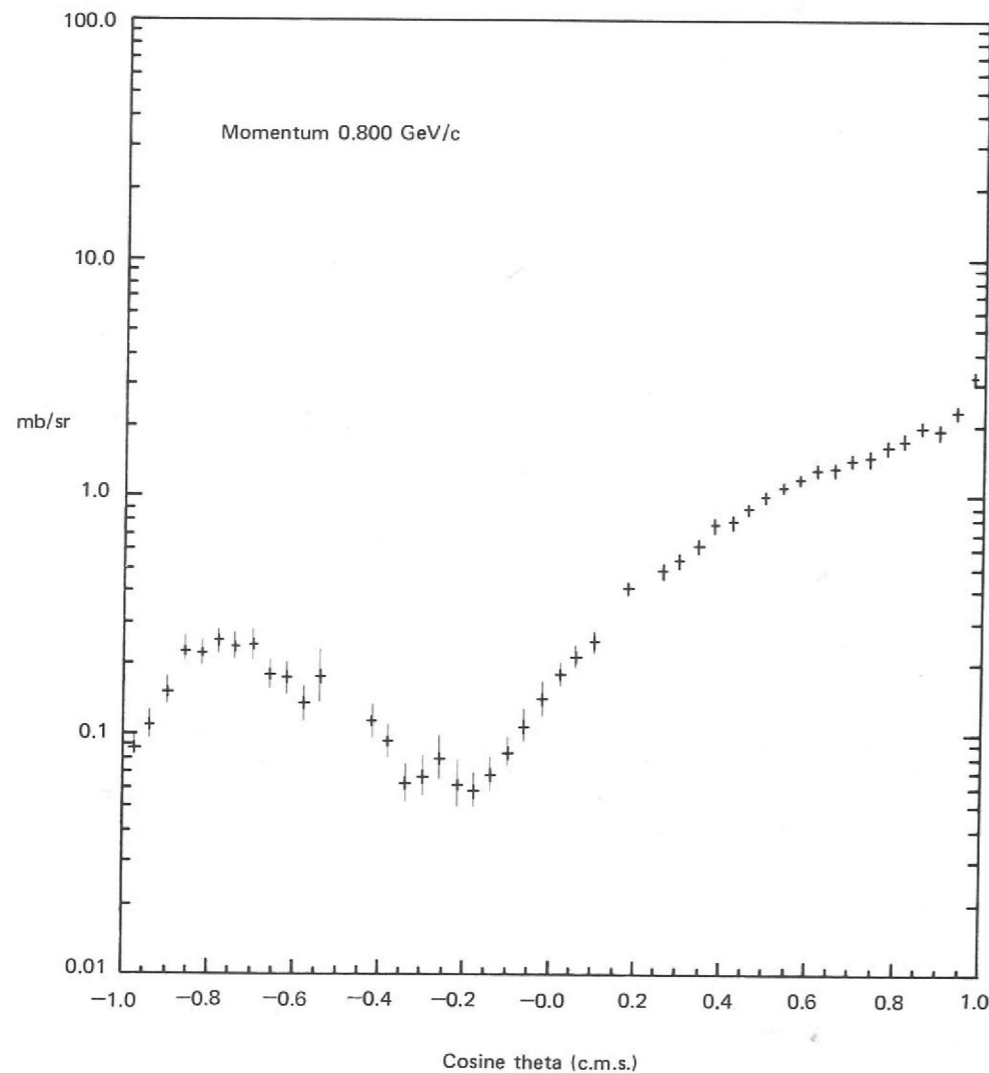
Figure 21. Differential cross-sections for π^+p elastic scattering at 1451 MeV/c from analysed data of Experiment 12.

Experiment 13

Nucleon resonances have been extensively studied through phase shift analysis of the elastic πp reactions. Very little information is available from inelastic channels. A study of the associated production reaction $\pi^-p \to K^\circ\Lambda^\circ$ is useful because polarization data is obtained simultaneously without recourse to a polarized target by measuring the decay asymmetry $\Lambda^\circ \to p\pi^-$, and the reaction is pure $I = \frac{1}{2}$ without diffraction scattering. The objective of a detailed low energy programme is an inelastic phase shift analysis to

Differential Cross-Sections and Polarization in the Reaction $\pi^- + p \to K^\circ + \Lambda^\circ$ between Threshold and 1·5 GeV/c

(a) identify baryon states in an inelastic channel for confirmation that the elastic channel Argand diagrams do represent evidence for resonant states;

(b) search for "daughter" states in the threshold region where angular momentum barriers inhibit higher spin states;

(c) determine branching ratios; and

(d) provide input for analyses in terms of the finite energy sum rules which may allow inferences about high energy amplitudes to be made.
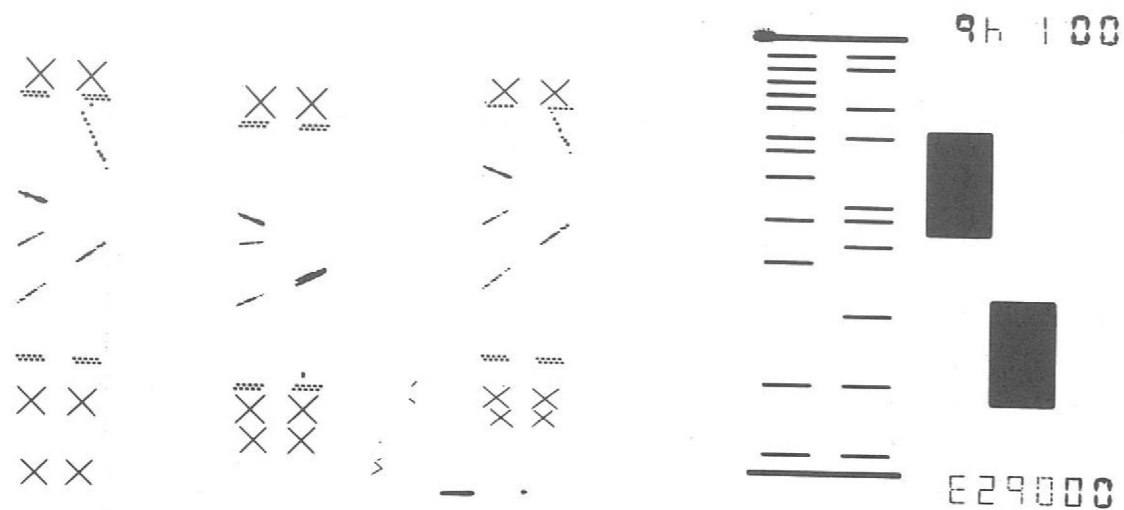
Figure 22. A possible $\pi^- p \to K^\circ \Lambda^\circ$ event taken in a setting up run for Experiment 13.
Three views of two ten-gap chambers are shown with the Brenner mark and data box alongside.

Setting up is in progress. Figure 22 shows a $K^\circ \Lambda^\circ$ candidate obtained in a run to investigate triggering. The film will be automatically digitised using Cyclops. Prototypes of magnetostrictive chambers which will supplement the film information have been tested. Data taking is scheduled during 1972.

Experiment 14

UNIVERSITY OF BIRMINGHAM
WESTFIELD COLLEGE, LONDON
RUTHERFORD LABORATORY

*Search for S = 0
Bosons in the Omega
Spectrometer at CERN*

An important development in the experimental technique of high energy physics is the use of very large magnets filled with spark chambers. The Omega system, nearing completion at CERN, will be the biggest magnet spark chamber system in operation. Its first use in an experiment is expected in mid-1972. Such devices are starting to encroach on what was formerly the territory of the bubble chamber, namely the detection of multi-body final states. These final states may come from a quasi two body process in which one (or both) of the intermediate state particles is unstable and decays. Thus, by being able to deal with this situation, a whole new range of interaction studies is opened up. The Omega system should have a number of important advantages over present day bubble chambers. These include:

(a) it is a triggered device, so that an enriched sample of events of a selected type can be studied.

(b) higher data taking rates are possible. The Plumbicon television camera spark co-ordinate recording system can cope with up to 30 events (pictures) per burst. This is in contrast with 1 picture per burst for most bubble chambers.

(c) the accuracy in determining particle trajectories (momentum and direction) is higher than with present day bubble chambers.

(d) the pictures are expected to contain fewer unwanted tracks than bubble chamber pictures, making automatic analysis simpler.

With these significant advantages, the Omega project has already developed a large following (some twelve European collaborations). The many groups hoping to make use of Omega have contributed to the planning and building of the device and its ancillary equipment. Equipment is being prepared by the collaboration for an experiment which will be carried out in the Omega project in late 1972 and 1973. It will bring together counter and bubble chamber physicists. It is a study of neutral bosons in the mass range 1-2 GeV/c² using a recoil neutron trigger.

The number of events expected is in the region of one million, very much larger than in any experiment carried out so far in which the decay products of bosons have been observed.

Two major pieces of equipment are in preparation: these are the neutron trigger counter array and the Plumbicon television camera read-out system for the 110 spark chamber gaps shown in Figure 23. The neutron counter has been tested in a charged particle beam and has achieved the expected ±0·25 ns time resolution. Efficiency tests using neutrons will take place at the Harwell synchro-cyclotron early in 1972.

Tests of the prototype Plumbicon cameras carried out at CERN and the Rutherford Laboratory have proved to be satisfactory, and show that the cameras have adequate resolution and sensitivity.

The group is contributing to the development of other aspects of the project at CERN including the beam, beam detectors and both on-line and off-line software.

Preparations for the analysis of the bulk of the data at the Rutherford Laboratory and Birmingham University are in hand. The digitised spark co-ordinates from the Plumbicon cameras, together with information from the beam detectors and trigger counters, will be submitted to a chain of programs similar to those used in bubble chamber analysis. Automatic pattern recognition will be an important feature of the method, but some events which fail this stage of the analysis will be recovered, if possible, by means of an interactive display system.

Figure 23. Diagram of the Plumbicon television camera system for the Omega Magnetic Spectrometer at CERN. (Experiment 14).
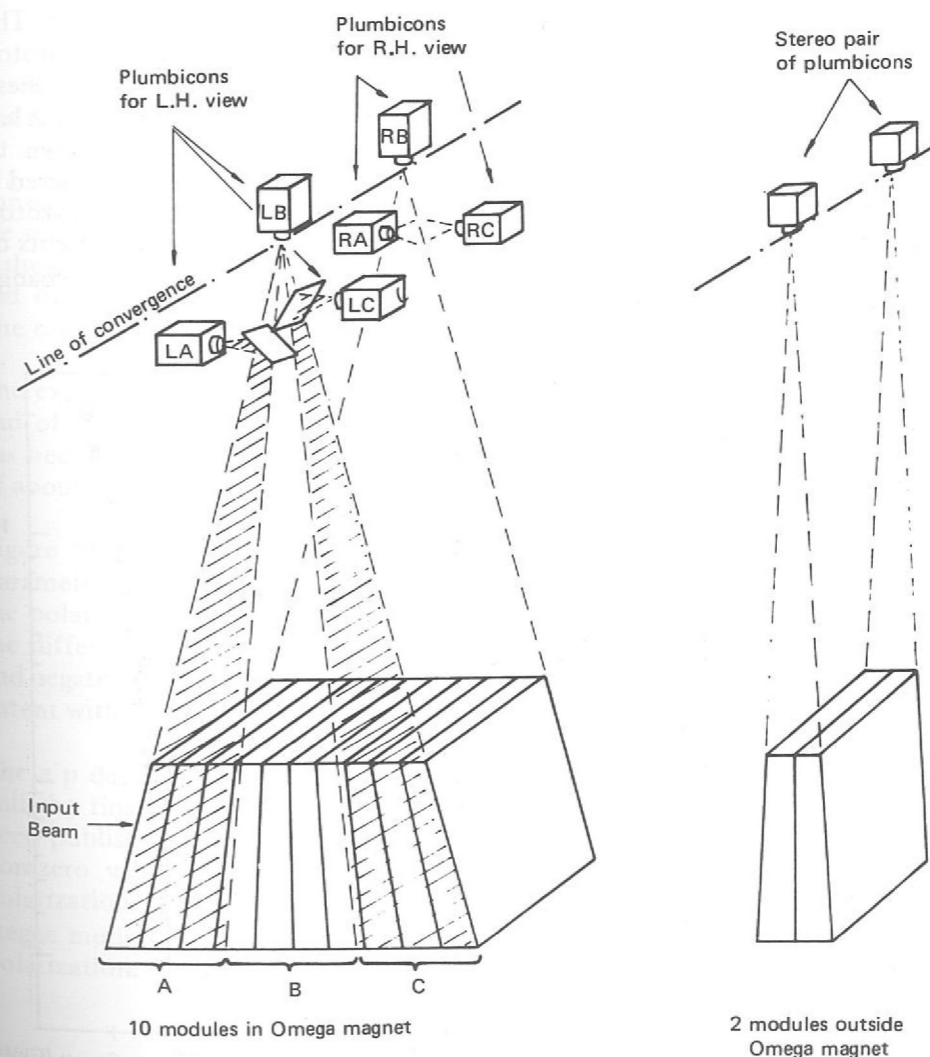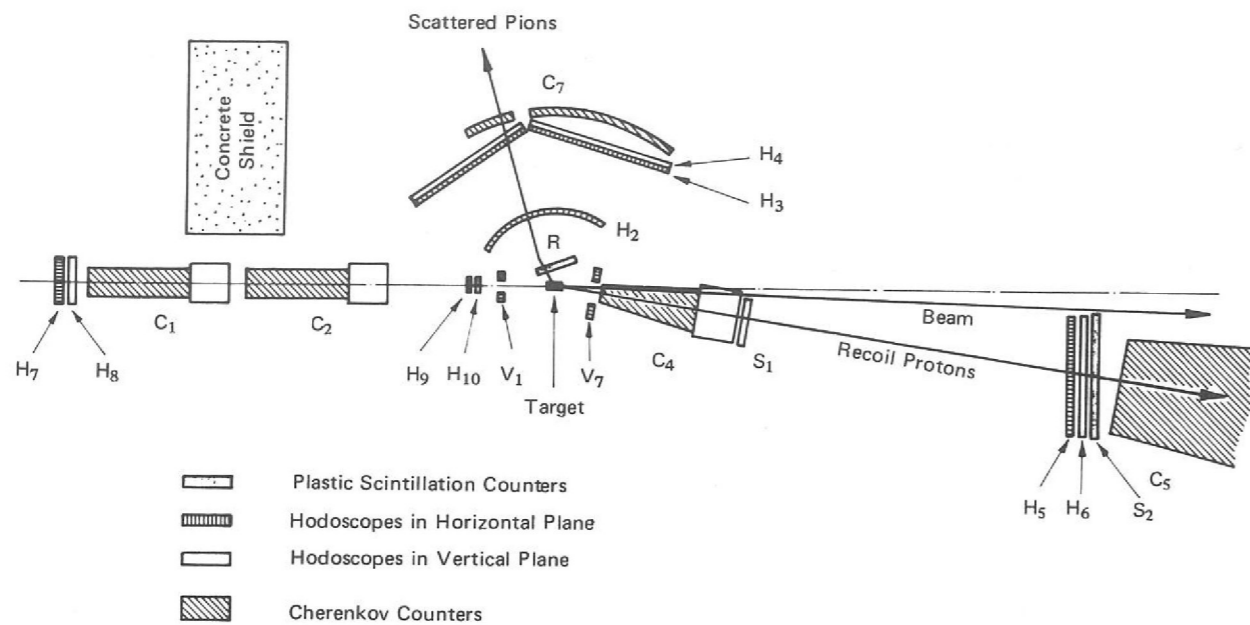
Figure 24. Experimental arrangement for polarization measurements in backward $\pi^\pm p$ elastic scattering. (Experiment 15).

Experiment 15

CERN
UNIVERSITY OF PARIS-SUD
UNIVERSITY OF OXFORD

Measurement of the Polarization Parameter in $\pi^\pm p$ Backward Elastic Scattering at 6 GeV/c (ref. 4, 127, 150)

This experiment is a continuation of the programme at CERN to study the spin-dependence of elastic scattering at high energies. The programme was initiated by the CERN-Orsay groups who over the course of the last four years have published detailed measurements of the polarization parameter in $\pi^\pm p$, $K^\pm p$ and pp forward scattering at high energies with four momentum transfer $|t| < 2$ (GeV/c)². The present collaboration has utilised the most recent developments in polarized proton targets (Butanol at 0·55K with a free proton polarization $\simeq$ 70%) to extend these measurements in $\pi^\pm p$ at 6 GeV/c to the region of backward scattering where it has been possible to make measurements of the polarization parameter down to differential cross-section levels of 1μb/(GeV/c)². The kinematic region covered is that of four momentum transfer from the incident pion to the outgoing proton $|u| \leq 1\cdot0$ (GeV/c)² equivalent to $|t| = 9\cdot42$ to $10\cdot42$ (GeV/c)². Measurements of backward scattering at high energy investigate the region where baryon exchange processes are expected to be dominant.

Figure 25. Measured polarization at 6 GeV/c from the analysis of all the $\pi^+ p$ backward elastic scattering data taken in Experiment 15. Also shown is the differential cross section $\frac{d\sigma}{du}$ as a function of four momentum transfer u.
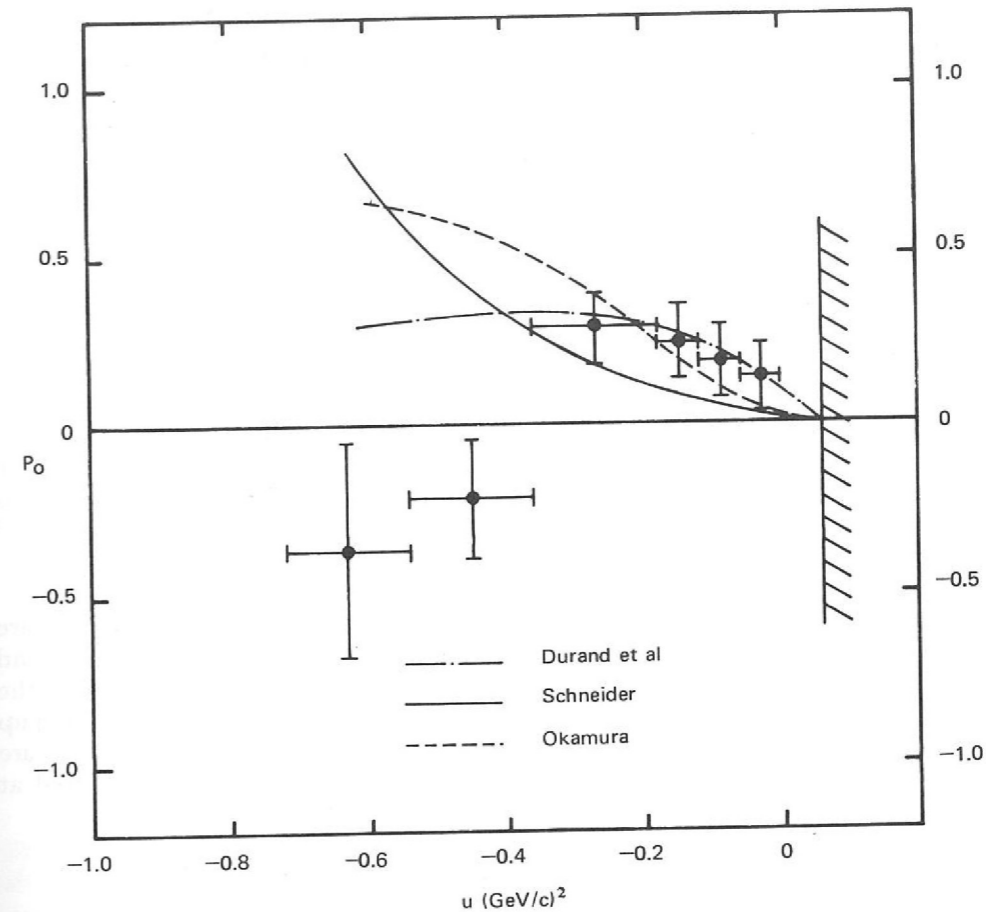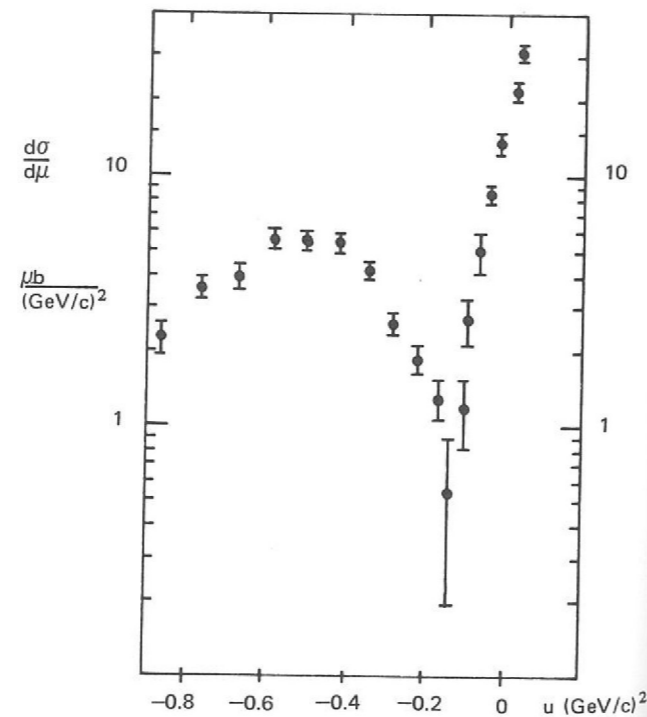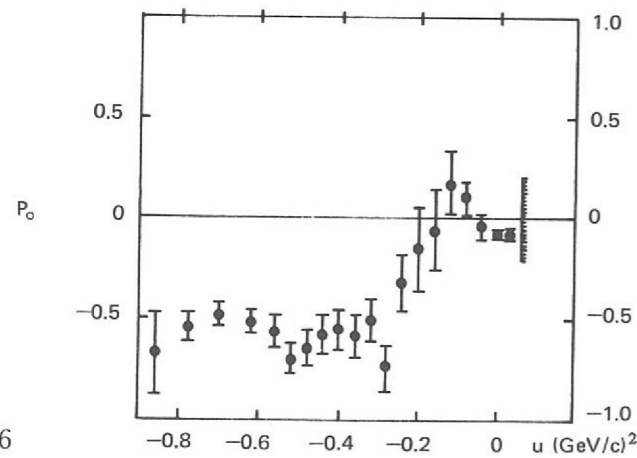
Figure 26. Measured polarization at 6 GeV/c from the analysis of about half the $\pi^- p$ elastic scattering data taken in Experiment 15. The curves are the theoretical predictions from three different models of $\pi^- p$ backward scattering.

The experiment uses arrays of plastic scintillator hodoscopes to record positions on the trajectories of the incident, forward scattered and backward scattered particle in the process $\pi^\pm p \to p\pi^\pm$. The elements of each hodoscope are typically 6 mm wide and over 600 photomultiplier tubes are used in the five large hodoscope arrays. The experimental layout is shown in Figure 24.

The experiment has been set up and run in the P4 beam of the CERN PS. By the end of 1971 about 10 weeks of data taking had been completed. The $\pi^+ p$ data has been completely analysed and a subset of the data already published. A total of about 15,000 elastic events have been recorded with $|u| < 1$ (GeV/c)².

Figure 25 shows the results of the differential cross-section and the polarization parameter in $\pi^+ p$ backward scattering from the complete data set. A small value for the polarization parameter can be observed in the region of the backward peak in the differential cross-section which goes to zero at the dip and then becomes large and negative beyond the dip in the differential cross-section. These results are consistent with the idea of N_α, Δ_δ exchange scattering with a dominant N_α trajectory.

The $\pi^- p$ data taking has still to be completed but 3000 events, representing about half the final data set, have been recorded and analysed. Preliminary results have been published and are shown in Figure 26. The striking feature of the data is its non-zero value at small $|u|$ values and a cross over from positive to negative polarization values at $|u| \sim 0\cdot4$ (GeV/c)². This data is in disagreement with simple Regge models having a single trajectory (Δ_δ) exchange which would predict zero polarization.

Experiment 16

UNIVERSITY OF ROME
RUTHERFORD LABORATORY

Study of the Production of Neutral K Meson Resonances

The object of this counter-spark chamber experiment is to study the peripheral production of neutral K*'s in the reaction:

$$\pi^- + p \rightarrow \Lambda^\circ + X^\circ$$
$$\downarrow\text{neutrals}$$
$$\downarrow p + \pi^-$$
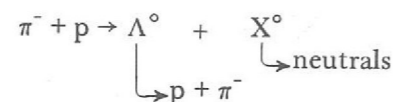
in the momentum interval 5 to 10 GeV/c. The experiment is planned to yield over 100,000 events in the mass range 1000 to 1800 MeV/c² with a mass resolution of ± 6 MeV. All the information presently available on the mass spectrum of the I = ½ strange mesons comes from bubble chamber experiments and consequently there is a limited number of events. There is considerable interest in both the mass range 1200 to 1350 MeV/c² (the Q region) and the range 1600 to 1800 MeV/c² (the L region).

By a system of veto scintillation and water Cherenkov counters, slow lambdas are selected in association with neutral K*'s. Measurement of the Λ° decay angles and the decay proton momentum, together with the momentum and direction of the incident π⁻, are sufficient to determine the mass of the missing system. Setting up is in progress at CERN. Range chambers to measure the decay proton energy are under construction. Film from the spark chamber system will be digitised at Rutherford Laboratory using HPD II. Data taking is expected during 1972.

Experiment 17

QUEEN MARY COLLEGE, LONDON
DARESBURY LABORATORY
UNIVERSITY OF PISA
UNIVERSITY OF MAINZ

The Pion-Nucleon Scattering Lengths

A precise measurement of πp scattering in the S wave at very low energies is of interest for the information it gives on long range nuclear forces due to exchange of two pions (σ exchange). Previous accurate experiments have been in the momentum range 100 to 400 MeV/c. The present experiment is aimed at providing a precise anchor point at zero energy.

The idea is to stop π⁻ in hydrogen or deuterium gas, when the π⁻ is eventually captured by a proton or deuteron, and cascades down through the Bohr orbits, emitting X-rays. The radius of the Bohr orbit in the ground state is 2×10^{-11} cm. The wave function of the pion overlaps the nucleus sufficiently to shift the ground state by 8 eV in the case of πp.

The X-ray emitted in the transition from the first excited state 2P to the ground state is observed. This X-ray is shifted from 2429 to 2437 eV in πp and is at 2595 ± 4 eV in πd: the uncertainty in the latter case arises from the present errors in the scattering lengths.

The apparatus is shown schematically in Figure 27. A π⁻ beam of 1.5×10^5/sec from the CERN Synchro-cyclotron is slowed down in a beryllium moderator inside the target containing gas at a pressure of 8 × atmospheric pressure. A counter 30 microns thick defines heavily ionising pions close to the end of their range. A veto counter almost completely enclosing the stopping region defines pions which stop. X-rays are measured in the proportional counter which views the target gas through a membrane 12 microns thick.
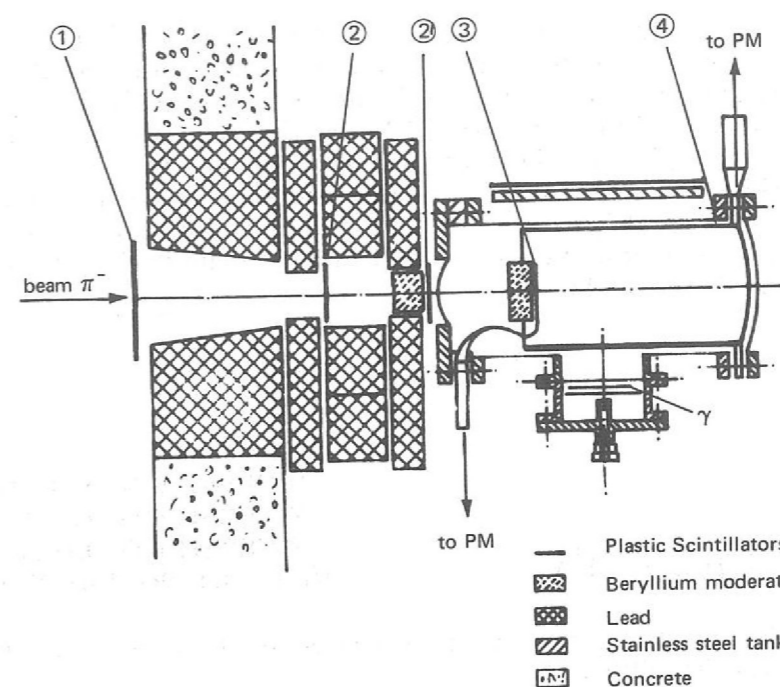
Figure 27. Schematic drawing of the apparatus for Experiment 17. 1, 2' and 3 are beam defining counters; 2 is a Cherenkov counter to veto electrons. 4 is the anti-coincidence shield inside the target vessel. γ is the proportional counter.

The first run took place in August and after a number of refinements to the electronics the spectrum of X-rays shown in Figure 28 was obtained from deuterium. This is the first item that π-mesic X-rays have been observed in deuterium. The experimental problem is that very few pions stop in the gas and counting rate is only 30 X-rays/hour. The signal/noise ratio is of paramount importance. Liquid hydrogen cannot be used because Stark mixing causes absorption of all the pions before they reach the 2P state.

Figure 28. π-mesic X-ray spectrum obtained from deuterium. (Experiment 17).
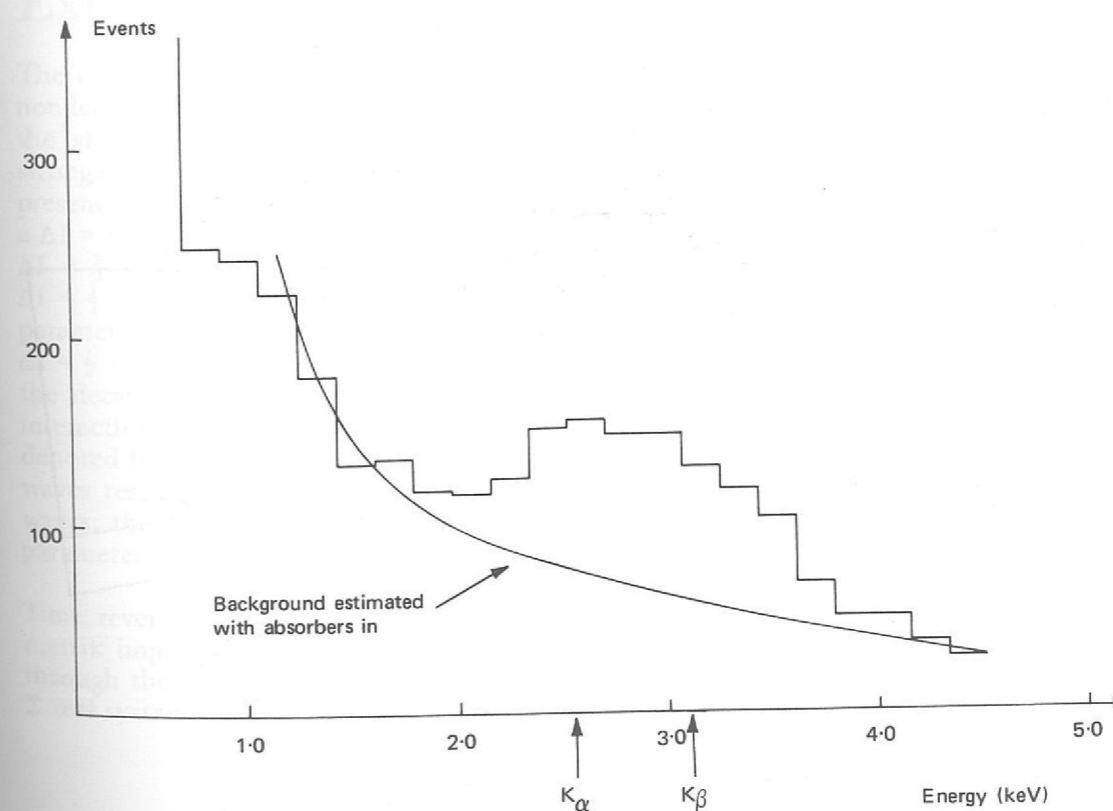
To establish the energy of the X-rays their absorption in a foil of Bismuth will be measured. Bismuth has a photoelectric absorption edge centred at 2603 eV and 20 eV wide. This absorption edge can be measured accurately by conventional X-ray techniques, and thus provides a delicate calibration of the energy scale of the X-ray. It is hoped that the energy of the X-ray can be measured to about $\pm$ 0·5 eV, which will give a factor of 8 improvement in the πd scattering length. Transitions to the πd ground state from higher excited states have energies $\geqslant$ 2·8 keV and are filtered out with a foil of Saran, containing Chlorine, which has a photoelectric K edge at 2820 eV.

Data taking will continue until April 1972.

CERN
UNIVERSITY OF STOCKHOLM
UNIVERSITY OF GENOA
UNIVERSITY OF BIRMINGHAM
RUTHERFORD LABORATORY

Experiment 18

The Line Reversal Reactions
$\pi^+ + p \to \Sigma^+ + K^+$
and $K^- + p \to \pi^- + \Sigma^+$
and other Two-Body Processes

The following two-body hypercharge exchange reactions will be studied at 10 GeV/c using the CERN PS

$$\pi^+ + p \to K^+ + \Sigma^+ \qquad (1 + 2 \to 3 + 4) \qquad (1)$$

and the line reversed reaction

$$K^- + p \to \pi^- + \Sigma^+ \qquad (\bar{3} + 2 \to \bar{1} + 4) \qquad (2)$$
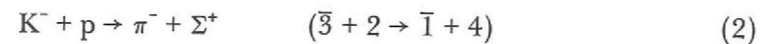
where $\bar{1}$ and $\bar{3}$ imply the anti-particles of 1 and 3 respectively in reaction (1).

Line reversal invariance requires equality of the differential cross-sections, and although separate measurements of these reactions at lower momenta have given indications of a breakdown of this invariance principle, there are large systematic uncertainties in the data.
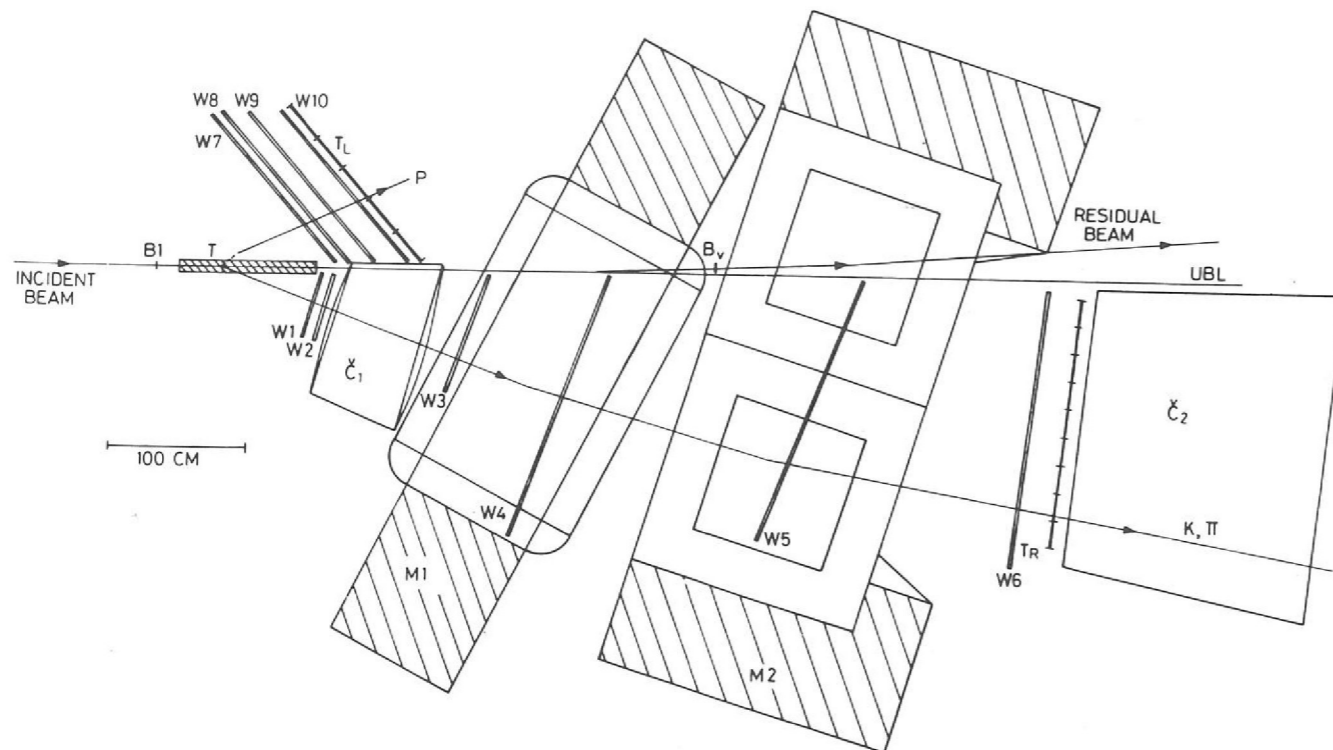
Figure 29. Schematic diagram of apparatus to be used in Experiment 18.

To reduce such systematic effects and to extend measurements to higher energies, this experiment proposes to measure both reactions in the same apparatus. This experimental equipment is designed to measure cross-sections out to large momentum transfers (t ~ -8 (GeV/c)^2). After scattering, the fast forward particles, namely K$^+$ for reaction (1) and π^- for reaction (2), are detected with scintillation (T$_R$) and Cherenkov counters (C$_1$ and C$_2$), and are momentum analysed in a magnetic spectrometer fitted with capacity read-out wire spark chambers (W$_1$-W$_6$). In addition the proton from the decay of the Σ^+ ($\Sigma^+ \to p + \pi^\circ$) is detected in the wire chambers, W$_7$-W$_{10}$. See Figure 29. This information will enable the determination of the Σ^+ polarization in the two reactions to be made, this being an important additional quantity, also related by line reversal invariance.

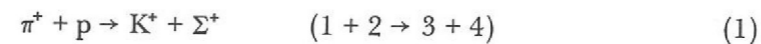Independent of the line reversal tests, it is necessary to obtain precise cross-section measurements for such two body reactions out to large t values, in order to complement the accurate data already existing for the elastic channels (πp, Kp, $\bar{p}$p, pp) in this energy region. These should be of value in assessing or formulating theoretical models for these processes (e.g. Regge pole, Regge cuts, etc).

Several other processes could be studied in the apparatus, in particular the two body coplanar reactions such as πp and Kp elastic scattering and $\bar{p}p \to X\bar{X}$ (where X = π, p, K). Another pair of related reactions which will be studied are

$$\pi^+ + p \to K^+ + \Sigma^+(1385)$$

and the line reversed reaction

$$K^- + p \to \pi^- + \Sigma^+(1385)$$
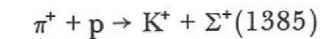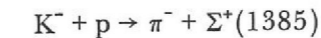
The experiment should be ready for installation in a beam at CERN by the end of 1972. The analysis of the data will mostly be done at the Rutherford Laboratory.

UNIVERSITY OF SUSSEX
WESTFIELD COLLEGE, LONDON
RUTHERFORD LABORATORY

Experiment 19

Test of the $\Delta I = \frac{1}{2}$
Rule in the Decay
$\Sigma^+ \to p\pi^\circ$
(ref. 193)

The current-current structure of the weak interaction Lagrangian, gives rise to non-leptonic $\Delta S = 1$ transitions with both $\Delta I = \frac{1}{2}$ and $\Delta I = \frac{3}{2}$. (ΔS is the change in the strangeness quantum number and ΔI the isotopic spin change.) There is strong experimental evidence for a $\Delta I = \frac{1}{2}$ selection rule. The only evidence for the presence of a $\Delta I = \frac{3}{2}$ amplitude comes from K$^+ \to \pi^+ \pi^\circ$ decay, which would require a $\Delta I = \frac{3}{2}$ amplitude that is $\sim$5% of the $\Delta I = \frac{1}{2}$ amplitude observed in K$^\circ_S \to 2\pi$. The $\Delta I = \frac{3}{2}$ may be suppressed for dynamical reasons or there may be an explicit $\Delta I = \frac{1}{2}$ selection rule in the weak interaction. The decay rates and asymmetry parameters of the non-leptonic sigma hyperon decays are sensitive tests of the $\Delta I = \frac{1}{2}$ rule. Angular momentum conservation in the decay $\Sigma \to N\pi$ requires that the decay nucleon and pion be in an S or P state; parity violation in the weak interaction allows a linear combination of these two states. The decays $\Sigma^- \to n\pi^-$ denoted by Σ^-_- and $\Sigma^+ \to n\pi^+$ (Σ^+_+) have been determined to be almost pure S and P waves respectively. The decay $\Sigma^+ \to p\pi^\circ$ ($\Sigma^+_\circ$) has approximately equal S and P waves; the exact ratio of S/P can be determined by measuring the asymmetry parameters α, β and γ in the decay of polarized sigmas.

Time reversal invariance and the requirement of unitarity in the π-N scattering matrix imply that β will be small. The Σ^+ polarization P$_\Sigma$ is readily observable through the up-down asymmetry of the decay proton angular distribution in the Σ rest system. The polarization of the proton is a function of P$_\Sigma$ and α, β and γ.

Polarized Σ^+ particles were produced by the reaction $\pi^+ p \to K^+ \Sigma^+$ using a separated π^+ beam of momentum 1·11 GeV/c incident on a target of liquid hydrogen. Thin foil spark chambers measured the direciton of the K^+ and the decay proton from $\Sigma^+ \to p\pi^\circ$, and the polarization and range of the proton were measured in a 60 gap aluminium spark chamber. The image of the spark chamber tracks were digitised on-line using a vidicon system.

From the observed scattering asymmetries in the aluminium range chamber a maximum likelihood method yielded the following result (assuming $\beta = 0$)

$$\alpha = -0.95^{+0.05}_{-0.04} \text{ and } \gamma = +0.32^{+0.14}_{-0.16}$$

This experiment yields the first umabiguous determination of the sign of γ.

Figure 30 shows that it is possible to fit simultaneously the S and P wave amplitudes for the Σ decays. The vectors should form a closed triangle in the (S, P) plane for a pure $\Delta I = \frac{1}{2}$ rule.

Figure 30. The $\Delta I = \frac{1}{2}$ rule for the Σ decays $\Sigma^+ \to p + \pi^\circ$ (Σ_0^+), $\Sigma^+ \to n + \pi^+$ (Σ_+^+) and $\Sigma^- \to n + \pi^-$ (Σ_-^-) requires a closed triangle for the S- and P-wave amplitudes of these decays. The present situation including the data from Experiment 19 is shown.
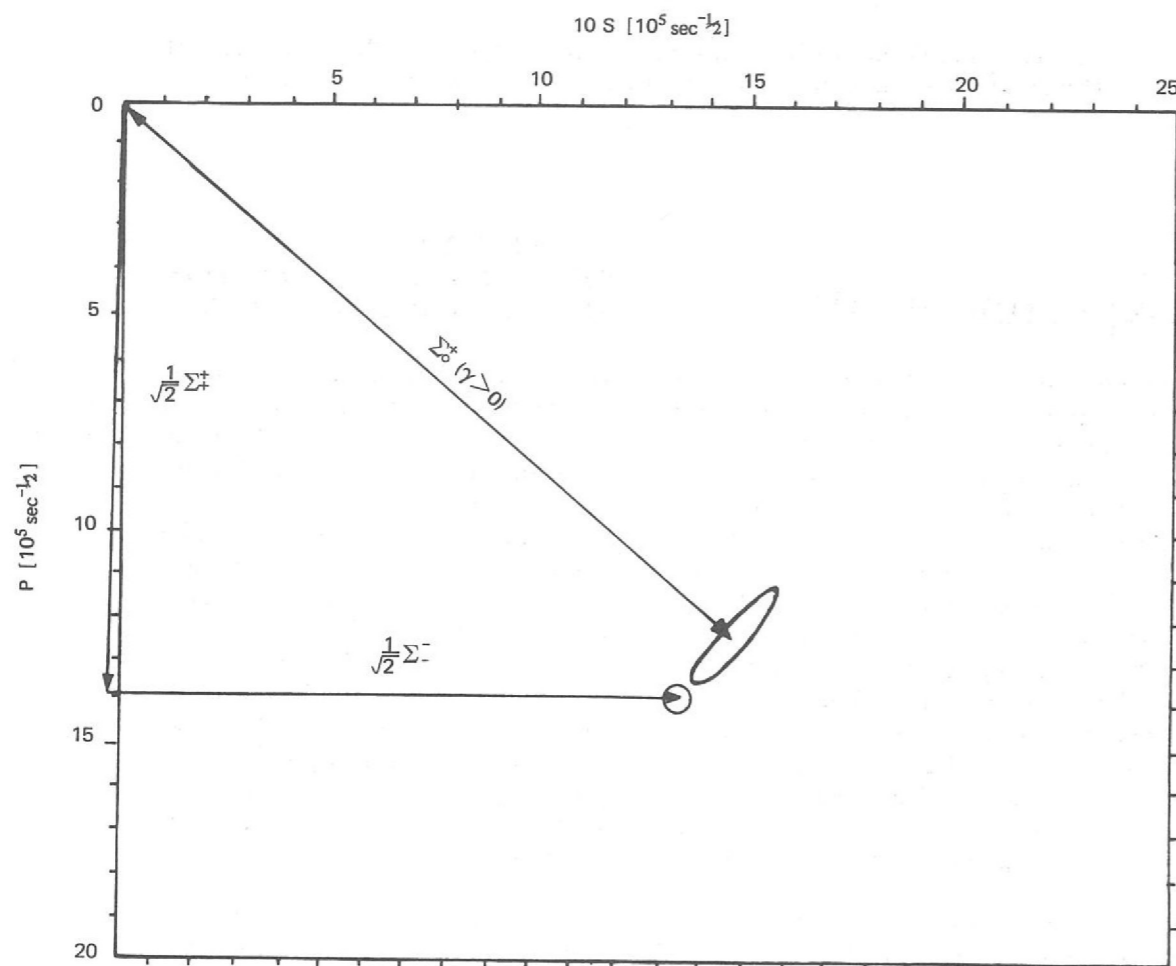
Experiment 20

UNIVERSITY OF CAMBRIDGE
RUTHERFORD LABORATORY

Test of the $\Delta S = \Delta Q$ Rule for K° Leptonic Decays

The present theory of weak interactions based on a current-current Lagrangian has had considerable success in predicting the properties of particle decays. One of its more fundamental consequences is the $\Delta S = \Delta Q$ rule which states that, in strangeness changing leptonic decays, the total change in strangeness (ΔS) is equal to the change in charge (ΔQ) carried by the strongly interacting particles.

The rule may be tested by studying the time dependence of the $K^\circ \to \pi^- e^+ \nu$ and $K^\circ \to \pi^+ e^- \bar{\nu}$ decay rates, from which the amplitude ratio

$$x = \frac{\Delta S = -\Delta Q \text{ amplitude (forbidden)}}{\Delta S = \Delta Q \text{ amplitude (allowed)}}$$

may be calculated. Many experiments have been performed to do this over the past decade, but the desired precision has been difficult to achieve.

This experiment obtained a large sample of $K \to \pi e \nu$ decays resulting from the decay of a pure K° state produced in the reaction $\pi^- p \to \Lambda K^\circ$ by 1·02 GeV/c pions incident on a polythene target. The Λ and K° decays were detected in optical spark chambers, and the electron from $K \to \pi e \nu$ decay identified by means of a threshold Cerenkov counter and steel plate spark chambers which induced shower formation.

Over 5,000 $K \to \pi e \nu$ events have been obtained in which the sign of the electron is known, and all these have been examined by physicists after measurement and kinematic fitting. In addition a number of $K^\circ \to \pi^+ \pi^-$ decays have been measured to provide a check on the Monte Carlo program which was used to calculate the detection efficiency of the apparatus. Satisfactory agreement was found between the observed and predicted Λ and K° lifetime distributions for these events.

In determining the detection efficiency for $K \to \pi e \nu$ decays, it was also necessary to take into account the effect of the Cerenkov counter. Internal checks have shown that this had a uniformly high efficiency for the sample of events from which a preliminary value of x has been calculated.

The chief sources of background in the experiment were $K^\circ \to \pi^+ \pi^-$ decay and $K^\circ \to \pi^\circ \pi^\circ$ decay followed by Dalitz decay, $\pi^\circ \to \gamma\, e^+ e^-$. Cuts on the data sample removed the majority of these events and a correction for the residual background was made in calculating x.

The preliminary result, based on two-thirds of the total data (1800 events after cuts), is

$$\text{Re } x = -0.14^{+0.08}_{-0.09}$$

$$\text{Im } x = 0.07 \pm 0.08$$

Although further investigation of the systematic errors is required this result provides no evidence for violation of the $\Delta S = \Delta Q$ rule.

Experiment 21

WESTFIELD COLLEGE, LONDON
UNIVERSITY OF SUSSEX
RUTHERFORD LABORATORY

Search for Charge Asymmetry in Eta Decay

This experiment is designed to look for a possible charge asymmetry in the decays of the eta meson

$$\eta \to \pi^+\pi^-\pi^° \qquad (1)$$

and also

$$\eta \to \pi^+\pi^-\gamma \qquad (2)$$

Such an asymmetry if it exists will show itself as an unequal sharing of the energy by the π^+ and π^- particles, studied statistically over a large number of events.

The π^+ and π^- are particle and antiparticle, and C symmetry requires that nature should treat them both with equal respect. Thus if:

N^+ is the number of times the π^+ is more energetic than the π^-, and

N^- is the number of times the converse is true, then C symmetry implies:

$$A = \frac{N^+ - N^-}{N^+ + N^-} = 0$$

The most recently published value for this quantity is:

$$A = 1\cdot5\% \pm 0\cdot5\%$$

for a measured sample of 36,000 η decay events. This is a result with three standard deviations of significance, and clearly requires confirmation.

Violation of C symmetry in this electromagnetic process — if it is confirmed — would have very important repercussions on the theory of electromagnetic interactions.

This experiment is a measurement of the possible asymmetry with ten times higher statistics. Construction of the apparatus was completed in September 1970 and data was collected in 1971. Some 6 million events were recorded on magnetic tape.

Data from the spark chambers which recorded the trajectories of the π^+ and π^- from the η decay was digitised by the TV camera system and transferred to an IBM1130 computer. This computer enabled a continuous watch to be kept on the quality of the data and all the fixed parameters of the experiment, and in turn transferred all events on to magnetic tape. Tapes were filled with 5,000 events at the rate of one tape every 2 hours. Analysis of the data is well under way and some typical kinematic plots are shown here. In Figure 31 the separation of η events from the
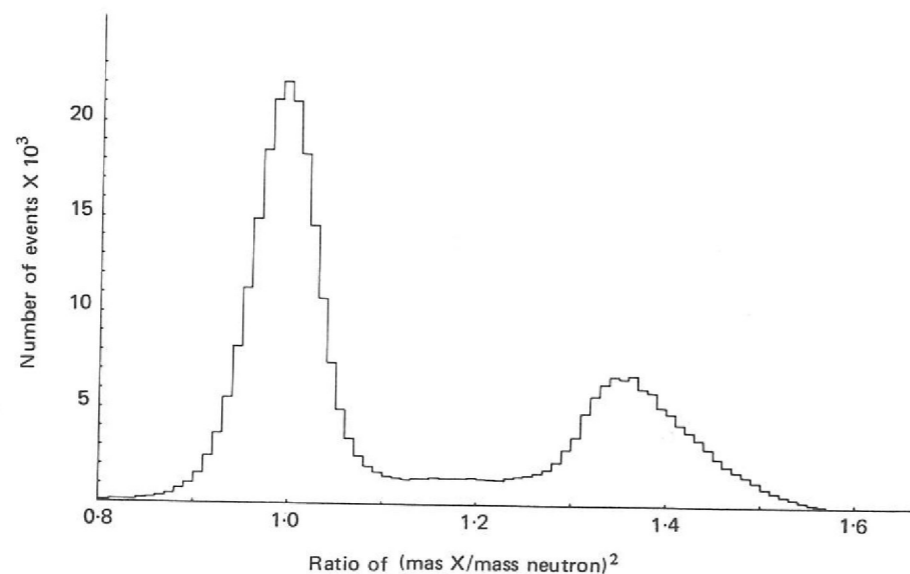
Figure 31. Plot of $[(\text{mass X/mass neutron})]^2$ where X is the total missing neutral mass in the reaction $\pi^-p \to \pi^+\pi^-X$ (Experiment 21).
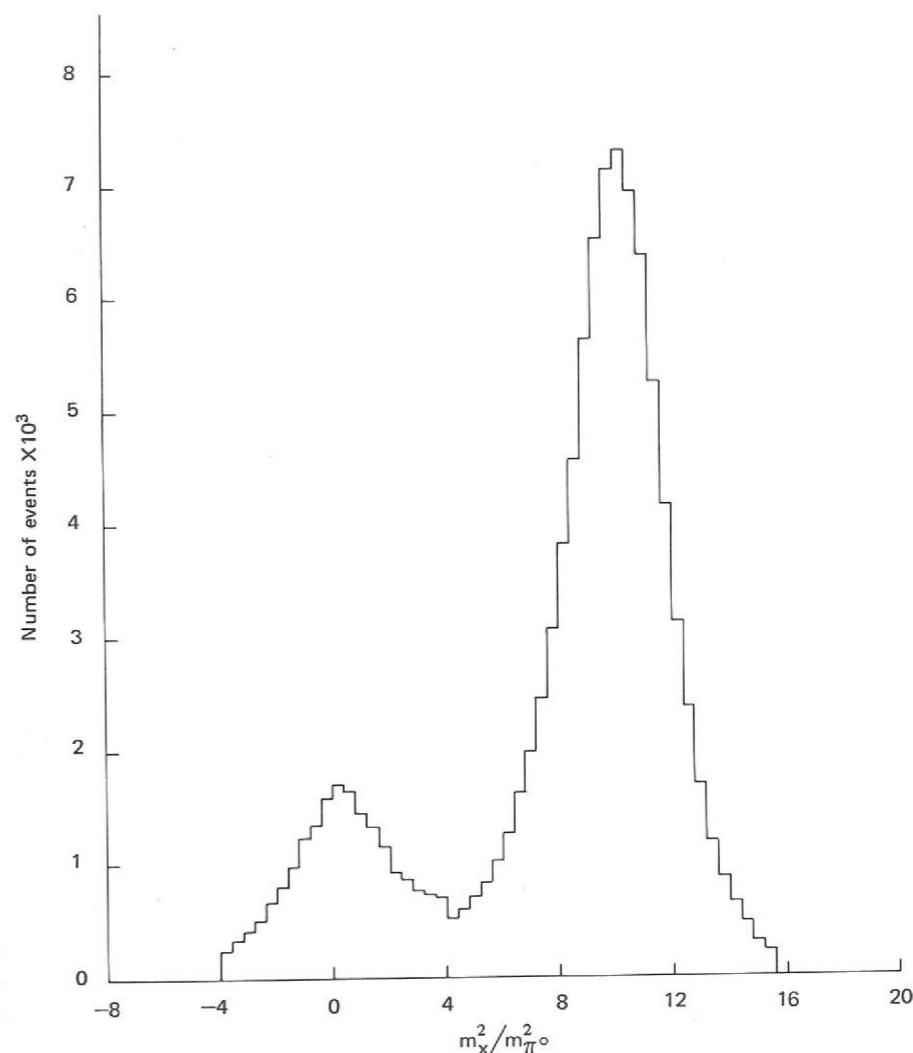
Figure 32. Missing Mass X in $\pi^-p \to n\,\pi^+\pi^-X$ (Experiment 21).

main background ($\pi^-p \to n + \pi^+ + \pi^-$) is obtained by plotting the missing mass to the two charged decay particles ($\pi^+ + \pi^-$) whose momenta are measured in the spark chambers inside the magnet. The background has a missing neutron only and hence gives a missing mass squared of 1 unit. The required events

$$\pi^-p \to n + \eta^°$$
$$\qquad\quad \hookrightarrow \begin{cases} \pi^+\pi^-\pi^° \\ \pi^+\pi^-\gamma \end{cases}$$

have a missing mass of two neutral particles $n + \begin{cases} \pi^° \\ \gamma \end{cases}$. The higher peak is essentially the $\eta \to \pi^+\pi^-\pi^°$ events and the flat region between the two peaks the $\eta \to \pi^+\pi^-\gamma$ events. By this means the eta events have been separated.

A further separation is obtained when the kinematic information on the detected neutron is used. In Figure 32 the missing mass to the $\pi^+ + \pi^- + $ neutron is plotted. In the case of process (1) a $\pi^°$ is missing and a peak occurs at $m^2 = m^2_{\pi^°}$. For process (2) a γ ray is missing and a peak indeed occurs at an m^2 of zero. It is seen that both kinematic tests are giving a clean and very satisfactory separation of the processes of interest. Final yields of the two decays of interest should be:

$$\eta \to \pi^+\pi^-\pi^° \qquad 350,000 \text{ events}$$
$$\eta \to \pi^+\pi^-\gamma \qquad 90,000 \text{ events}$$

Prior to publication of asymmetries for these two electromagnetic decays, a detailed study is being made of any possible geometric biasses in the apparatus. This study makes use of data runs in which the magnetic field was turned off. The straight particle tracks through the detectors are used to check the geometrical efficiency and reconstruction of events.

Experiment 22

WESTFIELD COLLEGE, LONDON
RUTHERFORD LABORATORY

*Search for the
C-Violating Decay
$\eta \to e^+e^-\pi^\circ$*

One way of looking for C violation (i.e. violation of charge conjugation invariance) in the electromagnetic interaction is to search for the decay $\eta \to e^+e^-\pi^\circ$. Estimates of the C-conserving two photon exchange rate yield a branching ratio of $\sim 10^{-9}$ compared with all η decay modes. This is far below present experiment accessibility. Thus observation of this decay must mean that the (e^+e^-) pair are in a C-odd (one photon) state and hence a violation of charge conjugation in η decay. In certain respects measurements of a non-zero rate is more favourable than measurement of a non-zero asymmetry in $\eta \to \pi^+\pi^-\pi^\circ$ since the decay is relatively insensitive to possible systematics in the apparatus. The basic problem is background reduction but once achieved the result is unambiguous.

The basic trigger for the $e^+e^-\pi^\circ$ decay remained the same as Experiment 21 but to identify the charged particles as electrons the top half of the decay spark chambers were backed up by gas Cerenkov counters. The primary requirement of these counters is that they have a low probability for detecting π's or μ's; their efficiency for electron detection is required to be well known rather than fully 100%. This led to the design of three relatively large counters filled with Freon 12 at one atmosphere and viewed radially by 32 RCA 4522 5 inch phototubes. The electron trajectories are relatively straight and radially directed outward (to $\sim \pm 20^\circ$) in this part of the magnet and since the Cerenkov light is emitted in a narrow forward cone a spatial requirement can be made to further supress randoms.

Another process under study with this detector is the C-allowed Dalitz decay $\eta \to e^+e^-\gamma$. The interest in this reaction is to determine the distribution of events as a function of the mass of the Dalitz pair and hence to measure the "timelike" form factor of the η.

Figure 33. A schematic diagram showing the electron Cherenkov counters over the decay spark chambers used in search for the $\eta \to e^+e^-\pi^\circ$ decay. (Experiment 22).
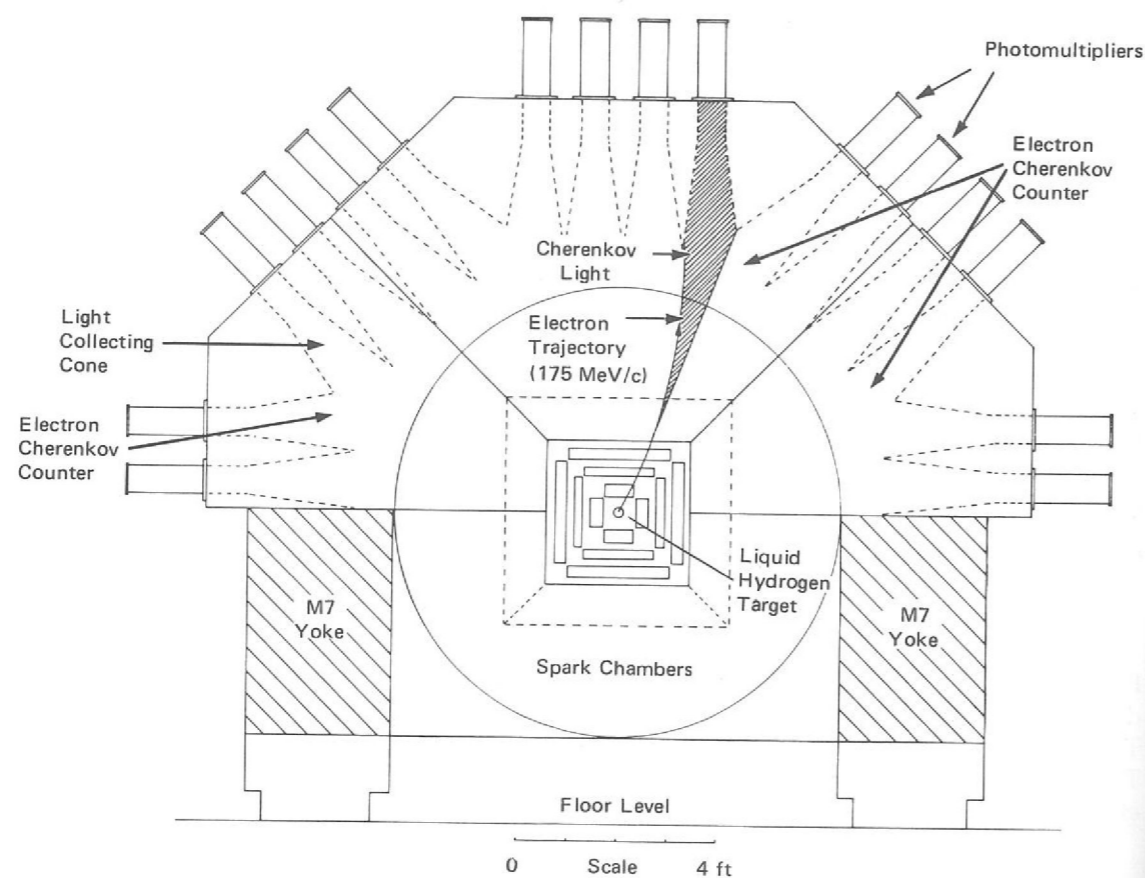
Dalitz decays or γ conversions are characterised by a peak at low opening angles and hence at low pair mass. Figure 34 shows such a plot for the raw data treating both charged particles as electrons. The first bin corresponds to a pair mass of ≤ 55 MeV and after further kinematic separation may be used to calibrate the efficiency of the counter for detecting electrons. Figure 35 shows the same data after requiring at least one electron tube to have fired and Figure 36 after a preliminary tube alignment is added.

Figure 34. Data from Experiment 22 analysed as $\pi^-p \to e^+e^-Xn$. All data
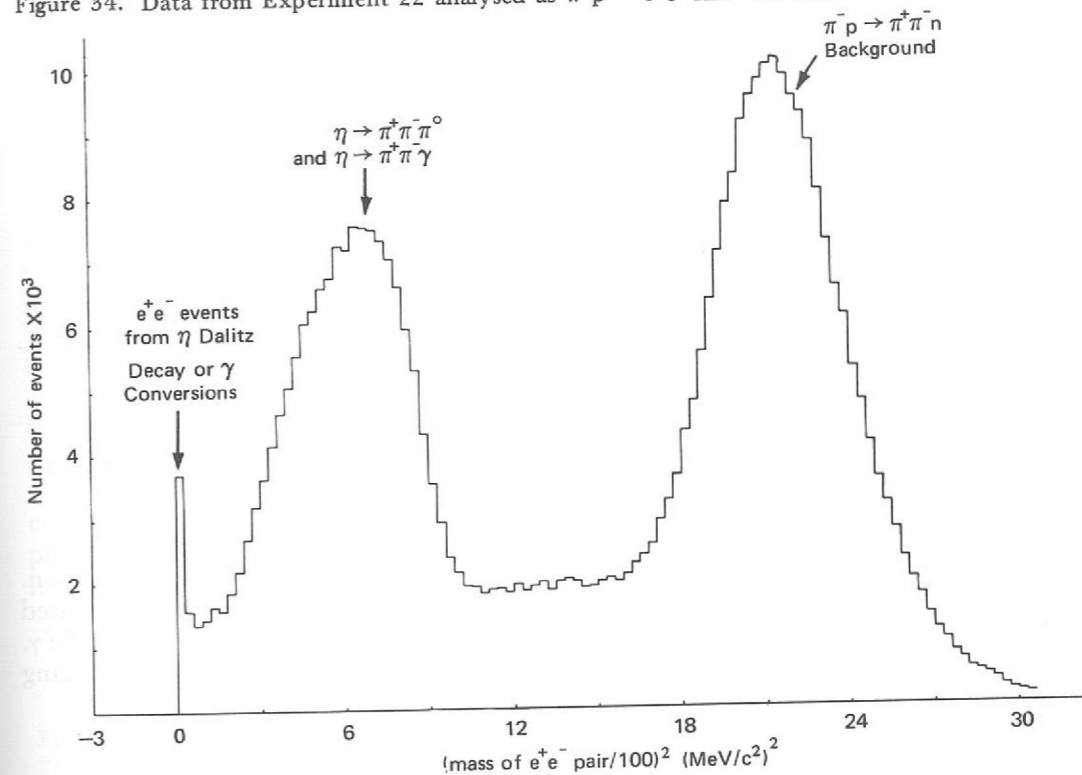
Figure 35. Data from Experiment 22 analysed as $\pi^-p \to e^+e^-Xn$ after demanding at least one Cherenkov tube to have fired.
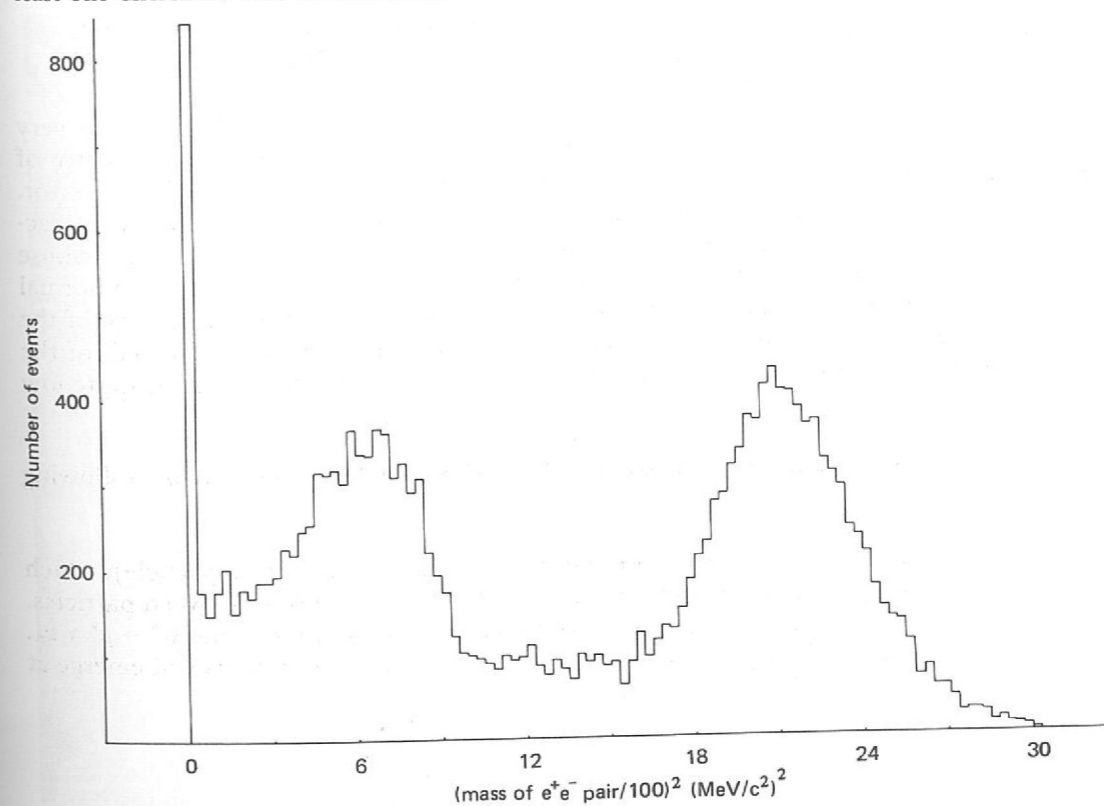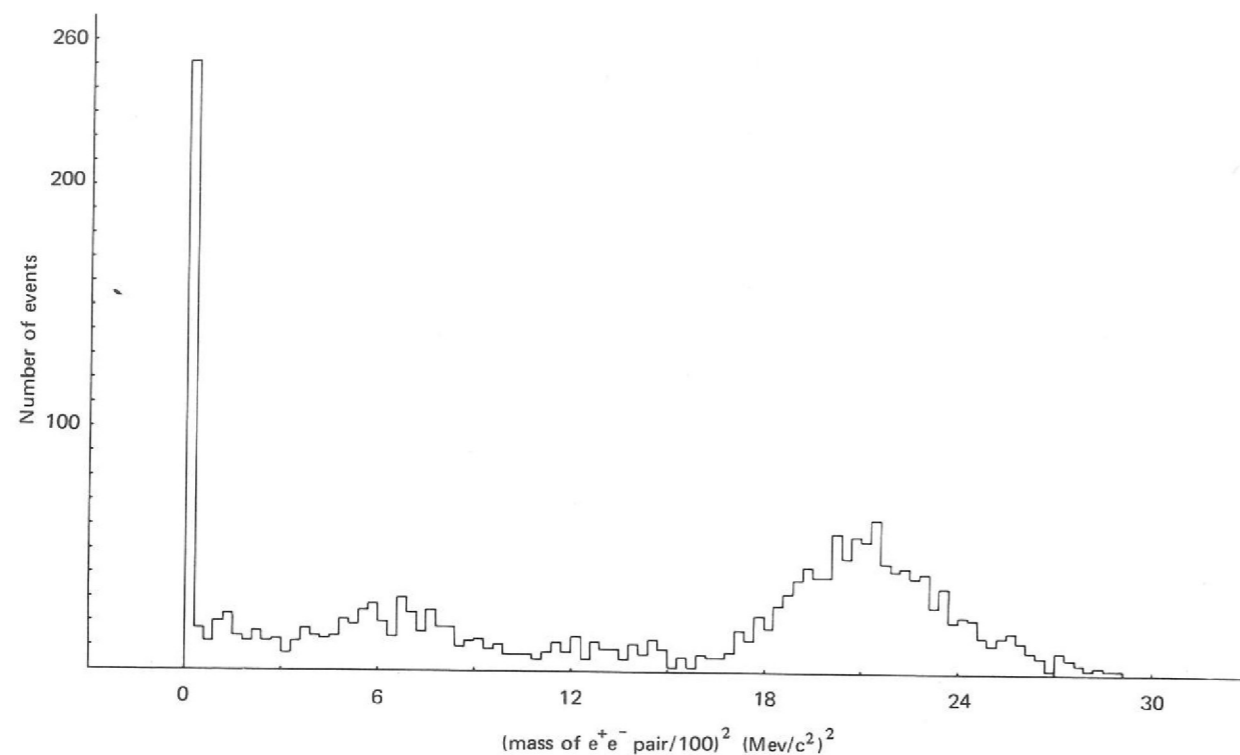
Figure 36. Data from Experiment 22 analysed as $\pi^- p \to e^+ e^- X n$ after demanding tube-track alignment.

A total of 3×10^6 triggers were taken with the Cerenkov counter in position. The present upper limit of 2×10^{-4} for the process $\eta \to \pi^\circ e^+ e^-$ leads to an estimated signal of 60 events with a background of less than 5%. For the reaction $\eta \to e^+ e^- \gamma$, with the pair mass >50 MeV, we expect 120 'useful' events (branching $\frac{\eta \to e^+ e^- \gamma}{\eta \to \pi^+ \pi^- \pi^\circ} = 6 \times 10^{-3}$).

Experiment 23

UNIVERSITY COLLEGE, LONDON
UNIVERSITY OF BRISTOL
UNIVERSITY OF LIVERPOOL
RUTHERFORD LABORATORY

ISR Search for the Intermediate Boson and other Massive Particles

The CERN Intersecting Storage Ring (ISR) facility came into operation very successfully during the course of 1971. The machine provides a total centre of mass energy of up to 56 GeV, equivalent to a 1600 GeV conventional accelerator. It is hoped that this machine will open a new 'window' into high energy interactions and, in particular, will allow the possibility of discovering particles whose mass is so large as to exclude their production at the energies available in normal accelerators. By the end of November 1971 the currents of protons in each of the storage rings had reached a level that was between one quarter and one half of the design value. Serious experimental measurements have begun, even for quite low cross-section processes.

The ISR experiment being carried out by this collaboration has the following objectives:

(a) The first aim is to search for the intermediate boson (or W particle), which has been postulated as the 'carrier' of the weak interaction between particles. The W is thought to decay into various leptonic modes, including $W^\pm \to \mu^\pm + \nu_\mu$. The suspected large mass of the W will mean that the muons will emerge at large angles with high momenta.

(b) Massive virtual γ-rays may be produced in electro-magnetic interactions and these will produce muon pairs whose mass spectrum will be observed.

(c) The experiment is one of a number around the ISR which will be carrying out a search for 'quarks'. These particles have been suggested as the constituents of baryons and mesons and are likely to have fractional charge and a high mass.

(d) Finally, the experiment aims to carry out a systematic measurement of the yields of strongly interacting particles, including their momentum spectra, over an angular range from 30° to 90° in the laboratory. These measurements are of intrinsic interest as tests of various models of high energy particle interactions and are also required for the detailed interpretations of the first three aims of the experiment.

The apparatus consists of two large detector systems. First, there is a large volume thick plate optical spark chamber system interleaved into an array of magnetized iron plates, for the identification of muons (in connection with aims (a) and (b) described above). This system, which occupies a volume of about $67m^3$ and weighs 300 tons, has been assembled on one side of Intersection Region 2 at the ISR, together with an array of approximately 100 mirrors. Scintillation counter banks are inserted into the spark chambers to provide a suitable trigger. Studies have already been carried out which have resulted in machine background triggers being reduced to a manageable level, so that the major contribution to unwanted triggers arises from the cosmic radiation. In January 1972 it is planned to install veto counters which will largely remove this source of background. In the meanwhile, preliminary data has been taken and some of the first film strips have been measured on the HPD II measuring machine at the Rutherford Laboratory.

Figure 37. A view of some of the apparatus at ISR Intersection 2 at CERN (Experiment 23). The equipment shown here was constructed in collaboration with a Scandinavian group and consists of a large movable arm carrying an arrangement of two magnets, eight scintillator hodoscopes and thirty-six magnetostrictive wire spark chamber planes. (CERN Photo).
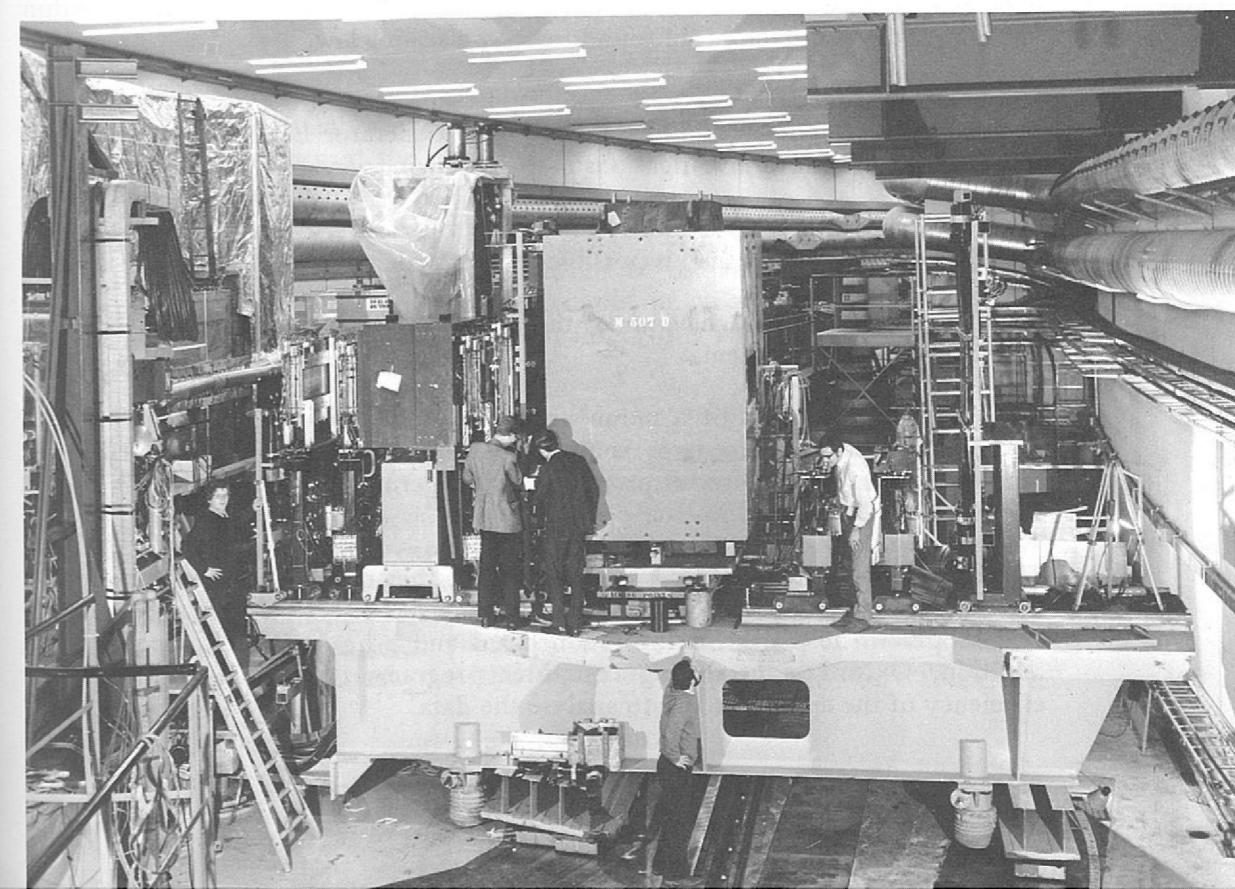
On the other side of Intersection 2, the wide angle spectrometer arm has been mounted and this forms the second detection system in the experiment (see Figure 37). This part of the equipment has been constructed in collaboration with a Scandinavian group at the ISR. The large moveable arm can carry various arrangements of detectors depending on whether high or low momentum measurements are in progress. The first arrangement that has been assembled consists of two magnets, eight scintillator hodoscopes and thirty-six magnetostrictive wire spark chamber planes. Two separate momentum measurements and four independent time-of-flight measurements are made on every particle and the pulse heights from each counter bank are noted. Particle identification is thus carried out with a high precision and it is hoped that any massive particles (e.g. quarks) will be detected down to a level of 1 in 10^9 of all particles produced. This arrangement is also suitable for the low momentum yields experiments, but for momenta above 2 GeV/c additional high pressure gas Cerenkov counters will be added and only the larger magnet will be used.

A considerable quantity of data has already been taken at a range of centre of mass energies, with the first arrangement on the arm, and the first analysis of the data indicates that the equipment is reliable. By early 1972 preliminary physics data should be available on the yields of particles at low momenta.

Experiment 24

UNIVERSITY OF OXFORD
UNIVERSITY OF CHICAGO
HARVARD UNIVERSITY

A Study of Inelastic Muon-Proton Scattering at NAL (USA)

The study of inelastic scattering of electrons on nucleons at the Stanford Linear Accelerator Centre has lead to the discovery of cross-sections greater than expected and with magnitudes suggestive of 'point-like' structures within nucleons. The form factors are found to obey a scaling law.

Muon inelastic scattering should explore the same structure and this experiment aims, by using a muon beam at the National Accelerator Laboratory at Chicago, to extend the Stanford investigations in the following ways:

(a) To investigate cross-sections and scaling over a very much wider range of kinematic variables than is possible at Stanford.

(b) To investigate the behaviour of the cross-sections in various channels of the hadronic recoil system.

The equipment consists of a muon beam adjustable from 50 to 200 GeV/c, a liquid hydrogen target, a large analysing magnet and various detectors for the scattered muon and the recoil products. The experiment is scheduled to begin on 5th July, 1972.

The University of Oxford, supported by the Rutherford Laboratory, is designing and building three large scintillator hodoscopes in the detection system, six smaller hodoscopes to be placed in the muon beam and a beam Cerenkov counter. In addition, Oxford is producing computer programs to predict the detection efficiency of the apparatus and to analyse the data.

Bubble Chamber Experiments

The bubble chamber technique continues to supply a large part of the data used by high energy physicists in their efforts to understand the interactions of elementary particles. The Rutherford Laboratory is supporting a varied programme of projects in bubble chamber physics, involving physicists both from within the Laboratory and from outside institutes and universities. The progress achieved in 1971 relates both to the development of new techniques in bubble chamber physics, as well as to the increasingly efficient analysis of film taken in conventional bubble chamber experiments.

Technical Developments

The year's most significant advance in bubble chamber technology came in November with the successful operation of the neon-hydrogen track-sensitive target in the 1·5 m bubble chamber. The design of the target and an account of its development are described in detail in pages 116-117 of this report. The importance of this achievement, for the experimental physicist, lies in the fact that a new class of reactions, namely those containing several photons in the final state, have become accessible to investigation using bubble chambers. The chamber was expanded 200,000 times in the successful run in November-December; during this period 65,000 pictures — the first part of 250,000 approved — were obtained with a 4 GeV/c π^+ beam and these are being used for physics analysis.

A second development which has extended the range of reactions accessible by the bubble chamber technique was the successful operation in July of a lambda hyperon ($\Lambda^°$) beam for the 2 m chamber at CERN. A high field pulsed magnet designed at the Rutherford Laboratory was used to deflect charge particles out of the beam, and allow the short-lived neutral $\Lambda^°$ particles into the chamber to produce hyperon-nucleon interactions before their decay. A total of 350,000 pictures were taken for Experiment 38 and a test was conducted on the feasibility of running with a Σ^- beam; thus a detailed study of the hyperon-nucleon interaction is becoming possible.

Bubble Chamber Experiments

Turning to the analysis of more conventional experiments, Table 5 shows a list of all the bubble chamber experiments being undertaken or supported by the Rutherford Laboratory at the present time, together with an indication of their status and of the groups involved.

Most of these experiments are investigations of the strong interaction, both in a continuing search for new resonances and in an attempt to elucidate the mechanism of the interaction. The most interesting results are described briefly in this summary.

The K^-p survey experiment (Experiment 25) represents a very thorough search for baryon resonances with strangeness quantum number $-$ 1, called Y*'s or hyperon resonances, and in the last year the phase shift analysis technique used in this experiment has been extended to allow analysis not only of pure two-body final states (such as $\Lambda\pi$), but also of quasi two-body final states (such as $\Lambda\omega$) where either or both particles may themselves be resonances, detected by their decay to more stable particles. These states carry an intrinsically richer information content and exploitation of this fact has led to the discovery of two new Y* resonances.

Table 5

Bubble Chamber Experiments

Expt. No.	Reaction	Momentum range GeV/c	Team	No. of pictures × 10⁶	Status
25	K⁻p	1·25 to 1·85	College de France Saclay Strasbourg Rutherford Laboratory	1·65	Analysis
26	K⁻p	0·96 to 1·36	Rutherford Laboratory	0·43 at CERN	Analysis
27	p̄p	1·23 to 1·43	Univ. of Liverpool Rutherford Laboratory	0·1 at CERN	Analysis
28	K⁻p	14·25	Ecole Polytechnique Saclay Rutherford Laboratory	0·8 at CERN	Analysis
29	π⁺d	4·0	Univ. of Birmingham Univ. of Durham Rutherford Laboratory	0·42 at CERN	Analysis and data taking
30	π⁺p	0·8 to 1·6	Univ. of Cambridge Imperial College Westfield College	0·42	Analysis
31	K⁻d	1·45 and 1·65	Univ. of Birmingham Univ. of Edinburgh Univ. of Glasgow Imperial College	0·71	Analysis
32	K⁺p	2·1 to 2·9	Saclay College de France Imperial College Westfield College	0·21	Analysis
33	K⁺d	2·2, 2·45 and 2·7	Imperial College Westfield College	0·75	Analysis
34	np	1·0 to 3·5 1·0 to 8·0	Univ. of Cambridge	0·09 0·11	Analysis Analysis
35	K⁻ in heavy liquid	2·2	Univ. College Univ. of Brussels CERN Tufts University	0·68	Analysis
36	Electromagnetic Processes		Univ. of Cambridge	0·29	Analysis
37	π⁺p in neon-hydrogen track sensitive target	4·0	Univ. College Univ. of Durham CERN Rutherford Laboratory	0·06	Development and data taking
38	Hyperon Interactions	10 to 20	Univ. of Cambridge	0·35 at CERN	Data taking and Analysis
39	K°L decays and Interactions	0·4 to 0·85	Univ. of Bologna Univ. of Edinburgh Univ. of Glasgow Univ. of Pisa Rutherford Laboratory	To be taken at CERN	Approved proposal

On the other hand, the search for direct channel boson resonances remains elusive: an investigation of p̄p annihilations into π or K mesons over a range of energies, Experiment 27, reports no evidence for formation of a resonance in the mass region around 2200 MeV/c² where existence of the T meson has been claimed.

An unusual effect has been observed in a K⁻ experiment in the heavy liquid bubble chamber (Experiment 35): looking at events with two Λ° decays in the final state, a resonant-like enhancement in the Λ-Λ system is observed. Up to now this has been the subject of very few investigations.

A very interesting result has been observed in Experiment 28. The exponential decrease in cross-section with incident energy for the reaction K⁻p → K*p, observed in lower energy experiments, cannot be extrapolated to their result at 14 GeV/c; instead, there appears to be a flattening-off of the cross-section in this high energy region.

At somewhat lower energy, a collaboration of several university groups is conducting a large-scale analysis of the K-nucleon system. This study has led to new results on cross-sections and on certain final states in K⁻d interactions in the 1-2 GeV/c region (Experiment 31), while the study of K⁺p interactions from 2-3 GeV/c (Experiment 32) has been completed.

Data Processing

During 1971 the Rutherford Laboratory bubble chamber group has processed data obtained from exposures in three high statistics experiments in the 2 m chamber at CERN. These are the 14 GeV/c K⁻p experiment, mentioned above, with 800,000 pictures, of which 400,000 were taken during the year; the new K⁻p survey experiment (Experiment 26), which, with 430,000 pictures, forms a continuation of the K⁻p study started with Experiment 25; and a 4 GeV/c π⁺d experiment for which 420,000 pictures have already been taken, and a further 400,000 are expected in 1972.

It is clear that a powerful data reduction system is necessary to cope with data on this scale. In 1971 the system of twelve measuring machines connected to an IBM 1130 computer, which was set up in the previous year, has produced a consistently high flow of digitised events ready for precision automated measurement on the flying spot digitiser (HPD). Figure 38 is a histogram of the number of events digitised per week, with entries for 37 weeks during 1971. The average is over 8,000 events per week, double the rate of the previous year. Further improvements in this rate are expected early in 1972 when a new multiplexor designed at AERE, Harwell, with interfaces designed at the Rutherford Laboratory,

Figure 38. Histogram of the number of events digitised per week.

52

53
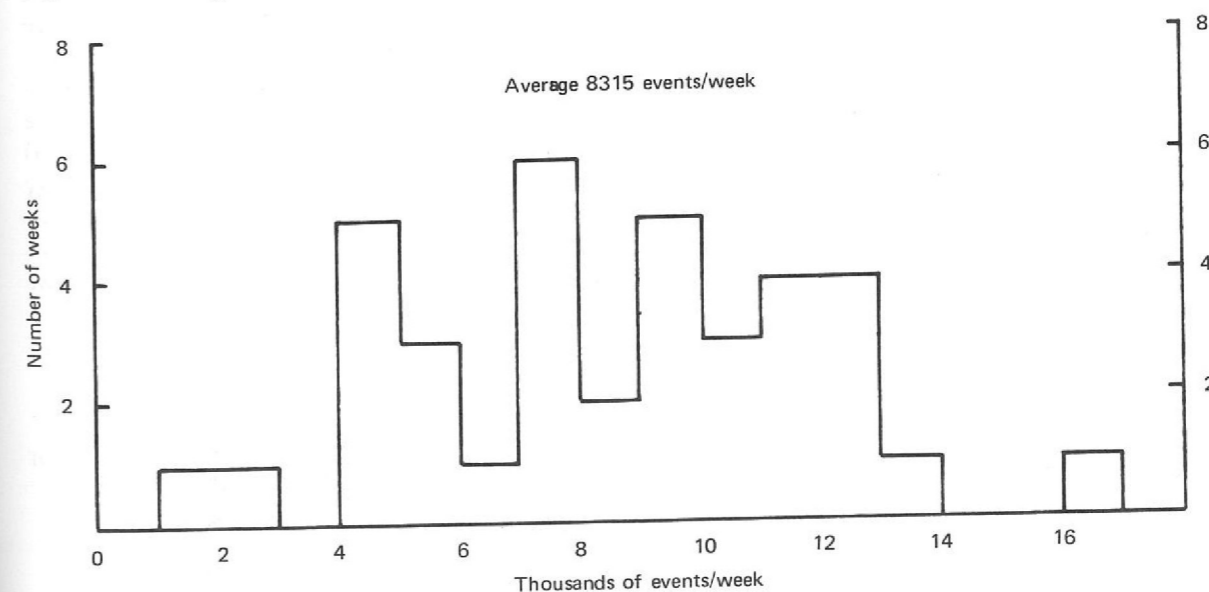
will be connected between the IBM 1130 and peripherals of the IBM 360/195, the Laboratory's central computer. This will permit much faster transfer of data between these two computers and thus reduce the main cause of delay in the present system.

After pre-digitisation, events are measured on the HPD. With over 300,000 events measured in 1971, the HPD has had a very successful year's running; details of its performance are given in pages 177-178 of this report.

The two film plane measuring machines which were acquired in 1970 for measurement of events which prove difficult on the HPD are being connected to a PDP8L computer. The system developed for them will include machine controlled track prediction, so that manual intervention during measurement will be minimal.

The group is looking ahead to receiving film from the 3·5 m European bubble chamber (BEBC) being assembled at CERN. Two BEBC scanning tables have been ordered for delivery in 1972 and they will be incorporated in the IBM 1130 system to pre-digitise film for measurement on the HPD.

COLLEGE DE FRANCE
CEN, SACLAY
UNIVERSITY OF STRASBOURG
RUTHERFORD LABORATORY

Experiment 25

K^-p Interactions in the Centre of Mass Energy range 1915-2168 MeV (ref. 19, 20, 51, 92, 132)

The K^-p system in the centre of mass energy range 1915 to 2168 MeV is being studied in terms of the formation of resonances in the s-channel. 1,650,000 pictures were taken at 13 equally spaced incident beam momenta in the range 1·263-1·843 GeV/c in the Saclay 180ℓ bubble chamber at Nimrod. Approximately 150,000 events have been measured.

Emphasis has now shifted from the study of genuine two-body reactions such as $K^-p \to \bar{K}N$, $\Lambda\pi$, $\Sigma\pi$ to the analysis of the large number of quasi two-body states such as

$$K^-p \to \Lambda\omega \qquad (1)$$
$$\to K^*(890)N \qquad (2)$$
$$\to \Sigma(1385)\pi \qquad (3)$$
$$\to \Lambda(1510)\pi \qquad (4)$$
$$\to \bar{K}\Delta(1236) \qquad (5)$$

found in the three and four body final states $K\pi N$, $\Lambda\pi\pi$, $\Sigma\pi\pi$, $\Lambda\pi\pi\pi$. Dalitz plot analyses are under way in all these channels in order to measure the relative fractions of the various final states as a function of total centre of mass energy. Hopefully resonant effects in these channels will show up as bumps in the cross-sections for the reactions. As an example Figure 39 shows Dalitz plots for the reaction $K^-p \to K^-p\pi^\circ$. Strong bands corresponding to $K^*(890)$, $\Delta(1236)$ and $\Lambda(1520)$ production can be observed. By fitting the distribution of events on the plot by the maximum likelihood method, and including the effects of the decay angular distribution of the resonances and interference between the resonances, the cross-sections for the production of these resonances can be determined. Figure 40 shows the cross-sections for the reactions:

$$K^-p \to K^{*-}(890)p \qquad (6)$$
$$K^-p \to K^{*\circ}(890)n \qquad (7)$$

obtained from the final states $K^-p\pi^\circ$ and $K^\circ p\pi^-$ for reaction (6) and $K^-\pi^+n$ for reaction (7).

It can be seen from Figure 40 and from Figures 41 and 42 which show mass plots for $\Lambda\pi$ combinations from the $\Lambda\pi\pi$ final state and the $\pi^+\pi^-\pi^-$ from the $\Lambda\pi^+\pi^-\pi^-$ final states respectively that reactions (1) to (3) are very strongly and cleanly produced. It has thus been found possible to obtain samples of sufficient size and purity to perform partial wave analyses of these reactions. The application of the partial wave analysis technique to the quasi two-body reactions listed above has a greater advantage over its use in normal two-body reactions such as $K^-p \to \Lambda\pi^\circ$: one can obtain information about the partial wave amplitudes not only from the differential cross-sections and hyperon polarization, but also from the angular correlation in the decay products of the resonances e.g. ω, $K^*(890)$ which are produced. As an example, a single event in the $\Lambda\omega$ final state (reaction 1) supplies six times as much information as one from the final state $\Lambda\pi^\circ$.

The partial wave analysis of the $\Lambda\omega$ channel is complete. The branching fraction of the $\Lambda(2100)$ into $\Lambda\omega$ has been measured to be $(1\cdot0^{+3\cdot0}_{-0\cdot5})$% and two new resonances of mass 1950±30 and 2000±50 have been observed. The preferred spin parities of these two states are D_3 and F_5 respectively but other assignments cannot be ruled out. The Argand diagram for the best fit to the data including these resonances is shown in Figure 43. Preliminary results are also available from the partial wave analysis of $K^*(890)N$ and $\Sigma(1385)\pi$. Table 6 gives the values of the square root of the elasticity times the branching fraction into the given channel for the $\Lambda(2100)$ and $\Sigma(2030)$ and $K^*(890)N$, $\Sigma(1385)\pi$ and $\Lambda\omega$.

Table 6

	$K^*(890)N$	$\Sigma(1385)\pi$	$\Lambda\omega$
$\Lambda(2100)$	$0\cdot25 \pm 0\cdot05$	not observed	$0\cdot06 \pm 0\cdot04$
$\Sigma(2030)$	$0\cdot10 \pm 0\cdot05$	$0\cdot12 \pm 0\cdot03$	—

These are in good agreement with SU(3), which predicts the absence of the $\Sigma(1385)\pi$ decay mode of the $\Lambda(2100)$ and a value of $\stackrel{\sim}{\sim}\frac{2}{1}$ for the ratio

$$\frac{\Lambda(2100) \to K^*(890)N}{\Lambda(2100) \to \Lambda\omega}.$$
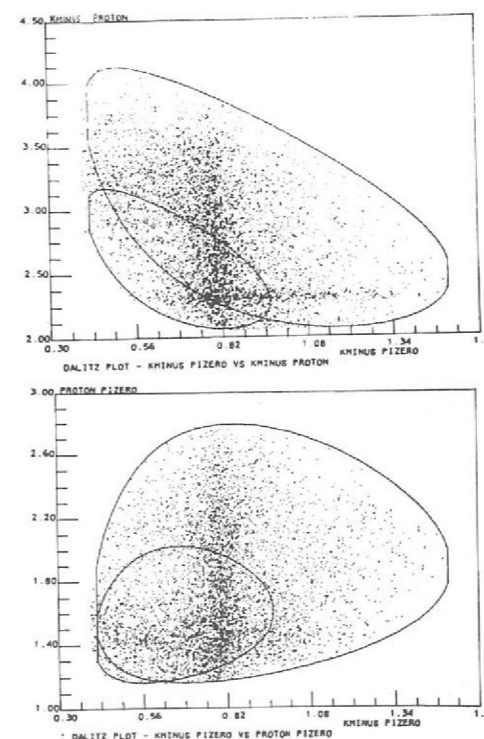
Figure 39. Dalitz plots for the reaction $K^-p \to K^-p\pi^\circ$ with incident K^- momenta in the range $1.26 - 1.84$ GeV/c. (Experiment 25).
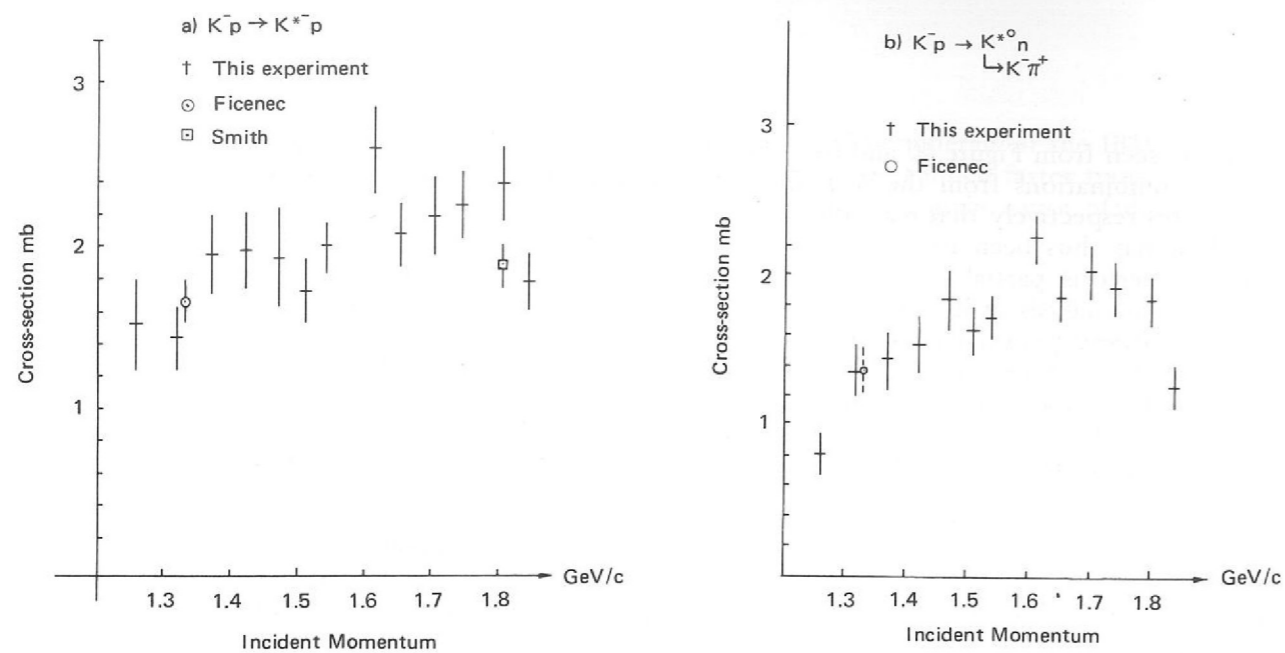
Figure 40. Variation of cross-section with incident momentum for reactions (6) and (7). (Experiment 25).
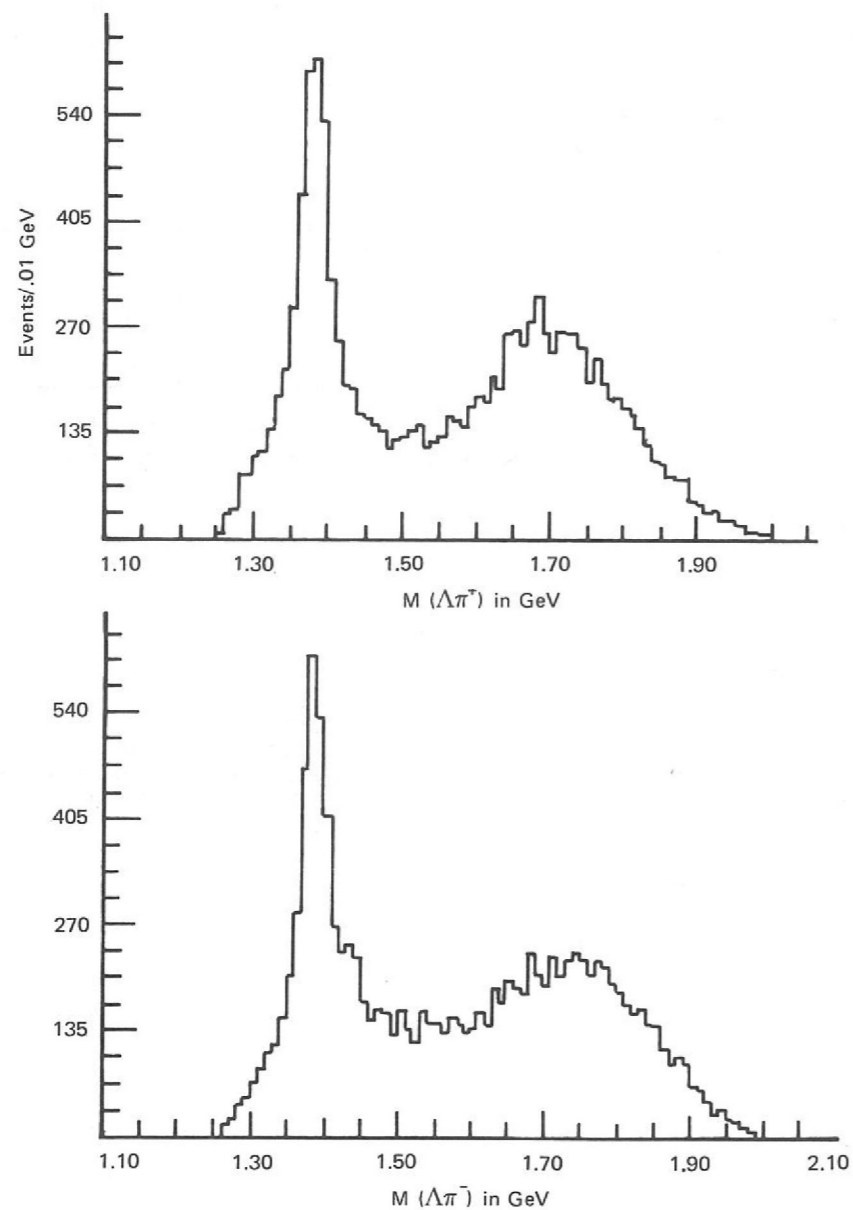
Figure 41. Invariant mass distributions $M(\Lambda^\circ\pi^+)$ and $M(\Lambda^\circ\pi^-)$ from the reaction $K^-p \to \Lambda^\circ\pi^+\pi^-$ with incident K^- momenta in the range 1.26 to 1.84 GeV/c. (Experiment 25).
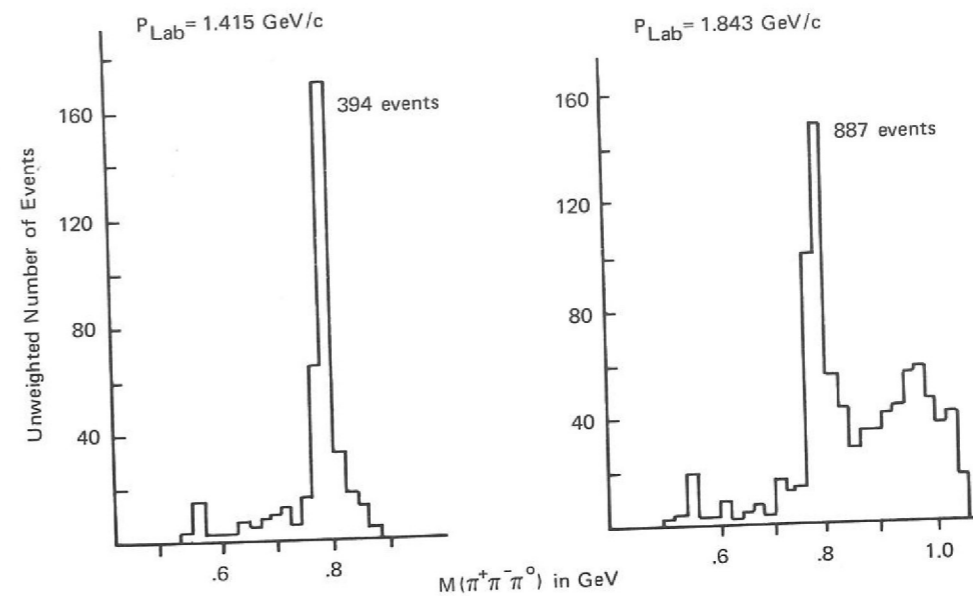
Figure 42. Invariant mass distributions $M(\pi^+\pi^-\pi^\circ)$ from the reaction $K^-p \to \Lambda^\circ\pi^+\pi^-\pi^\circ$ at various K^- momenta. (Experiment 25)
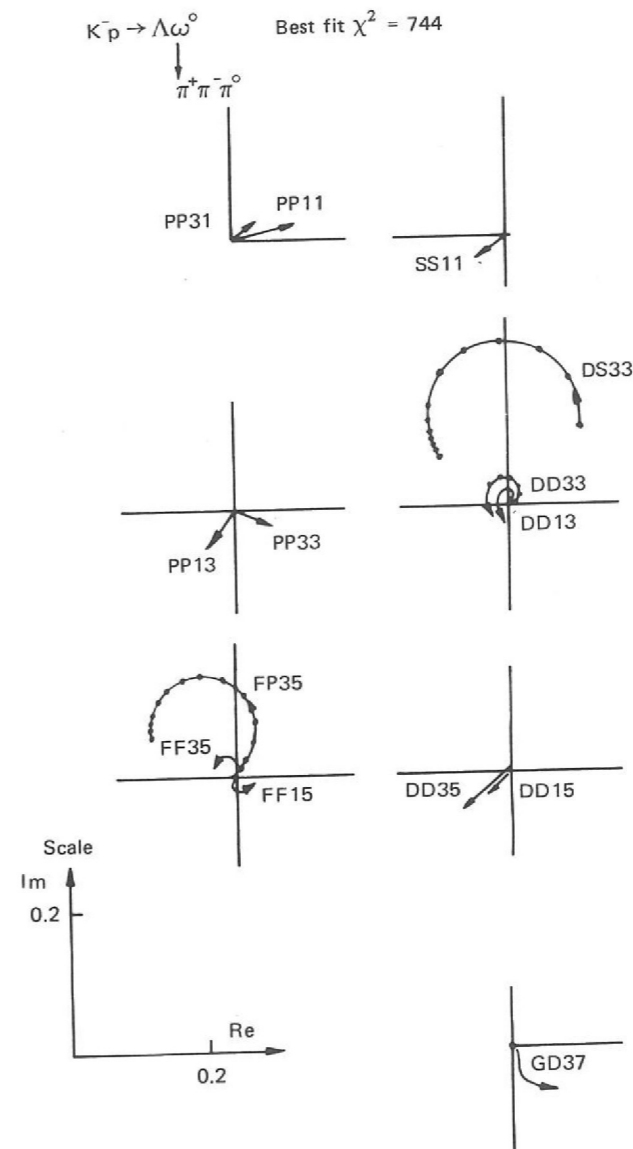
Figure 43. Argand diagrams for the partial wave amplitudes corresponding to the reaction $K^-p \to \Lambda^\circ\omega^\circ$. (Experiment 25).

Experiment 26

K⁻p Interactions in the Centre of Mass Energy Range 1775-1960 MeV

Very high statistics K⁻p formation experiments are now required to resolve the ambiguities in the partial wave analysis which extends over the range from threshold to 2·0 GeV/c. This experiment covers the momentum range 1·0-1·4 GeV/c and will provide a uniform distribution of events within this region. Approximately 300,000 events have now been measured from the 420,000 pictures taken in the CERN 2 m hydrogen bubble chamber, and the measurement will be completed by the summer of 1972. The number of events in any channel in this experiment will be a factor four greater than that in previous experiments.

Experiment 27

p̄p Annihilations into Two Charged Particles with Centre of Mass Energies in the Region of 2200 MeV.
(ref. 5, 176)

The two prong annihilation channels of the p̄p interaction in the cm energy range 2150 to 2240 MeV are being studied. This range approximately covers the width of the isospin-one structure seen in the NN total cross-section at 2190 MeV and contains the T-meson observed in the CERN missing mass spectrometer experiment. The film was taken using the CERN 2 m bubble chamber with four antiproton momentum settings centred at 1·23, 1·30, 1·36 and 1·43 GeV/c. A total of 75,000 two prong events were measured by the HPD of which about half are annihilations. The events were analysed through the standard Rutherford Laboratory geometry and kinematics programs.

$\bar{p}p \rightarrow \pi^+\pi^-$ and $\bar{p}p \rightarrow K^+K^-$. The cross-sections measured for these reactions are shown in Table 7. They fall rapidly with beam momentum and, when taken in conjunction with results at neighbouring momenta, show no obvious structure in the T-meson region. The centre of mass angular distributions are shown in Figure 44. None of the coefficients of the Legendre polynomial expansion for the di-pion final state show any structure which could be attributed to the narrow T-meson.

$\bar{p}p \rightarrow \pi^+\pi^-\pi^\circ$. The amount of di-pion resonance production in this channel was determined by a maximum likelihood fit to the Dalitz plot density distribution. The results are shown in Table 7 from which it can be seen that ρ and f° production account for almost half of the channel. Again, there is no striking evidence of direct channel effects.

$\bar{p}p \rightarrow \pi^+\pi^-$ + neutrals. The majority of two prong annihilations occur with more than one accompanying neutral. The ρ contributes to this channel but to a much smaller extent than in the three pion final state. Those events which fitted to the $\pi^+\pi^-\eta$ hypothesis showed some indication of a small enhancement in the $\pi^\pm\eta$ mass spectrum at the δ mass.

Figure 44. Centre of mass angular distributions for the reactions $\bar{p}p \rightarrow \pi^+\pi^-$ and $\bar{p}p \rightarrow K^+K^-$ shown as a function of the laboratory momentum of the incident $\bar{p}$ in the range 1.23 GeV/c to 1.43 GeV/c. (Experiment 27).

Table 7

p̄p Annihilation Cross-Sections

Momentum	1·23 GeV/c	1·30 GeV/c	1·36 GeV/c	1·43 GeV/c	Mean Value
Final State	Cross-sections in µb				
$\pi^+\pi^-$	235 ± 23	211 ± 24	171 ± 21	153 ± 19	—
K^+K^-	59 ± 11	52 ± 11	66 ± 13	44 ± 10	—
$\pi^+\pi^-\pi^\circ$	2019 ± 75	1894 ± 78	1719 ± 72	1742 ± 71	1843 ± 46
$\rho^\pm\pi^\mp$	313 ± 84	308 ± 85	151 ± 82	215 ± 78	260 ± 39
$\rho^\circ\pi^\circ$	255 ± 61	304 ± 71	216 ± 64	251 ± 61	264 ± 32
$f^\circ\pi^\circ$	356 ± 71	300 ± 78	290 ± 76	295 ± 73	313 ± 38
$\pi^+\pi^-+n\pi^\circ (n>1)$	17660 ± 360	17100 ± 360	16740 ± 350	15860 ± 330	—
$\rho^\circ+n\pi^\circ (n>1)$	—	—	—	—	624 ± 60
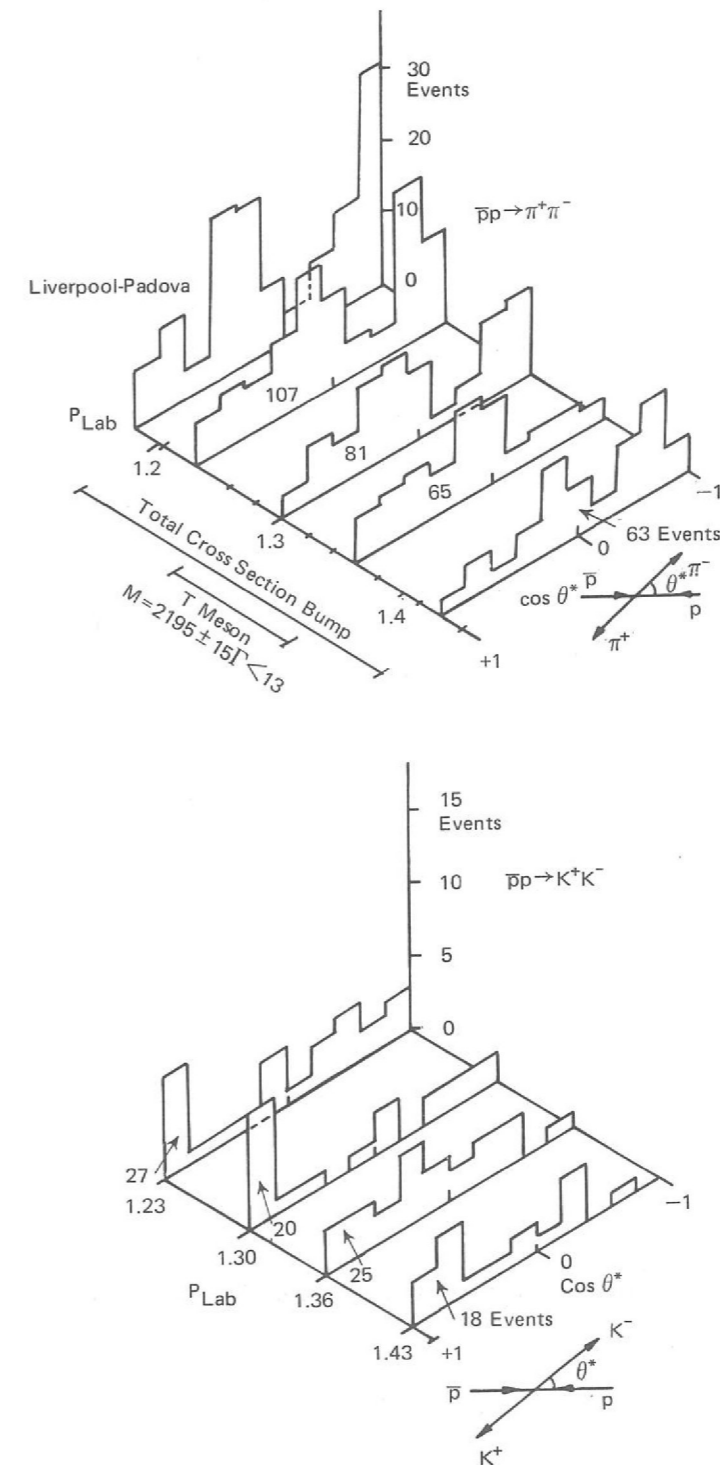
Experiment 28

ECOLE POLYTECHNIQUE, PARIS
CEN SACLAY
RUTHERFORD LABORATORY

14 GeV/c K⁻p Interactions (ref. 13, 27, 58, 118, 119, 136)

The CERN 2m hydrogen bubble chamber is being used to study the interactions of K⁻ mesons with protons at high energy. A total of 800,000 stereo photographs have been taken at a beam momentum 14·25 ± 0·10 GeV/c, using the CERN r f separated beam. A further 500,000 pictures have been proposed for the coming year, which would make this experiment the largest such exposure taken at any laboratory to date. The first published result of the experiment was a relatively accurate measurement of the K⁻p elastic scattering cross-section.

At the Amsterdam International Conference on Elementary Particles, preliminary results were presented on the production of the K*(890) resonance in the reaction

$$K^-p \rightarrow K^{*-}(890)p.$$
$$\hookrightarrow \bar{K}^0\pi^-$$
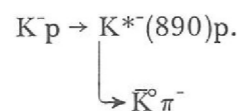
The $\bar{K}^0\pi^-$ effective mass distribution is shown in Figure 45, clear peaks due to the production of the K*(890) and K*(1420) resonances are observed above a very small background.

A new and unexpected effect was observed when the cross-section for the above reaction was plotted against beam momentum (or total energy); as seen in Figure 46, the cross-section decreases with energy much more slowly than expected from the lower energy measurements of earlier experiments. The theoretical interpretation of this effect is not straight-forward and it provides a test of various exchange models for particle interactions.

Analysis is continuing on other quasi two body reactions. These studies are greatly aided by the high energy of the experiment since the meson resonances (associated with the incident K⁻) and the baryon resonances (associated with the proton) are well separated in the laboratory system.

Figure 45. The invariant mass distribution $M(\bar{K}^0\pi^-)$ from the reaction $K^-p \rightarrow K^{*-}(890)p$ at 14.25 GeV/c. (Experiment 28).
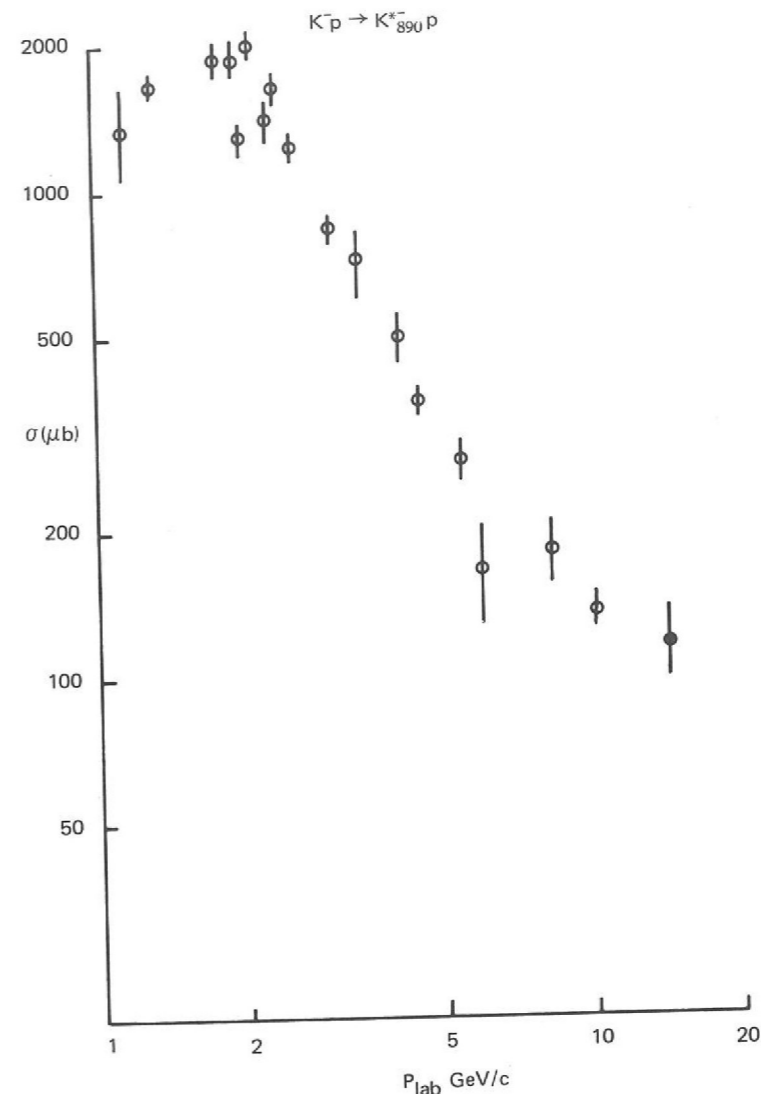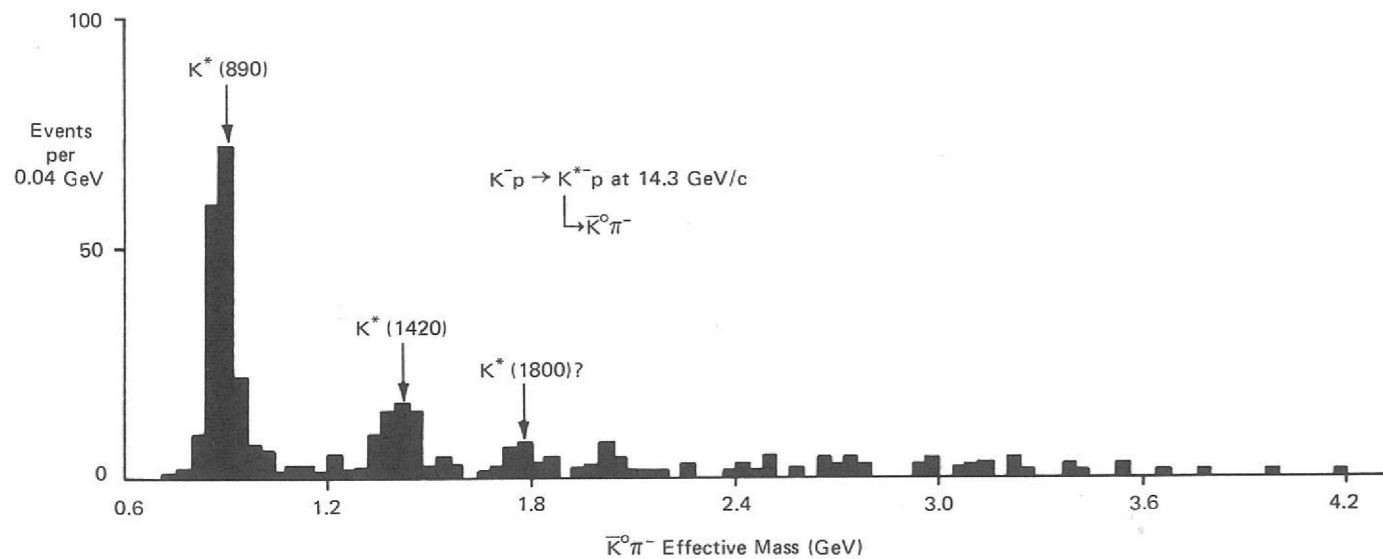
Figure 46. The variation of the cross-section for the reaction $K^-p \rightarrow K^{*-}(890)p$ with incident momentum. (Experiment 28).

Experiment 29

UNIVERSITY OF BIRMINGHAM
UNIVERSITY OF DURHAM
RUTHERFORD LABORATORY

The Study of 4 GeV/c π⁺d Interactions

Although the study of boson resonances has up to now produced some firmly established results, there are still a large number of possible boson states whose existence is doubtful, or whose properties are not well known. This experiment is intended to study some of these states, produced in the reaction $\pi^+d \rightarrow ppB^0$, where B° is a neutral boson whose decay products are fitted from bubble chamber measurements.

A total of 800,000 pictures in the CERN 2 m chamber have been approved, and roughly half of these have been taken. A further 200,000 pictures are expected to be taken shortly.

Scanning and digitising of the film (and also digitising of film pre-scanned at Durham) is under way at the Rutherford Laboratory, and is expected to be completed by mid-1972.

Preliminary results obtained from analysis of a sample of the film, show evidence for production of well-known boson resonances such as f°(1260).

Experiment 30

CAMBRIDGE UNIVERSITY
IMPERIAL COLLEGE, LONDON
WESTFIELD COLLEGE, LONDON

*π^+p Interactions in the Range 0·8-1·6 GeV/c
(ref. 7, 87, 186, 188)*

A systematic study of the inelastic decays of Δ resonances in the mass range 1550 to 1950 MeV/c^2 is being undertaken using film from the 80 cm and 1·5 m hydrogen bubble chambers exposed at the Rutherford Laboratory.

0·9 to 1·05 GeV/c. Work on this experiment, which was carried out by Imperial College and Westfield College, was completed last year. A paper on the constrained phase-shift analysis of the elastic data has been published and a paper describing the single pion production channels has been submitted for publication.

1·1 to 1·6 GeV/c. Most of the 130,000 events at the seven momenta of this exposure have been measured and are currently being processed through the geometrical reconstruction and kinematic fitting programs. A remeasurement pass has been started for part of the film. Data summary tapes for some of the momenta should be available within a few months.

0·8 to 1·25 GeV/c. In August 1970 110,000 pictures were taken in the 1·5 m bubble chamber at four momenta between 0·8 and 1·25 GeV/c. Measurement of the 45,000 events in the film is nearing completion.

Experiment 31

UNIVERSITY OF BIRMINGHAM
UNIVERSITY OF EDINBURGH
UNIVERSITY OF GLASGOW
IMPERIAL COLLEGE, LONDON

*K^-d Interactions in the Total Energy Range 1·8 to 2·1 GeV
(ref. 32, 34, 174)*

Activity has continued at a reduced level on the analysis of this experiment. The pictures (equivalent to 1·6 events/μb at 1·65 GeV/c and 3·0 events/μb at 1·45 GeV/c K^- momentum) were taken in the deuterium filled Saclay 80 cm bubble chamber in the K1 beam at Nimrod. Event selection at the scanning stage concentrated on K^-n reactions, having an initial pure state with I = 1, S = -1 and B = 1.

An analysis of cross-sections and a description of the general features of various channels has been published. The cross-sections observed in two particle final states (not including K^-n elastic scattering and $K^-d \rightarrow K^-d$), 3 particle and >3 particle states are given in Table 8. However, almost all ($\sim$90%) of the observed 3 body states, and a large proportion of the 4 body states can be accounted for by quasi-2 body states. The production mechanisms of these quasi-2 body states in the s and t channels continues to be of interest.

The difficulties and resultant uncertainties inherent in experimentation with virtual neutron targets have been discussed in two publications:

(i) Intermediate state rescattering in the $\pi^-(\Sigma N)$ state leading to the $\Lambda^\circ p\pi^-$ final state could explain all of the enhancement in the Λp mass observed at 2·129 GeV/c^2.

(ii) A major problem in the treatment of the $K^-n(p)$ elastic scattering is the separation of this reaction from both $K^-p(n)$ elastic scattering and the coherent K^-d scattering. All of these reactions are dominantly peripheral leaving the nucleons with low laboratory momenta, of the same order of magnitude as the Fermi momenta internal to the deuteron.

Table 8

Cross-Sections in Observed Channels

Beam Momentum	1·45 GeV/c	1·65 GeV/c
2 body (excluding K^-n, K^-d elastic)	3·16 mb	2·98 mb
3 bodies	9·71 mb	9·70 mb
>3 bodies	1·01 mb	1·53 mb

Experiment 32

CEN, SACLAY
COLLEGE DE FRANCE, PARIS
IMPERIAL COLLEGE, LONDON
WESTFIELD COLLEGE, LONDON

*K^+p Interactions in the 2 to 3 GeV/c Region
(ref. 23, 24, 110, 183, 187)*

In this experiment K^+p interactions have been studied at four momenta spanning the third bump observed by Cool and his collaborators in the K^+p total cross-section.

Analysis of the 200,000 photographs taken in the 1·5 m hydrogen bubble chamber is now complete and four papers presenting final results are being submitted for publication.

Cross-Sections. Cross-sections for the elastic scattering channel, all single pion production channels and those two pion and three pion production channels which do not involve more than one unseen neutral particle have been determined. The results when combined with data from other experiments show no enhancements which could be associated with s-channel resonances. The third Cool bump might be associated with threshold effects in the three pion channels but a considerable increase in statistical accuracy would be needed before this could be established with certainty.

Elastic Scattering. The slopes of the forward and backward peaks of the elastic differential cross-sections at four of the momenta have been measured and compared with results from other experiments. There is no evidence, from the present experiment, for resonance formation in the elastic channel.

Single Pion Production. Resonance fractions for all three single pion production channels have been computed. A study has been made of the production mechanisms of the K*(892) and Δ⁺⁺(1236) resonances in the K°π⁺p final state. For the K*⁺, there is evidence that the slope of the forward differential cross-section and the ρ_{oo} density matrix element (see Figure 47) show structure in the energy range of the present experiment. The K°π⁺p channel will be investigated in more detail when data from the K⁺d experiment discussed below becomes available.

Multi-Pion Production. Cross-sections and density matrix elements for K*(892) and Δ(1236) production in the two and three pion channels have been determined. The K*°Δ⁺⁺, K°η°p and K°ω°p final states also have been studied.

Figure 47. Momentum dependence of the observable density matrix elements of the K*⁺(892). The dotted line is the result of an absorption model calculation at 3 GeV/c. (Experiment 32).

P_{K^+} (GeV/c)
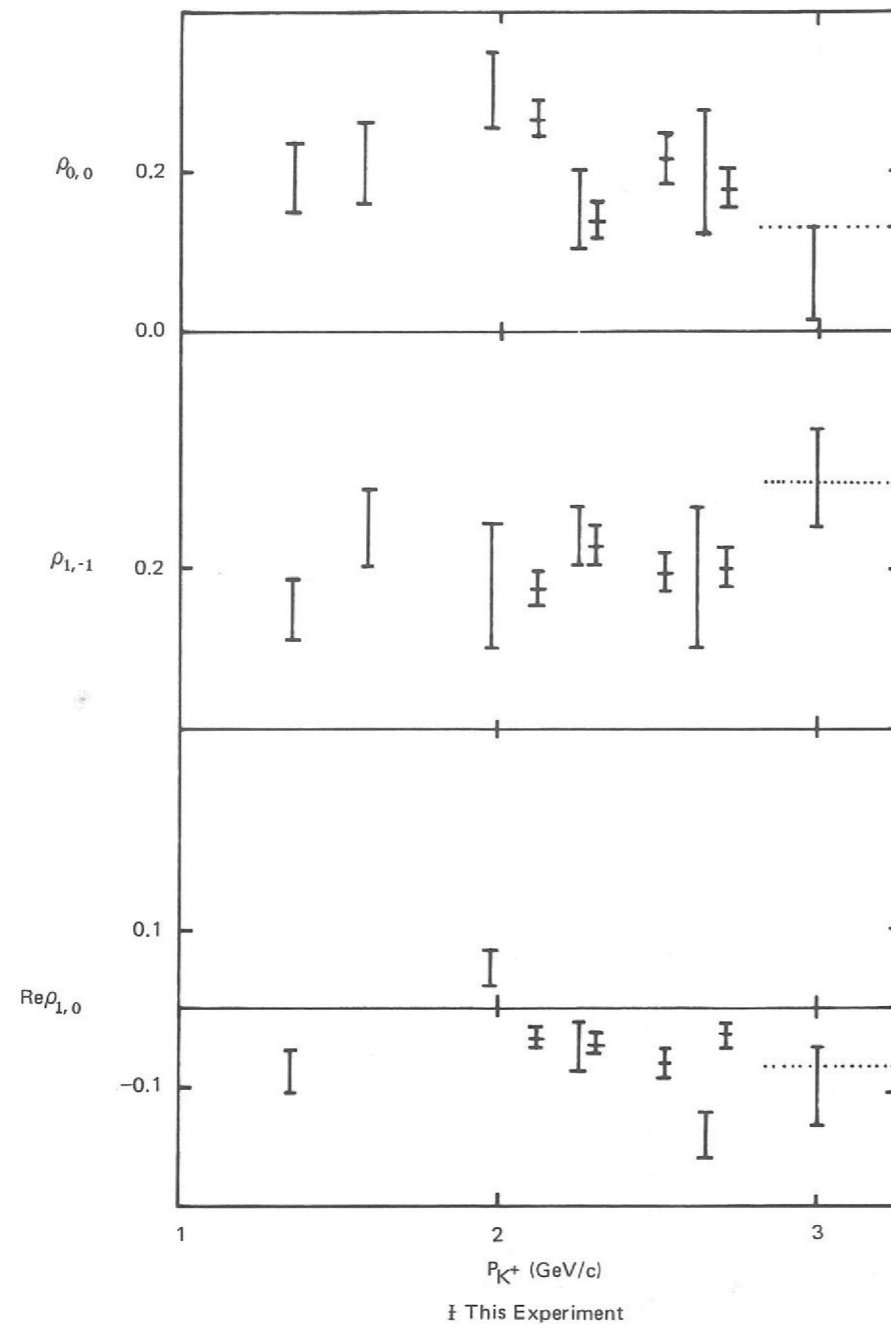
I This Experiment

Experiment 33

K⁺d Interactions in the 2-3 GeV/c Region

The data for this experiment comes from an exposure of the 1·5 metre deuterium bubble chamber at Nimrod. A total of about 750,000 pictures were taken at K⁺ beam momenta of 2·2, 2·45 and 2·7 GeV/c. The Fermi momenta of the individual target nucleons smears the centre of mass energy distribution, so approximately the same range as in experiment 32 is uniformly covered.

Almost all of the scanning and road-making is complete. Measurement has begun on the Imperial College HPD. About 20% of the total sample has been measured. HPD measurement of bubble density is being used to determine the reaction channel for events as far as possible.

The scanning criteria are designed to select all events on a neutron target (spectator proton) and events on a proton target in which two charged particles and a seen K° are produced. These last contain the K*⁺p final state mentioned in Experiment 32. Coherent deuteron events are also accepted. The initial analyses are concentrated on K⁺n charge exchange and single pion production channels. Preliminary results are expected early in 1972.

Experiment 34

UNIVERSITY OF CAMBRIDGE

Pion Production. The following channels are being studied using longitudinal phase space techniques:
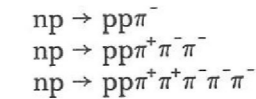
np Interactions in the Range 1 to 8 GeV/c (ref. 172)

$$np \rightarrow pp\pi^-$$
$$np \rightarrow pp\pi^+\pi^-\pi^-$$
$$np \rightarrow pp\pi^+\pi^+\pi^-\pi^-\pi^-$$

No evidence has been found for N(1470) production in the np → ppπ⁻ channel which is at variance with the findings of Shapira et al.

Figure 48. Distribution in angle ω for 250 events of the type np → Σ⁻pK⁺. q_Σ, q_K and q_p are longitudinal momenta in the c.m.s. (Experiment 34).

Events per 12 degrees

Van Hove Angle 'ω' (degrees)
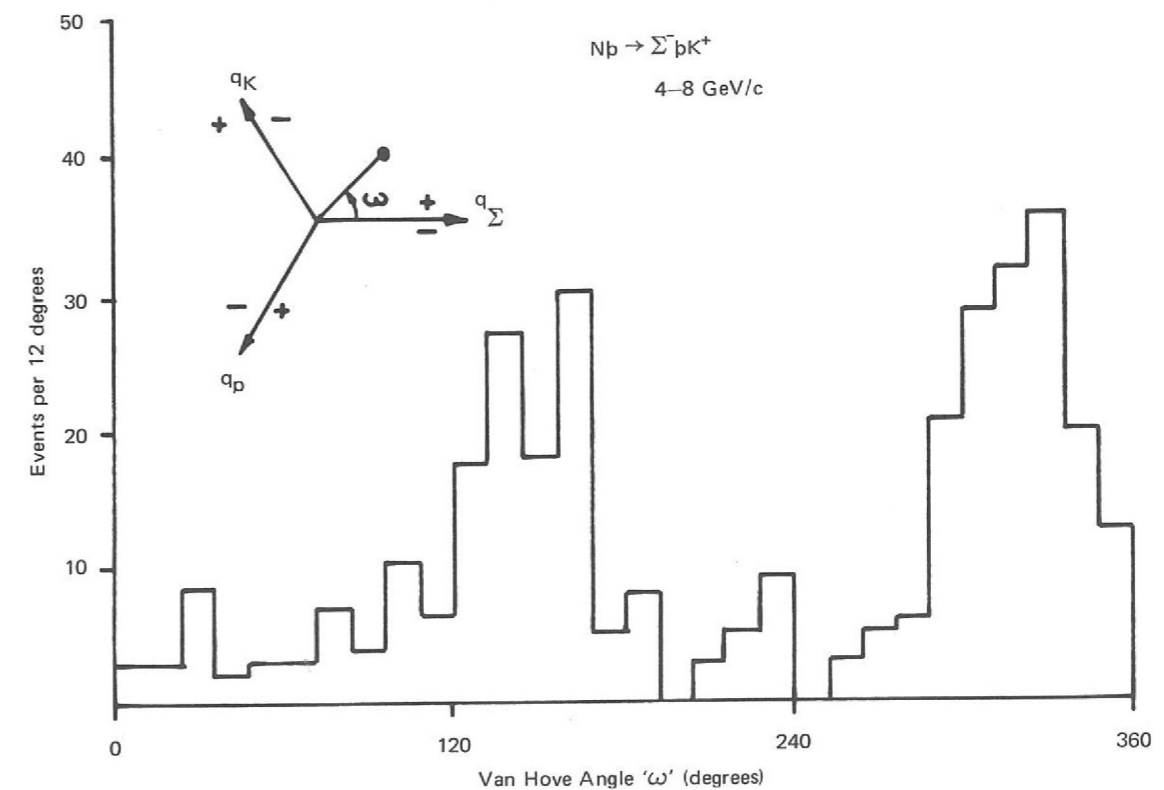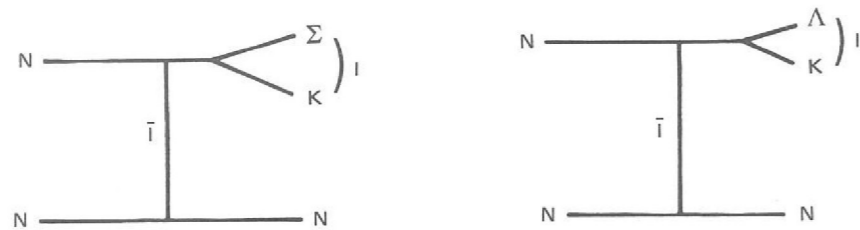
Figure 49. Diagrams corresponding to isospin amplitudes $M(\bar{I},I)$. $M(0,\frac{1}{2})$ and $M(1,\frac{1}{2})$ occur for both $NN \to \Lambda KN$ and ΣKN, whilst $M(1,\frac{3}{2})$ occurs for $NN \to \Sigma KN$ only. (Experiment 34).

Strange Particle Events. The 3-body processes

$$np \to \Lambda pK^{\circ}$$
$$np \to \Sigma^{\circ} pK^{\circ}$$
$$\text{and} \quad np \to \Sigma^{-} pK^{+}$$
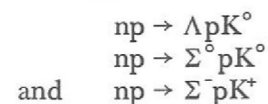
have been studied at mean neutron momenta 5·2 GeV/c and 6·8 GeV/c. Figure 48 shows the distribution in the Van Hove angle ω for 250 $\Sigma^{-}pK^{+}$ events, the peaks centred at $\omega \approx 145°$ and $\omega \approx 235°$ belonging to events in which the $(\Sigma^{-}K^{+})$ combination is produced from the neutron vertex and target proton vertex respectively. When our np data is taken with existing pp data in the same momentum range, cross-sections for a total of 7 charge channels for $NN \to \Sigma KN$ and 3 charge channels for $NN \to \Lambda KN$ are available. This data has been used to perform a complete isospin analysis in terms of the 3 isospin amplitudes $M(\bar{I},I)$, where $\bar{I}$ and I are as defined in Figure 49. Preliminary results for $NN \to \Sigma KN$ indicate that $\bar{I} = 0$ exchange occurs approximately 20% of the time, and that $\bar{I} = 1$ exchange with production of an $I = 3/2$ (ΣK) — system is predominant with 43% of the total amplitude.

Figure 50. Distribution in Van Hove angle ω for the reaction $np \to \Sigma^{-}(1385)pK^{+}$. (Experiment 34).
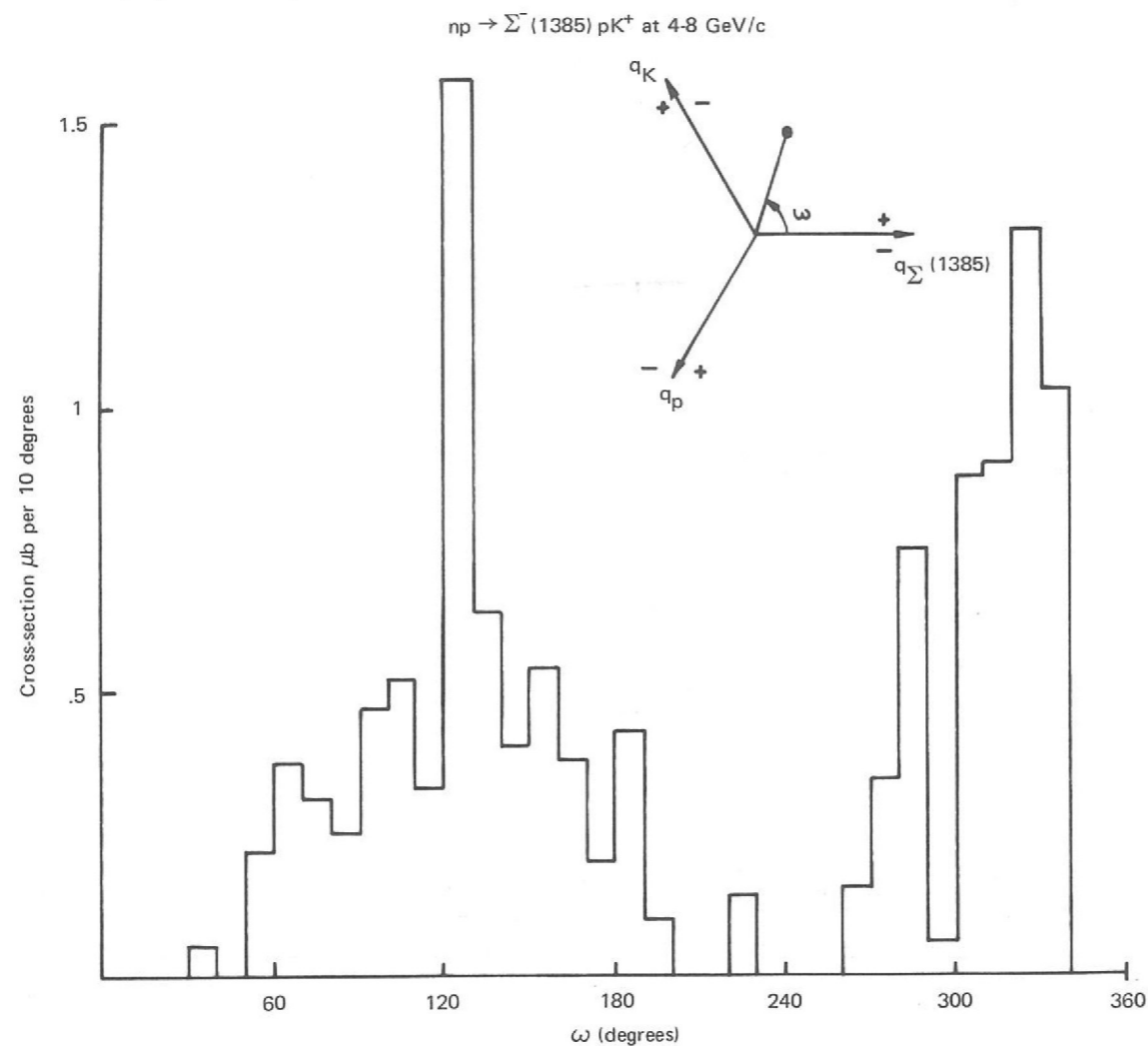
The 4-body processes

$$np \to \Lambda pK^{+}\pi^{-}$$
$$np \to \Sigma^{\circ} pK^{+}\pi^{-}$$
$$np \to \Sigma^{\mp} pK^{\circ}\pi^{\pm}$$
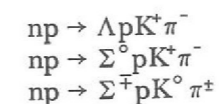
show very strong production of the $\Sigma(1385)$ resonance, which enables an isospin analysis of the reaction $NN \to \Sigma(1385)KN$ to be made in similar fashion. Figure 50 shows an ω-distribution equivalent to that of Figure 49 for 75 events of the type

$$np \to \Sigma^{-}(1385)pK^{+}$$
$$\qquad \hookrightarrow \Lambda\pi^{-}.$$
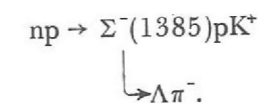
A general analysis of 4-body events using reduced longitudinal momentum techniques to identify reaction mechanisms is proceeding.

In November 1970 about 90,000 pictures containing on average two 3-prong events per picture were taken in the 1·5 m hydrogen bubble chamber. The neutrons are contained within a band 2 cm wide.

It is proposed to measure $\sim$ 40,000 3-prong events (about 8000 have been measured so far, on Sweepnik), which on the basis of a preliminary analysis should yield $\sim$ 25,000 events of the type $np\pi^{+}\pi^{-}$ and $\sim$ 12,000 events of the type $np \to pp\pi^{-}$ the remainder being $np \to pp\pi^{-}\pi^{\circ}$ and $np \to 5$ bodies events. As expected it seems possible to resolve the few ambiguous solutions ($\sim$ 10% of the events) on the basis of ionization estimates. A special study will be made of single and double $\Delta(1236)$ production from threshold up to 3·5 GeV/c.

UNIVERSITY COLLEGE, LONDON
TUFTS UNIVERSITY, USA
UNIVERSITY OF BRUSSELS
CERN

Experiment 35

670,000 pictures were taken in an exposure of the 1·4 m Rutherford Laboratory Heavy Liquid Bubble Chamber to a 2·2 GeV/c K⁻ beam at Nimrod. The liquid used was a propane-freon mixture with radiation length of 30 cm.

The main purposes of the experiment are to determine the lifetimes and the decay parameters of the cascade particles and to study the Λ-Λ, Λ-γ and the Λ-p final states.

In a search for the radiative decay $Y_{\circ}^{*}(1327) \to \Lambda + \gamma$, which had been reported by Bogachev et al, no evidence was found for the existence of this state. As mentioned in last year's report, our experiment has placed an upper limit of 98 μ-barn on the cross-section for the reaction

$$K^{-}+p \to Y_{\circ}^{*}(1327) + \pi^{+}\pi^{-}(+n\pi^{\circ}, \text{ where } n>o)$$
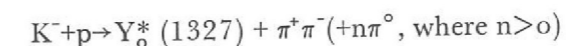
To study the properties of the cascade particles (Ξ^{-}, Ξ°) the entire film was doubly scanned and 3640 events were measured. 2400 of these had an acceptable topology for the reaction:

$$K^{-}+A \to K_{\circ}^{+} + \Xi^{\circ} + A^{1} (+n\pi)$$
$$\qquad \hookrightarrow \Lambda\pi$$
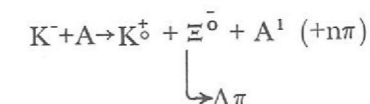
where A and A¹ represent the initial and final nuclear states. In scanning for these events detection of at least one gamma ray was essential. Further inspection of the events, and the application of kinematic fitting, reduced the sample to 232 Ξ°'s and 840 Ξ^{-}'s.

The big reduction in the number of Ξ°'s is due to the elimination of the events with spurious gamma rays. The existing sample of 232 Ξ°'s contains some background and various cuts must be applied to remove it. The effects of these cuts are being studied and the results will be published in the near future. An attempt will also be made to determine the masses of the cascade particles.

A Russian group claims that they have observed four peaks in the invariant mass distribution of the Λ-p system produced in n-C^{12} reactions. Since the interactions in our experiment are on complex nuclei a similar effect could be observed. A small fraction of the film has been scanned for the $\Lambda^{\circ}p(n\pi)$ final states, obtaining 1500 events. The preliminary results show only one peak which may be significant just above the Λ-p threshold. The observed peak is not in the same place as any of the peaks reported by the Russian group or by K^{-}-deuterium experiments.

Using events with two visible Λ° decays in the final state — (we have over 400 of these) — it is possible to study the Λ°-Λ° interaction. There is no sign of strong S-wave correlation at low Λ-Λ mass. There is, however, a significant mass peaking at 2370 MeV/c^2 in the Λ-Λ system. This seems consistent with a Λ-Λ resonance, probably as a final state interaction in the process $\Xi N \rightarrow \Lambda\Lambda\pi$. This result has been reported at a number of conferences in 1971 and will be published soon.

Experiment 36   UNIVERSITY OF CAMBRIDGE

Anomalies in Electromagnetic Processes

Approximately half the 290,000 pictures taken in the 1·5 m hydrogen bubble chamber at the Rutherford Laboratory in 1970 have been fully analysed. Separate studies of the electromagnetic processes of electron bremsstrahlung and electron positron pair production by photons in hydrogen have been made. In each case good agreement with the Bethe-Heitler theory for these processes has been obtained, no evidence for the previously reported anomalies being found.

Figure 51. Shows the distribution obtained for the bremsstrahlung energy losses of 1 GeV/c momentum e⁻ in hydrogen based on measurements of 139,000 tracks. (Experiment 36).
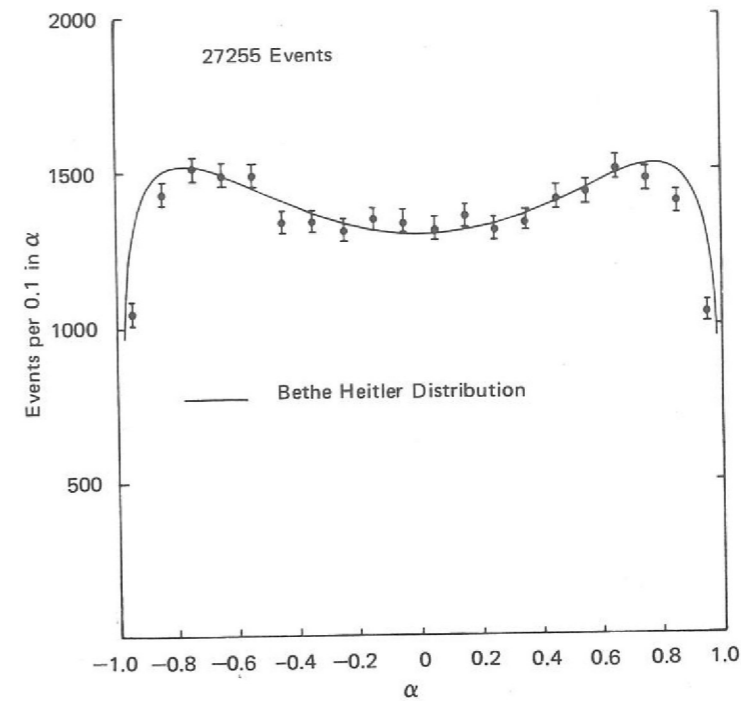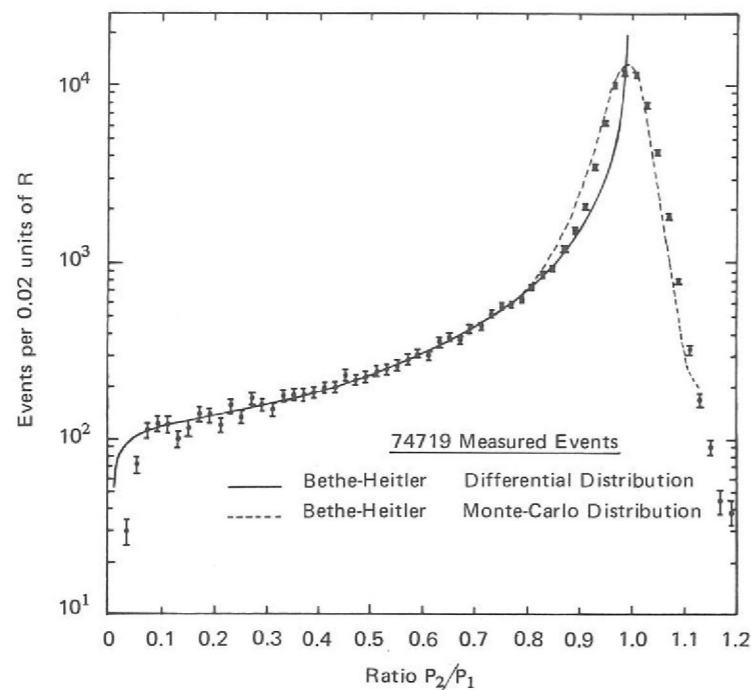
Figure 52. The distribution of the momentum partition function, α, obtained for a sample of 27255 electron positron pairs of energies between 80 MeV/c and 2000 MeV/c. (Experiment 36).

Experiment 37

UNIVERSITY COLLEGE, LONDON
UNIVERSITY OF DURHAM
CERN
RUTHERFORD LABORATORY

The Track Sensitive Target Facility in the 1·5 m Bubble Chamber

November 1971 saw the successful operation of the Track Sensitive hydrogen target in the 1·5 m bubble chamber filled with neon-hydrogen. The design and operation of the target are discussed in detail on page 116. From the viewpoint of high energy physics the principle is simple. The hydrogen is contained in a perspex walled chamber 4·5 cm deep situated centrally inside the main chamber so that beam interactions occur in hydrogen. The walls of the target are 6 mm thick and the expansion is transmitted from the main chamber by movement of the target walls (maximum deflection less than $\sim$ 1 mm). Products of reactions occuring in the hydrogen pass through the perspex into the heavy liquid neon-hydrogen mixture. This allows the increased stopping power and gamma conversion efficiency of the neon-hydrogen to become effective and so combines the merits of the hydrogen chamber — simple production kinematics and near vertex precision — and the heavy liquid chamber. The system is shown diagramatically in Figure 53.

Figure 53. Diagrammatic view of the neon-hydrogen track sensitive target facility. (Experiment 37). The central target chamber is 4·5 cm deep and contains pure hydrogen. The outer region, extending for 20 cm on either side of the target chamber contains a mixture of Neon and Hydrogen.
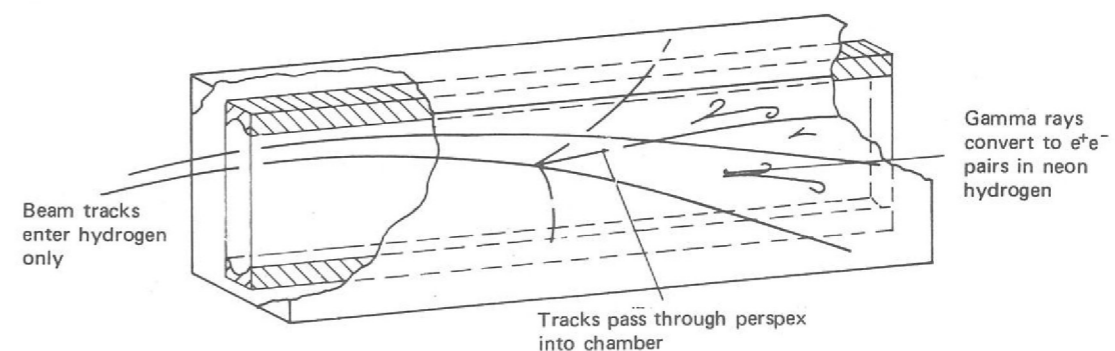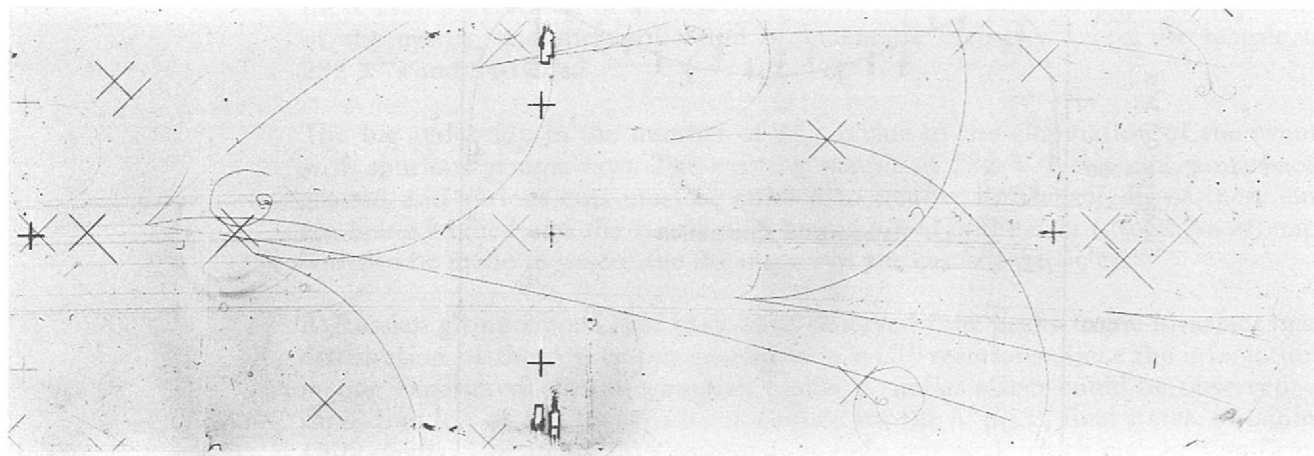
Figure 54. An example of the reaction $\pi^+p \to p\pi^+\pi^+\pi^-\pi^\circ\pi^\circ$ observed in the neon-hydrogen track sensitive target. All four gamma rays coming from the decay of the π°s convert into electron-positron pairs in the neon. (Experiment 37).

A photograph taken with a 4 GeV/c π^+ beam is shown in Figure 54. The hydrogen inside the target is clearly less sensitive than the neon-hydrogen mixture. Gamma conversions into electron-positron pairs in the neon point back to the production vertex in the hydrogen. The event shown has four gammas converted and is an example of two π° production — a class of events which cannot be analysed in a pure hydrogen chamber. The reaction shown is:

$$\pi^+p \to p\pi^+\pi^+\pi^-\pi^\circ\pi^\circ$$
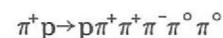
The application of the system to high energy physics is thus derived from the following properties:—

(i)   The detection of gamma rays and the ability to analyse final states with more than one neutral (π°) produced.

(ii) The stopping power of the heavy liquid yields precise momentum measurements from range.

(iii) The heavy liquid will identify electrons at the scanning stage because of their energy loss characteristics and hence, combined with the hydrogen production Kinematics, will be value in the study of hyperon β-decays.

The radiation length in the 45 mole percent mixture used in the first run is $\sim$73 cm so that the gamma conversion efficiency is $\sim$25%. Figure 55 shows the radiation length as a function of the neon concentration in the mixture. It is clearly desirable to increase the concentration to $\sim$80 mole percent which will be tried early in 1972. Later in 1972 we would hope to operate with deuterium in the target and $\sim$93 mole percent neon in the chamber (radiation length $\sim$28 cm) as has been shown feasible at DESY.

The first physics run will be with 4 GeV/c π^+ to study, in particular, the final states

$$\pi^+p \to \Delta^{++}\rho\pi^\circ \qquad \ldots\ldots\ldots \quad (1)$$
$$\pi^+p \to \Delta^{++}\pi^\circ\pi^\circ \qquad \ldots\ldots\ldots \quad (2)$$
$$\pi^+p \to pA_2^+ \qquad \ldots\ldots\ldots \quad (3)$$
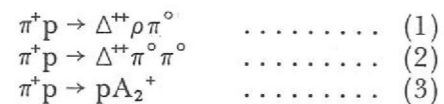
Reaction (1) was reported to contain the H-meson (mass 960 MeV/c^2) in $\rho^\circ\pi^\circ$ — with a cross-section $\sim$150 μb. The existence of the H-meson is now in doubt however because of the possibility of kinematic confusion between $\eta' \to \rho^\circ\gamma$ and H $\to \rho^\circ\pi^\circ$. In previous experiments the neutrals were not detected and the kinematics not sufficiently good to resolve a missing gamma from a missing π°. The direct observation and measurement of one or two gammas associated with the events in the H peak will resolve the question.

Reaction (2) can be used to study the $\pi^\circ\pi^\circ$ system. This is interesting because the quantum numbers are restricted to $J^P = 0^+, 2^+, \cdots$ i.e. natural parity even spin, and I = 0 or 2. It is therefore possible to study scalar mesons without vector meson background. It is necessary to observe at least one pair of gammas making a π° to allow a 1C fit to channel (2) or to observe all four gammas for a 4C fit.

Reaction (3) is interesting because the range of recoil proton gives a precise momentum measurement ($<\frac{1}{2}$%) in the momentum transfer region below and including the Jacobian peak. This, coupled with a good angle measurement between the proton and the incident π^+ should yield a good mass resolution on the A_2^+. We would expect $\Gamma \sim \pm 6$-8 MeV/c^2 for $t < 0.55(\text{Gev/c}^2)^2$.

Figure 55. Variation of radiation length in a hydrogen-neon mixture as a function of neon concentration in the mixture at 29 K. (Experiment 37).
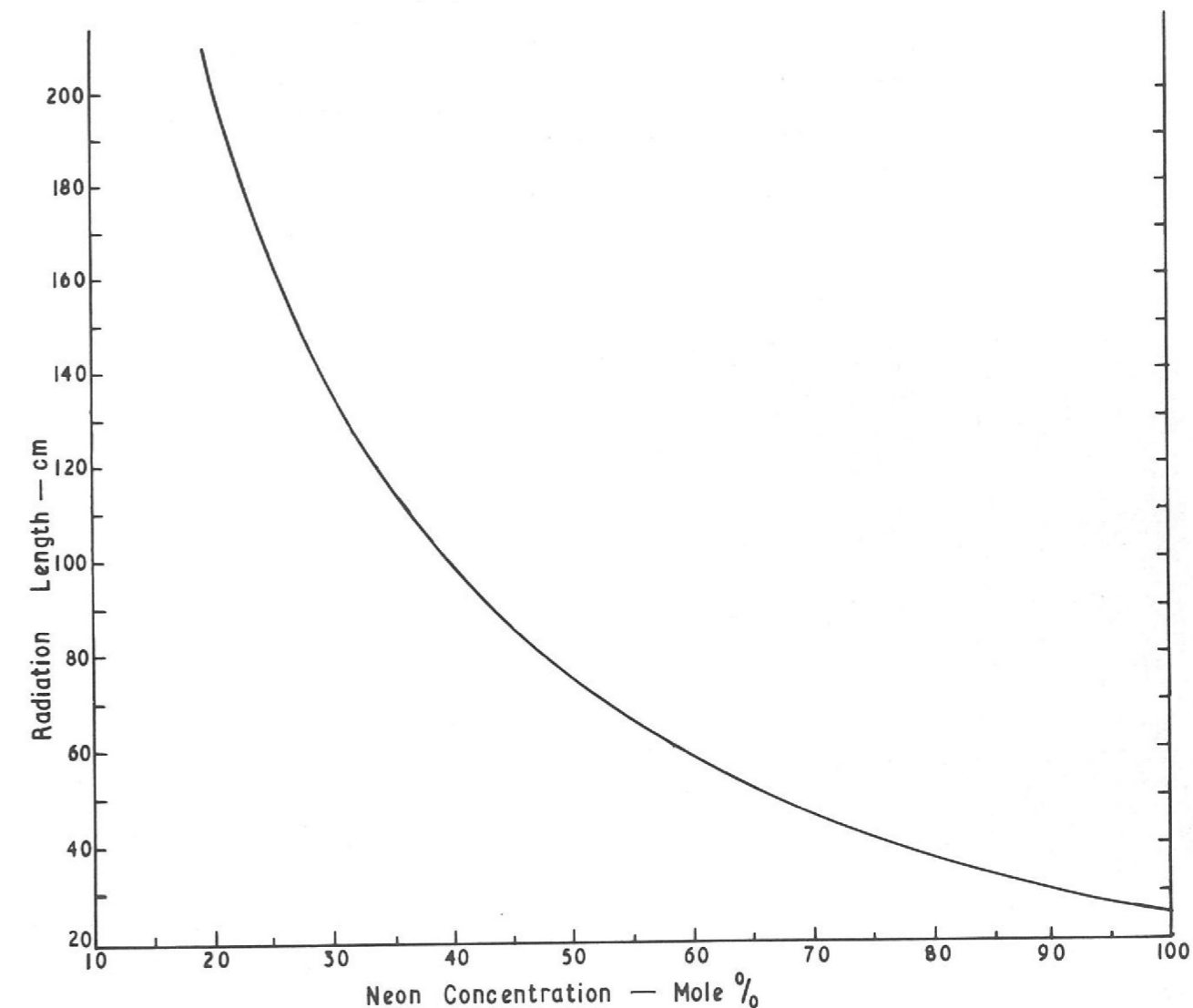
Experiment 38

UNIVERSITY OF CAMBRIDGE

Hyperon-Nucleon Interactions

In July and August 1971 some 290,000 pictures were taken in the 2 m hydrogen bubble chamber at CERN by the Cambridge Bubble Chamber Group, in order to study Λp interactions with Λ momenta in the range 10 to 20 GeV/c.

The experiment was performed by allowing a 24 GeV/c proton beam of intensity $\sim 3 \times 10^4$ protons per pulse to strike a 5 cm long copper target 3·3 m from the start of the visible region of the chamber. The neutral particles produced were allowed to enter the chamber whereas the primary proton beam and the charged particles were removed by means of a specially designed high field pulsed magnet (HFPM) of length about 50 cm, followed by a brass collimator having a straight channel of length 1·6 m and angular acceptance of 72 μsr. The collimator was surrounded by extensive uranium and lead shielding. Figure 56 shows the HFPM installed at the 2 m chamber.

Figure 57 shows a frame from the exposure, with a visible Λ° decay. There is an estimated flux of about 30 fast neutrons in the chamber and several multi-prong neutron interactions can be seen. The frame shown in Figure 58 is taken under the same conditions as Figure 57 but with the HFPM switched off and dramatically illustrates the useful sweeping effect of the HFPM. Scanning of the Λ film has started and preliminary results indicate that the flux of Λ's observed is roughly in accord with the predictions of the Hagedorn-Ranft model.

In addition to the Λ film some 66,000 test pictures were taken with a proton beam of higher intensity to study the feasibility of making a high momentum Σ⁻ bubble chamber beam. The straight channel in the collimator was replaced by a curved channel, the magnetic field in this region permitting the separation of a high momentum negative beam. Initial study of this test film indicates that such a negative beam can be made but further work is necessary to reduce the muon background in the chamber to a tolerable level.

Figure 56. The high field pulsed magnet installation at the 2m bubble chamber, CERN. (Experiment 38).
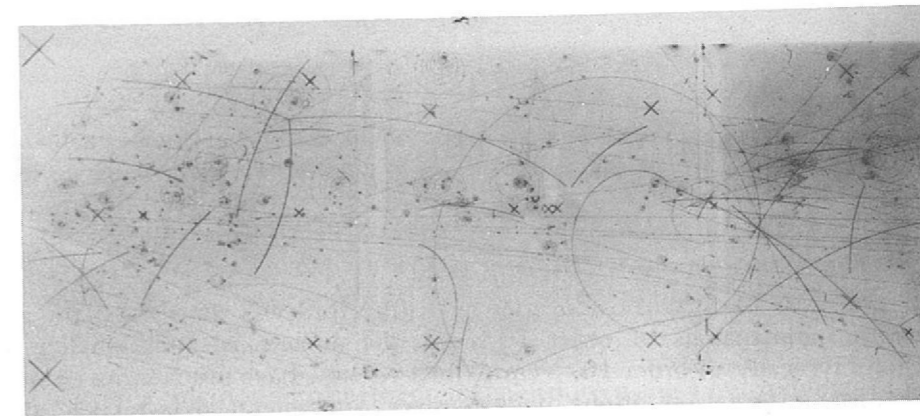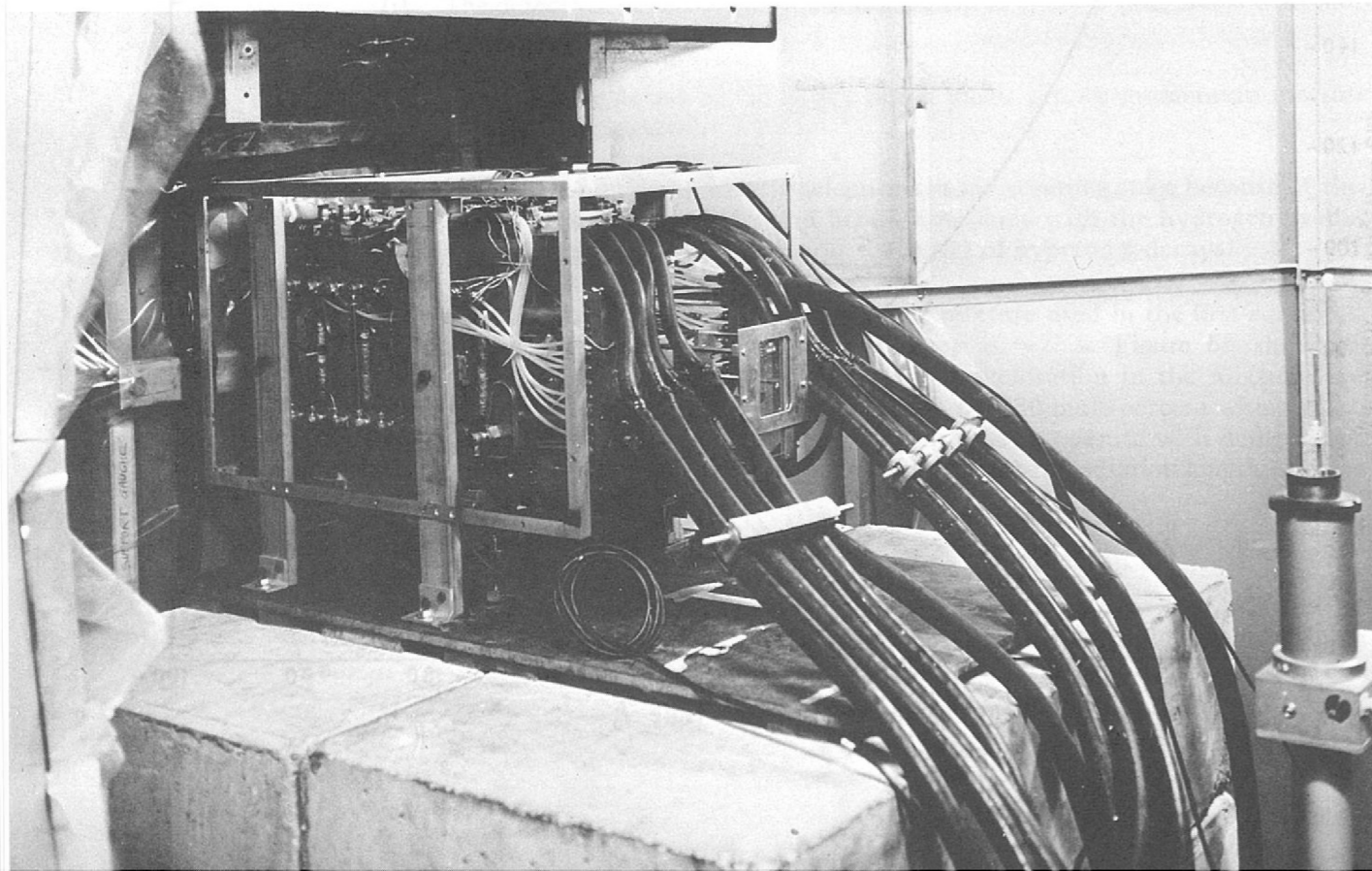
Figure 57. A typical frame from the Λ° exposure, showing a Λ° decay and several neutron interactions. (Experiment 38).
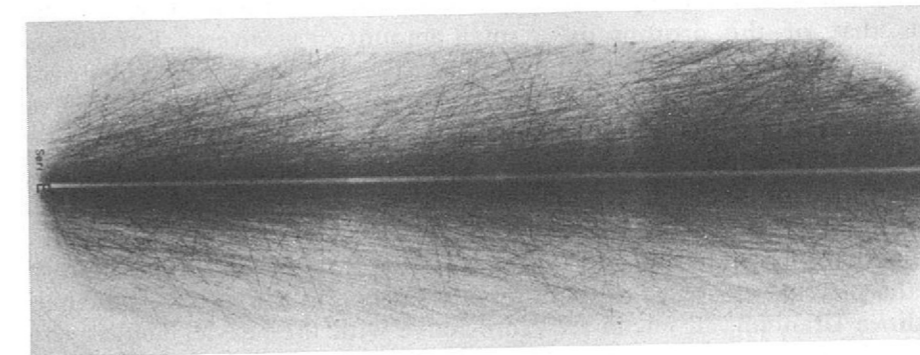
Figure 58. Another frame taken in the Λ° beam, but with the high field pulsed magnet turned off. (Experiment 38).

Experiment 39

UNIVERSITY OF BOLOGNA
UNIVERSITY OF EDINBURGH
UNIVERSITY OF GLASGOW
UNIVERSITY OF PISA
RUTHERFORD LABORATORY

Parameters of the τ and Semi-Leptonic Decays of the K°_L; $K^\circ_L p$ Interactions in the Range 400-850 MeV/c.

Preparations are being made for an exposure of the 2 m hydrogen bubble chamber at CERN to a beam of K°_L. A π^- beam will be passed into a hydrogen target and K° produced in the forward direction, via the reaction $\pi^- + p \rightarrow \Lambda^\circ + K^\circ$, will be passed into the chamber 7 metres away. By varying the momentum of the π^- in steps a range of K° momentum can be covered. The exposure will consist of a total of 300,000 pictures for eight π^- momentum settings to allow coverage of the range 400-850 MeV/c in K°_L momentum. At the lower momenta the resultant K°_L beam will be monoenergetic.

The weak interaction part of the experiment is concerned with the elucidation of the mechanisms responsible for the decays:—

$$K^\circ_L \rightarrow \pi^\pm e^\mp \nu$$
$$\pi^\pm \mu^\mp \nu$$
$$\pi^+ \pi^- \pi^\circ$$

A knowledge of the beam momentum allows the avoidance of the kinematic ambiguity which has beset previous investigations.

Of particular interest in the strong interactions is the reaction $K^\circ_L + p \rightarrow \Sigma^\circ + \pi^+$. There is some previous evidence for I = 1, S = -1 baryon states with large branching ratios into Σπ. The channel is more amenable to study using a neutral rather than negative K beam. Preparations are being made for the provision of counting equipment to monitor the π^- beam, a hydrogen target, shielding and an optimised absorber assembly to remove photons from the K°_L beam.

Nuclear Structure Experiments

One of the most important discoveries by Rutherford was that whilst the atom typically has dimensions of order 10^{-8} cm, the nucleus is much smaller with dimensions typically of order 10^{-13} cm. Whilst we now have much more complete and detailed information about nuclear sizes, in general this relates to the proton distribution which is measured through its electrical charge. Our information about the distribution of neutrons is much more sparse; for example, it is thought that in heavy nuclei the density distributions of neutrons and of protons are similar but it is still not known whether the radius of the neutron distribution exceeds that of the protons by a small amount or vice-versa. Experiment 40 describes a measurement of the total reaction cross-sections for pions on nuclei to gain information about neutron density distributions. A preliminary analysis of the results indicates that in heavy nuclei the radii of the neutron and proton distributions are almost equal.

Recently there has been considerable speculation by nuclear structure physicists about the possible existence of superheavy elements. In the region of the periodic table above Uranium, all nuclei are radio-active with the heavier nuclei generally having shorter life times before decay. The heaviest element known at present has the atomic number 105 and a half-life for decay measured in seconds. The general expectation would be that nuclei heavier than this would have even shorter half-lives. However, it has been predicted that, due to the stabilising effect of a closed shell of protons at atomic number 114, nuclei in this region could have quite long half-lives for decay with values as long as 10^6 years being predicted in some cases. These nuclei are known as the superheavy elements. Attempts in the Rutherford Laboratory to produce superheavy elements by secondary reactions in targets irradiated by high energy proton beams have continued throughout the year. However, despite a great deal of work (both in this Laboratory and elsewhere) it has not so far been possible to confirm with certainty, or to disprove, the earlier results reported last year for the possible production of a superheavy element with the atomic number 112. Towards the end of the year a further irradiated target was obtained from CERN and it is hoped that a repeat of the earlier work with this target will clarify the situation.

The Laboratory continues to support university groups carrying out experiments at the accelerators available at AERE (Harwell), particularly those groups previously associated with the Proton Linear Accelerator at the Rutherford Laboratory (PLA). These experiments are included in Table 9 and reported below.

Several members of the resident nuclear structure physics group have participated in theoretical studies relating to nuclear structure problems, particularly with reference to the question of nuclear sizes. The Microscopic Model has been applied to the elastic scattering of α-particles from ^{204}, ^{206}, ^{208} Pb and ^{209} Bi for energies below and near the Coulomb barrier. The analysis showed that the rms radii of the nuclear mass distributions did not exceed the values of the charge radii by more than $0 \cdot 1$ fm. This work was later extended to study the effective alpha-nucleon interaction in nuclei where a comparison was made between the effective interactions used to describe elastic α-nucleus scattering and those derived from free nucleon-alpha scattering.

An analysis has been made of reaction cross-sections for negative pions, on a range of nuclei, at momenta from 20 to 60 GeV/c measured at Serpukhov. Data for C, Al, Sn and Pb were analysed in terms of nuclear sizes. Assuming that the neutron and proton distributions in C are identical it is found that for Pb the best agreement with experiment is obtained using neutron density distributions which have similar geometrical parameters to that of the proton distribution.

Results from a calculation of neutron distributions using a hydrodynamical model are found to be in good agreement with the analyses of pion and α-particle scattering data mentioned earlier. The model has been used to examine the "anomaly" in the radii of the orbits of excess neutrons in heavy nuclei.

Data on the depolarization parameter for proton-nucleus scattering measured on the PLA and elsewhere have been analysed in terms of a spin-spin dependent potential. In general the potential values obtained are very small, in agreement with analyses of the scattering of polarized neutrons by aligned nuclei.

Table 9

Nuclear Structure Experiments

Expt. No.	Experiment	Location	Team	Status
40	Total Reaction Cross-sections for Pions on Nuclei	π10 beam Nimrod	Univ. of Birmingham Univ. of Surrey Rutherford Lab.	Analysis
41	Search for Super-heavy Elements	CERN Proton Synchrotron	Univ. of Manchester Univ. Res. Reactor, Risley AERE, Harwell AWRE, Aldermaston Rutherford Lab.	Analysis
42	Correlation Studies on Light Elements	AERE, Harwell Variable Energy Cyclotron (VEC)	King's College, London Queen's Univ. Belfast	Analysis
43	Scattering Studies with Helions and Alpha Particles	AERE, Harwell VEC and Tandem Accelerators	King's College, London Univ. of Birmingham	Data taking and Analysis
44	Studies of 'Few Nucleon' Reactions	AERE, Harwell Synchro-Cyclotron	King's College, London Queen Mary College, London AERE, Harwell	Data taking and Analysis
45	Elastic Scattering of 400 MeV/c $\pi^{\pm}$ by Deuterium	CERN Synchro-Cyclotron	Univ. of Oxford CERN	Data taking

Experiment 40

UNIVERSITY OF BIRMINGHAM
UNIVERSITY OF SURREY
RUTHERFORD LABORATORY

Total Reaction Cross-Sections for Pions on Nuclei (ref. 16, 36, 37)

The objective of this experiment is to measure the total reaction cross-sections for π^+ and π^- mesons on a range of nuclei at energies in the range 0·5 to 2·0 GeV. The purpose of the measurements is to obtain further information about the density distribution of neutrons in nuclei, a currently controversial topic in nuclear structure physics.

In heavy nuclei both π^+ and π^- mesons are strongly absorbed in the nuclear interior. However, if for the pion-nucleon total cross-sections (σ_T), the ratio:

$$Q = \frac{\sigma_T(\pi^-p)}{\sigma_T(\pi^+p)} = \frac{\sigma_T(\pi^+n)}{\sigma_T(\pi^-n)}$$

is much greater than 1 then in the surface region the π^+ will be mainly absorbed by neutrons and the π^- by protons. Hence the ratio of the total reaction cross-sections for pion-nucleus interactions

$$R = \frac{\sigma_R(\pi^-N)}{\sigma_R(\pi^+N)}$$

will be sensitive to the properties of the surface region around the 50% density point and in particular to the relative distributions of neutrons and protons. The ratio R has been measured before for 700 MeV π^+ and π^- mesons where Q = 2·6, but the measurement was only made for lead and at one pion energy. In the present experiment these measurements have been repeated and extended to cover both a wide range of nuclei and a number of pion energies.

The experiment itself consists of a "bad-geometry" transmission measurement in which the number of particles transmitted through the target is measured as a function of the solid angle subtended by the elements of an array of scintillation counters. By moving the counters relative to the target, measurements have been taken at 20 different solid angles. After various small corrections have been applied the results are then extrapolated to zero solid angle to obtain the measured total reaction cross-section. Since the aim of the experiment is to measure the ratio of the reaction cross-sections for π^+ and π^- mesons to high accuracy (better than 1%) effective identification of the incident pions and measurement of count-rate effects are very important. This is particularly so for positive beams where the incident π^+ mesons are accompanied by a large flux of protons. A DISC Cerenkov counter is used to distinguish between protons and π^+ mesons and a threshold Cerenkov counter is used to reject electrons and muons. Scalers recording the data are interfaced using the CAMAC system to a PDP-8 computer which is used for on-line checking and calculation of the results.

Measurements have been taken for the series of nuclei, C, Al, Ca, Ni, Sn, Ho and Pb chosen to cover a range of A values at momenta of 0·71, 0·84, 1·0, 1·36, 1·58 and 2·0 GeV/c. Ho was included as a good example of a badly deformed nucleus. At 1·36 and 1·58 GeV/c the Fermi-averaged π^+ and π^--nucleon total cross-sections are equal so that the calculated ratio of π^-/π^+ reaction cross-sections is independent of the neutron density distribution assumed. At the lower momenta the π^+ and π^--nucleon total cross-sections differ by a factor of two, whilst the 2·0 GeV/c measurements will give a check of momentum dependent effects in the theory. Measurements have been taken for the separated isotopes ^{120}Sn and ^{208}Pb at 0·84, 1·0 and 1·36 GeV/c as for these nuclei the proton density distributions are particularly well-known.

A preliminary analysis of the date gives R = 1·0437 ± 0·0038 for Pb at 1·36 GeV/c to be compared with the model-independent calculated value of 1·0470. At 1·0 GeV/c the value 1·0230 ± 0·0024 is obtained, compared with calculated values of 1·038 if the neutron and proton distributions are identical and 0·979 if the radius of the neutron distribution is taken to be 0·5 fm larger than the corresponding value for protons.

Experiment 41

UNIVERSITY OF MANCHESTER
UNIVERSITY RESEARCH REACTOR, RISLEY
AERE, HARWELL
AWRE, ALDERMASTON
RUTHERFORD LABORATORY

Search for Superheavy Elements (ref. 18, 55, 56)

In last years report an experiment was described in which the observation of spontaneous fission in a mercury source separated from a tungsten target which had been irradiated by 24 GeV protons was taken as evidence for the possible existence of a superheavy element with atomic number 112. It was suggested that secondary reactions in the tungsten target might be able to produce the superheavy nuclei which have been predicted to exist in the region of the possible closed shell of protons at around Z = 114.

The evidence that the observed activity might be due to a superheavy element was based entirely on the prediction that element 112 will be the chemical homologue of mercury. Such an identification may, of course, be in error due to the possibility of contamination of the sources and this possibility was considered in some detail.

Since the earlier experiments, attempts have been made to identify the source of the observed fission activity more directly by trying to measure nuclear properties which depend in some way on the Z or A of the nucleus undergoing fission. A more uniform source was prepared by chemically exchanging the Hg activity onto an evaporated film of PbS on a 240 ± 20 μg/cm^2 polycarbonate backing. About 50% of the fission activity was transferred onto the PbS film. With this source it was now possible to measure the kinetic energy spectrum of the fission fragments and energy spectra were recorded for both single and coincident summed kinetic energies. The observed singles and coincidence spectra are shown in Figure 59. Also shown in Figure 59 are the spectra obtained in the same apparatus from a ^{252}Cf source which was prepared by sublimation of ^{252}Cf onto successive layers of PbS to simulate the HgS-PbS source as closely as possible. ^{252}Cf (which undergoes spontaneous fission) is the most likely contaminant element.

It can be seen that the two spectra appear to differ in shape, particularly in the low energy region, and that the Hg energy spectrum seems to have a peak at slightly higher energy than that for ^{252}Cf (about 194 MeV as compared to 182 for ^{252}Cf). A statistical χ^2 analysis indicates that the probability that the observed spectrum is consistent with that of pure ^{252}Cf is less than 1%. The probability increases to 30% if the point with the largest value of χ^2 (at channels 120-130) is removed from consideration.

The fission data were printed out sufficiently often that about 50% of the individual singles and coincidence events could be correlated with each other. In these cases, it is possible to determine the energy of the fission fragments striking the back detector by a simple subtraction. The energies of the correlated fragments are plotted in Figure 60 along with a contour which encloses the region in which 90% of the ^{252}Cf fragments would be found. The relatively large number (30%) of the observed fissions from the Hg source which do not fall within the contours can be regarded as evidence of spontaneously fissioning material other than ^{252}Cf in the Hg source.

Figure 59. Energy spectra of fission fragments observed with the mercury source. In (a) the summed kinetic energy spectrum is given and in (b) the singles spectrum observed with the front detector. The continuous lines show similar measurements with a ^{252}Cf source with much better statistics. (Experiment 41).
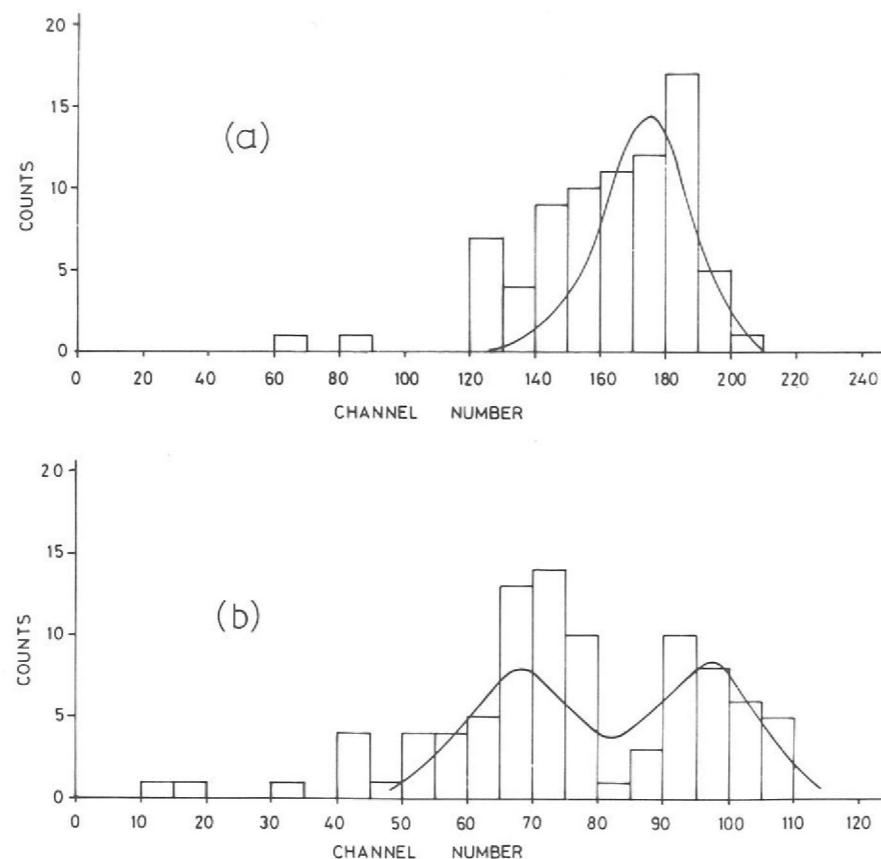
Figure 60. Correlated energies of fission fragments from the Hg source. The pairs of numbered points show the alternative interpretations when the analysis of the events is ambiguous. The contours enclose the region in which 90% of ^{252}Cf fragments would be found and are asymmetric because of energy loss in the source backing. (Experiment 41).
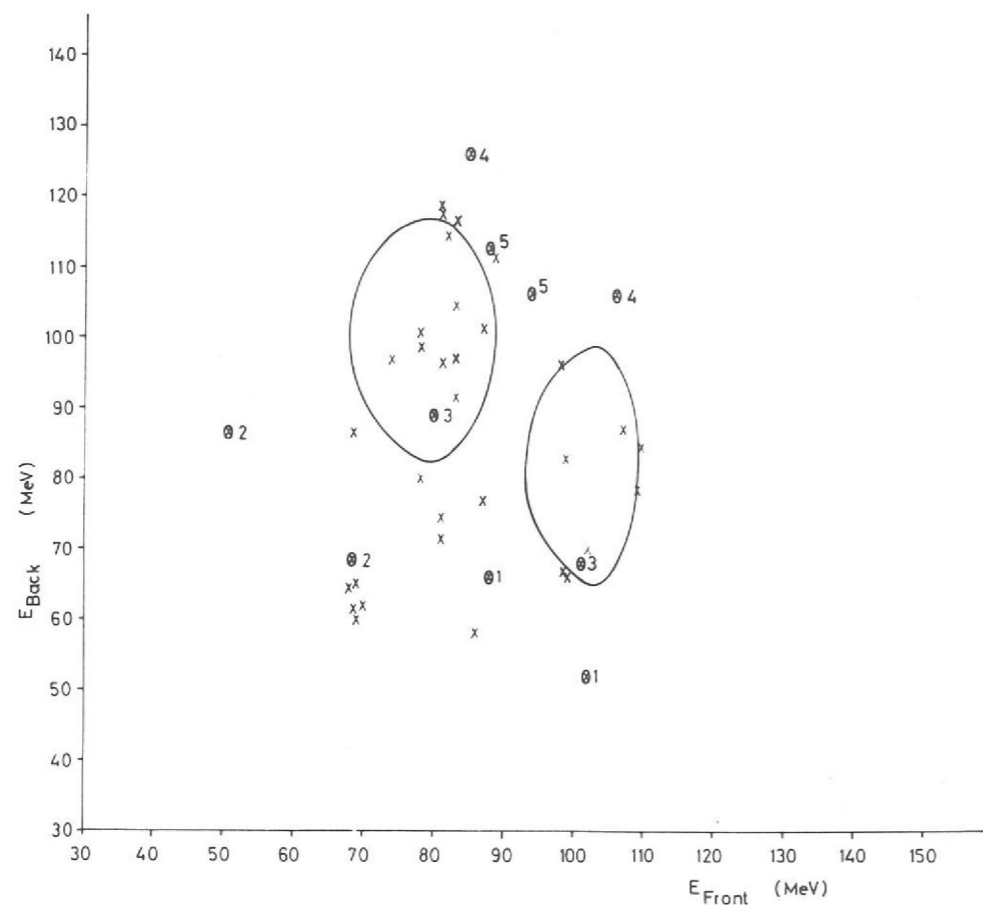
Measurements of the fission energy spectra, the mean number of neutrons per fission and the alpha/fission intensity ratio all suggested that a significant fraction of the observed fission activity from the thin source could have been due to ^{252}Cf. Some further chemical separations were therefore carried out. The fission and alpha activity of the resulting actinide source showed that $73\pm7\%$ of the fission activity observed at the time of the kinetic energy measurements now appeared in the actinide fraction and here the intensity ratio of 6·1 MeV alpha particles to fission fragments was $16\pm2 : 1$, a characteristic value for ^{252}Cf.

From these and other measurements, it appeared that approximately 70% of the fission activity observed was due to ^{252}Cf although the remaining 30% is unlikely to be due to this element. As early alpha spectra showed smaller amounts of alpha activity having an energy of around 6·1 MeV for comparable rates of fission activity we conclude that after the original separation either the source has been contaminated or the ^{252}Cf has grown in.

The fact that the mean number of neutrons emitted per fission for the total Hg source was close to that of ^{252}Cf indicates that the remaining 30% of the fission activity has a neutron multiplicity in the range of 2 to 5. The kinetic energy spectra and the value of neutron multiplicity do not agree with the published predictions for the binary fission of superheavy elements; however, neither do the kinetic energy spectra appear to fit those of any known spontaneously fissioning actinide isotope.

Finally some attempts have been made to measure the mass of the spontaneously fissioning activity in the Hg fraction using a mass separator. A thin Nickel foil was used in the focal plane of the separator to collect nuclei over the mass range 260 to 320 amu. Polycarbonate foils exposed to the Nickel plate give some slight evidence for spontaneous fission activity corresponding to masses in the region of A = 308. Scanning of nuclear emulsions exposed to the Nickel plate is in progress.

Experiment 42

KING'S COLLEGE, LONDON
QUEEN'S UNIVERSITY, BELFAST

The value of single-nucleon transfer reactions for determining the single-particle characteristics of nuclear states is well established. Neutron transfer reactions have been widely used but the use of proton transfer reactions has been limited by the availability of particle beams. Analysis difficulties are encountered in these reactions due to the composite nature of the particles and the complexity of the reaction mechanisms. These difficulties are partly removed by the (p, 2p) reaction as the use of correlation techniques restricts the mechanism almost entirely to the simple 'knock-on' or 'quasi-elastic' process. Provided the distortion effects, which become appreciable below 100 MeV, can be satisfactorily described the better resolution of low energy experiments makes them preferable for nuclear structure studies. The distortion of the incoming and outgoing proton waves can now be well described by the optical model.

Correlation Studies on Light Elements (ref. 42)

Of the 1p shell nuclei, ^{16}O is particularly interesting as its structure has been widely considered and its ground state appears to be largely a closed p$\frac{1}{2}$ shell. By using a combination of measurements from $C_{10}H_8O_4$ (mylar) and MoO_3 targets the nucleus ^{16}O has been investigated together with ^{12}C for comparison with previous work.
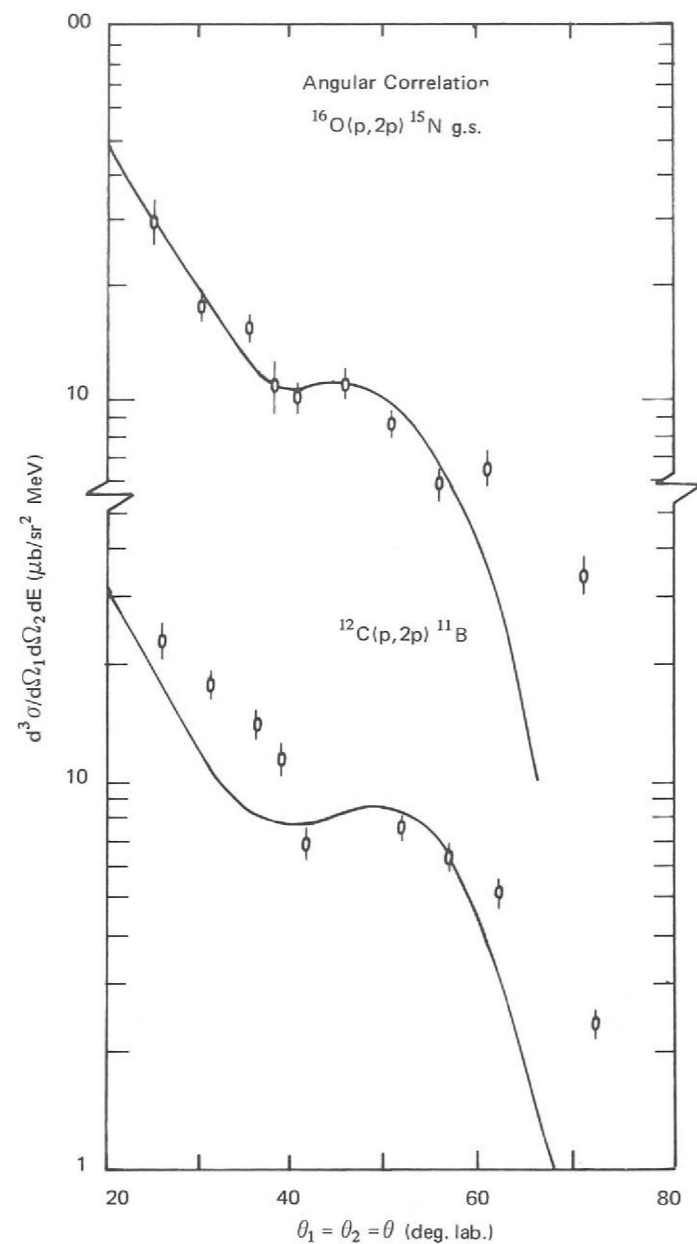
Figure 61. Angular correlations for the $^{16}O(p,2p)^{15}N$ and the $^{12}C(p,2p)^{11}B$ reactions at 49.5 MeV. The solid curves are the results of distorted wave impulse approximation calculations. (Experiment 42).

The UKAEA Harwell Variable Energy Cyclotron was used to produce a well defined beam of $49 \cdot 5 \pm 0 \cdot 3$ MeV protons. After scattering from targets of either $1 \cdot 70 \pm 0 \cdot 02$ mg cm^{-2} mylar or $1 \cdot 60 \pm 0 \cdot 02$ mg cm^{-2} MoO$_3$ the reaction products were detected in semiconductor detector telescopes at equal co-planar angles on either side of the beam. Each telescope consisted of a 400 μm surface barrier transmission counter, a 4 mm Si(Li) transmission counter and a 5 mm Si (Li) veto detector to remove high energy elastically scattered protons. The total energy resolution as measured from free proton-proton scattering was 250 keV.

For the purpose of a preliminary comparison distorted wave impulse approximation calculations have been performed using the di-proton model of Jackson and Jain. The angular correlation curves for $^{16}O (p,2p)^{15}N$ and $^{12}C(p, 2p)^{11}B$ ground states are shown in Figure 61. Measurements to other states of ^{15}N observed at excitation energies of $5 \cdot 3$, $6 \cdot 3$ and $7 \cdot 3$ MeV will require a more detailed analysis. The salient feature of the results is the location of a minimum in the correlation curves close to the angle corresponding to zero momentum transfer. The extra diffraction structure observed in the previous ^{12}C data is not in evidence.

Experiment 43

The inelastic and elastic scattering studies, which determined with precision the optical model parameters for protons, using the PLA have been continued using the helion beams of the UKAEA Variable Energy Cyclotron (VEC) and Tandem Accelerators.

Scattering Studies with Helions and Alpha Particle Beams (ref. 29, 86, 181, 191)

Using the $53 \cdot 4$ MeV helion beam of the cyclotron elastic and inelastic scattering measurements have been made for ^{56}Fe over an angular range of $12°$ to $150°$. The value of precise large angle measurements in reducing the ambiguities of the optical potentials has been amply demonstrated. The preference for surface absorption potentials is shown in Figure 62. Coupled channels (SCA) calculations based on the ground state and principal 2^+ and 3^- states indicate that such coupling effects are not as dominant as the inclusion of a spin-orbit potential in the regular optical model for helions.

Figure 62. Regular optical model best fits for surface (full line) and volume (dashed line) absorption potentials with $J_{RS}/A\rho A_T = 445$ MeV fm^3 but without any spin-orbit component. (Experiment 43).
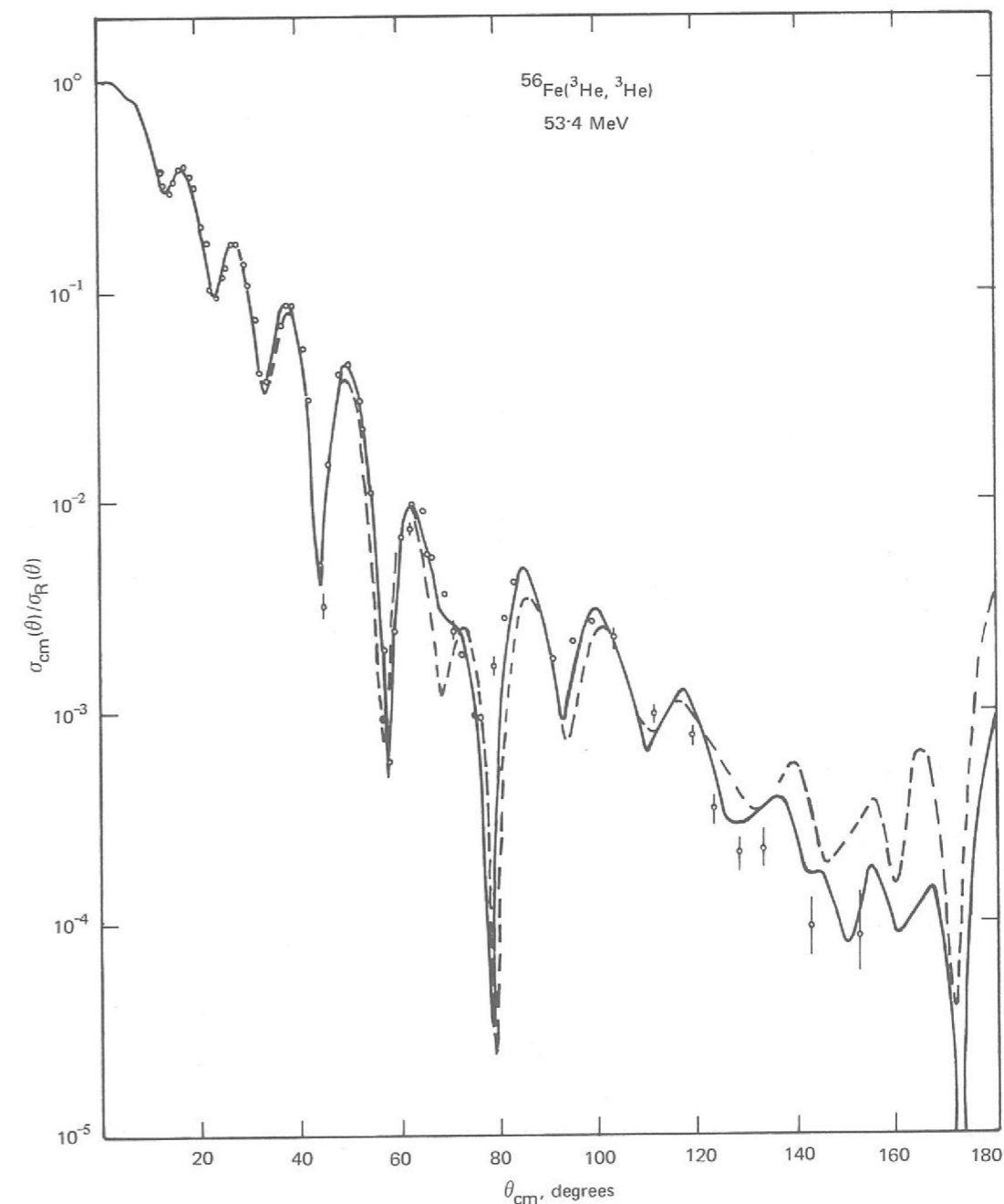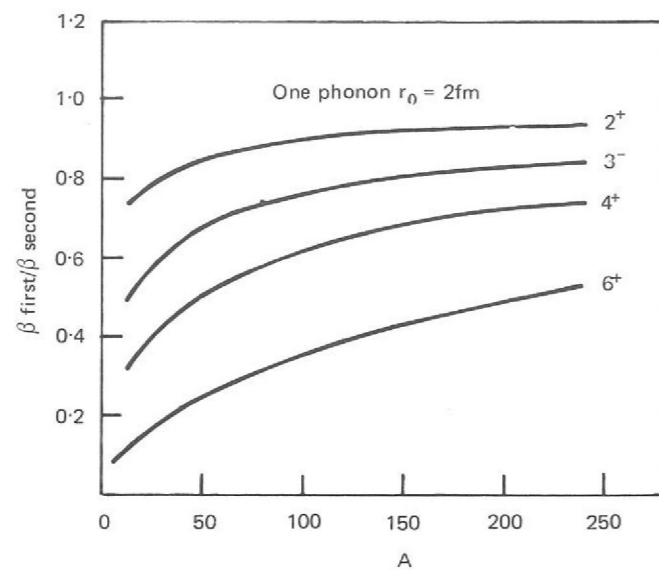
Figure 63. The ratio of the optical potential and nuclear density deformations calculated for a Gaussian force of 2 fm range as a function of A number for 2^+, 3^-, 4^+ and 6^+ states. (Experiment 43).

The previous detailed proton study on the even isotopes of Samarium shed considerable light on the transition region between vibrational and rotational nuclei. Elastic and inelastic scattering helion studies on ^{144}Sm have been completed at 53·4 MeV and 18 MeV and studies of the other isotopes are planned. The low energy measurements used the UKAEA Tandem accelerator and were combined with a study of the (h, α) reaction. Comparison of the spectroscopic factors obtained with those of the (p, d) reaction show a factor of six difference between the values obtained for the $l = 0$ transition at 0·107 MeV. This failure of the DWBA analysis is attributed to the large momentum mismatch in the (h, α) reaction.

Elastic and inelastic scattering cross-sections of ^{3}He and α particles have been measured for ^{11}B and isotopes of Mg at several energies using the Harwell VEC and the Oxford Tandem accelerator. This data is being employed to study two step processes in the stripping reactions ^{12}C $(d, ^3He)$ ^{11}B and ^{26}Mg $(^3He, \alpha)^{25}$Mg. Both Collective and Microscopic Models are being used to treat the excitation of the intermediate states involved in such processes.

The presently accepted formalism for inelastic scattering of nucleons from collective nuclei is based on a deformed optical potential. A simple Microscopic Model has been used to compare this formalism with an alternative one based on a deformed nuclear density. The results show that there are very large differences between the nuclear and the optical potential deformation parameters (see Figure 63) and that quite different shapes are obtained for the inelastic formfactors with these two prescriptions.

Table 10

Comparison of spectroscopic factors(S) obtained in neutron pickup reactions leading to final states in ^{143}Sm.

E (MeV)	Level	S (p, d)	S (h, α)
0·0	$d_{3/2}$	4·0	4·24
0·107	$s_{1/2}$	1·6	0·26
0·748	$h_{11/2}$	9·86	10·8
1·10	$d_{5/2}$	2·57	1·86
1·36	$h_{11/2}$	1·04	2·28

KING'S COLLEGE, LONDON
QUEEN MARY COLLEGE, LONDON
AERE, HARWELL

Experiment 44

The first three experiments in this series, n-p differential cross-section, n-p bremsstrahlung and n-d differential cross-section, have been completed and data analysis is in progress. Preliminary results were presented at the Budapest Conference on the Nuclear Three-Body Problem, 1971.

Studies of 'Few Nucleon' Reactions (ref. 154)

Kinematically complete data has been obtained from the reaction d(n,np)n, using a multi-parameter data acquisition system developed previously for n-p bremsstrahlung reaction studies. The system uses a neutron beam obtained from the AERE synchro-cyclotron, collimated onto a target of liquid deuterium, designed and built at the Rutherford Laboratory. Data is digitised and recorded on magnetic tape.

Twenty-five million events, each characterised by eleven parameters, have been recorded, covering a range of incident neutron energies from 50 to 150 MeV. Neutrons and protons were detected in coincidence in the final state, at fifty pairs of angles, chosen to enhance three final state processes:

(i) the n-n final state interaction
(ii) the n-p final state interaction
(iii) n-p quasi-free scattering.

In addition it should be possible to extract data on the n-d bremsstrahlung reaction.

Figure 64 shows data obtained in a preliminary run (December 1970). The kinematically allowed locus of proton energy, E_p against neutron energy E_n is
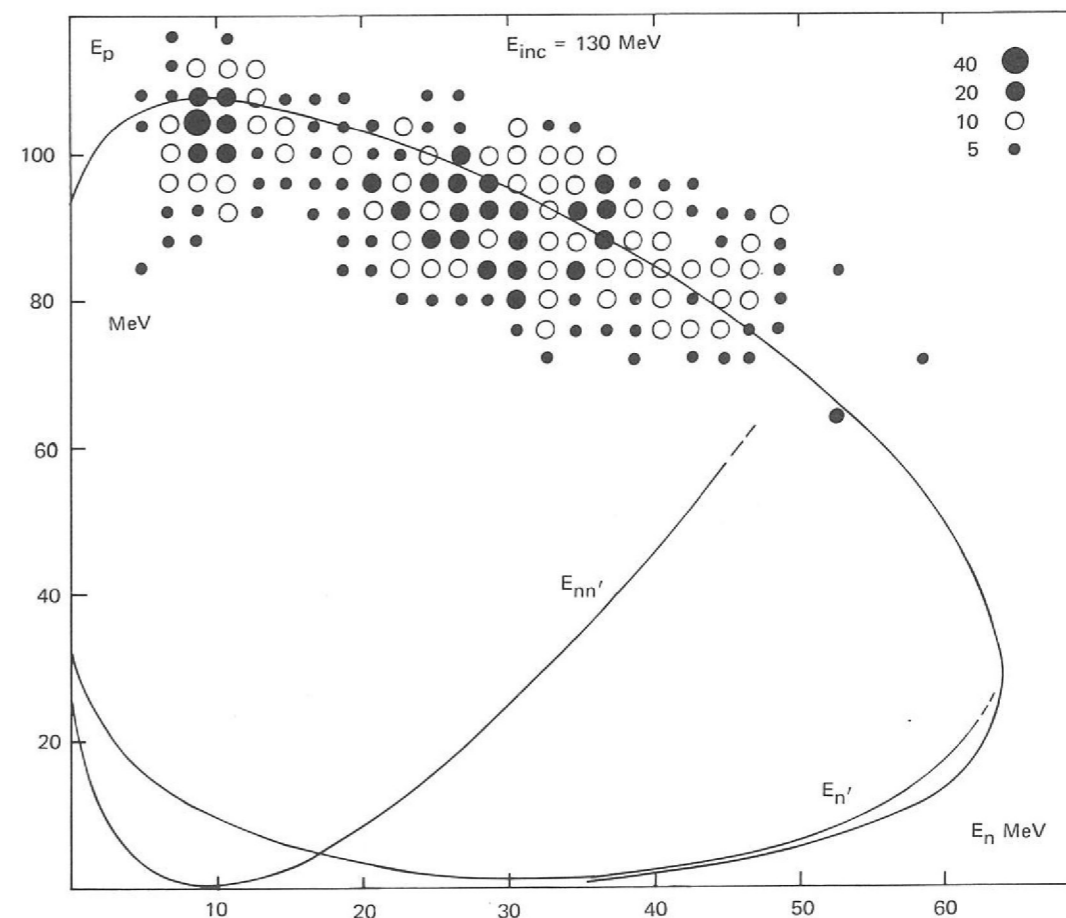
Figure 64. Proton energy versus neutron energy for an energy bin 120—140 MeV, $\theta_p = 32.0°$, $\theta_p = -65.1°$. (Experiment 44).

drawn, together with the relative energy, $E_{nn'}$ of the observed and unobserved neutron, and the spectator particle energy, $E_{n'}$. Events are observed to populate the kinematic locus with enhancements at $E_{nn'} = 0$ due to the n-n final state interaction, and at $E_{n'} = 0.9$ MeV (minimum), due to the n-p quasi-free scattering process.

In a later run, in July 1971, thirty times this number of events were obtained. Analysis will include extraction of absolute cross-sections for both final state and quasi-free interaction and extraction of an accurate value for the n-n scattering length using Watson-Migdal theory. The existence of data from a variety of kinematic conditions should indicate the reliability of this method in the proximity of the spectator particle process.

The next experiment in the series, n-d polarization at 130 MeV, is currently being set up.

Experiment 45

UNIVERSITY OF OXFORD
CERN

The Elastic Scattering of 400 MeV/c π^+ by Deuterium (ref. 43, 179)

The analysis of data from elastic π-nucleus scattering in terms of multiple scattering on the individual nucleons, requires the use of many approximations because of the complexity of the target particle. In this respect the deuteron (because of its simpler spin structure) has advantages over other nuclei. Of the existing πd scattering data the best in quality is that measured at energies greater than 1 GeV. It is the purpose of this experiment to provide good data at a point in the lower energy region which can be used to seriously test various theoretical approaches.

Figure 65. Typical pulse-height spectra from π^+d scattering using a $C_6 D_{12}$ target. (Experiment 45).
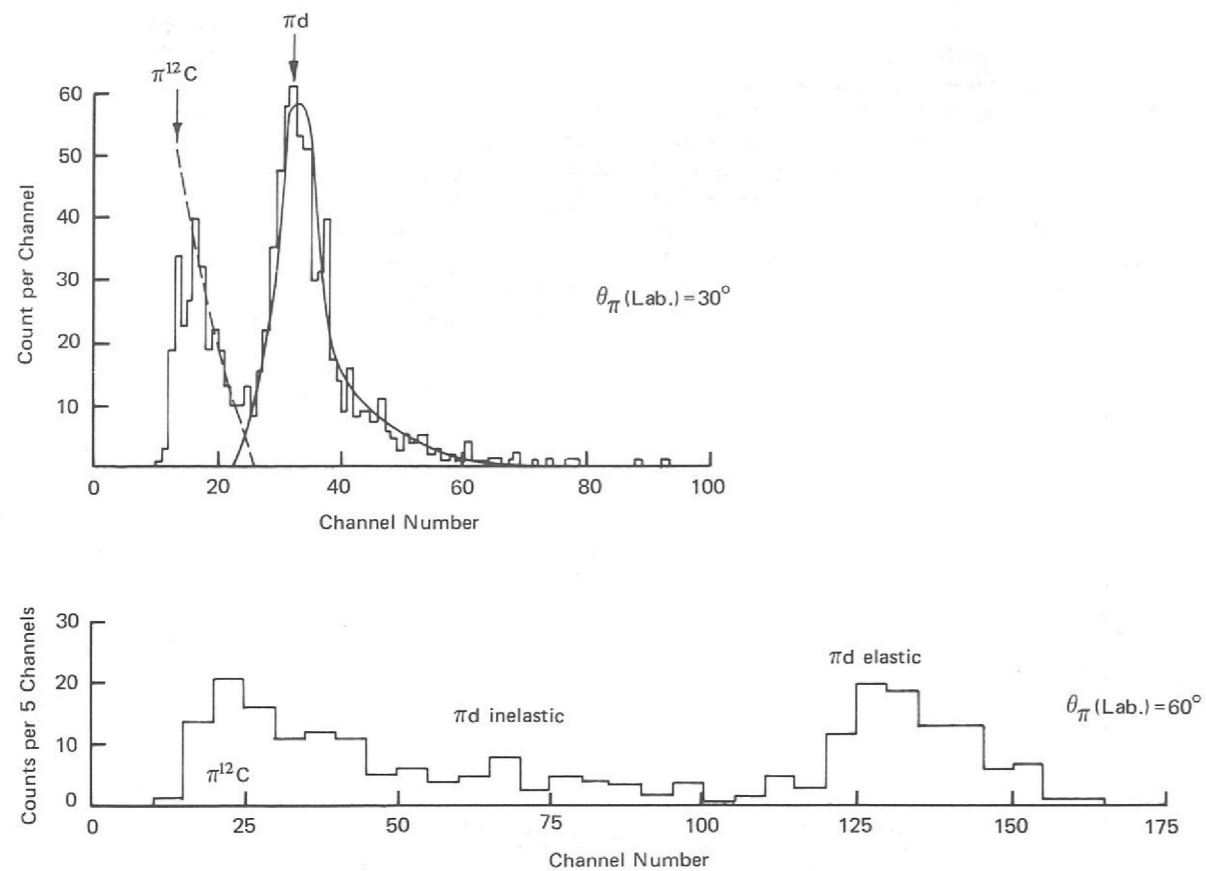
At 400 MeV/c and for large pion scattering angles ($\geqslant 120°$) the recoil deuteron can escape from the target material and is detected in this experiment by a counter telescope, Cerenkov system. At smaller angles a magnetic spectrometer measures the momentum of the incident pion and the recoil deuteron is stopped in a scintillating target composed of deuterated cyclohexane.

Preliminary measurements have shown that the technique of identifying the recoil deuteron by pulse height from the scintillating target gives adequate resolution provided the momentum of the incident pion is known. Some typical pulse height spectra from πd scattering and from πp scattering used for calibration, are shown in Figure 65. Preliminary analysis of the present data has yielded points on the πd angular distribution that are in good agreement with calculated values (Figure 66).

Figure 66. Angular distribution for πd scattering from a preliminary analysis of data from Experiment 45. Solid lines are from calculated values.
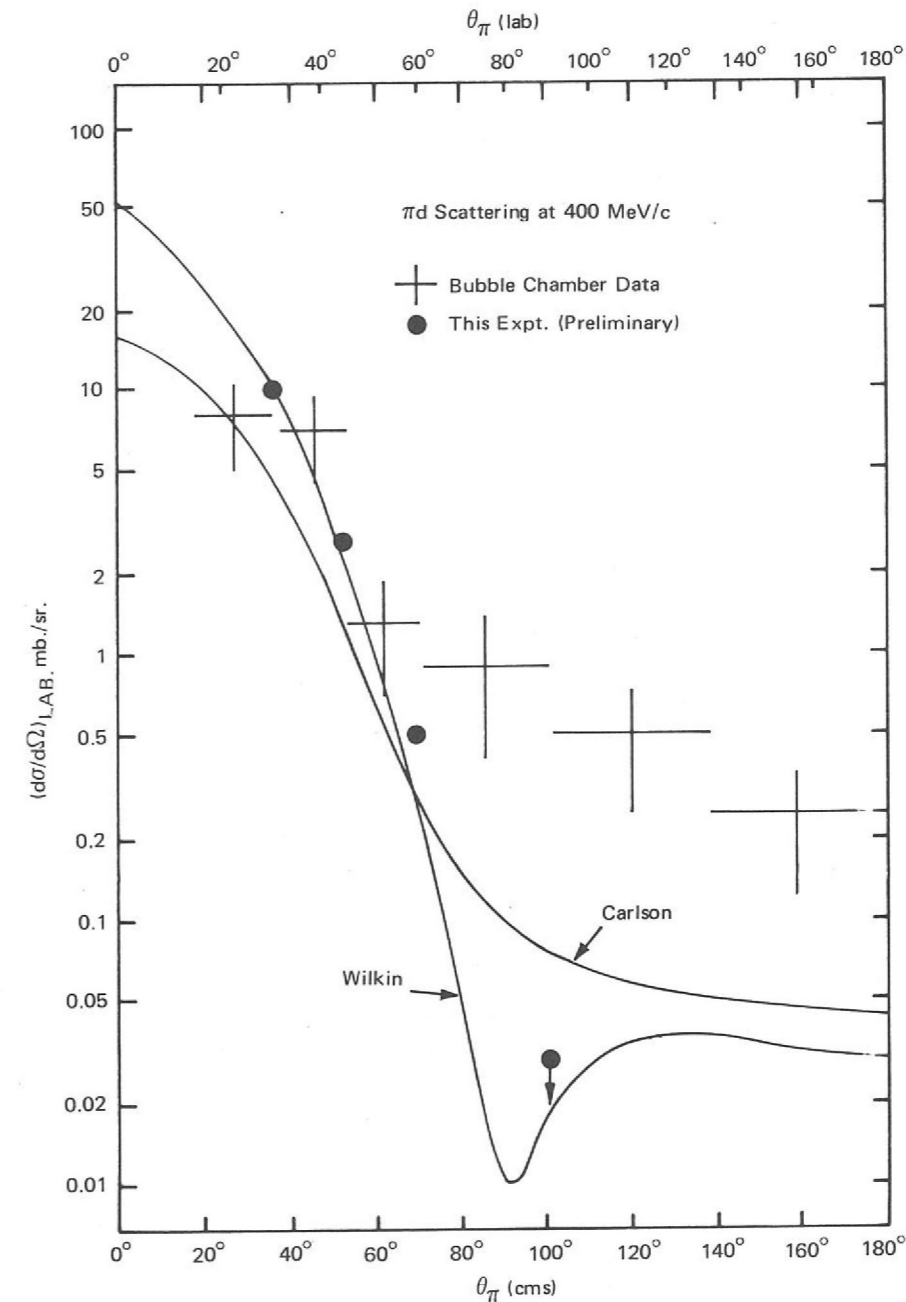
Theoretical High Energy Physics

The high-energy theory group maintains a particular interest in phenomenology, which means learning from experiment. There is a wide gap between experimental data on the one hand and fundamental theory on the other. In this middle ground the phenomenologist works, trying to bridge the gap, seeking to identify theoretical implications of the data and practical consequences of given theories. Often he proceeds by building models, in which basic ideas are supplemented by plausible assumptions, to see how far they will succeed. Even when they fail there is something to be learned.

A new direction in high-energy phenomenology is amplitude analysis. Experimental quantities are typically bilinear combinations of several scattering amplitudes. If the amplitudes themselves can be extracted, they represent the data in the most transparent form; they give the best test of given models and also the clearest indication of what modifications are needed. In connection with this development, recently the πN data at 6 GeV/c have become complete enough for a direct amplitude analysis. In other situations, the phenomenologist can eke out incomplete data by adding reasonable assumptions, or by exploiting analytic continuation.

This year has seen a lot of work on the Regge-absorption model. Regge poles are just a sophisticated formulation of Yukawa's old idea, that interparticle forces come from exchanging virtual particles. However, Regge poles alone cannot explain all the high-energy scattering data, and a plausible assumption is that corrections must be made for absorption in the initial and final states. This gives the Regge-absorption model, in broad outline; in fact there are several versions, differing in their assumptions about the Regge poles and the nature of the absorption. The first problem was to find experiments to discriminate between rival models. Eventually, results were found that disagreed with all existing models. A period of reconstruction has followed; some old assumptions have been abandoned and some new ones have been introduced. It appears that the basic idea of the Absorption Model may survive, but that the details are more subtle than originally supposed.

The theory group has also been concerned in many other areas of research. Some of the results achieved may be seen in the following summaries.

A Case for Medium-Energy Hadron Physics (ref. 256)   A report has been prepared, surveying some of the important questions that are still unanswered in medium-energy hadron physics, and also what light may be shed on high-energy dynamics. The relevant experiments lie within the range of accelerators such as Nimrod, and pose no essential difficulties beyond the reach of present techniques.

Duality   The underlying idea of duality is that there is a connection between the interactions of the strongly interacting particles (hadrons) in the low energy "resonance" region and in the high energy "Regge-pole exchange" region. Thus, in principle, results in one region can be used to predict the behaviour of the other. Various developments of this idea are discussed below:—

(i) **Dual Models of πN and $\pi\pi$ Scattering.** Two of the most serious problems of dual models are the proper treatment of fermions and the introduction of finite width resonances — an important first step to unitarisation. Work has continued on a dual model for πN scattering without parity doublets. Numerical calculations with this model indicate that it is much more peripheral than was expected from approximations to previous models of this nature, and that it can fit $d\sigma/dt$ for $\pi^- p \rightarrow \pi^\circ n$ and $d\sigma/du$ for backward $\pi^\pm p$ scattering. This emphasizes the importance of being able to calculate the model explicitly. *(ref. 100)*

Calculations have also been started on a dual model for $\pi\pi$ scattering which satisfies the Mandelstam representation and has finite width resonances. For the first time we have a model which does not violate any of the principles that are required for strong interactions. One surprising result is that the Regge trajectory does not have to rise linearly in order to produce Regge asymptotic behaviour.

(ii) **Unitarity effects.** The problem of incorporating unitarity effects in dual models has been investigated. Various possible forms for such models have been considered, and a detailed physical interpretation in terms of absorption effects has been suggested. A specific model demonstrates that amplitudes of the desired kind do exist and that one can work with them. *(ref. 93)*

(iii) **Planar versus Local Duality.** The planar version of duality, which forms the basis of the Veneziano representation, is shown to be a considerably weaker hypothesis than two-channel local duality, which assumes a local or semi-local equivalence between the s-channel resonances and t-channel Regge poles. Accordingly the planar version is less predictive. However, most of the successful predictions of local duality (e.g. exchange degeneracy) are contained in the planar version, whereas most of the unsuccessful ones are not. *(ref. 73)*

There have been two main philosophies, in applying absorptive corrections to Regge-pole exchanges. In one, the Regge poles are assumed to have wrong-signature zeros (suggested by duality) that lead directly to dips in cross-sections; the absorption modifies this structure a little, but essentially it comes from the poles. In the other approach, the Regge poles have no such zeros, and structure is generated instead by destructive interference with absorptive corrections. *Polarization Test for Absorption Models (ref. 66)*

The scattering amplitudes predicted with these two approaches differ in many details, but nevertheless both models can be fitted to most of the cross-section data. This is because a differential cross-section is the sum of squares of moduli

of helicity-flip and non-flip amplitudes; it does not tell us which amplitude dominates, nor what its phase is. To discriminate between theories, we need to separate the amplitudes.

Polarization is a flip-nonflip interference effect: $P \, d\sigma/dt = \text{Im} \, [f \, (\text{nonflip}) \, f^*(\text{flip})]$. Because elastic scattering is dominated by an essentially imaginary non-flip Pomeranchuk amplitude, elastic polarization picks out the real part of the helicity-flip amplitude, that is supposed to be given by Regge exchanges plus absorption. So here we have a clean test. For $\pi^{\pm}p$ elastic scattering, polarization measures $\text{Re} \, f(\text{flip})$ from ρ exchange. The first kind of absorption model predicts a double zero at $t = -0.5$, the second kind tends to predict a single zero. Experiment favours the former.

Modified Strong-cut Absorption Model (ref. 98, 99)

The original strong-cut absorption model, with no exchange degeneracy or wrong-signature zeros for the Regge poles fails the polarization test (above). However, it has been shown that if the elastic amplitude defining the absorption has an appreciable real part, qualitatively different from what was previously supposed, the model can be adjusted to agree with the πN high energy data, including the amplitude analysis at 6 GeV/c.

Real Part of the $\pi^-p \to \pi^\circ n$ Non-Flip Amplitude (ref. 67)

It is illuminating to separate the various components of scattering amplitudes, whenever possible. In π^-p charge exchange, the helicity flip amplitude is known to be represented rather well by the ρ Regge pole term. Such features as the cross-over phenomenon between the π^-p and π^+p cross-sections give a reasonable measure of the imaginary part of the non-flip amplitude; in particular, it is known to be peripheral in impact parameter distribution, as expected for an absorptive Regge or optical type model. The real part of the non-flip amplitude is the only element missing from a complete analysis. It can be found, however, from the recent charge-exchange polarization measurements, when all the other information above is fed in. The result agrees qualitatively with phase shift information at lower energies; in particular they both show a strongly non-peripheral character in the impact parameter representation. This result disagrees with simple absorptive Regge models, but fits nicely in to the systematics proposed by Harari on the basis of duality and peripheral resonance domination.

Polarization Reactions in Charge and Hypercharge Exchange (ref. 106)

There is still some mystery about the absorptive corrections, that have to be added to Regge-pole exchanges. In the one case where experiments permit a complete analysis of the high-energy amplitudes, namely πN scattering, it appears that none of the existing absorption models are wholly correct.

On the other hand, whatever the details may be, we expect that the net amplitudes for ρ and K_{890}^* exchange will be very similar; also the net amplitudes for A_2 and K_{1400}^* exchanges should be similar. This is because the two mesons in each case belong to the same SU_3 octet; since the leading absorptive corrections are presumably generated by the Pomeron (an SU_3 singlet), we expect these too will follow the same octet symmetry. Thus the amplitudes for meson-baryon charge-exchange processes (ρ and A_2 exchange) can be related to those for hypercharge-exchange (K_{890}^* and K_{1400}^* exchanges).

No simple relations emerge for differential cross-sections. This is because the SU_3 F/D ratios for the flip and non-flip amplitudes are different. But there are simple relations for polarization, or more precisely for $P \, d\sigma/dt$. From existing data on $\pi N \to K\Lambda$, $K\Sigma$ and $\bar{K}N \to \pi\Lambda$, $\pi\Sigma$ it is possible to predict the polarizations in $K^+n \to K^\circ p$ and $K^-p \to \bar{K}^\circ n$, that will soon be measured.

This kind of idea can be extended to predict polarization in regeneration $K_L^\circ p \to K_S^\circ p$, and in baryon-baryon or baryon-antibaryon processes such as $np \to pn$, $\Lambda p \to p\Lambda$, $\bar{p}p \to \bar{n}n$, $\bar{p}p \to \bar{\Sigma}\Sigma$, $\bar{\Lambda}\Lambda$, $\bar{\Sigma}\Lambda$, $\bar{\Lambda}\Sigma$.

Complex Regge Poles and Line Reversal (ref. 74)

The notion of resonance — Regge pole duality leads to many strong constraints, relating the parameters of different Regge poles. As a result, there are pairs of reactions $a + b \to c + d$, $\bar{c} + b \to \bar{a} + d$ (said to be related by "line-reversal"), in which the Regge-pole contributions are equal within a phase factor. For one reaction the phase is real, for the other it is rotating. Thus the cross-sections should be equal, for Regge poles alone. Experimentally, this relation is violated; generally the reaction with the real amplitude has a bigger cross-section than the other. Simple absorption corrections also break the line-reversal equality, but in the wrong direction. However, if real Regge poles are replaced by complex conjugate pairs of Regge poles, line-reversal breaking has the correct sign.

A Modified Absorption Model with Exchange-degeneracy

A new approach was motivated by the failure of simple absorption models to explain line-reversal breaking (see above), and also their failure to fit $\pi^-p \to \pi^\circ n$ charge exchange polarization. It was realized that agreement would be restored if the phase of the absorptive cut was modified in a simple way, for non-planar graphs. The usual absorptive cut is retained for planar graphs, and all cuts are restricted to non-flip amplitudes. The Regge poles have exchange degeneracy and wrong-signature zeros. Although a theoretical basis for this prescription is still lacking, the resulting model gives a good description of the amplitudes that can now be directly extracted from high-energy two-body data.

Inclusive Reactions (ref. 69, 103)

In the expanding field of interest of processes of the type $a + b \to c +$ anything, several problems have been studied:—

(i) One feature of these reactions is the phenomenon of "scaling". One way of stating this is to say that a single particle distribution is a function of the ratio s/M^2, (where s = total cm energy, M = the missing mass of "anything") rather than of the variables s, M^2 separately. This indicates that we expect the dependence on s at a fixed value of M^2 to be closely connected to the M^2 dependence at fixed s. It was shown that the general shapes of the inclusive distributions (e.g. M^2 spectrum) could be well understood in terms of the more familiar behaviour of pseudo-two-body cross-sections as a function of beam-momentum.

(ii) Since an inclusive reaction is the sum of several (usually many) "exclusive" reactions (i.e. processes in which the entire final state is known), it may be possible to understand features of the inclusive reaction in terms of the

constituent exclusive reactions. In specific kinematic regions, e.g. the triple-Regge (T-R) region, the missing mass may not be too large and the average multiplicity consequently low. It turns out that the diffractive production of certain resonances contributes significantly to the T-R region. Therefore such a process can allow one to set bounds on the Regge trajectory appearing in T-R expressions. Somewhat surprisingly, these bounds turn out to be extremely good estimates of the relevant trajectories.

A_1 Production
(ref. 68)

Recent techniques for analysing data on 3π meson production allow one to study the individual partial waves of the diffractively produced 3π-system. New features revealed by this sophisticated method include:

(i) the A_1 cross-section shows a distinct falling-off with energy and

(ii) in contrast to evidence in favour of s-channel helicity conservation in other diffractive processes, it is the t-channel helicity which appears to be conserved.

A dual six pion amplitude has been used to describe the production and decay of the A_1 with no extra parameters. The above features appear naturally in such a model which also successfully predicts the S- to D-wave ratio in the A_1. The energy dependence of the A_1 production will be much better understood once the cross-section is known at Serpukhov.

Polarization in
Multi-Particle
Reactions
(ref. 94)

There is potentially a lot of information to be gained from studying polarization in multi-particle production. Simple models indicate the sort of thing that can be learned, for instance, the way in which the phase of an amplitude depends on relative orientations that do not appear in two-body reactions. Also, the dependence of polarization on a mass variable provides a new way to detect resonances.

Impact Parameter
Representations
(ref. 102)

A critical examination of the approximations made in deriving the Glauber and Blankenbecler-Goldberger representations of the scattering amplitude, leads to a unified treatment of the two. This brings out the heirarchy of approximations both in coordinate space and momentum space.

The Charge Radius
of the Pion
(ref. 101)

The slope of the pion charge form factor has been calculated using the Gilbert-like dispersion relations for the form factors. The slope is calculated to be $\approx 2\cdot40$ GeV^{-2}. The ρ-dominance value of this slope is $\approx 1\cdot72\ GeV^{-2}$.

Nomlinear SU_3
Symmetry
(ref. 52, 53)

When SU_3 is treated as a nonlinear symmetry realised by the appearance of massless scalar mesons in the symmetry limit, and Regge asymptotics are imposed on the scattering amplitudes of the theory, the Gell-Mann -Okubo mass formula can be derived without ad hoc assumptions. Pursuing this approach to SU_3 symmetry leads to some further interesting results. In particular, the F over D ratio for the coupling of the A_2 Regge trajectory to baryons has been related to the baryon masses, and the ratio of meson mass differences to baryon mass differences has been expressed in terms of total cross-sections.

Small-angle proton-proton scattering has an approximately exponential form, $d\sigma/dt = A\ exp(bt)$, where $t = -(momentum\ transfer)^2$. Up to 70 GeV bombarding energy, the celebrated "shrinking" phenomenon is seen; b increases logarithmically with energy. This suggests a dominant Regge pole — the Pomeron — in the high energy limit. The rate of shrinking then depends on the slope $d\alpha/dt$ of the Pomeron trajectory $\alpha(t)$.

Shrinking in
High-Energy pp
Scattering
(ref. 8, 9)

Colliding proton beams at CERN have now reached much higher energies, corresponding to 1500 GeV on a stationary target. First results indicate that the shrinking is much less at these energies, contrary to the simple Regge pole picture. There are various ways to explain this. One interesting possibility is that the Pomeron trajectory actually has zero slope $d\alpha/dt = 0$. The observed shrinking is then due to secondary trajectories: b does not increase indefinitely, but tends to a finite limit; the apparent logarithmic increase at lower energies is only approximate. Another possibility is that $d\alpha/dt$ is not zero, but is nevertheless smaller than previously believed: again, secondary effects must be invoked.

Pion-Pion Scattering is a perennial topic because experimental information is indirect, yet theoretically it is a very simple process. There are problems both in extracting the $\pi\pi$ signal in various experimental situations, and in interpreting it. A renewed attack on extracting $\pi\pi$ phase shifts from πN elastic scattering information has been made, with emphasis on the recent very accurate $\pi^{\pm}$ data over the Δ region. This approach depends on interpreting the contribution to πN elastic scattering from the exchange of a pair of pions, which contain information on $\pi\pi$ scattering. Greatly improved precision has now been achieved, so that it is becoming competitive with other sources of $\pi\pi$ information. Secondly, there has been continuing study of the S* effect, the $K\bar{K}$ I = 0 threshold enhancement, and its coupling to the $\pi\pi$ system. The status of the S* is important for classification schemes, such as the quark model. In addition, the coupling of the $\pi\pi^-$ channel is interesting in its own right. There is a pronounced cusp phenomenon, the detailed form of which can resolve the long-standing "up-down" ambiguity of the I = 0 S-wave phase shift. In another piece of work, unitarity corrections to Weinberg's celebrated prediction of low energy $\pi\pi$ scattering parameters from Current Algebra have been re-examined. It seems that rather definite statements can now be made. The parameters are still not empirically determined with any precision, although this should shortly change. Finally, a new slant on the famous Chew-Low extrapolation method for extracting $\pi\pi$ scattering information by identifying the pion exchange contribution to $\pi N \rightarrow \pi\pi N$ has been discussed. The idea is to adopt the currently fashionable "inclusive" approach and measure $\pi N \rightarrow N + anything$. The pion exchange contribution, if it can be identified, contains information on $\sigma_{tot}^{\pi\pi}$. The experimental requirement is to measure slow neutrons with great precision, so it is at once both simple and demanding.

Pion-Pion
Scattering
(ref. 108, 134)

Dispersion relations are of great use in extending our knowledge of elementary particle physics — for example, by predicting quantities which may be difficult to measure directly, in terms of integrals over other quantities which are much simpler to measure. Our experimental knowledge of the πN interaction below 600 MeV/c has progressed little in the last few years except for the Cambridge-Rutherford Laboratory total cross-section measurements. Nevertheless dispersion relations enable us to use the wealth of information above 600 MeV/c together with the low energy $\pi^{\pm}p$ total cross-sections to make accurate predictions for the low energy amplitudes. The level of accuracy is such that Coulomb and mass difference effects cannot be ignored but it turns out that only the S and large P-waves are influenced by these corrections, the predictions for the small P and for the D and F waves being remarkably stable.

Dispersions
Relations
(ref. 60, 61, 63, 64,
96, 109)

These predictions can equally well be continued below threshold and by extending them towards the region of the $\pi\pi \rightarrow N\bar{N}$ process we obtain valuable information on the $\pi\pi$ interaction. The πN D-waves are particularly important in distinguishing between various forms proposed for the low energy S-wave $\pi\pi$ interaction.

Dispersion relations have proved most fruitful in connection with the πN system but now there starts to be sufficient data for their application to the KN and $\bar{K}N$ systems to be profitable. For example backward dispersion relations particularly favour the Sens γ set of K^+p phase shifts and work is now underway to see whether the individual partial waves of this set of phases are consistent with partial wave dispersion relations.

Phase Shift Analysis (ref. 3) One of the main themes of the Rutherford Laboratory experimental programme is two-body scattering measurements, the data from these experiments being usually subjected to some form of amplitude analysis. In this field there is a particularly close collaboration between members of the theory group and the Bristol-Rutherford Laboratory experimental group who are now measuring K^+p and π^+p elastic scattering distributions to a high precision. Rapid phase shift analysis of preliminary data affords the chance of feed-back while the experiment is still in progress and enables detailed examination of regions of potential interest.

Data Representation (ref. 71, 72) The problem of continuing a scattering amplitude throughout its domain of analyticity, given inexact information about the amplitudes in the physical region, is of practical interest in many applications of S-Matrix theory. Conventionally this has been done using Cauchy's integral formula to write a dispersion relation, finite energy sum rule, etc., for the amplitude.

However, given the experimental errors in the amplitude it has been found possible to express, in integral form, the analytic function that minimises the difference between it and the data, weighted according to the statistical errors. Thus, for the first time it is possible to find the optimum values for coupling constants, Regge parameters, etc., together with realistic statistical errors for these constants.

A Solution of the Reaction Matrix Equation in Nuclear Matter (ref. 85) A new mathematical solution of the integral equation for the reaction matrix has been presented. This quantity is used in nuclear matter calculations, where the energy etc. are expressed by the help of it. The method can be applied if the two-nucleon potential acts in a limiting number of orbital states, and possesses a first order singularity at the origin.

Nucleon-Nucleon Potential The latest Dubna and Livermore two-nucleon phase shift data have been used to improve the phenomenological two-nucleon potential. The potential obtained describes the two-nucleon data with $\chi^2/($number of data $-$ number of parameters$) = 2$.

Calculation of ^4He Properties A calculation of the fundamental characteristics of the ^{4}He nucleus has been undertaken. The many-body approach was chosen and the corresponding method developed. The binding energy, the mean square radius and the density of nucleons

can be expressed by the help of the reaction matrix for finite nuclei. The computation consists of two parts: the calculation of the two-nucleon singlet state contribution to the physical quantities and the triplet state contribution. The first part is completed and gives already as a final result that the Coulomb energy of the ^{4}He nucleus is 0·82 MeV, in full agreement with the experimental value. The triplet state calculation is in progress. It is hoped that the method can be used also for ^{12}C and ^{16}O.

Part of the muon detector used in the ISR search for the intermediate boson and other massive particles. This part of the apparatus is enclosed in a light tight "igloo". (CERN Photo).

INSTRUMENTATION FOR
HIGH ENERGY PHYSICS

Instrumentation for High Energy Physics

The work described in this chapter is concerned mainly with the designing and commissioning of apparatus to enable experiments in particle physics, as described in the preceding chapter, to be carried out.

The setting up of a new experiment often requires new and unique apparatus to be provided. A particular example this year is the experiment to search for the Intermediate Boson, the postulated "carrier" of the weak interaction, although this is not the only purpose for this experiment. The experiment is being carried out at the Intersecting Storage Rings, CERN, Geneva, which is the highest available energy source for proton-proton interactions in the world. A large part of the instrumentation described below is for this experiment. The preparation of the apparatus has required the solution of novel problems, e.g. in the construction of very large mirrors. Another aspect, not directly related to the instrumentation, has been the problem of transportation of both heavy and delicate equipment safely to CERN after assembly and testing at the Rutherford Laboratory. The absorber and magnet assembly has a total weight of 245 tons, with each of the 26 magnet plates weighing 8 tons. To solve the overall problem, a system of pallets and large aluminium containers was used, and shipment of the complete apparatus, with a total weight of 470 tons, required 33 vehicle loads.

Other instrumentation described below involves the continuous process of improving existing apparatus and development of new equipment, e.g. particle detectors. Reports on electronic instrumentation, development of targets and bubble chamber operations complete this chapter.

INSTRUMENTATION FOR THE SEARCH FOR THE INTERMEDIATE BOSON AT THE ISR, CERN. (EXPERIMENT 23)

The Muon Magnet Construction and assembly of the full scale Muon Magnet at the Rutherford Laboratory was completed in February 1971. A magnetic field survey, prior to shipment to CERN, compared favourably with the model magnet results.

After re-assembly of the magnet at CERN a preliminary field survey was made to check the reproducibility of the results previously obtained at the Rutherford Laboratory, since this would allow other construction work around the magnet to go ahead with confidence. The comparison of fields was complicated by the re-distribution of the magnet plates that has been carried out to optimise the gap spacing. This was done to ensure that the 4 m x 2 m double gap optical spark chambers could be slotted into the air-gaps between the plates, in spite of irregularities in thickness and flatness of the plates. At the working current of 600A the plate to plate field variations were no more than the measuring error of ±1·5% except in the case of four plates. Two of these varied from the mean field by only −2% whilst the remaining two nearest to the beam intersection region had fields 3·5% lower than the mean value perhaps due to the plate ends being outside the projected area of the coil.

The effect of the stray field from this magnet on the ISR beams has been made small by introducing shield plates. It is measured by determining the path integral $\mathrm{Bd}\ell$, where B is the stray field, along the path (ℓ) of the ISR rings. In situ measurements appear to give a result 25% larger than expected, although the measurement is difficult, the estimated error being ±20%. However, the magnet is being operated with no apparent effect on the ISR beams.

Figure 67. The assembled magnet for Experiment 23 (*CERN Photo*).
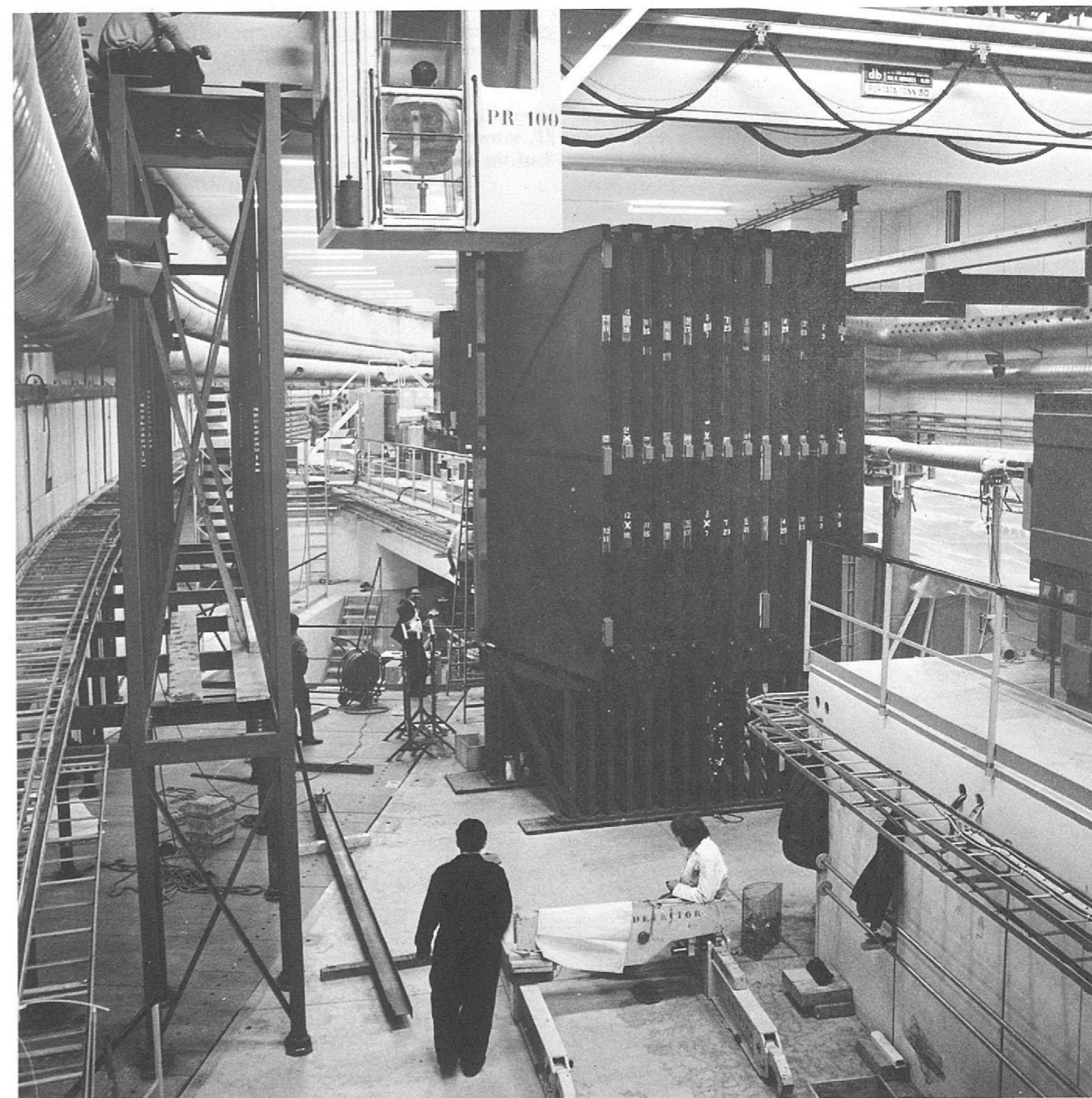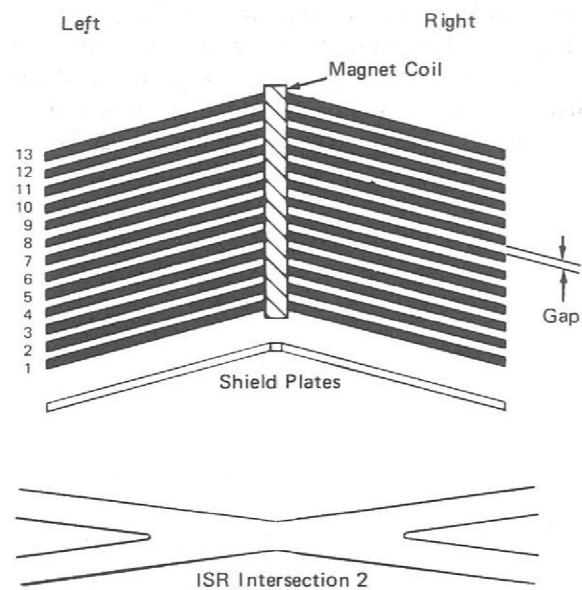
Figure 68. Schematic diagram of the magnet for Experiment 23, showing its position relative to Intersection 2 of the ISR.

The Thick Plate Spark Chambers

The thick plate spark chambers are double gap optical chambers having an active area of 4 m x 2 m. The chambers are suspended in 100 mm wide gaps between the 100 mm thick steel plates of the muon detector magnet. Each chamber is viewed through a vertical edge and the bottom edge. A total of 24 units (48 single gaps) were required, each unit weighing approximately 600 kg.

It was important to arrive at a simple yet effective design because of the number and size of the units to be manufactured and therefore the large multiplying costs. The most important design and construction features were:—

1. To achieve a spark chamber as free from optical obstruction as possible (as few clamping bolts and internal spacers as possible).

2. To achieve an assembly as flat as possible to ensure an unobstructed view of sparking and also to prevent uncontrolled electrical breakdown.

3. To design a low cost edge joint (approx. 1200 metres total length) which would be leak tight against neon and helium gas and would withstand the considerable handling and transportation between Rutherford Laboratory and CERN.

4. Material finish and cleanliness consistent with good practice in high voltage work.

Each single gap comprised two 4·4 mm thick aluminium sheets spaced 1 cm apart by perspex optical strips around the perimeter and cross-linked polystyrene spacers in the centre, positioned to cause the minimum optical obstruction. The curvature of each sheet was measured and they were matched to achieve an overall flatness for each chamber. The perspex spacer strips are bonded to the sheets to form a gas seal. Use of steel leaf springs enable these edge joints to be maintained under compression with relatively few bolts, giving good optical access to the chambers.

An overall production rate of one gap per week was attained. To achieve this, jigs and tools were designed and built at the Rutherford Laboratory and loaned to a manufacturing company which produced kits of parts. A Rutherford Laboratory team of craftsmen carried out bonding, gas testing, final assembly, spark testing and packaging for shipment to CERN. Each spark chamber was assembled on to a timber frame at the Rutherford Laboratory and remained on this frame for all tests and handling until final assembly in the magnet at CERN.

The optical spark chambers are energised by spark-gap type pulser units which *Pulser Units* connect directly on to the spark chambers. Each unit contains clearing field coupling components. A small metal cylinder, approximately 9 cm long by 7 cm diameter and designed for pressurising at up to 60 lbf/in² with high purity nitrogen, houses the spark-gap which is fixed at 1 mm between hemi-spherical electrodes of heavy alloy. The operating voltage may be varied over a wide range by altering the gas pressure.

An interesting feature of the spark-gap is that the co-axial trigger electrodes and feed-through insulator are conveniently formed using a slightly modified automobile sparking plug.

Figure 69. A view of the large muon detector system used in Experiment 23. The large mirrors can be seen to the right. (*CERN Photo*).
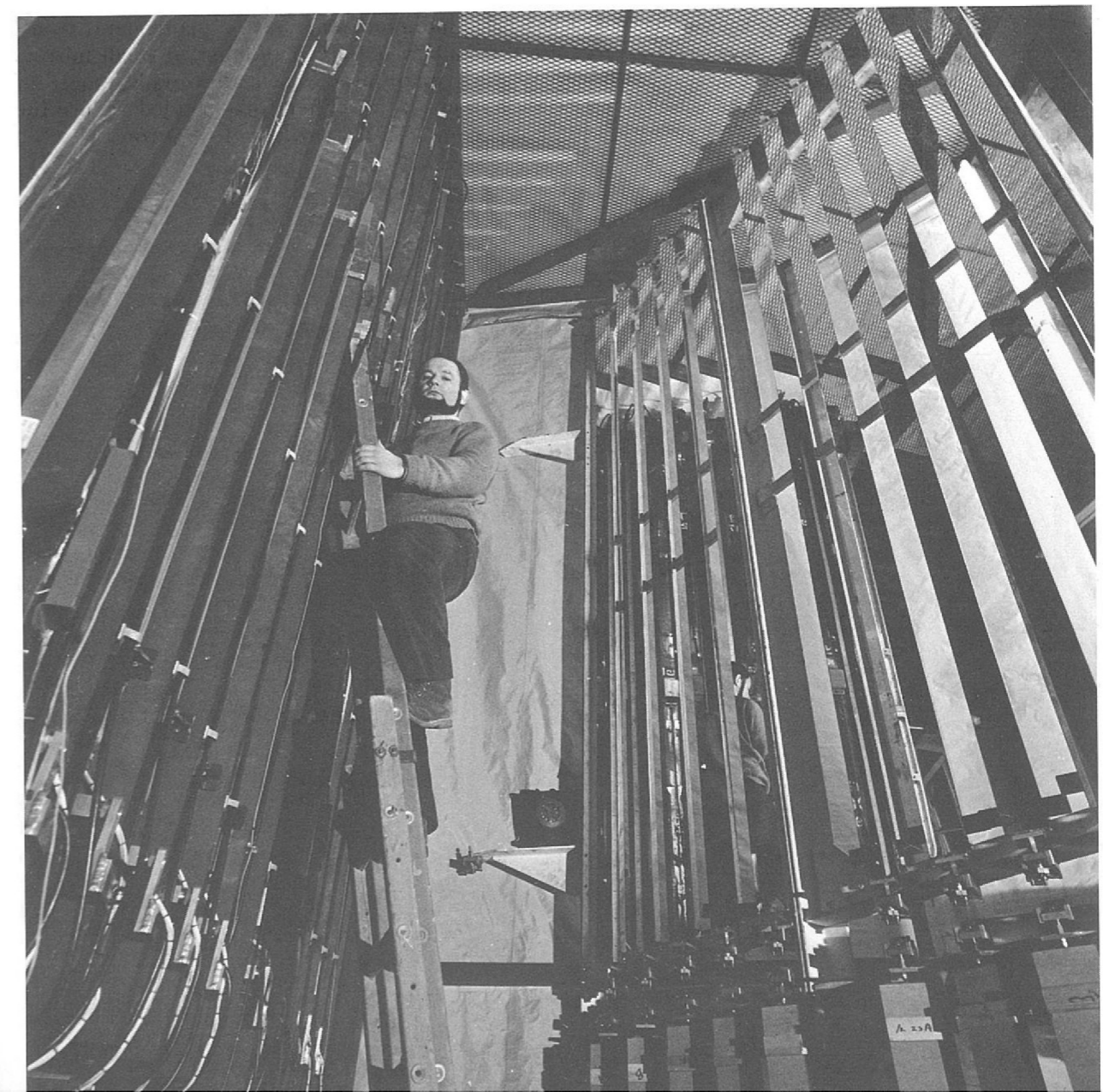
Special Handling Equipment The installation of the large spark chambers between the magnet plates required development of special handling equipment. This was partly because of their size and weight (see above) and limited clearance between the magnet plates, but more particularly because of the restricted access due to the fact that the whole assembly is inside a light tight enclosure which is required for the photographic recording system. The solution was to use a modified fork-lift truck and guide rails, to accurately control its position, when installing the chambers.

The Light Tight Enclosure The light tight enclosure referred to above is formed by attaching panels of a laminate composed of nylon fabric, mylar film and aluminium foil to a steel frame surrounding the entire apparatus. This covering material, combining light-tightness and electrical screening, is both light in weight and strong.

The Optical System The 4m x 2m optical spark chambers in the muon magnet require a complex system of mirrors to enable the two orthogonal views of each chamber to be viewed by one camera, using 70 mm film. These mirrors also equalise the optical paths from each chamber to the camera. A total of 100 mirrors, ranging in size from 400cm x 9cm down to a few centimetres square, are used. The optical system is shown in Figure 70. It has a focal length of 17 metres with a depth of focus of approximately ±2½ metres.

In addition to calculation of the optical paths, actual assembly of the system required accurate positioning of the mirrors with well-defined axes of rotation for the final alignment.

The Large Mirrors Because of the limited size of existing aluminium evaporation plants, large front-aluminised plate-glass mirrors are difficult to obtain. A number of small mirrors butt-jointed together, although possible in principle, have the disadvantages of visible join lines and poor overall flatness. It was therefore decided to use the aluminised melinex plastic film that is commercially available for mirrors.

Figure 70. The optical system for Experiment 23.
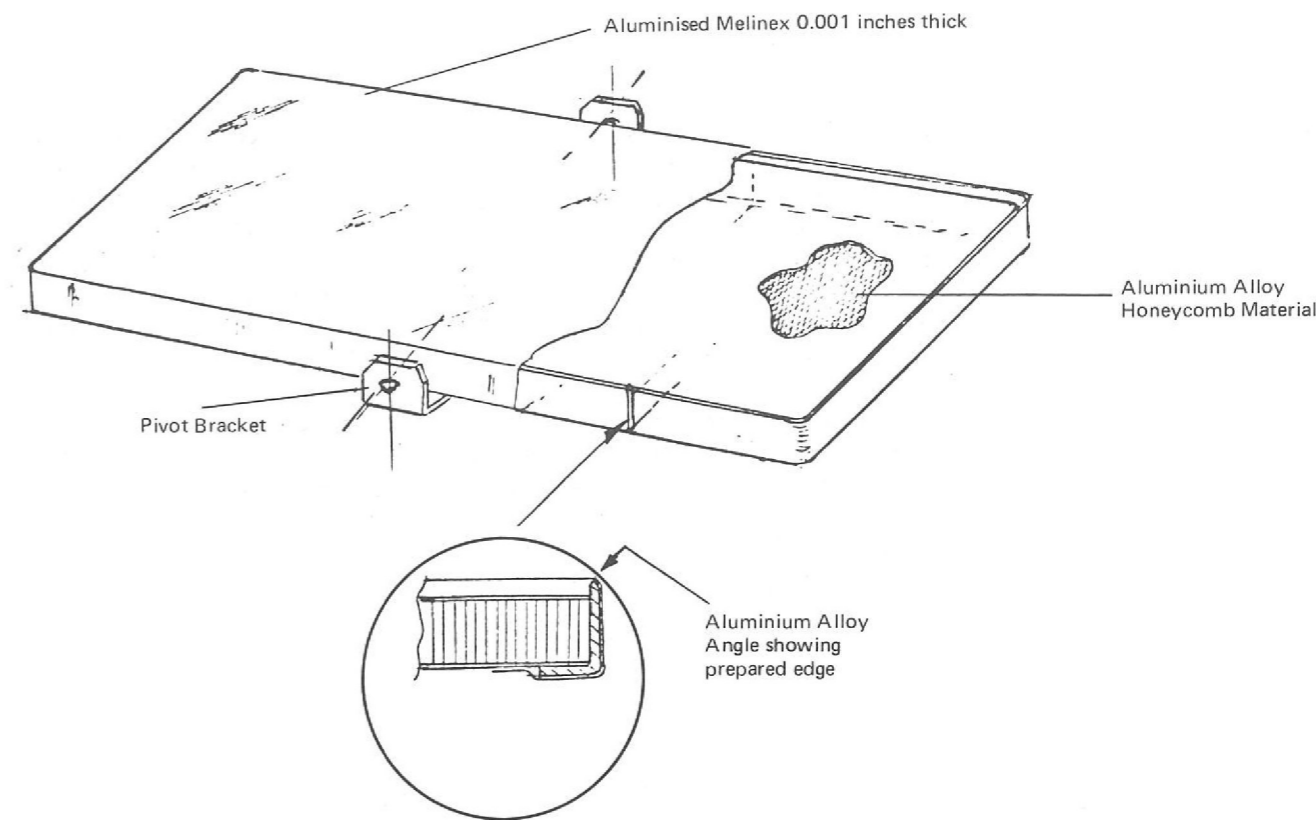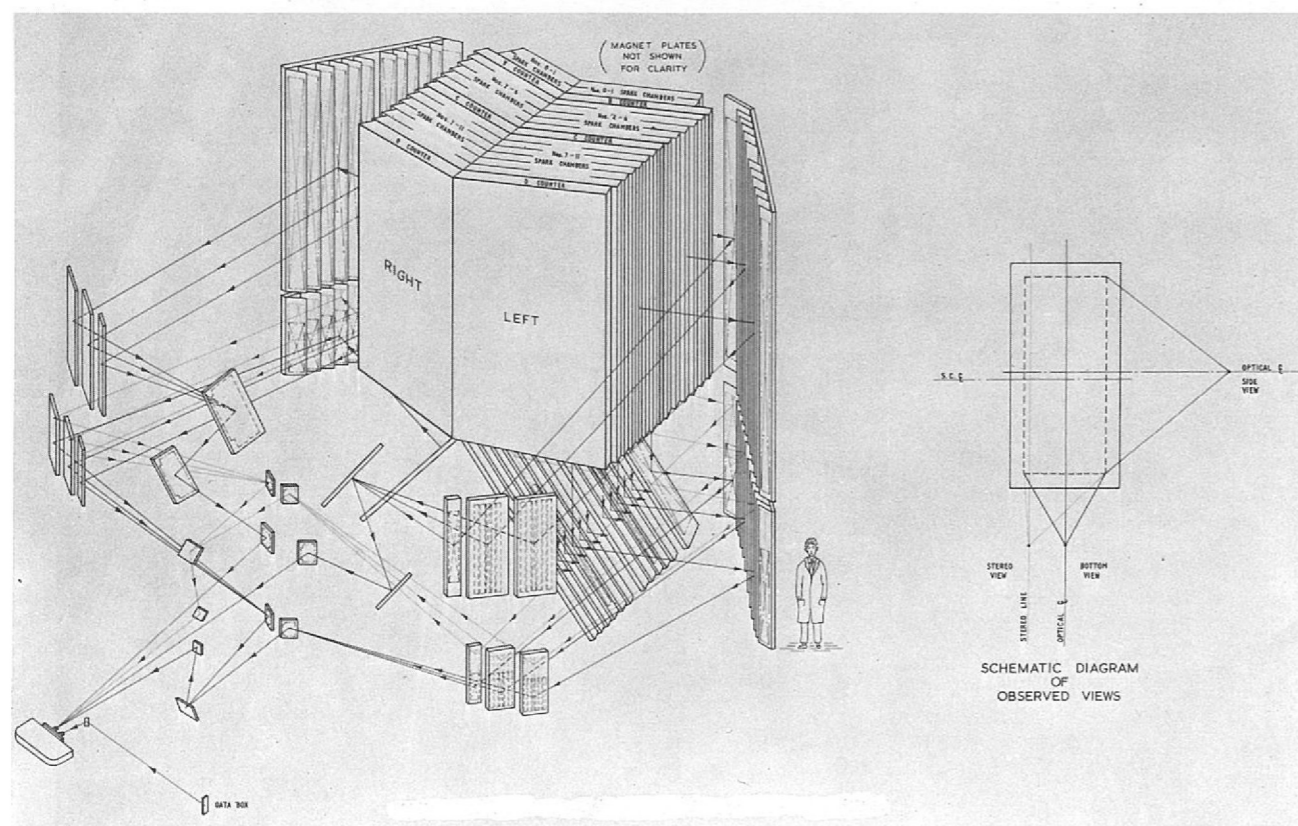
Figure 71. Constructional details of the large mirrors (Experiment 23).

A mirror is formed by stretching the film over a baseboard which has a narrow, very flat, raised edge as the only region of contact. The film is stuck down at the edges and then heat shrunk to obtain a flat surface. The baseboard materials are extruded aluminium alloy channel for the long, narrow mirrors and 50 mm thick sheets of a commercially available honeycomb material for the large mirrors. The latter consists of an aluminium foil honeycomb sandwich between thin sheets of glass-epoxy resin, and the raised edges are formed by aluminium angle extrusion fixed to the edge faces. The raised edges were machined flat to better than 100 μ m over distances of up to 4 metres.

The mirrors were checked for distortion using an auto-collimation technique with an optical path of 17 metres. In this, the position of an object is compared with the position of its image after reflection in the mirror. The largest deviation measured was ½ mm, well within the specification.

The advantages of this type of mirror are:—

1. They are very light so that an inexpensive and lightweight support structure may be used.

2. They remain flatter than glass mirrors when subject to temperature cycles.

The Camera Turret Assembly Three cameras, operating in sequence, are used to record data from the optical spark chambers. They are mounted, together with a TV camera, laser and theodolite base, on a turret with six stations. The cameras are positioned alternately between the other devices.

The turret can be rotated by six steps of 60° through 300° so that each camera or other device can be accurately positioned at the spark chamber viewing station by remote control; the cameras are used for recording events and the other devices for checking alignment of the optical components and operating condition of the spark chambers. All the equipment is required to operate consistently and reliably throughout an experimental run of several days duration since access to equipment in the area during runs is not possible because of the radiation danger.

Banks of scintillation counters are required to reduce the number of triggers due to cosmic rays in the experiment to search for the Intermediate Boson. The largest and most complicated bank consists of 24 sheets of scintillation material 20 mm thick x 100 cm wide x 69 cm high, arranged so that two assemblies hang either side of the central spine 2 sheets wide x 6 sheets high. To provide for easier handling during construction, shipping and assembly, each bank was divided into an upper and lower assembly of six sheets each (see Figure 72); the two assemblies when bolted together measure 5·4 m x 2·1 m x 83 mm thick, and weigh 550 kg.

The phototubes are sited at the top and bottom of the assemblies to keep them outside the stray field of the magnet plates; also the upper tubes are orientated at right angles to fit into the restricted clearance between the top of the magnet and the underside of the ISR cranes. To minimise cost, the amount of perspex used in the light guides was reduced by adopting a multi-strip design. The light guides are "adiabatic", that is each light pipe in each assembly is the same length within a few centimetres. The other advantage of this design is that the amount of Cerenkov light generated in the perspex light guides is kept to a minimum.

Figure 72. Lower half of a scintillation counter before fitting light tight covers. This was inverted as shown to simplify assembly. (Experiment 23).
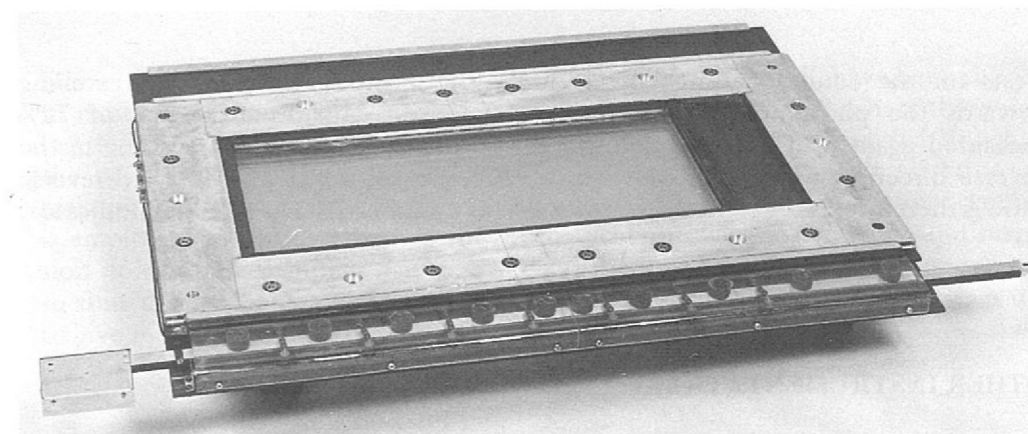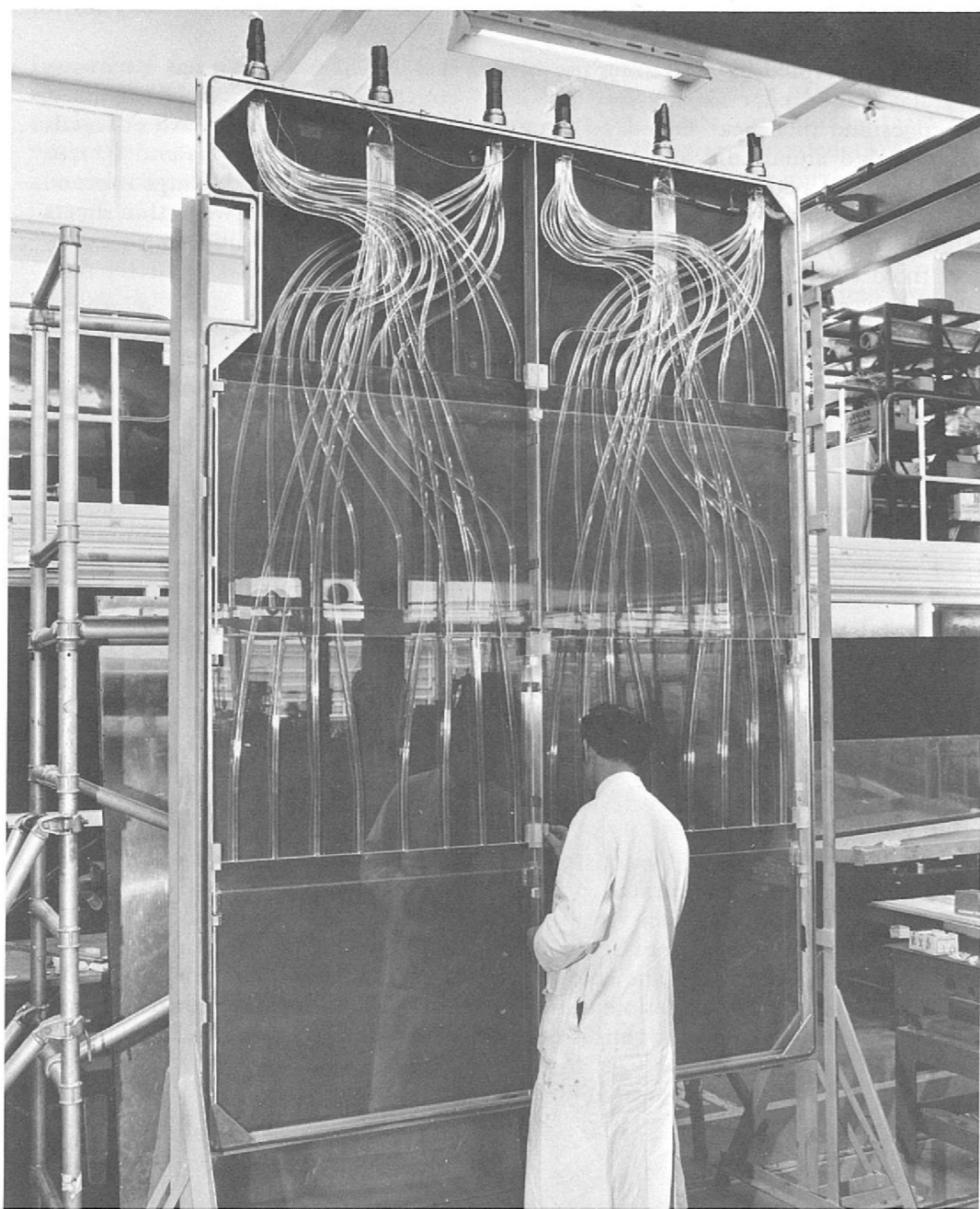
Figure 73. Wire spark chamber with magnetostrictive read-out.

On the other side of the ISR intersection point to the Muon Magnet (described above) is a large wide angle spectrometer. Part of its detection system is a set of wire spark chambers comprising a total of 30 gaps. For the quark search 6 modules each of 3 gaps are used. The other chambers will be required at a later date in various configurations on the British and Scandinavian experiments to be mounted on the spectrometer arm. *Magnetostrictive Wire Spark Chambers*

The chambers are designed with magnetostrictive read-out, the wands (see below) being readily demountable, and have active regions ranging from 177 cm x 90 cm down to 50 cm x 25 cm. The pitch between wires is 1·0 mm and wires are mostly wound at 0°, 30° and 90° to the vertical. A few chambers have been wound with wires at other angles. The chambers can be easily dismantled, should repairs be required: they are required to remain gas-tight during operation with high purity neon/helium gas continuously circulating via a gas purification system. All chambers were manufactured commercially.

The wire spark chambers are activated by twelve "line-type" thyratron pulsers. A ceramic tetrode is used to discharge a line consisting of up to twelve paralleled 30 metre lengths of co-axial cable. Connection to the spark chamber inputs is made via corresponding 8 metre lengths of similar cable. *Pulser Units*

A general purpose clearing field unit has been developed for use with the wire spark chambers. This enables the clearing field voltage to be applied in the form of a pulse, for a pre-set period of time, immediately following the firing of the chamber. Thereafter the clearing field is reduced to a lower level (15 volts) until the next high voltage pulse in the chamber. The unit is designed to operate over a voltage range up to 400 V and the pulse width is variable over the range 10 to 160 ms. *Pulsed Clearing Field Units*

A Cerenkov counter is used to veto cosmic radiation of comparable energies and directions to particles produced in proton-proton interactions at the intersection region. *Cerenkov Veto Counter*

The counter consists of four sections arranged in an arc about the intersection region. Each section contains a perspex block 45 cm wide x 38 cm high x 19 cm thick in which the Cerenkov light is produced when charged particles pass through. Six photomultipliers are mounted on the 45 cm x 38 cm face nearest the intersection region, the opposite face being roughened and coated with matt black paint to give minimum reflection. The tubes are positioned on a circle concentric with the horizontal axis of the block, and alternate tubes are electronically grouped to produce two outputs in coincidence. Therefore for an event to be recognised, two adjacent tubes must record the event.

Tests on the counters using cosmic radiation showed that particles travelling towards the photomultiplier tubes were counted with an efficiency of 72% measured against an external counter telescope, while particles travelling in the reverse direction were counted with an efficiency of 0·3%. The forward/reverse ratio is therefore 240:1, and the counter acts as a very efficienct direction indicator.

OTHER INSTRUMENTATION

Multi-Wire Proportional Counters The demand for Multi-wire Proportional Counters has increased during the year. Several experiments now use them for making beam profile measurements, since they allow rapid beam tuning during the setting-up phase of an experiment. Operational experience over several months has shown these counters to be robust, reliable and to require very little adjustment.

The design of larger Multi-wire Proportional Counters has continued during the year. One type having an active area of 200 mm x 200 mm is now in use. It has a wire plane for the high voltage electrode, instead of foil or mesh, giving the chamber greater transparency. Also, since the high voltage wires can be wound perpendicularly to the sense wires, surface tracking problems on the frame are considerably reduced making a guard strip unnecessary. The counter frames have been fabricated using a low-cost polyester glass laminate. The wires can be wound with the manual winding technique developed originally for wire spark chambers but slightly modified to handle the 20μ m diameter sense wire. The wires are uniformly tensioned by inflating a pneumatic tube placed between the wires and the frame before fixing them to the frame.

A unit is formed from two of these 200 mm x 200 mm counters mounted in an aluminium alloy box which provides both electrical screening and mechanical support for the amplifier cards. The box is so constructed that the sense wires have an accurately known spatial relationship to indexing pegs on the outside of the box allowing alignment to be carried out externally.

Three units of this type have been supplied for use in the π9 beam line. One unit is set at the first focus of the beam and has both its counters orientated to have their sense wires vertical and offset to each other by 1 mm to provide the best momentum resolution. Two other units are placed in the beam near the polarized target. These have counters with both vertical and horizontal sense wires to determine the profile and direction of the incident beam. A photograph of one such unit is shown in Figure 74.

Further work is in hand on larger counters with active dimensions of up to 2 m x 2 m. It is expected that counters measuring 1 m x 1 m will be available in the first half of 1972.

Magnetostrictive Wands Magnetostrictive read-out in a wire spark chamber is accomplished by placing a magnetostrictive delay line over the spark chamber wire plane. A spark current induces a mechanical disturbance in the magnetostrictive material and travels down the line at the local velocity of sound. The delayed disturbance eventually passes through a coil situated in a magnetic field where it is transformed into an electrical pulse and amplified. The position of the spark is then directly related to the time delay. The delay line with its acoustically-damped suspension, coil, magnet and amplifier are usually mounted on a "wand" which is readily detachable from the spark chamber.

During the year a total of 90 wands, up to 2·5 metres in length, have been supplied to experimental teams. Most of these were for Experiment 23 where there was a restriction on the wand thickness. This meant finding a new material to achieve the necessary rigidity. Tests with various materials resulted in the selection of a resin-impregnated wood and aluminium alloy sandwich. Special acoustic damping is employed to avoid reflecting the mechanical pulse at the delay line and suspension points. The damping materials are synthetic rubber and PTFE tape arranged so that the mechanical loading is applied gradually. An improved amplifier is used to give increased gain with an increase in signal to noise ratio.

Figure 74. A multi-wire proportional counter unit consisting of two 200 mm x 200 mm counters with local amplifiers.
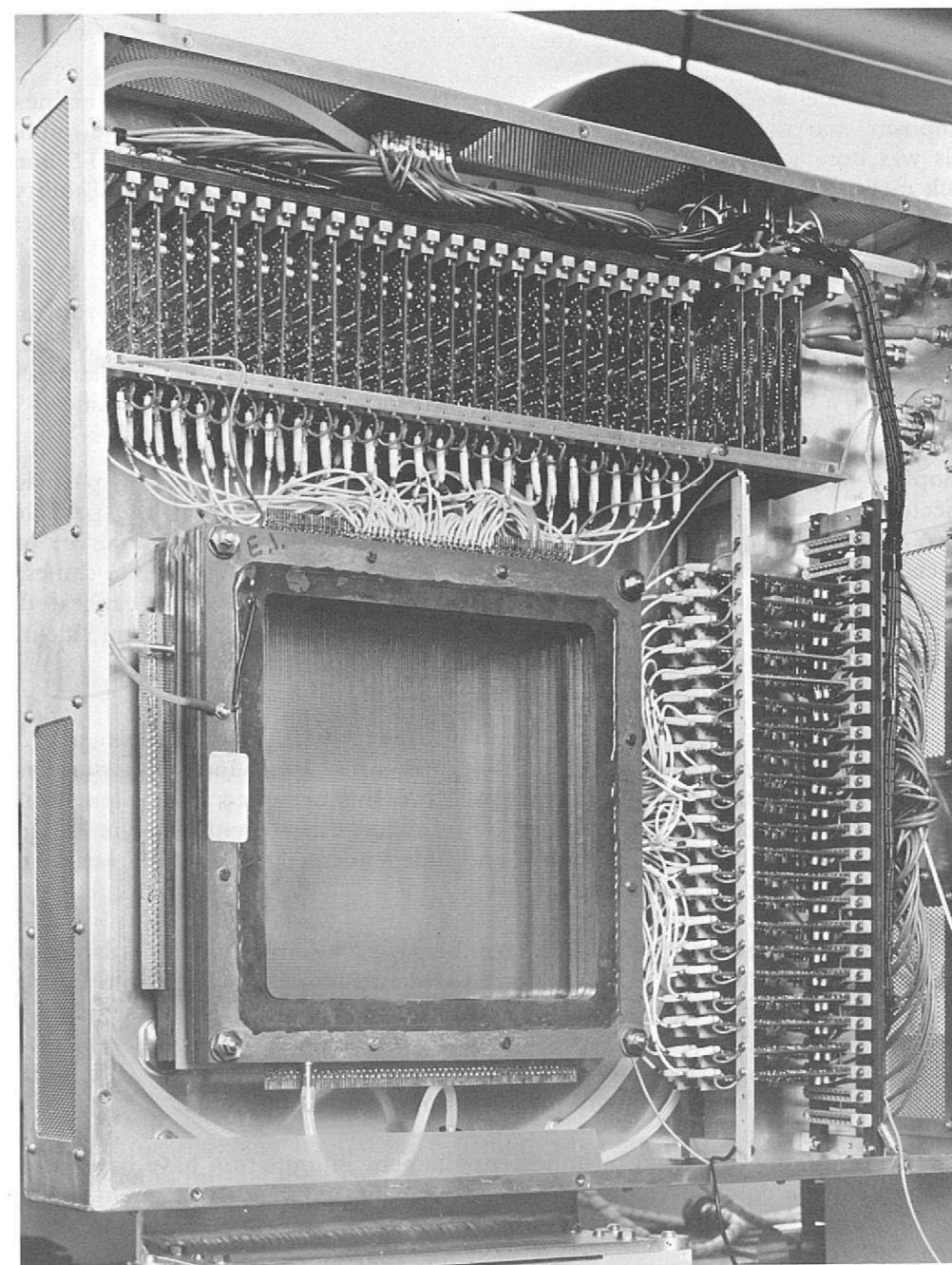
A High Voltage Power Supply for Spark Chambers A high voltage unit based on an idea originating from Bristol University has been developed to supply the large magnetostrictive spark chambers used in Experiment 13. These chambers are fed by a number of co-axial lines having a total capacitance of 35,000 pF charged to 15 kilovolts and discharged ten times a second by a thyratron pulser. Recharging is accomplished in 30 ms. Few commercially-made units were available. These provided less current and had inferior voltage ranges as well as being expensive.

The new unit employs modern, high power, high voltage switching transistors and as a result is compact (it is housed in a 19in x 12in x 5½in chassis) and has a high conversion efficiency so that special cooling is not required. Circuits are built up in modular form to aid fault finding and repair. Some twenty units are being manufactured at present.

Low Mass Chambers Sixteen low mass magnetostrictive read-out spark chambers have been produced for Experiment 3. They are located around the hydrogen target. The most important requirement was to produce spark chambers from low density materials so that particles scattered from the hydrogen target would suffer minimal Coulomb scattering when they pass through the chambers.

The wire planes for the chambers were produced from a sheet of copper-melinex composite material etched to give wires 0·4 mm wide with a pitch of 1·00 mm. This was bonded to a 1·5 mm thick expanded polystyrene sheet and a 0·5 mm thick melinex sheet to produce a low mass, rigid laminate having low permeability to helium gas. Each chamber consists of two of these low mass etched wire planes bonded to each side of a thin section perspex frame.

Another small but important feature which presented a manufacturing problem was the 64 coils required for the magnetostrictive read-outs. Each coil consists of 200 turns of 0·02 mm diameter insulated wire wound on to a 0·5 mm diameter former with a 0·325 mm hole through the centre, fully potted in epoxy resin.

Fiducials and Data Boards for Optical Spark Chambers In optical spark chambers images of sparks which are formed along particle trajectories are recorded photographically. The reconstruction of the particle trajectories in space is made possibly by recording, on the same film, survey or fiducial marks at known positions in the spark chamber with the same camera system. Measurement of these fiducials enables the optical system to be calibrated, taking into account distortion in the mirrors, lenses and in the transparent side of the spark chambers; thus accurate reconstruction can take place.

The fiducial system for the large optical spark chambers in Experiment 23 consisted of a series of slits spaced at 134 mm intervals around the perimeters of all the spark chambers so that a total of 2100 slits occupied a total length of 280 metres. Illumination was provided by miniature fluorescent tubes mounted behind the slits, with switching control and independent light intensity variation of the front and rear slits in each chamber.

Another requirement for optical spark chambers is provision of data boards which provide a sequential numbering system to identify every photograph. Three experiments have been supplied with electro-luminescent fiducail marks and data board displays during the year. All used an organic material on a glass substrate which proved to be very reliable. The data boards for Experiments 13 and 23 had, in addition to the usual binary information, displays in decimal.

Both electro-luminescent and incandescent filament illumination have been used and found to be equally reliable but the latter is preferred since filament lamps may be directly connected to the TTL integrated circuits used for decoding binary and decimal data.
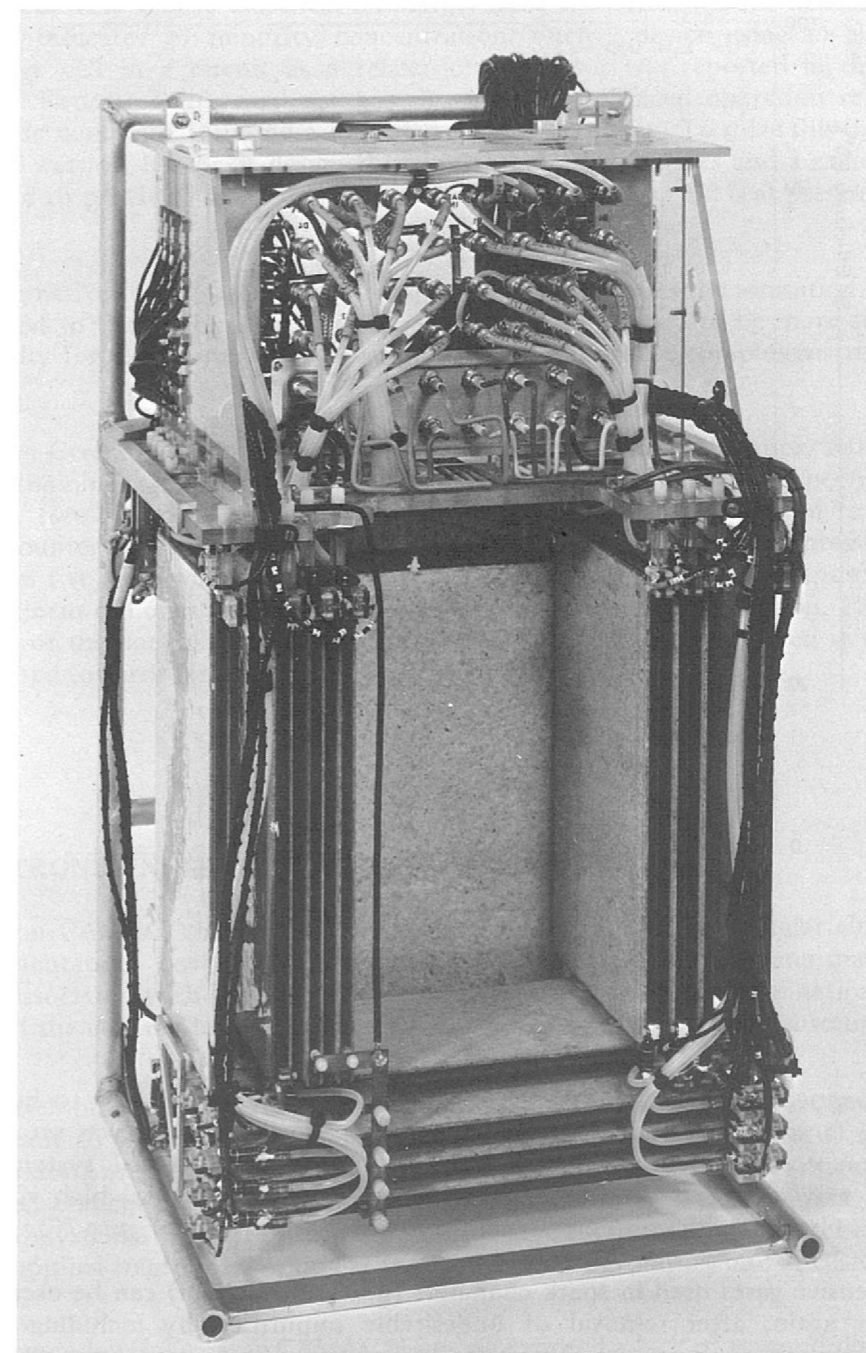
Figure 75. Low mass magnetostrictive spark chamber assembly for Experiment 3.

Spark chambers are routinely tested following their construction. Testing typically involves:— *Spark Chamber Testing*

1. Ensuring gas leak-tightness.

2. Checking that any high voltage breakdown that does occur is random. This is done by pulsing the spark chamber using a pulse generator trigger.

3. Obtaining high voltage-efficiency characteristics for a number of positions within the active area. Cosmic rays or a β-active source is used.
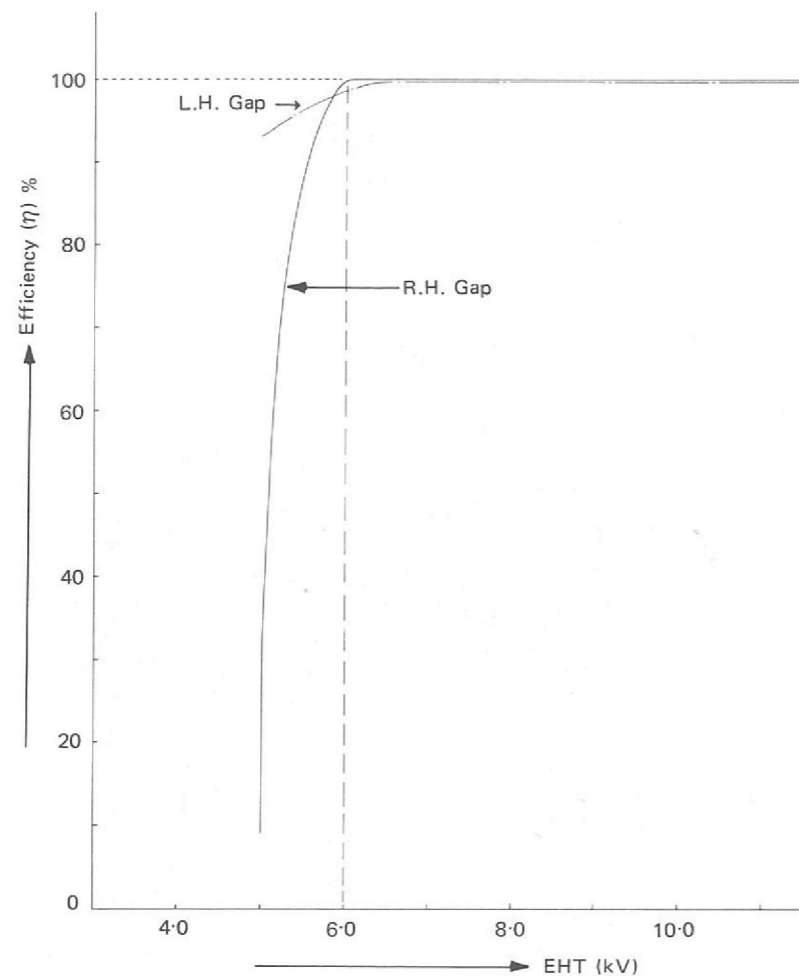
Figure 76. Typical EHT-efficiency curve for 2m x 4m
optical spark chambers. Experiment 23.

For the optical spark chambers a large light-tight housing had first to be constructed. A scintillation counter telescope and associated logic was set up to trigger on cosmic ray particles. A camera, mirror and fiducial system was installed and many pictures of cosmic ray events taken. Typical high voltage-efficiency characteristics obtained from these tests are shown in Figure 76.

Spark Chamber Gas The expensive gases used in spark chambers (neon and helium) can be used over
Purification and and over again, after removal of undesirable impurities, by including a gas
Recirculation purifier-recirculator in a closed system. Six of these units have been put into operation during the year. Four were for experiments at CERN and two for Nimrod experiments. The cost saving has been substantial for large spark chamber systems as in Experiments 10 and 23 where as much as 15 litres of gas per minute is required.

There have been other advantages. It is now possible to flush air out of a system and have the gas sufficiently pure for spark chambers to operate in hours rather than days. This is because a purifier-recirculator can handle large gas flows. It also becomes economically possible to use the large gas flows needed when spark chambers are to be triggered at high rates.

Noble Gas Purity Noble gases used for filling spark chambers (as described above) may contain
Monitor minute quantities of certain impurities that tend to "poison" the chamber. The effect of "poisoning" is to reduce the spark energy or inhibit spark formation altogether. Thus it is desirable to monitor the concentrations of these impurities, as a check on the spark chamber efficiency.

One method is to use electrical discharge, since the colour of the discharge is a reliable indicator of impurity concentration. Such a device using an electrical discharge cell in a circuit as a relaxation oscillator was reported in the 1969 Annual Report. Two years' use has shown that prolonged operation results in electrode contamination and a loss of frequency stability. To solve this problem, a Mk 3 version has been designed, using rotatable electrodes and a radio-active β source to provide ions in the gas between the electrodes, and is at present under test.

An alternative device is currently being developed that uses the ionisation current produced in the gas by a radio-active source. It is expected to be more sensitive especially for electro-negative gases, but may require more complex instrumentation.

Electron Cerenkov counters used in Experiment 22 enclose the upper half of the *Electron Cerenkov*
spark chamber array around the hydrogen target within the M7 spectrometer *Counters*
magnet (see Figure 33) to identify the decay of the η (eta) meson to $e^+e^-\pi^\circ$. Each counter consists of a box filled with Freon 12 at atmospheric pressure and lined on five sides with aluminised melinex. The remaining side is composed of an arrangement of cones that transform from a square to a circular section. The inner surface of the cones is reflecting so that the Cerenkov light produced in the box is directed towards photomultiplier tubes at each apex.

ELECTRONIC INSTRUMENTATION

Work on CAMAC, the internationally accepted standard for modular electronic *The CAMAC*
instrumentation, has continued with the Laboratory's effort being mainly on *System*
work associated with the higher level of system control and co-ordination, while most of the user modules have been bought directly from commercial sources.

The development at the Rutherford Laboratory of the System Crate concept is a significant step towards the rapid implementation of complex CAMAC systems. It provides a method of allocating one of many sources of control to one of many CAMAC branches. It can also be used as a powerful method of linking several isolated systems into a network. A total of seven System Crate assemblies have been supplied to groups working at the Rutherford Laboratory and at CERN.

The tremendous increase in CAMAC usage has exposed a lack of test and diagnostic equipment. To meet this situation, a range of indicator modules which monitor all parts of CAMAC systems, the control lines, the data lines and the interrupt lines, has been developed. Further developments will add units which could be used to implement computer controlled diagnostic programs for CAMAC systems as well as CAMAC modules.

While CAMAC provides a control structure and defines a set of basic commands, it does not define how the various components are combined to implement a given operational function. One common requirement is data transfer between the CAMAC system and an external device. Though many such interface modules are available there is a surprising difference in the detailed facilities provided. A skeleton interface has been developed at the Rutherford Laboratory which can easily be extended to match particular input/output devices. This approach will be increasingly important as greater use is made of the data transmission facilities for the control and monitoring of experiments as it will allow the use of device independent driver routines.

Counter The CAMAC units developed for counter hodoscope applications have now been
Electronics in use for several months. They provide discrimination, strobing, storage and read-out facilities. Fifty-six channels (7 modules each of 8 channels) are in use and a further batch of improved modules is being manufactured.

The Miniature Logic System continues to be used and is still the best solution for very large scintillation counter experiments which require a flexible method of implementing complex trigger logic.

Proportional The electronics for a 300 wire system is being commissioned and further small
Chambers systems are being manufactured.

Hybrid integrated circuit elements already developed for this field are being evaluated and a study of the use of emitter coupled circuit techniques has been initiated. These should provide better performance in terms of speed and inter-connection simplicity.

TV Camera The read-out system for the Omega project at CERN, using lead oxide target
Read-out System vidicons is nearing completion. The system will consist of six cameras, a control unit which provides the complex frame scanning program, and a display unit. Though evaluation and further development is still needed in some areas, most of the components are now in an advanced stage of production.

Film Scanning The data acquisition and measuring stage control electronics, developed for the
Electronics Vanguard measuring machines, has now been evaluated.

Automatic film advance has been fitted to one scanning machine. Eventually this will be available for all scanning and measuring machines.

Module Testing Computer programs exist for the testing of complex modules so that they can be easily evaluated under a large number of operating conditions. Not only will this speed up testing but it will reduce the number of data dependent faults which might otherwise escape detection.

LIQUID HYDROGEN/DEUTERIUM TARGETS

Targets in use During the year 1971, 6 liquid hydrogen and 1 liquid hydrogen/deuterium targets
at Nimrod have been operated simultaneously at Nimrod. Of these, 3 were Type I targets in which refrigeration is provided in the form of liquid hydrogen from dewars, and 4 were Type II targets, each with its own closed circuit refrigerator.

The N4 experiment uses an existing target which has been previously used on the K8 beam line. A Type I system is used for this target but new features are employed for the safety ventilation system. The hydrogen dewar is placed in a separate igloo, constructed of structurally weak panels of 'perlite' based material to allow for little restraint in the event of an explosion. Where further security is required a wire mesh screen surrounding the igloo prevents large fragments being projected into the experimental area. The separate target-reservoir assembly is protected by a conventional ventilated HYVE system.
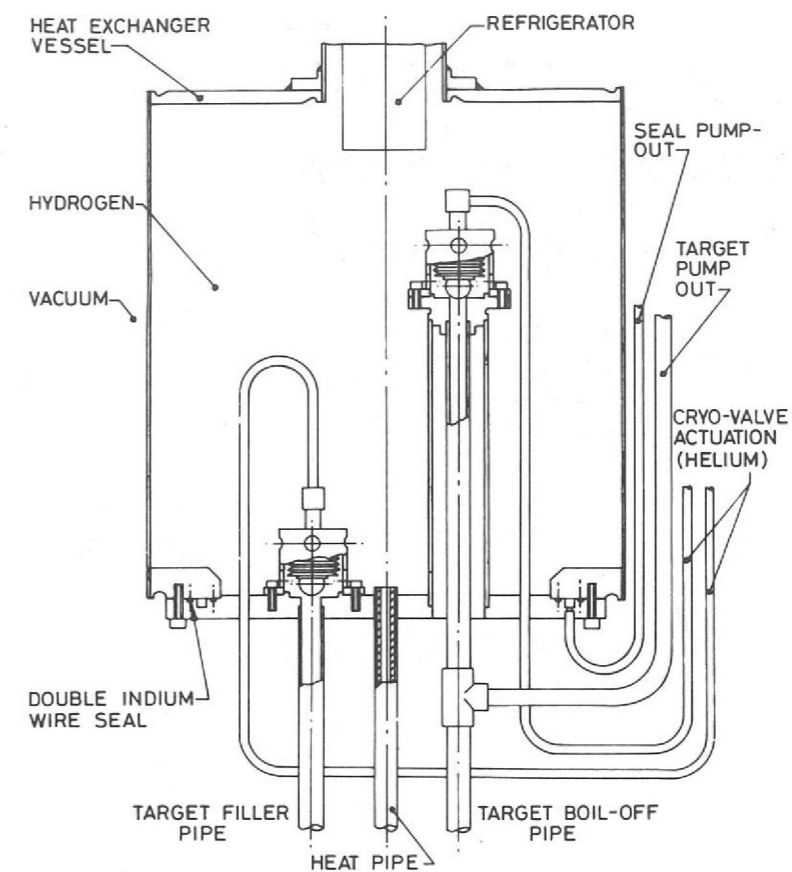
Figure 77. The heat exchanger vessel for the liquid hydrogen target of Experiment 13.

The latest target for K13C employs a Type II condensing system and has a total liquid hydrogen capacity of 0·25 litres. The design of this target is directed towards the elimination of all hydrogen system joints within the vacuum system other than those produced by either brazing or welding. In order to achieve this, the cryogenic valves are repositioned in the heat exchanger vessel and the target flask has a welded seam joint produced after the manufacture of the Melinex flask (see Figure 77). The only remakeable joint is at the base of the heat exchanger vessel and consists of a double indium seal with an interspace pump-out. The target flask is mounted on a thin wall tube tripod from the beam entry window flange (see Figure 78).

Detailed modifications to the control system allows restart after mains failure to be automatically accomplished. All the targets have operated in a very satisfactory way and a high standard of reliability in the components has now been achieved.

Figure 78. The target flask. (Experiment 13).
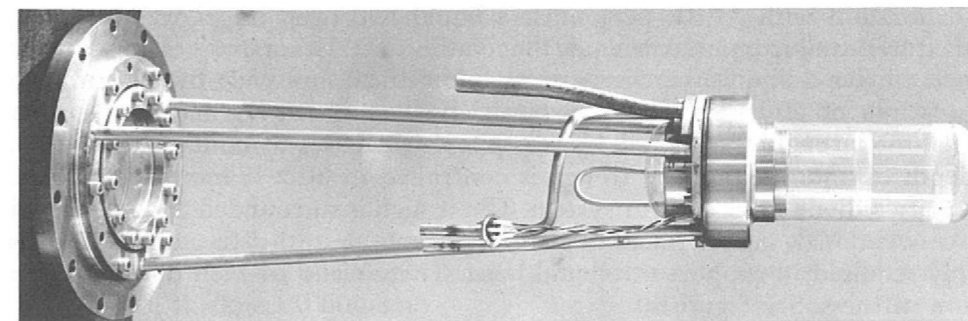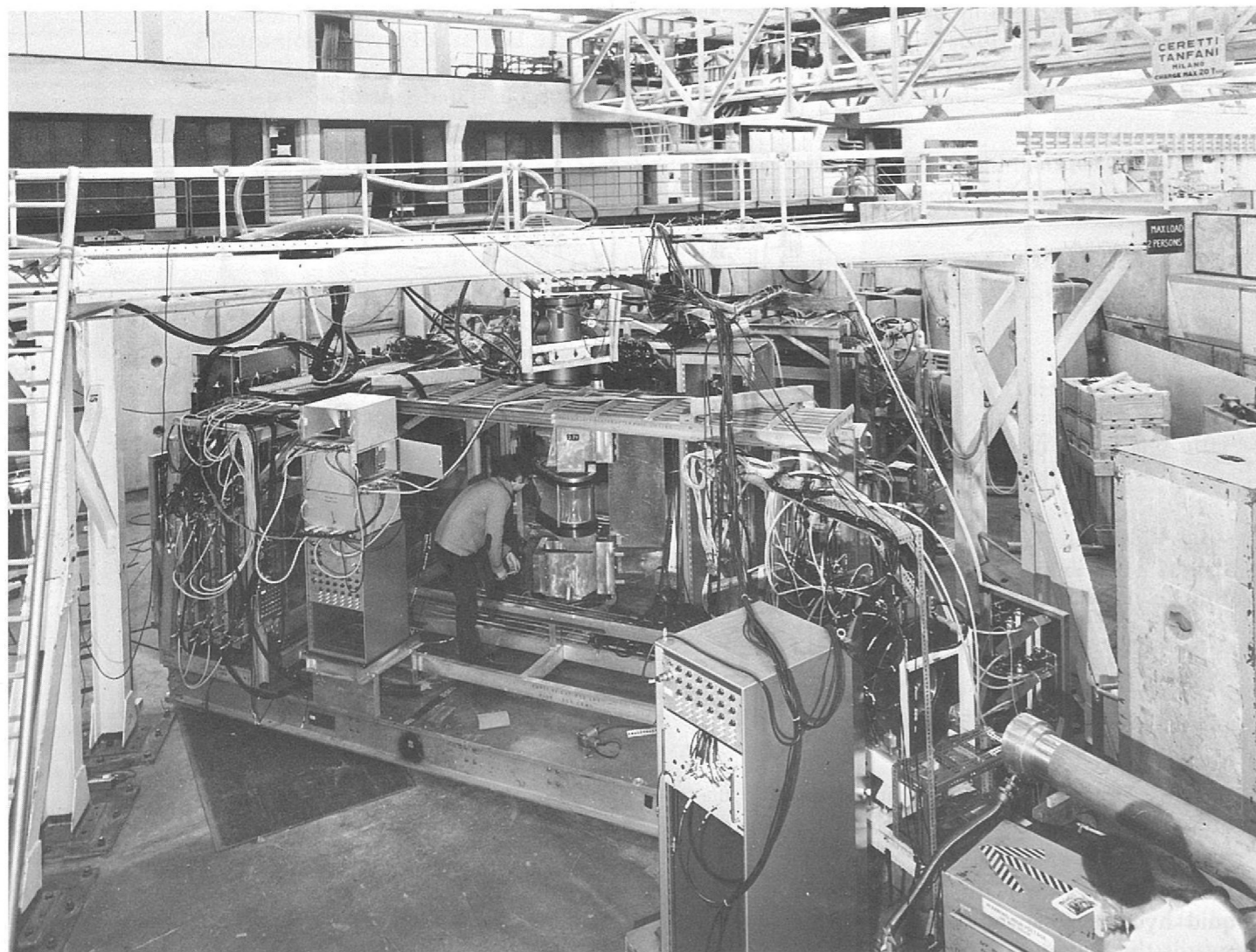
Figure 79. The liquid hydrogen target for the p̄-p experiment at CERN (*CERN Photo*).

Target for a p̄-p Experiment at CERN

The liquid hydrogen target for this experiment was designed and manufactured at the Rutherford Laboratory in collaboration with CERN PS Target Section personnel. After trial assembly at the Laboratory, the components were despatched to CERN where the Melinex flask and vacuum vessel windows were assembled and tested. The conventional CERN liquid hydrogen and vacuum service vessel was attached to the assembly and the complete system was successfully tested and commissioned in the experiment in April 1971. Figure 79 shows the target assembly in position in the experiment at CERN.

A Target for AERE Cyclotron Experiments

In collaboration with AERE personnel, a liquid hydrogen target was designed, manufactured and commissioned at the Rutherford Laboratory. The target is designed to give a liquid hydrogen cross-section of 20 mm wide by 60 mm high with a length of 200 mm. This is achieved by manufacturing a 0·08 mm-thick wall Melinex trough, supported by a copper strip base, to contain the liquid. The depth of liquid within the trough is controlled to 60 ± ½ mm by use of the Laboratory's diode level control system. The trough is surrounded and supported by a conventional vapour-filled target flask, such that the flat through walls are only required to support the liquid head. These walls are also ribbed to give addition stiffness. See Figure 80.
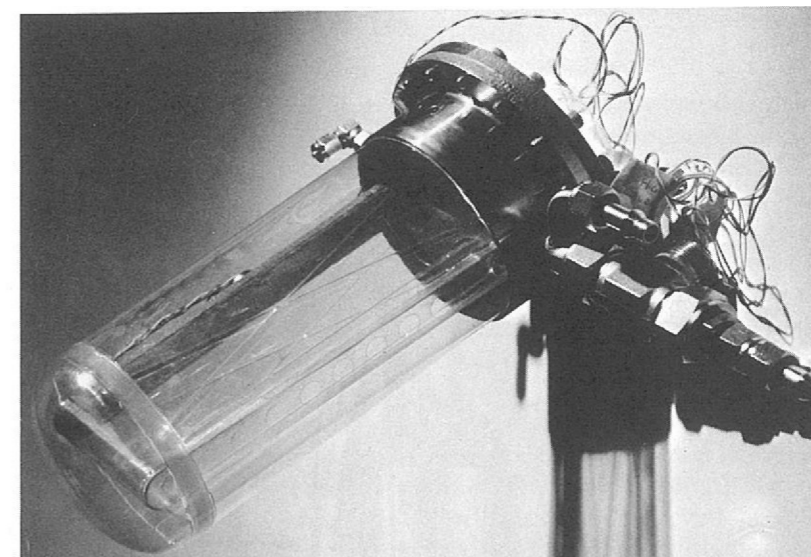
Figure 80. The liquid hydrogen target flask for AERE Cyclotron experiments.

POLARIZED PROTON TARGET

A new type of polarized proton target of advanced design is currently undergoing commissioning tests. The target is of the separated function type in which processes of polarization and subsequent use for data collection are separated in time and, in this particular target, in space too. In this way conditions pertaining to polarization and data collection can be optimised separately. This procedure allows a degree of angular access that would be unattainable otherwise using existing techniques.

(ref. 160, 211, 215, 264, 265, 266, 282)

The major portion of the cryogenic system has been assembled and tested. It consists of a closed cycle ³He refrigerator with a power of 1 W at 0·9 K and capable of cooling the target to a working temperature of 0·3 K during data collection. Difficulties with thermal oscillations in this system were successfully solved by application of a new type of heat exchanger embodying metal foam.

The success of this type of heat exchanger has led to a small development programme with the objective of determining the physical characteristics of metal foams of different materials for more general use in heat exchangers. The principal features of this new type of exchanger are good efficiency, compactness, low cost and elimination of thermal oscillation conditions.

The magnet system of the frozen target consists of a 50 kG superconducting polarizing magnet, a split-pair arrangement giving 27 kG central field with a 90° access and two trimming coils, all within one cryogenic enclosure. The performance of the complete magnet system with both magnets fully energised follows closely that predicted, and the required field homogeneity — of a few parts in 10^4 over the volume of the target — is achieved. The partially assembled system is illustrated in Figure 81.

Special procedures have been developed to minimise heat inleaks to the target. A new type of thermal break for microwave guides has been developed of extreme simplicity giving the equivalent thermal break of 2 cm of thin walled stainless steel tubing yet giving no measureable attenuation of the microwaves at 4 mm wavelength.

To minimise eddy-current heating of the cavity during movement from the polarizing to holding positions the cavity is constructed from gold plated stainless steel foil of thickness 0·008 cm.
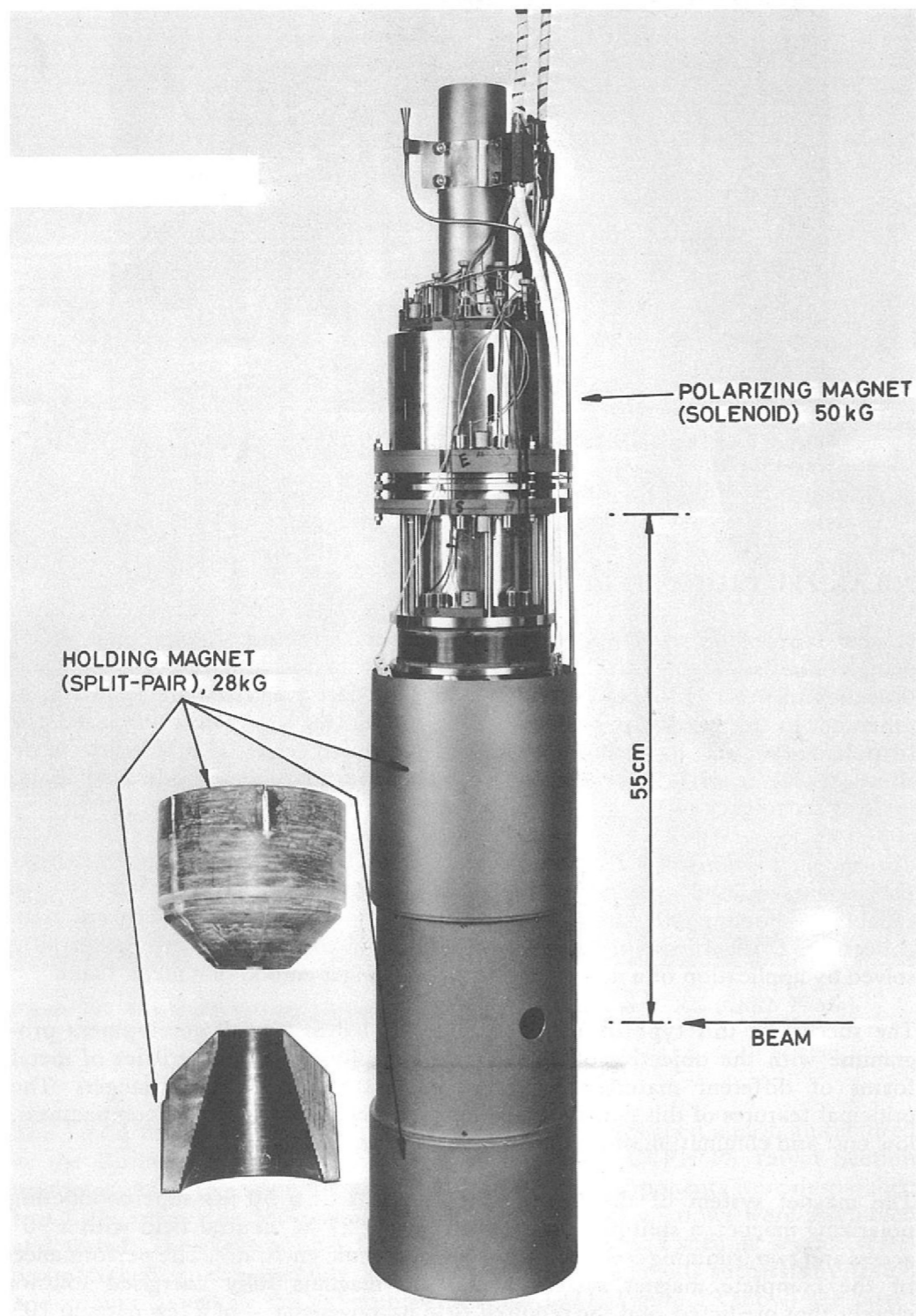
Figure 81. The partially assembled magnet system for the polarized proton target.

Both the microwave and nuclear magnetic resonance (NMR) systems of this target have been designed for use at two different frequencies, corresponding to operation with 4 mm and 2 mm wavelength microwaves. Developments of the NMR system include use of a multiple half wavelength coaxial line of low r.f. attenuation and low thermal conductance, totally enveloping double screening, a balanced low level monitor and second order correction to improve the overall noise levels and accuracy of measurement. Part of the NMR system was used to make magnetic field surveys of the frozen target polarizing magnet.

Following the demonstration that glycerol-water-porphyrexide was a suitable material for use in the frozen target, research on this material was continued. Studies were made of the build-up and decay rates of polarization.

Design studies also have been made of several new polarized targets. In one of these the direction of polarization would be along the beam axis. The design incorporates a trigger counter very close to the cavity thus requiring the scintillation counter to work in a cryogenic environment. Tests are being made to check the operation of typical scintillation materials down to $\sim$ 1K.

The range of magnetic fields and temperatures now available for polarized targets are indicated in Figure 82. For successful operation of a separated function type of target the ratio of magnetic field strength to temperature should exceed 100 kG/K. This condition could be achieved at low magnetic field strengths by using a dilution refrigerator. To explore this possibility and to examine the behaviour of target materials at temperatures of 100 mK or less a dilution refrigerator unit is being installed and will incorporate an existing 50 kG high homogeneity superconducting magnet.

Figure 82. Range of magnetic fields and temperatures now available for polarized targets.
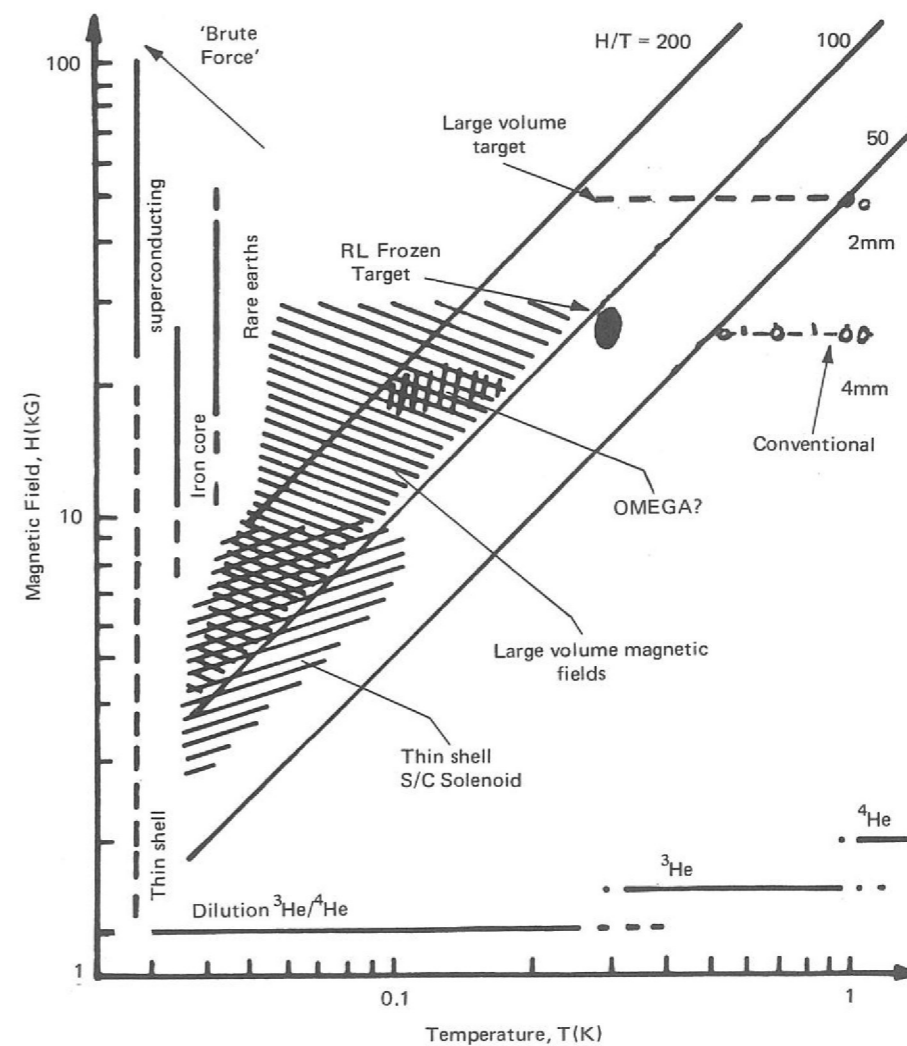
THE 1·5 METRE CRYOGENIC BUBBLE CHAMBER

Chamber Modifications (ref. 140, 226, 243)

The extensive modifications that were carried out on the Bubble Chamber expansion system during the 1970 shutdown were completed early in the year. These have resulted in very great improvements in the chamber operation. Leaks into the main insulating vacuum have been eliminated and the chamber has become much more manageable. Detailed modifications to the vacuum system have improved reliability and with the chamber in excellent condition, a full track sensitive target development programme was undertaken during the year.

The PDP8I computer has now been programmed to provide a monitoring system which gives the bubble chamber operators a means of keeping close control on the operation of the chamber. At present some 60 analogue signals are monitored by the computer and alarm messages are generated if signals exceed limits which are set by the chamber operator. Sixteen digital channels are also available and these are used at present for providing the computer with data from electro-mechanical counters and for "status bits". The counters are used for recording such information as film number and exposure number. The operator communicates with the computer through a teletype using simple command strip. Error messages are typed out on a second teletype. A "log command" allows the contents of the computer data table to be typed out on demand. Parameters which are synchronous with the chamber cycle can be read and stored in the form of a histogram which provides information on the long-term functioning of the chamber. A CRT display is available which allows any of the 64 possible analogue inputs to be displayed as a function of time. This facility has proved to be of great value during the track sensitive target development programme.

Track Sensitive Target (ref. 193, 240, 241, 268, 269, 281)

All the operating time of the chamber this year has been given to the development of a sensitive hydrogen target in the chamber the rest of which contains a sensitive mixture of neon and hydrogen. The advantages of this system for detecting uncharged particles were described in last year's report. A series of targets were tried during the year, culminating in a successful run during which 65,000 pictures were taken for a physics experiment. Full instrumentation was provided to enable data to be collected from strain gauge patterns and temperature and pressure sensors. This coupled with detailed examination of broken targets began to throw light on the problems that were standing in the way of success in this work. A theoretical analysis of the pressure transients in the chamber during the expansion cycle, and the stresses imposed on the target walls due to flexing was undertaken. As a result of this study a "composite" target was designed.

A photograph of this target installed in the chamber is shown in Figure 83. The target is made up of a rigid frame of stainless steel which is mounted in the median plane of the bubble chamber by a method which allows differences in contraction of the target and chamber body during cool-down. The frame is provided with refrigeration loop, the necessary valves for filling the target and a strain gauge transducer for measuring dynamic pressure. The side walls are made of 6 mm perspex. To allow for the large differential thermal contraction, the seals between the frame and the windows are made at the operating temperature of 29K by forcing the windows against indium wire set in grooves on the frame by inflating a flexible backing tube behind the perspex.

This target was installed in the chamber during October and successfully operated during November when 65,000 pictures were taken in a 4 GeV π^+ beam.
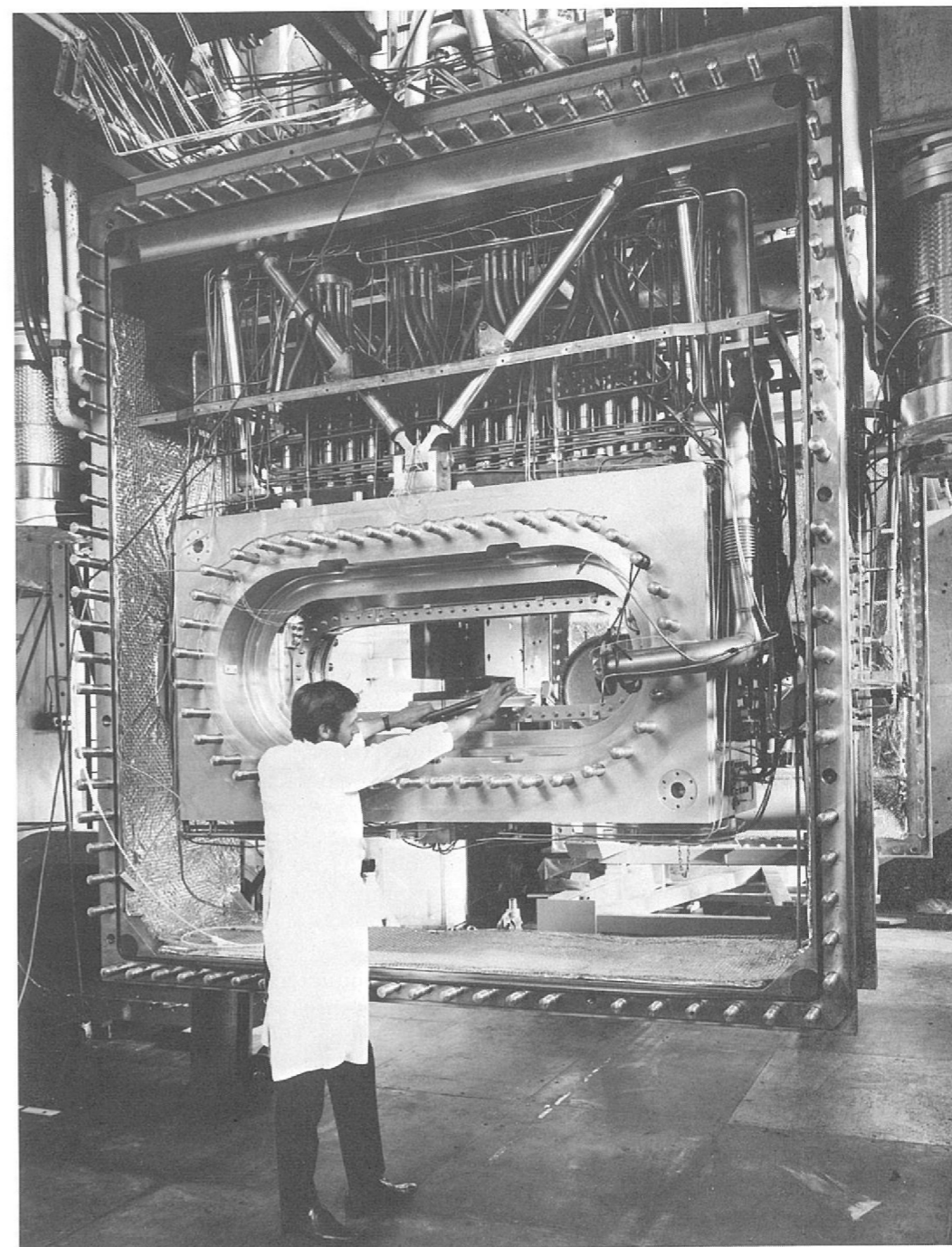
Figure 83. The track sensitive target installed in the bubble chamber.

The target was filled with hydrogen and the chamber surrounding it contained neon/hydrogen mixture with a neon concentration of 45 molecular per cent giving a radiation length of 73 cm. At this and similar concentrations homogeneous mixtures can be produced which, with a small change in the conditions of temperature and pressure, have a tendency to stratify into neon-rich and neon-poor regions which would be unsuitable for physics use. Operating techniques have now been developed for filling the chamber with uniform mixtures and many successful fillings have been achieved. During operation, the mixture is more sensitive than the hydrogen in the target, but by choosing suitable operating conditions, satisfactory track quality in both regions can be achieved. See Figure 54, Experiment 37.

The target has been operated for over 200,000 expansions without trouble up to the Nimrod shutdown (December 1971). On inspection, after dismantling, the seals and windows were in good condition. This facility will be fully used in the physics programme of the Laboratory during 1972.

SPECIAL PURPOSE MAGNETS

High Field Pulsed Magnets at CERN

For the successful data taking run for the Λ hyperon experiment conducted by the Cambridge Group in the 2 m hydrogen bubble chamber at CERN, two high field pulsed magnet assemblies, designed, developed, built and tested at the Rutherford Laboratory, were taken to CERN together with a 20,000 μF, 0·3 MJ capacitor bank and its power supply. Two spare coils were held in reserve.

Intended to provide 70 kG over 40 cm in a $40 \times 6 \times 11$ cm³ bore at a repetition rate of 20 pulses per minute with half sine-wave pulse lengths of 2-3 ms, the design lifetime was 100,000 shots minimum before coil failure. Figure 84 shows one such coil in a cut-away shock-absorbing and redistributing assembly.

Installation involved the fitting of lead and uranium shielding at the entrance to the bubble chamber, with a narrow acceptance-defining axial slot in a brass insert. The pulsed magnet, surveyed into place immediately upstream of this transport system, is used to sweep charged particles, produced in a target 3·3 m from the entry window of the bubble chamber, into the shielding, so that the remaining neutral beam is injected into the chamber.

After only 40,000 shots at 76 kG, the first installed magnet developed a water leak at the coil bore. Replacement with the back-up assembly took only 4 hours; this magnet went on to give over 250,000 shots and is still operational. About 150,000 of these were at 66 kG to permit magnet operation at the accelerator rate of 26 pulses per minute, whilst the remainder were either at half-rate and 76 kG, or at 30 ppm and 56 kG. See figures 57 and 58, Experiment 38, in which the bubble chamber pictures show the beam entering the hydrogen without the pulsed magnet operating, together with an example of a picture taken under normal operation when the magnet was running at 66 kG.

Before concluding the run, feasibility tests were conducted for a beam enriched in Σ⁻ hyperons, and involved about 80,000 magnet shots at 66 kG. Preliminary design tests are now being carried out for a 20 cm long 150 kG magnet for such an experiment.

Figure 84. High field pulsed magnet during assembly.
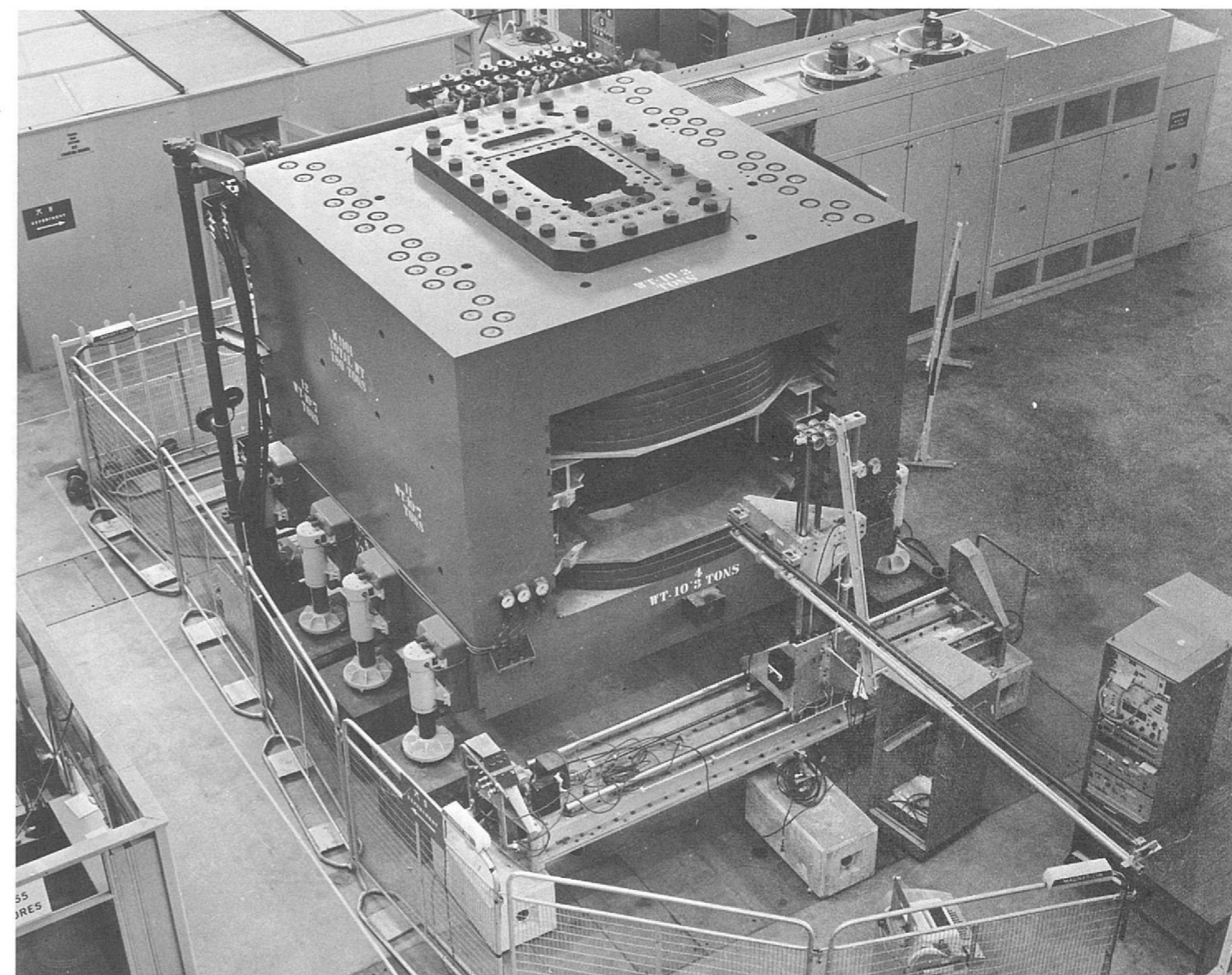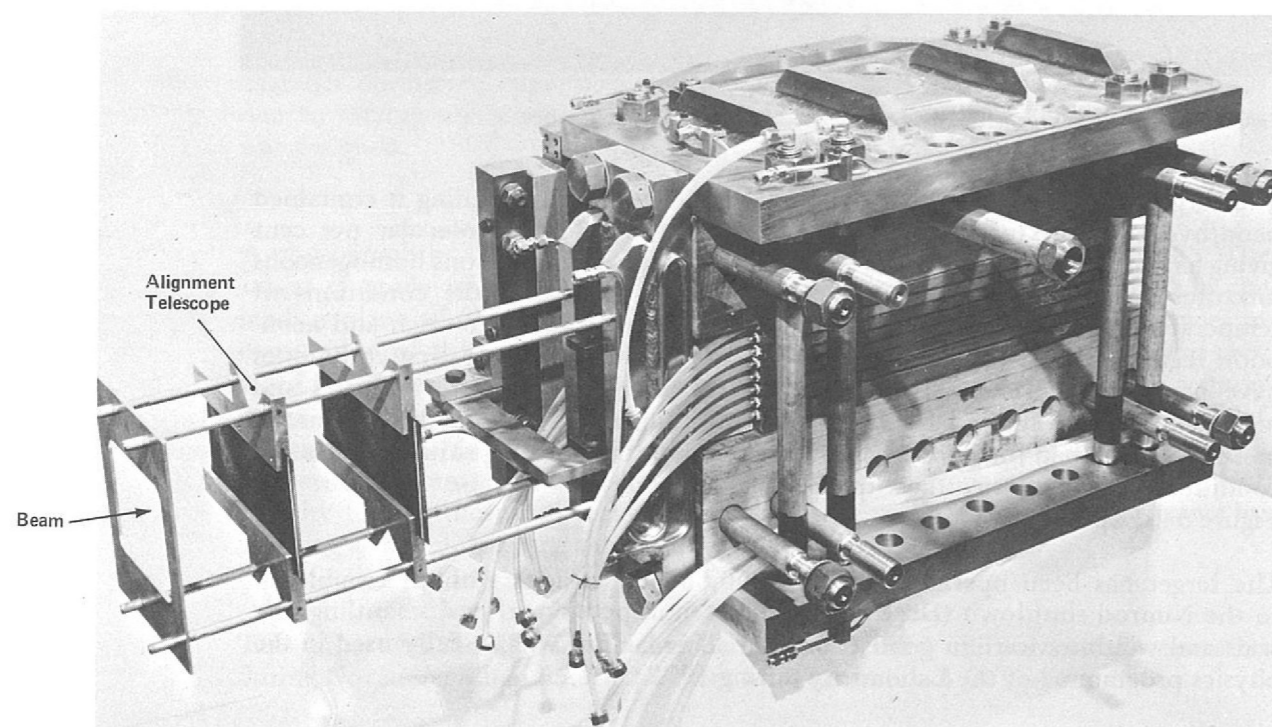
Figure 85. M11 spark chamber magnet with field plotting equipment.

The heavy liquid bubble chamber magnet has been rebuilt as a spark chamber magnet with an aperture of 78·8 cm and has achieved its design field of 10 kG. A turntable has been constructed to give small angular movements of the magnet, and its accuracy of positioning is being evaluated. A new power supply for the magnet has been tested and commissioned. The output is 1·2 MW at 250 V and 4,800 A, with a current stability of better than 1 part in 10⁴ between 480 A and full load.

M11 Spark Chamber Magnet
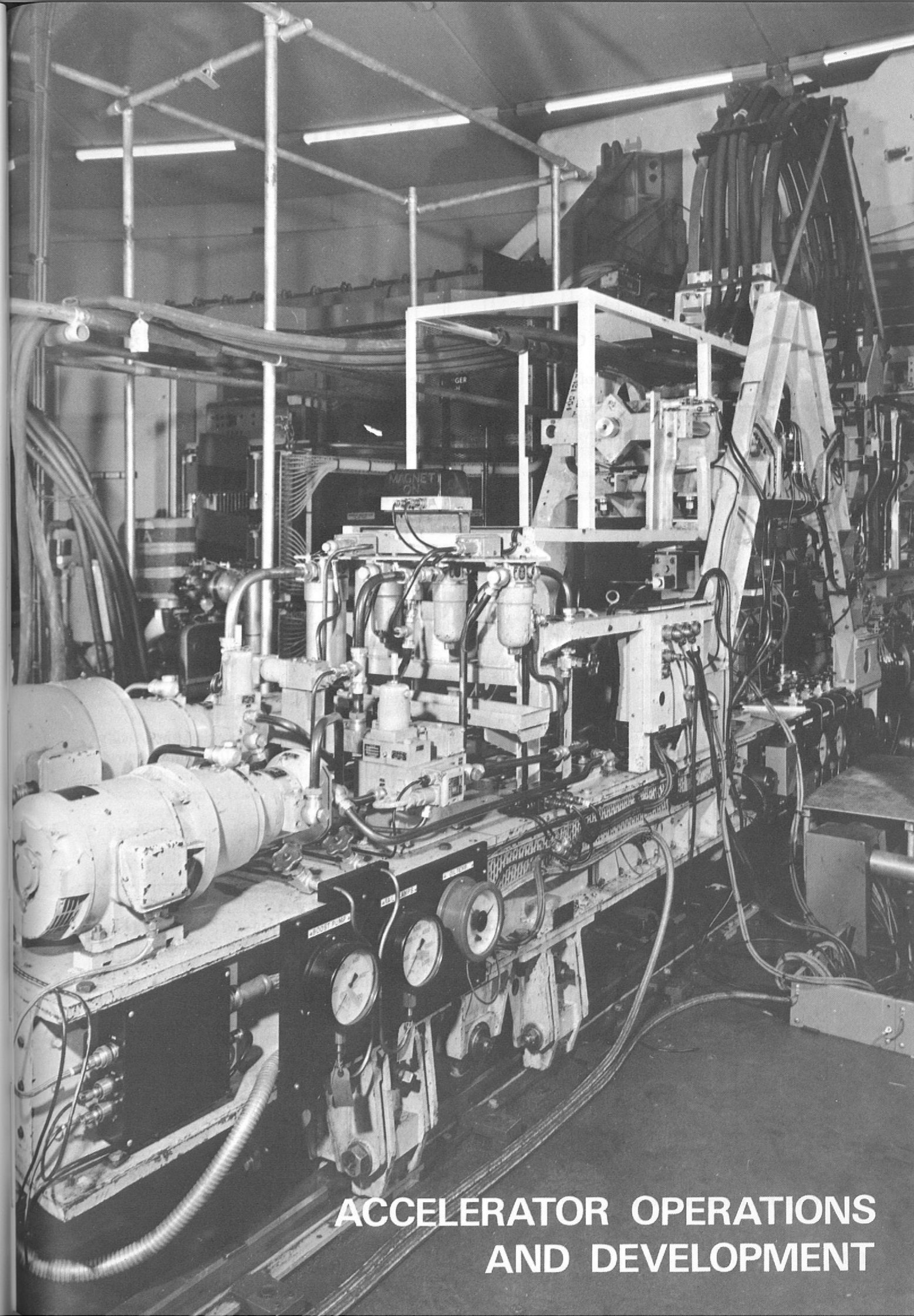
A Mk II Plunging Mechanism used in the thin septum Piccioni extraction system at Nimrod.

ACCELERATOR OPERATIONS
AND DEVELOPMENT

Accelerator Operations and Development

OPERATION OF NIMROD

The pattern of operation of the accelerator, as in recent years, has consisted of 3-week cycles, the major portion of each cycle, about 82% on average, being devoted to HEP research, with the remaining 18% being accounted for by accelerator development, maintenance and start-up time.

The operational record is summarised as follows:

HEP Research	Hours
Scheduled time	6010
Good beam time	4859

ie beam on for 81% of HEP scheduled operating time. This compares with good beam time realised last year of 4708 hours.

Accelerator Development	Hours
Scheduled time	895
Realised beam time	420
Machine available time	624

ie machine availability 70% of scheduled operating time for accelerator development. The operations record is detailed in the following Table:

Table 11

Nimrod Operations 1971

Date (From – To)	Hours Clock	Shut-down	Sched. Maint.	HEP Research Beam Sched.	Beam On	Set-Up	*Exp. Off	Nimrod Off	Nimrod Avail.	Machine Physics and Development Beam Sched.	Beam On	*Exp. Off	Nimrod Off	Nimrod Avail.
Jan 1 – Mar 31	2160·00	838·50	96·00	1082·00	724·08	19·98	4·37	333·57	728·45	143·50	73·72	4·62	65·16	78·34
Apr 1 – Jun 30	2184·00		143·96	1748·16	1418·24	6·38	1·80	321·74	1420·04	291·88	168·79	26·33	96·76	195·12
Jul 1 – Sep 30	2208·00		100·50	1840·27	1503·31	1·71	1·67	333·58	1504·98	267·23	94·11	79·43	93·69	173·54
Oct 1 – Dec 31	2209·00	644·41	32·38	1339·64	1213·40			126·24	1213·40	192·57	83·06	93·78	15·73	176·84
Totals	8761·00	1482·91	372·84	6010·07	4859·03	28·07	7·84	1115·13	4866·87	895·18	419·68	204·16	271·34	623·84
Percent Clock Time	100·00	16·92	4·25	68·61						10·22				
Percent HEP Scheduled Time				100·00	80·85	0·47	0·13	18·55	80·98					
Percent MP Scheduled Time										100·00				69·68

*Beam off at Experimenters request
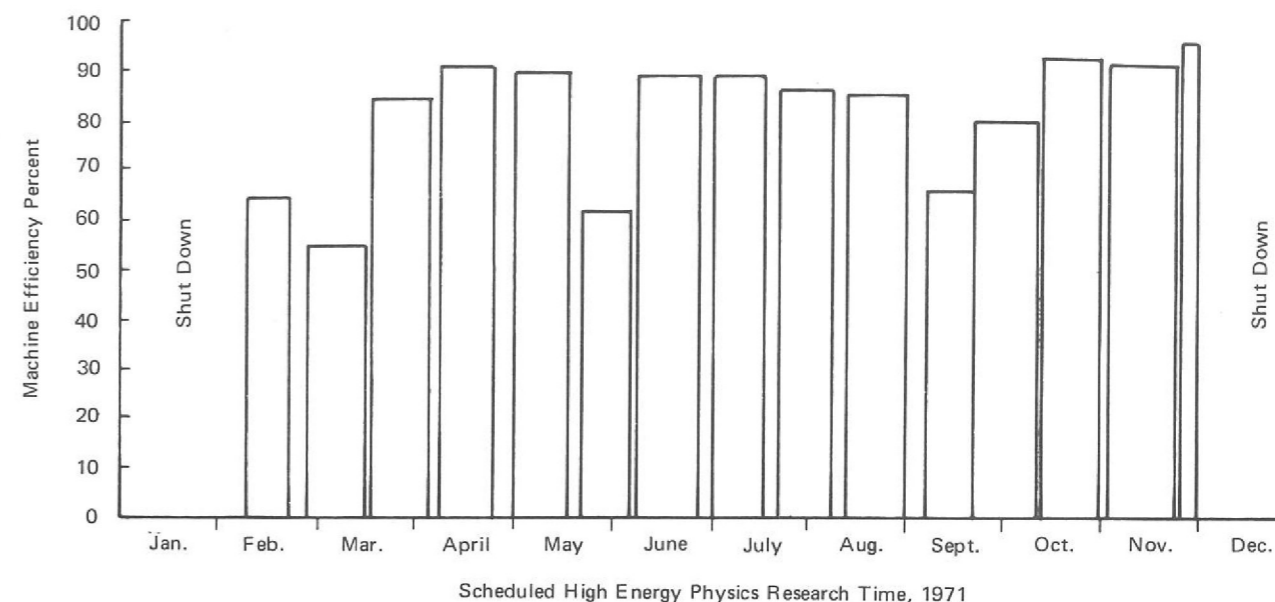
Figure 86. Nimrod operating efficiency during scheduled High Energy Physics research time. January to December 1971.

The total number of protons accelerated during the year is 35% greater than it was in 1970. The number of machine pulses, with beam, at almost $6·5 \times 10^6$, is 7% higher than last year.

The pattern of utilization for HEP research has been as follows:

1. X1/K9, the fast spill extracted beam to the bubble chamber has been available when required throughout the year, the actual usage being determined by the demands of the 1·5 m bubble chamber programme. The required fraction of the Nimrod beam is taken every pulse.

2. Because extracted beams X2 and X3 are mutually exclusive beams for flat-top operation, the mode of operation has been to run one system on flat top at 7 GeV for data-taking and the alternate system on current rise at 4, 5 or 6 GeV for setting up purposes. This permitted all of the secondary beams on the extracted proton beams to have some beam particles at all times and for every pulse. The flat top users have a spill of about 450 ms and the current rise users a spill of about 15 ms in length. About 5% of the circulating beam goes to the current rise users. Previously, sharing between X2 and X3 had been accomplished by, say, X2 taking 1 pulse in 5 on flat top, followed by X3 taking the next four pulses on flat top and so on.

3. Scattered out beams, π7, π10, P71 and K10S, operating from internal machine targets, were in use during the year, sharing beam with the flat top, slow spill, extracted proton beams X2 or X3, every pulse.

Machine pulse repetition rates continued at $\sim 20·3$ pulses per minute for the greater part of the year. However, improvements to the Nimrod magnet power supply brush gear environment permitted a significant increase in repetition rate and since mid-October rates of 21·9 pulses per minute have been the rule. The Mk 2 plunging mechanism system, installed in January 1971, in straight section 2 operated well throughout the year.

X1/X2 continued operation using a conventional 'thick septum' Piccioni extraction system. Extracted beams, as measured at the external target of X2, of 7×10^{11} protons per pulse have been readily obtainable, with a maximum of 10^{12} protons per pulse.

X3, using a thin septum extract magnet, continued in the mode of operation instituted mid-1970 and described in the 1970 Report. From February onwards the thin septum magnet was changed from a 4-turn design to an 8-turn design. The latter version requires 7000 A as against 14,000 A for the 4-turn type and has no water joints inside the vacuum system. Beam intensities, at the external X3 target, of $\sim 10^{12}$ protons per pulse, are easily obtainable. The maximum is $\sim 1 \cdot 2 \times 10^{12}$ protons per pulse.

Beam to the X3X target, a second target station, down-stream of, and in series with, the X3 target in Experimental Hall 3, was first transported on April 1. Protons not interacting in the X3 target are collected and focused on to the X3X target. As an indication of the gain in utilisation of protons, $3 \cdot 1 \times 10^{11}$ protons hit the X3X target when the normal 6 mm square $\times$ 100 mm long copper target is hit by 9×10^{11} protons. Using a shorter X3 target, more protons reach X3X and a very flexible system of operation is obtained. The secondary beams on the X3X target, $\pi 9$ and N4, were brought into use in June and October 1971 respectively.

Table 12

Analysis of Nimrod Off Time during scheduled Operating Time for 1971

Total Scheduled Operating Time	6905·3 hours		
Total Off Time	1386·5 hours (detailed below)		

	Beam Time Lost. Hours	% of Scheduled Op. Time	% of Nimrod Off Time
1. Faults and Routine Inspections			
*Extraction Systems			
(a) Magnets	192·73	2·79	13·90
(b) Power Supplies	100·86	1·46	7·28
(c) Plunging Mechanisms	80·61	1·17	5·81
Synchrotron RF/Beam Control/ Diagnostics	186·64	2·70	13·46
*Vacuum Systems	145·71	2·11	10·51
Coolant Systems	85·77	1·24	6·19
Straight Section No. 1 Environment	79·57	1·15	5·74
Injector	77·93	1·13	5·62
Nimrod Magnet Power Supply			
(a) Convertor Plant	77·04	1·12	5·56
(b) Ripple Filter Plant	11·28	0·16	0·81
(c) Rotating Plant	7·27	0·11	0·52
Targets and Target Mechanisms	68·06	0·99	4·91
Pole Face Winding Systems	62·95	0·91	4·54
Nimrod Magnet	39·61	0·57	2·86
Inflector System	13·27	0·19	0·96
Miscellaneous	40·84	0·59	2·94
2. Other Reasons			
Start-up	97·96	1·42	7·07
Public Electricity Supply	18·37	0·27	1·32
Totals	1386·47	20·08	100·00

An analysis of faults on equipment is a very important requirement and enables *Fault Analysis* the scale of spares, improvements and modification to operational routines to be determined. Table 12 gives a breakdown of the fault record of different parts of the accelerator.

During February/March, an elusive contamination of the vacuum system caused the Straight 1 electrostatic inflector to fail six times, necessitating "letting-up" and cleaning each time. A total of 80 hours was lost.

Extraction system components, particularly magnets and high current power supplies were responsible for the loss of a considerable amount of beam time. Improvements to extractor magnets and provision of standby power supplies will improve the reliability of the systems.

Failure of the accelerating gap insulators in the r.f. cavity was responsible for the loss of some 153 hours in June. (The previous failure of this insulator was 4 years ago in August 1967).

Radiation damage to the cooling water connecting tubes of the pole face winding adjacent to Straight 7 caused several interruptions to scheduled beam time. The opportunity is being taken during the shut-down December 71/January 72 to fit connectors of a new design in this area, which is the highest radiation dose area in the machine. The installation of the thin septum extraction system for X1/X2 will considerably reduce the radiation dose levels in the Straight 7 region where most of the proton loss occurs with the original extraction system.

A large programme of installation, modification and maintenance is currently in *Shut-down* progress, particularly: *December 1971- January 1972*

1. Conversion of the present thick septum extraction system associated with X1/X2 beams to the thin septum type which has been in use on the X3 beam since June 1970. This should lead to improved extraction efficiency, and also because of the fact that only one plunging mechanism is required (as against two for the existing thick septum system) it should be intrinsically more reliable in operation. The radiation dose levels in the accelerator will also be reduced.

2. Provision is being made for spare heavy current power supply capacity, in particular the installation of a 900 kW static power supply which could be used with both thin-septum extraction systems.

3. The installation and commissioning of a digital position control system on the Straight Section 4 plunging mechanism is proceeding.

4. Removal of the Straight Section 7 box, which is the area of peak radiation dose caused by protons hitting the septum of the plunged quadrupole of the original extraction system, so as to permit detailed examination of components in straight section regions after their 10 years of life since the accelerator commenced operation.

5. Installation of two new flywheels for the accelerator magnet power system. Also the repaired drive motor will be re-installed, thus releasing the spare bi-directional drive motor presently in service.

*Figures for Vacuum and Extraction Systems include routine inspection time.

6. Development of the computerised control system. Interactive graphics and diagnostic programs for pole face winding currents are being implemented. Interactive graphic presentations will be extended to other parameters in due course.

7. Introduction of the "second harmonic" r.f. system. Some preparatory work is under way, including the installation of beam control induction electrodes in Straight Section 3. (In due course a system using these electrodes will replace the existing system using electrodes in Straight Section 6. It is required to free this latter Straight Section in order to make room for the second harmonic r.f. accelerating cavity.)

Radiation Dosimetry   The integrated isodose contours at December 1970 when the last complete survey of the inner vacuum vessels was performed is shown in Figure 87.

During 1971, measurements of the radiation dose absorbed by the Nimrod inner vacuum vessels were confined to Octants 7 and 8. Both integrating and glass capsule hydrogen pressure dosimeters were used and the highest dose received since machine start up is estimated to be 435 megarad in Octant 7. This is well below the dose which the vessels can withstand. Dosimeters are still positioned to monitor the dose received by the outer vacuum vessels.

The radiation doses received by the coils of magnets adjacent to X3 and X3X targets are now being monitored.

Figure 87. Integrated isodose contours for the inner vacuum vessel of Nimrod.
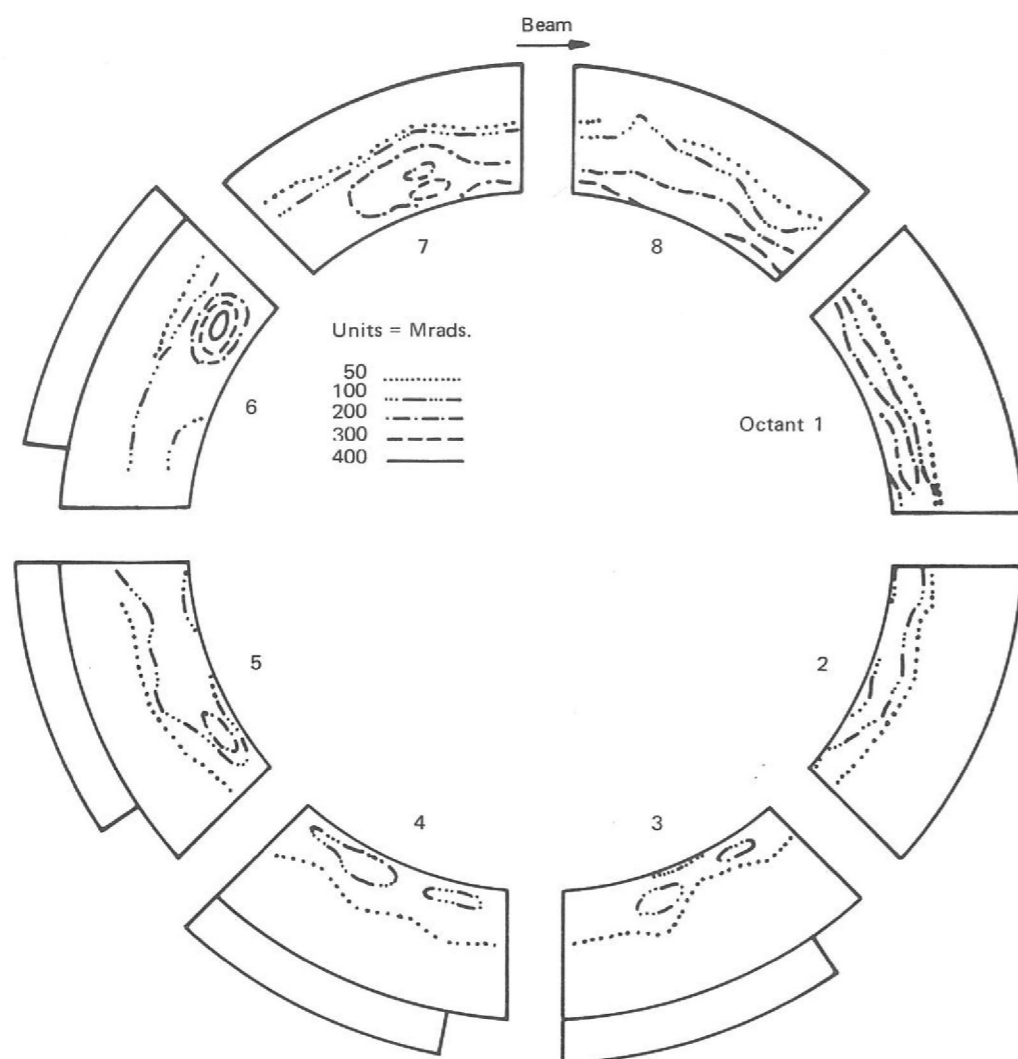
THE MAGNET RING POWER SUPPLY AND ANCILLARY PLANT

The magnet has been pulsed throughout the year using both motor-alternator sets and the complete converter plant except for the period 26 April-3 May when, due to a fault on the rotor of No. 2 drive motor, pulsing was carried out with No. 1 motor-alternator and both flywheels. Apart from this period, both alternators have operated in electrical parallel, with separate shaft systems, throughout the year. Each alternator now has a solid pole rotor and these are the first machines of this type to operate electrically paralleled and mechanically uncoupled on synchrotron pulsing duty. Their performance so far has been excellent. The mercury-arc converter plant has continued to operate very reliably with a negligible arc-back rate. The programme of installation of redesigned grid control gear on all 16 converter groups has been completed. The operating statistics for the year are as follows:

Machine running time	6295 hours
Machine pulsing time	6000 hours
Total pulses	$7 \cdot 2 \times 10^6$

On Friday, 29 October, the total of 50 million recorded magnet pulses, since the original commissioning, was achieved. This has involved about 48,000 hours of running time and 44,000 hours of pulsing time.

No. 2 Drive Motor   Following the re-winding of the rotor of No. 2 drive motor in 1970 the motor was re-assembled at the end of January 1971 prior to its return to service. The motor ran in service until 24 April when a stator earth fault developed. Temporary repairs to the rotor fan were made and two stator phases were re-wound. Meanwhile the decision was taken to re-assemble No. 2 drive motor using the stator of the original No. 1 motor, the rotor of which was scheduled for overhaul. This machine was put into service on 3 May and subsequent operation has been satisfactory. The short down-time of half the power supply indicates the advantage of a good spares availability.

No. 1 Drive Motor   This was taken out of service during the 1970/71 shutdown for examination of its rotor. Signs of fretting in the region of the main drive keys between the rotor core and the hub were seen and it was decided that a repair programme, similar to that described in the 1970 Report on the No. 2 drive motor failure, should be carried out. On this occasion, however, the opportunity was taken to increase the understanding of Dielectric Loss Analysis by permitting specialists in this field to carry out a series of tests on the rotor before rewinding and then again immediately afterwards. This was the first time that such tests had been carried out and, if successful, the state and probable life of rotor and stator insulation will be able to be assessed. Prior to this it had only been possible to obtain this information for the stator. The results of the tests, are at present being analysed.

No. 1 drive motor has now been rebuilt using the repaired stator from No, 2 motor and its own original rotor. This rotor has been rewound, and fitted with new drive keys. The new type of slip-rings and brushgear operating at a lower brush pressure, have also been installed. This motor is to be re-installed in the 1971/72 shutdown.

New Flywheels   Two new flywheels have been delivered during the year and are to be installed during the 1971/72 shut-down. These flywheels have one half-shaft forged integrally with the disc, thus eliminating the bolted and keyed construction between the alternators and the flywheels. The quality of the forgings for the new flywheels is excellent and a complete ultrasonic survey of each one has been carried out for record purposes. The new flywheels are shown in Figure 88.
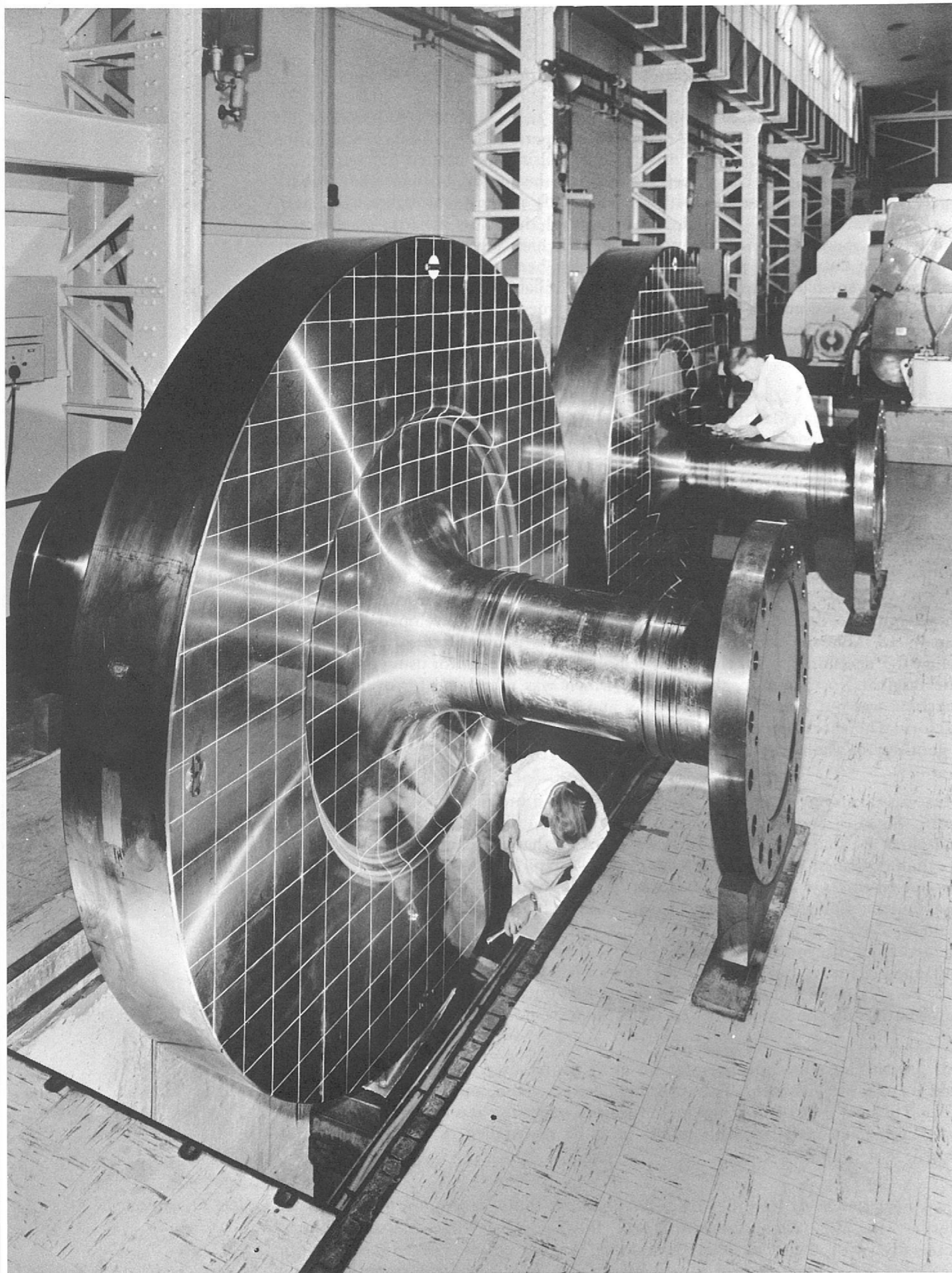
Figure 88. New 30 ton flywheel assemblies for Nimrod Magnet Power Supplies showing the integrally forged half-shaft. (The "grid-system" is for ultrasonic survey purposes).

Further testing to assess the condition of machine winding insulation has been carried out during the year, this time on the alternator stator removed during the 1970/71 shut-down from the No. 2 set position and on the stator from the original No. 1 drive motor. The condition of the alternator stator was found to be good and the motor stator, although giving results to be expected from its age (10-11 years) was marginally better than the No. 2 motor stator tested in November 1970. This latter stator has also been tested again this year, subsequent to the rewinding of two of the phases as described earlier in this report. *Insulation testing*

The new units intended for installation during the 1970/71 shut-down were not installed after all as doubts concerning their suitability were raised by news of failures of similar units experienced by other users. A critical examination of the units was made in conjunction with the manufacturers and the Welding Research Institute, and after correction it was decided to hold the units as spares. *Drive Motor Rotor Resistors*

The brushgear of the Nimrod Power Supply plant has always had to operate at, or very near to, its design limit. Several modifications have been carried out to the original brush gear system but the problem of high brush temperature, which can result in extremely rapid brush wear, has not been solved. The only way so far in which the temperature rise can be limited has been found to be by forced ventilation and control of atmospheric humidity. *Drive Motor Brushgear*

When the spare drive motor was ordered an attempt was made in conjunction with the manufacturer and the brush-gear supplier to improve the brush gear. Larger slip rings and larger but fewer brushes were decided upon. In addition, methods of increasing and optimising the distribution of the air flow through the brush gear have been investigated and significant reductions in brushgear operating temperatures have been achieved. However, the new design has not yet been finalised.

All 16 of the operational grid control equipments have now been modified so that the chassis and frameworks are now at earth potential. Replacement of faulty transistors in the impulse forming circuitry and the replacement of relay contacts by substantial switches in some control circuits have significantly reduced the lost beam time due to the converter plant as a whole. *Converter Grid Control Gear*

A new master timer for the control of the main converters is under construction. The original timer is becoming increasingly obsolescent and therefore difficult to maintain. Furthermore, in its present form it cannot easily be modified to provide additional facilities. It is planned to have the new timer in service on a trial basis after the 1971/72 shutdown. *Master Timer (ref. 233)*

Three of the heat exchangers in the cooling plant have been overhauled during the year. The shells were grit-blasted internally and then coated with epoxy based paint. With one more heat exchanger shell being similarly treated in the 1971/72 shutdown all 10 main heat exchanger shells will have been examined and treated within the last 3 years. *Heat Exchangers*

One of the 4 refrigerators used for chilled water has been completely overhauled. A new crankshaft and a complete new set of bearing shells were fitted. An order has been placed for a further 100-ton water chiller to meet increased demands for chilled water from extraction systems and from the second r.f. system. *Water Chillers*

The 150 hp pump purchased last year is in operation in Hall 1. A further similar unit is on order. One of these 150 hp pumps will meet the duty which was previously carried out by two 100 hp units. We shall therefore have a standby unit. All outstanding reservations on the Hall 3 installation were cleared up during the year and the system has operated satisfactorily. *Demineralised Water Systems*

Second Harmonic
RF System

The 1970 Report described a proposal to instal an additional accelerating stage in Nimrod, so adding a second harmonic r.f. field at eight times the orbital frequency. The effect of this field was calculated to yield higher beam intensities by increasing the phase stable area of the bunches. The accelerating voltage will be achieved using a drift tube in Straight 6 tuned by a pair of ferrite loaded resonators mounted respectively on each side of the containing straight section box. The box, drift tube and resonators have been designed and are now in an advanced phase of manufacture.

A 1/5 scale model of the drift tube box valve structure and resonators operating over a frequency range from 14 to 80 MHz, i.e. five times the second harmonic of the Nimrod r.f. frequency, was invaluable in assessing the permeability range required in the ferrite and enabling the mechanical design work to proceed independently of the high power r.f. tests which followed. The model is shown in Figure 89 side-by-side with the full-scale wooden prototype. This latter model was built to provide a realistic dummy load for use with the final r.f. power amplifier while the final load was being manufactured. It comprises a wooden carcase identical in internal dimensions to the straight section box with extended ends to simulate the vacuum vessel ends and the bellows extensions. The interior is lined throughout with 0·010 inch thick copper sheet, inside is a copper clad drift tube pattern (Figure 90). The final r.f. amplifier valve, a 33 kW tetrode, is mounted in the recess or 'top hat' in the box ceiling and the anode connects to the drift tube centre through an insulated vacuum window in the floor of the recess. Figure 89 shows the dummy loads attached to the side of the box adjusted to give similar losses to those calculated in the ferrite loaded resonators. Tests so far have shown that the box tunes accurately as predicted by the 1/5 scale model.

Figure 89. $\frac{1}{5}$ scale model of the drift tube box valve structure for the second harmonic r.f. system alongside the full-scale wooden prototype.
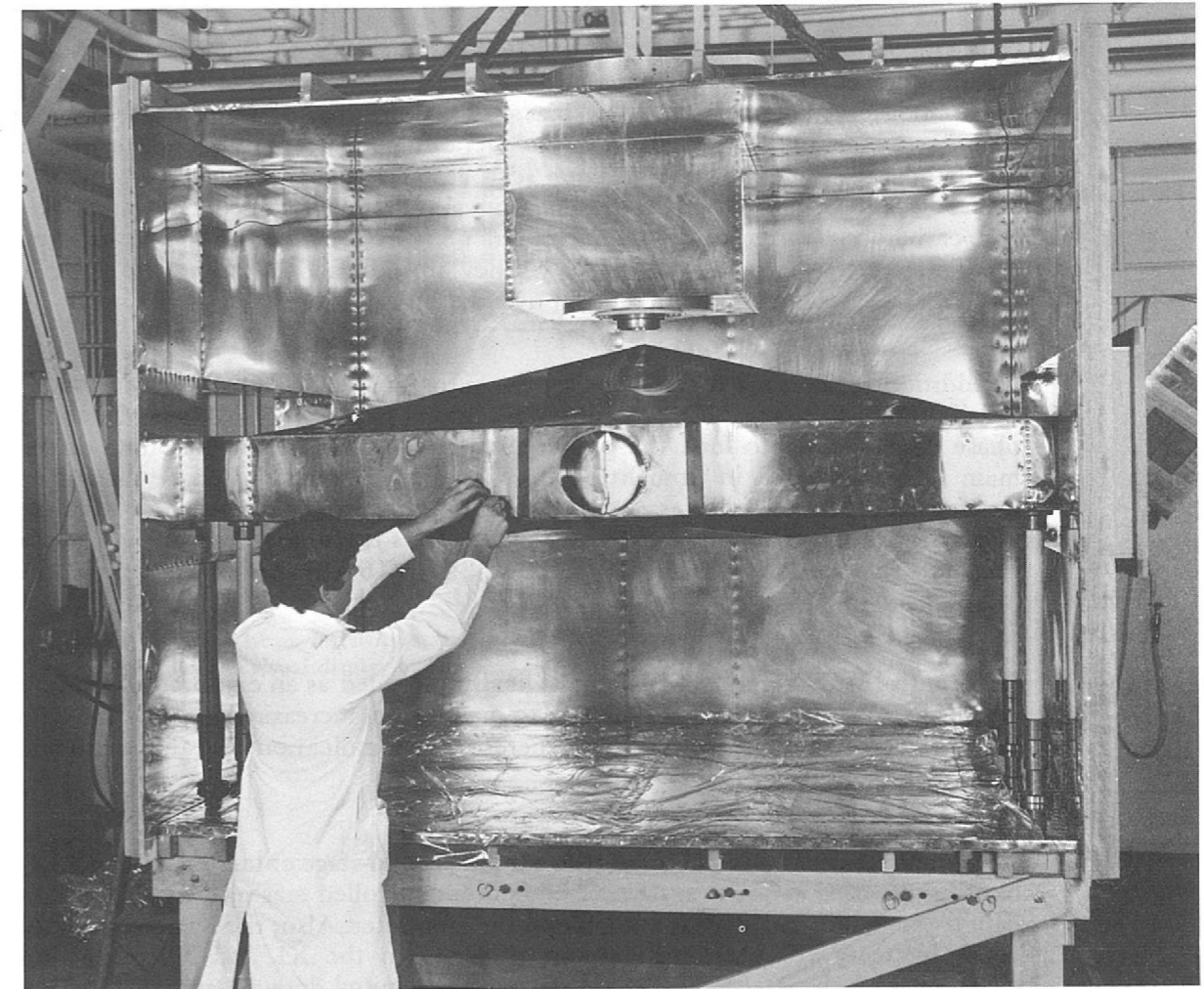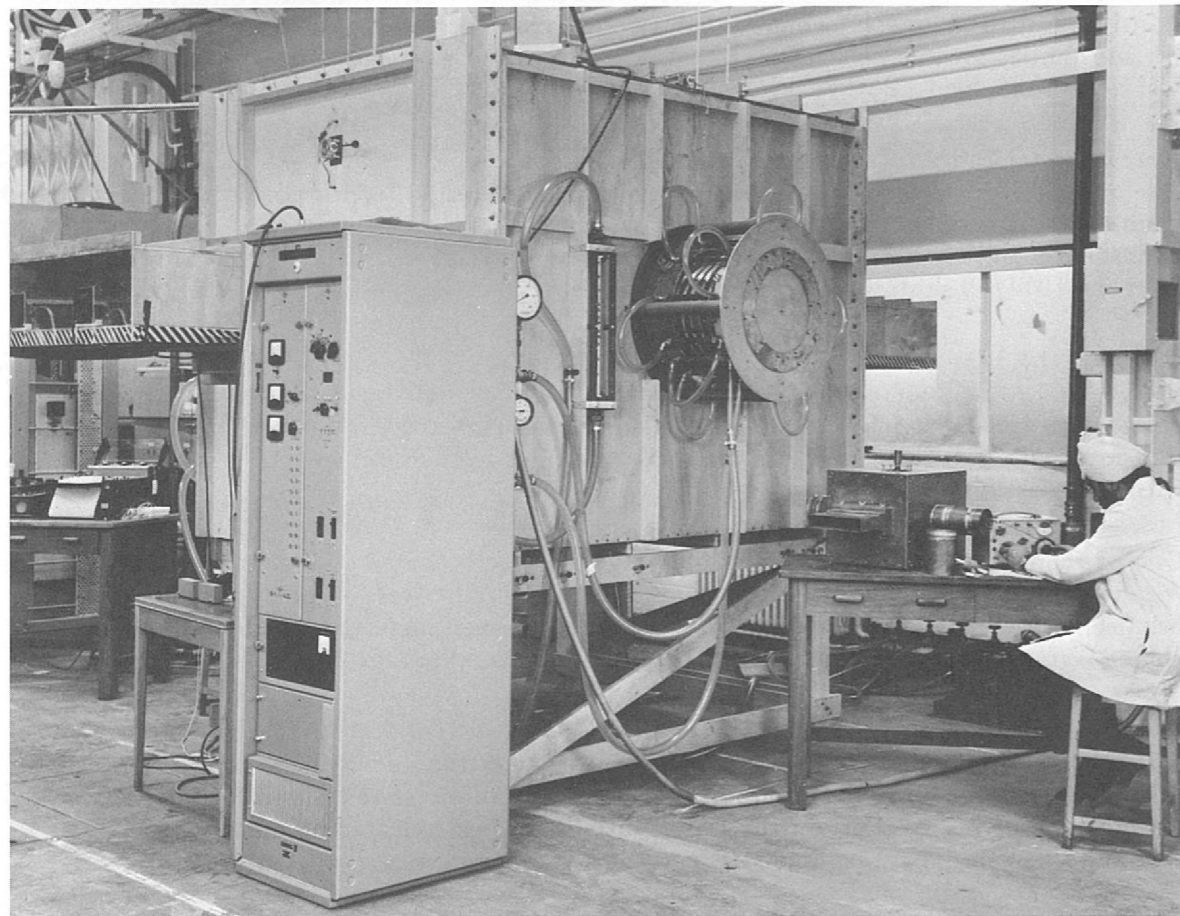
Figure 90. The interior of the wooden prototype for the second harmonic r.f. system.

The mechanical design problems associated with the drift tube cavity and resonators have proved particularly challenging. The straight section vacuum box must be tailored to maintain the existing Nimrod magnetic field shape. It will be constructed from 0·0625 inch copper cladding, to carry the radio-frequency currents, on 0·5 inch thick steel plate. Ribs are used to counteract the vacuum load and extra steel is bolted on to maintain the correct Nimrod magnet field configuration. New Ω-type bellows 61 in x 25 in in area, to join the straight section box to the Nimrod vacuum vessels, will be constructed. The drift tube is about 101 inches long and has an aperture for the circulating beam of 38 in x 9 in. It is manufactured from reinforced copper sheet and is shaped to connect to the resonators at each side and to the power amplifier valve above.

A detailed measurement programme on ferrite samples has been completed, and the required quantity of ferrite obtained. In addition a number of small sample rings have been assembled in a test cavity. This can be sweep tuned by a programmed bias supply and, when powered from an r.f. amplifier coupled to a second harmonic signal derived from the Nimrod primary frequency generator, can be operated at r.f. fluxes under working conditions similar to those expected in the final system. This will yield much useful information on the r.f. power required, the phase errors to be expected, and the bias current programme required to maintain the resonators on tune. So far the test cavity has been swept successfully up to 8 MHz.

The bias supply for the ferrite comprises a 250 kW motor generator set and a transistor bank similar to that used for the extraction magnets. The control circuits incorporate a current feedback loop giving very accurate control of the bias current under transient conditions. Twelve bias turns, consisting of water cooled nylon coated copper tube one inch in diameter, are supported in the centre of the resonators. They pass through vacuum seals and are then formed to surround the Nimrod beam aperture. The 12 return windings consist of nylon coated (uncooled) copper bars each 3·0 in x 0·75 in routed up the vertical sides and across the inside of the top of the r.f. cavity box. They are designed to carry up to 3000 A in a high vacuum environment without overheating.

In addition to the usual servo loops for the automatic level control of the Straight 6 drift tube r.f. voltage and the automatic tuning control, the system contains a phase control loop to lock the phase of the Straight 6 r.f. to the phase of the main accelerating r.f. in Straight 8. The system will keep the phase difference between the two r.f. voltages constant and null the initial phase error in less than a quarter of a synchrotron phase oscillation. Thus the phase detector and phase shifter have to work over the r.f. range of 2·8 to 16 MHz and have bandwidths of 100 kHz.

Computer Control of Nimrod

The control and acquisition system originally intended as an exploratory venture on the X3 beam line has expanded to handle an increasing amount of data relating to the accelerator itself, and there is every indication that this trend will continue.

The beam elements and collimators in the X3 second-stage extracted beam (X3X) have been added into the system of computer controlled magnets, and beam-flux data from the second stage is available to the computer. Also, the Nimrod primary beam intensity (BEAM), the amount of beam in the X1 and X2 extraction channels, and the X1 and X2 external target monitor data are monitored. The beam-element alarm scan has been arranged to trigger a channel in the main Nimrod alarm system when critical operator-specified beam line magnets go out of tolerance.

Effort has gone into providing adequate means for processing and displaying data, and thus there are now in use histogram and graph-plotting programs using a storage-CRT display (Figure 91). This display is available on the Nimrod closed circuit television system, and can be hard-copied when required. These data-display programs are usually run in a time-shared mode.

The most frequently-used time sharing programs have been linked permanently into the system, and have thus "disappeared" as far as operator call-up is concerned. In this category are a Nimrod BEAM history recording program, which outputs to a 36-hour cyclic disc buffer, and the digital display (nixie tubes) program. Other "operator-visible" programs can be called to interact with these; for instance, the BEAM data-buffer can be accessed by user programs which compile and output BEAM statistics in various forms.

These developments have meant increased core occupation for several parts of the software system, particularly the date table, the Nimrod interrupt program, and the core areas where various levels of programs are run. Consequently, the core store capacity was increased to 16K during the year. A certain amount of space is now free for extra facilities, one of which is a further history buffer on the discs, of real-time length about 30 minutes, in which 12 channels of pulse-by-pulse data are recorded.
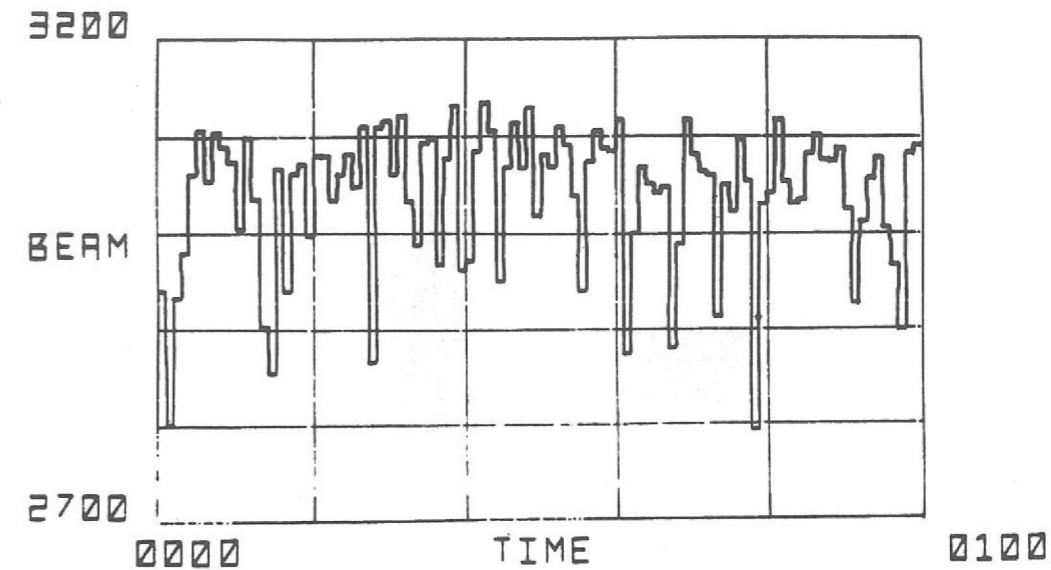
Figure 91. Nimrod beam intensity statistics, over a period of time, produced by the computer control — visual display system.

The extraction systems in use at Nimrod were described in some detail in the 1970 Report. After the initial success of the thin-septum system in X3, when an estimated 45% of the circulating beam was transported to an external target in Hall 3, innovations to equipment to improve reliability appeared to reduce the extraction efficiency. Although it has been possible to operate close to 40% during normal operation, the original 'high' as recorded early in 1970 has never been repeated, even when those conditions were reproduced as closely as possible.

Thin Septum Piccioni Extraction (ref. 208)

However, recent point-to-point surveys of the extraction channel by mounting foils at strategic locations and measuring induced activities, have revealed that 65% of the accelerated protons hitting the energy-loss target in the synchrotron are transported to hit the external target. This throws doubt either on the targetting principle involved, or on the measured circulating beam figures used for normalisation. Detailed cross-calibration, as yet incomplete, of the output signals at the beam-measuring electrodes, suggests that indicated circulating beam intensities are upwards of 40% high. Normal extraction efficiencies, after taking into account effects such as nuclear interaction loss during the lipping process and loss on the target support, would then be in the region 60-65%. An experiment devised to collect all the available circulating protons on a tall target for calibration purposes will be concluded as soon as possible to add further confirmation.

If the extraction efficiencies are in the 60-65% region there will be little gain in going to the more complicated resonant extraction system.

In addition to providing intensity date, a foil has been autoradiographed to show beam distribution across its section. By applying the technique to the 0·5 mm beryllium energy-loss target lip as well as to the foil just inside the target body, the beam at the X3 target location has been seen to be about 16 mm high.

Lip 0.5 mm thick

Target body
18.5 mm long

Target support
18.5 mm long

median plane

(a) at Octant 3 for X₃.

median plane
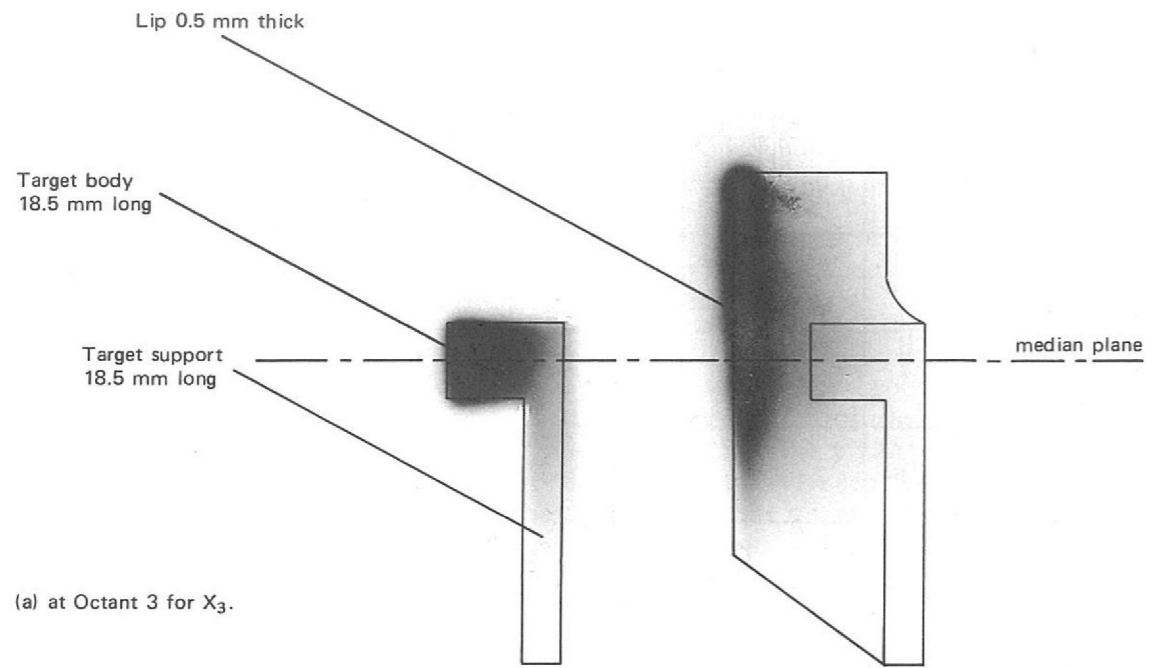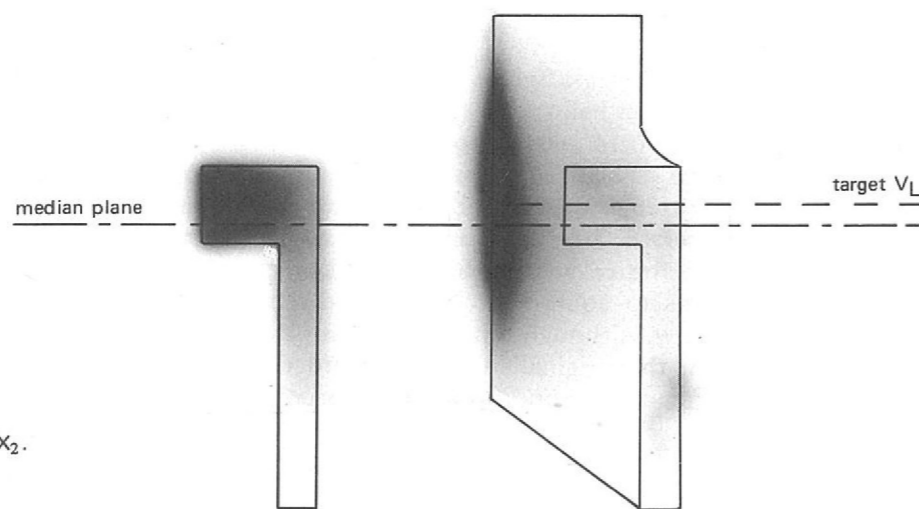
target V_L

(b) at Octant 1 for X₁/X₂.

Figure 92. Auto radiographs of foils showing the circulating beam cross section at the energy-loss targets for the extracted proton beams X₃ and X₁/X₂.

Figure 92 shows such a set of autoradiographs, together with an example exposed in Octant 1 at the location for the energy loss target for the X1/X2 extraction channel to be commissioned early in 1972. The beam is very nearly on the geometric median plane in this part of the machine.

Beam height correction has been achieved by energising pole face windings, using up to 60 A. Unfortunately, such a scheme upsets beam stability, so a compromise for X3 involves raising the target 8 mm and using only about 15 A median plane correction currents in the pole face windings. Another satisfactory scheme involves powering the pole face windings in adjacent pairs of Octants in reverse polarity with only low currents in such a way that the median plane is 'tilted' in the target region. Even without beam depression, the extraction efficiency is not much reduced when the raised target is used.

Throughout the year regular Machine Physics periods have also been used to test other suggested improvements. These have included using shorter targets after bringing the beam onto target height, since reduction in septum losses during the lipping process was expected to permit a closer approach of the extract magnet to the target radius, thus reducing beam spread and consequently lowering total losses. Angled targets have been used to nullify any angular errors. The original XM9 magnet with a laminated septum instead of the later stacked septum was tried. Although median plane fringe fields are of the same magnitude, they have opposite polarities and may be expected to introduce different closed orbit perturbations. However, none of these trials led to any significant improvement. Transport in the X3 beam line, from the machine outlet port to the external focus target, is about 90% efficient. From the header vessel quadrupole to the exit port, only 15% is lost. Overall the target-to-target transport efficiency is in excess of 65%. If the Piccioni targetting system is as efficient as has always been believed to be the case, then the X3 extraction channel runs close to its theoretical upper limit of 70%.

Thin Conductors for Septum Magnets (ref. 258)

The efficiency of extraction magnets and the first magnets in secondary beam lines frequently depends on the thickness of the 'septum', the dividing barrier between the accelerator magnetic field and the region where zero field is required. The septum is usually a thin energising conductor of the magnet. Work has continued on the basis of producing thin septa with coolant flow across the height of the septum rather than along the length which is then not a critical consideration in the cooling problem. Fluid flow and heat transfer rates have been measured for stainless steel and copper capillary tubes down to 0·3 mm diameter. From the test results, a septum of 0·5 mm thick and 20 mm high may be designed to carry 4500 A with a mean septum temperature of 90°C. A test magnet is being built which should produce a magnetic field of 2·4 kG (see Figure 93).

Figure 93. Schmetic diagram showing the assembly of a thin septum on an existing magnet yoke.

Return Windings

Main Manifold

Insulator

Sub Manifold

Pole

Pole

Septum

RX3 Yoke
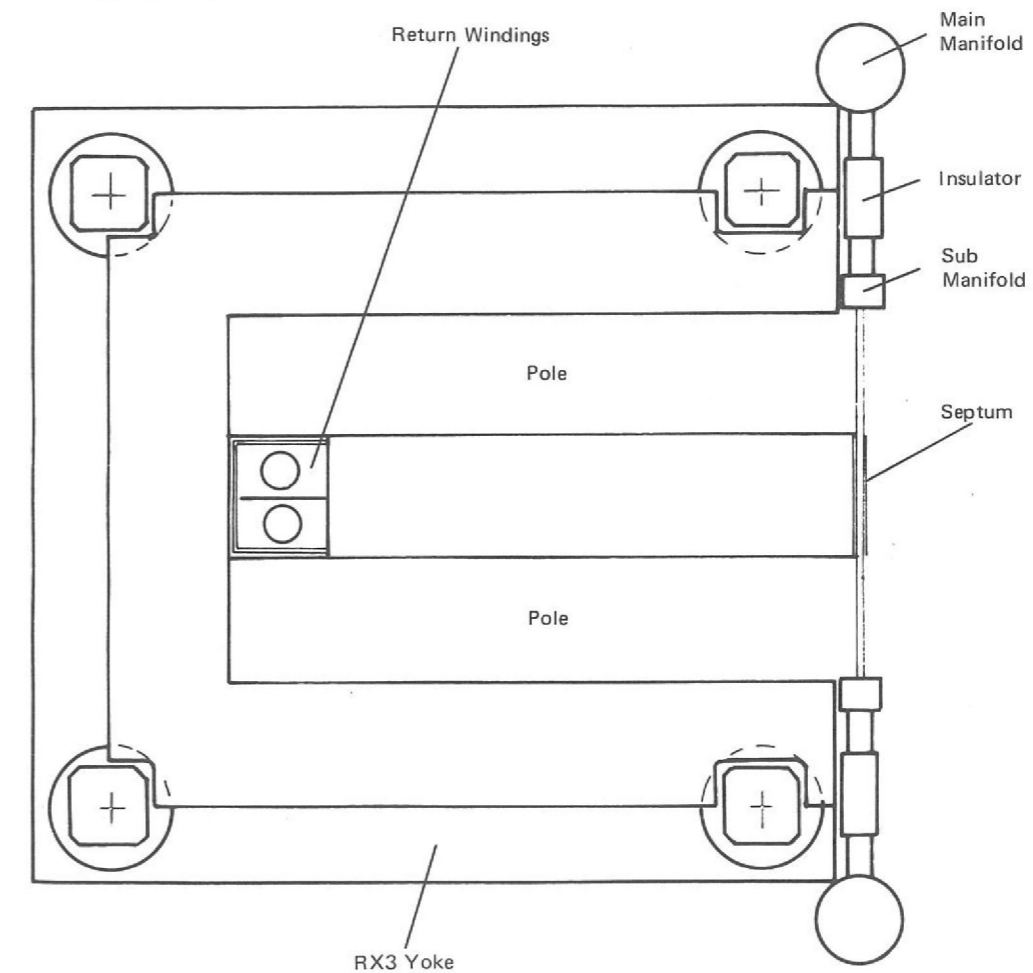
The internal target mechanisms have been fitted with improved target arm assemblies in order to simplify and speed up maintenance changes in high radiation areas. The mounting of external targets has been simplified and improved for easier setting up and changing. Again, the design emphasis has been on cutting down or simplifying tasks carried out in radio-active areas.

The range of physics which could be done using Nimrod as the secondary particle source could be much extended if the intensity of extracted beams were 10^{13} protons per pulse. Present intensities are $1 \cdot 2 \times 10^{12}$ ppp which with improvements already mentioned will bring it close to 2×10^{12} ppp. The extraction efficiency is now as high as one can reasonably achieve, so that the number of accelerated protons must be increased to give more extracted protons. We know that Nimrod is limited at injection into the magnet ring by transverse incoherent space charge effects in which the forces between the injected protons are sufficient to overcome the focussing forces of the synchrotron magnet to such an extent that the number of injected protons reaches a saturation level. The saturation level of protons goes up as the injection energy increases. A factor of five improvement requires the injector energy to be increased from its present value of 15 MeV to 70 MeV.

Figure 94. Layout of the proposed 70 MeV Injector for Nimrod.

Past reports have described various higher energy injectors for Nimrod. In 1966 a 70 MeV separated orbit cyclotron was described. A proposal was put forward in 1968 to modify the 50 MeV PLA, then still working, and to transport the protons to be injected into Nimrod. A small circular synchrotron booster between the present injector and Nimrod has also been considered. It is now considered that a 70 MeV linear accelerator (linac) is the new injector most likely to be within the Laboratory resources by diverting part of the resources currently given to experimental physics. Comparative studies have been done this year for a completely new linac based on the first part of the injector for the 200 GeV accelerator at the National Accelerator Laboratory at Batavia, USA, and a 70 MeV linac next to Nimrod using some of the components of the PLA. The latter is considerably cheaper and a scheme has been prepared in which the linac would be housed in a single lean-to building alongside the present linac. Injection would be one Straight Section away from the present injection point. Building and commissioning of the new linac would not interfere with operation of Nimrod at its present intensity. The time-scale envisaged for providing the new injector ready for commissioning is 2½ years from approval.

BEAM LINES AND ASSOCIATED EQUIPMENT

During the early part of the year the main effort in the experimental areas was directed to improving the flow monitoring devices of septum magnets, modifying the K9 collimators, repairing the K15 separator and installing components of the π9 beam line associated with the building of the X3X blockhouse. These tasks were all achieved on time, in particular the first beam onto the X3X target was achieved by 1 April and the K15 separator was fully conditioned and operational by 29 April.

(ref. 218)
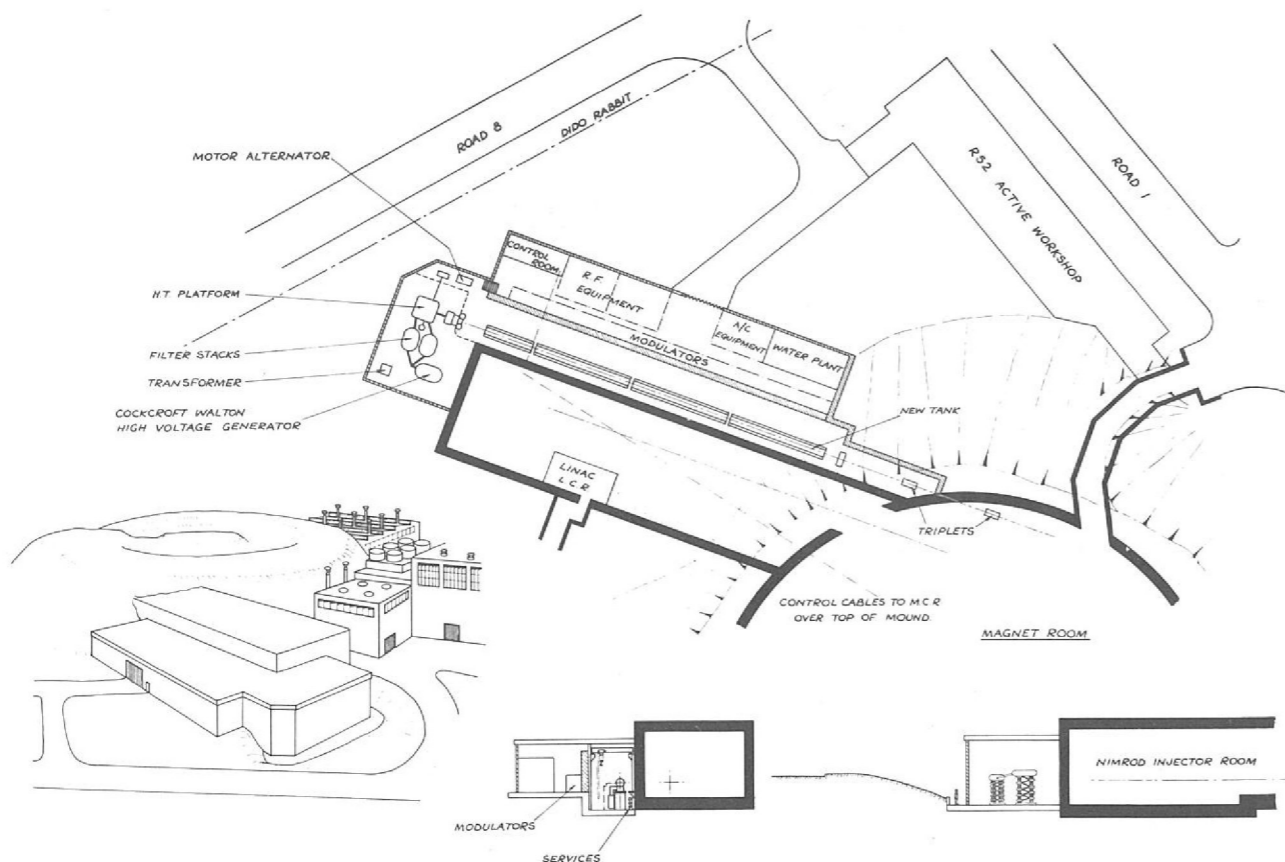
Further operation of X3X was stopped in April to enable the new "N4 Neutron Test Facility" beam to be installed. In addition to the usual beam-transport components, a 100 ton spectrometer magnet, type M5, was removed from K13 and installed in N4. The X3X beam stop was extensively modified to accommodate a new 10 ft long collimator slot. The first neutron beam was realised during October.

Beam Line Installation

The building of the X3X blockhouse, π9 and N4 beam lines completely absorbed the Laboratory reserve of steel shield blocks. The removal of these blocks from the old airfield runway provided the impetus to clear away and re-organise the storage of the remaining concrete shielding.

During the year a concerted drive to improve safety and cleanliness was conducted in the experimental halls. The "Permit to Work" system was extended to include work on the tops of block houses, warning lights were fitted to all gantry cranes, raised walkways and steps were built over floor-level magnet hoses and cables. The rust surfaces of steel blocks used in shield walls were painted. A start was also made in sealing the concrete floors. It is felt that these measures have all in some way contributed in maintaining the low level of accidents in the experimental halls. 15 accidents were reported during the year 1971 in these areas of which only one caused loss of time.

Safety in Experimental Areas

Work has been proceeding on the updating of some of the older 100 kW and 50 kW power supplies to give improved response times and a current stability of 1 part in 10^4. Also a digital-to-analogue converter has been incorporated in the control circuit to enable remote setting-up either by digi-switches or from a computer, a facility already existing on the more recent units. A total of 53 units have been modified to date.

Beam Line Magnet Power Supplies

Figure 95. General view of the Experimental Hall 3 showing the K15 beam line and the X3X blockhouse.

The rectifiers on X3, X3X and K9 beam lines are already on computer control. The rectifiers on π9 and K13C are on a digit control scheme ready to be interfaced to a computer, and the units on X1 and X2 are now being modified for digit/computer control.

X2 Complex (ref. 231, 255) A redesign of the X2 extracted beam blockhouse layout is in progress, primarily aimed at providing a stopped kaon beam for counter physics (referred to in the 1970 Report) with installation during the 1972/73 winter shutdown. The design takes account of other possible beams for X2, in particular the provision of a 2·5 GeV/c K⁻ beam for the projected rapid-cycling bubble chamber.

Low Momentum K⁻ Beam for 1·5 m Bubble Chamber (ref. 217) A two-stage electrostatically separated beam for the 1·5 m Bubble Chamber has been designed to allow K⁻ physics in the momentum range below 1 GeV/c (See Figure 96). Particular emphasis was placed on achieving low contamination, so that energy-loss degrading would allow experiments in the momentum range 0 to 0·5 GeV/c. The design should also provide antiprotons in the range 0 to 1 GeV/c, again using an energy degrader.

K9 Beam Line to the 1·5 m Bubble Chamber (ref. 137) **Installation of Computer Control.** The computer control system for the K9 beam line described in the 1970 Report was installed during the first half of the year, almost exactly on schedule. The beam has been required at approximately six-weekly intervals to meet the needs of the development work on the target facility in the 1·5 m hydrogen bubble chamber. In each successive operational period more computer control was used until in the last period of the year the beam was tuned and run completely under computer control.
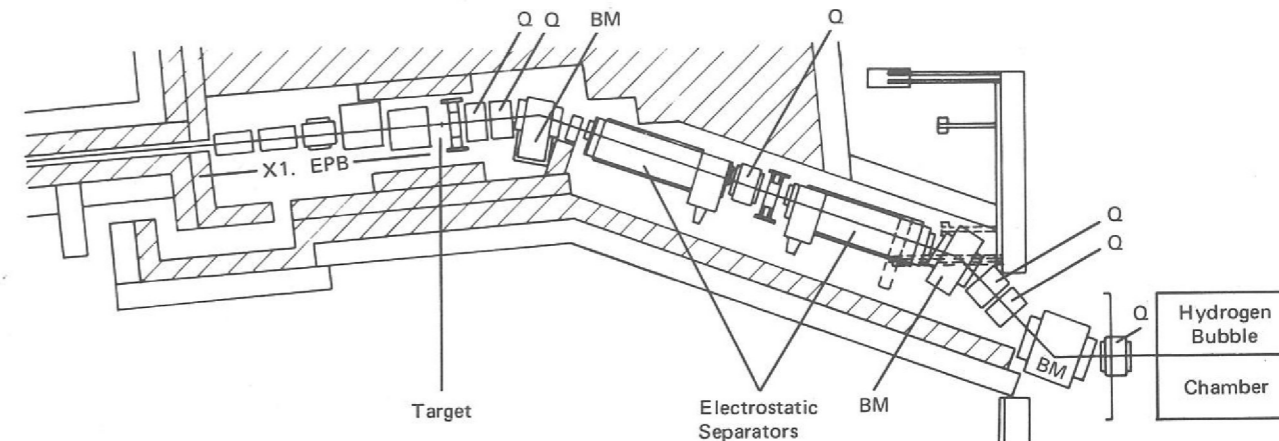
Figure 96. Layout of low momentum K⁻ beam for the 1.5 m Hydrogen Bubble Chamber.

Operating System. The operating system is entirely different from that used on the X3 extracted beam line in that programs are written and stored in an extension of the FOCAL language and are run under the control of an interpreter. The extended language and its operating system are given the collective name RTI-70, RTI standing for Real Time Interpreter. With RTI-70 a sequence of commands (a program) are translated (interpreted) into the computer's own instructions one by one as they are encountered.

By normal computer standards, such an interpretive system is inefficient and slow. However, in the case of a beam line, the equipment to be controlled is relatively slow in response and so the low speed has not proved to be a problem. In any case this slight disadvantage is far outweighed by the tremendous flexibility achieved.

Flux Measurements. An opportunity was taken early in the year to measure the *(ref. 219)* flux of anti-protons that might be provided by the beam and at the same time to check the earlier measurements of the negative kaon flux. The results showed that anti-proton experiments in the range 1·9 to 2·6 GeV/c are possible, while for negative kaons the usable range extends from 1·9 to beyond 3·0 GeV/c. These figures are based upon an estimated consumption of about 50% of Nimrod's accelerated protons. Figure 97 shows the results in more detail.

Figure 97. K⁻ and $\bar{p}$ yields for K9 beam.

Electrostatic Separators (ref. 197)
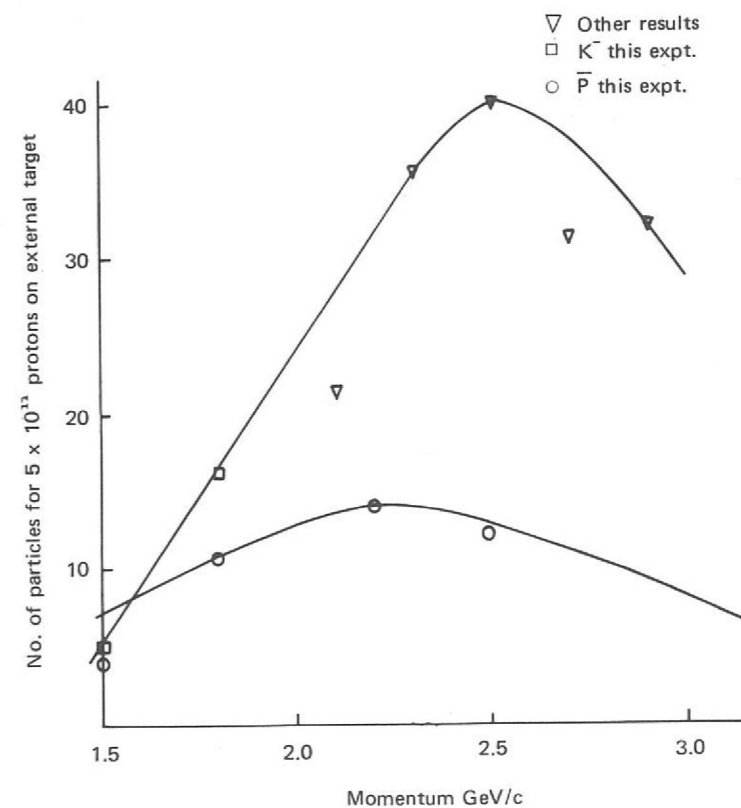
DC separators have been operational in four Nimrod beam lines during 1971, a total of nine separator tanks have been used in these systems. There have been no serious operational problems, potential gradients of up to 80 kV/cm have been used successfully.

Wire Grid Electrodes. Development effort has been concentrated this year on evolving the final design of a wire grid electrode and proving its performance ready for the installation of such electrodes in beam line separators. Two beam lines are to be fitted with wire grid electrode separators during the 1971/72 winter shutdown of Nimrod, namely K15 and one of the two separators on K9. It is hoped to change over all the separators at the Laboratory to these new electrodes as the opportunity arises.

During this final development work, two difficulties have become apparent. The first concerns the design of the supporting framework for the electrode. This framework has to be very stiff to achieve the required degree of flatness in the electrode surface and so it was intended to make it in the form of a rivetted box girder. However it was discovered that the presence of the flat top surface of the box girder immediately behind the wires spoilt the electrical performance by increasing the sparking rate. To overcome this defect the supporting frame was changed to an open ladder type of structure which completely overcame the problem.

The second problem arose with the decision to change only one of the two separators in the K9 beam. In the previous form of separator using heated glass cathodes, the cathode has to be the lower electrode because of its weight. Up to this time all tests on the wire grid electrodes had been performed with the wire grid electrode, which is best used as an anode, at the bottom. When the wire electrode was put at the top, using it as an anode, the performance was affected seriously. (This suggests that the ability of dust and other particulate matter to escape through the gaps between the wires is one reason for the improvement in the sparking rate with wire electrodes.) There was thus a dilemma for the K9 beam, the existing glass cathode separator required that the cathode be at the bottom, while the new wire grid electrode separator would ideally require the cathode to be at the top. The problem has been resolved by deciding to operate the new separator temporarily with the polarity reversed until the other separator can be changed as well. Even so the performance is still superior to that of separators with heated glass cathode.

The performance of the final form of wire grid electrode separator is given in detail below for a gap of 100 mm:

Total voltage (kV)	600	645	700	740
Sparks per hour	0·3	1	12	60

When operated with the polarity reversed the voltage at which the sparking rate is 1 per hour is reduced to 600 kV.

There still remains to be measured the performance at gaps other than 100 mm so that beam designers can select the optimum gap for any particular requirement.

Lead-in and Support Insulators. During the year long-term tests have been performed on the latest design of both lead-in and support insulators. The lead-in insulators are now thought to be able to withstand 500 kV on either polarity for long periods without significant deterioration, while the support insulators are good for long-term service in glass cathode electrode separators up to 350 kV at 80°C and in wire grid electrode separators up to 400 kV (at room temperature).

Fundamental Vacuum Breakdown Research. This work is manned in the main by students working at the Laboratory for one year as part of their undergraduate courses. The experiment attempted during this year led to a negative result. Attempts were made to detect an r.f. component corresponding to an ion-exchange process in the pre-breakdown current. Despite an extensive search it was concluded that any such currents must be below the limit of sensitivity of the available apparatus.

Figure 98. Interior view of an electrostatic separator with a wire grid anode.
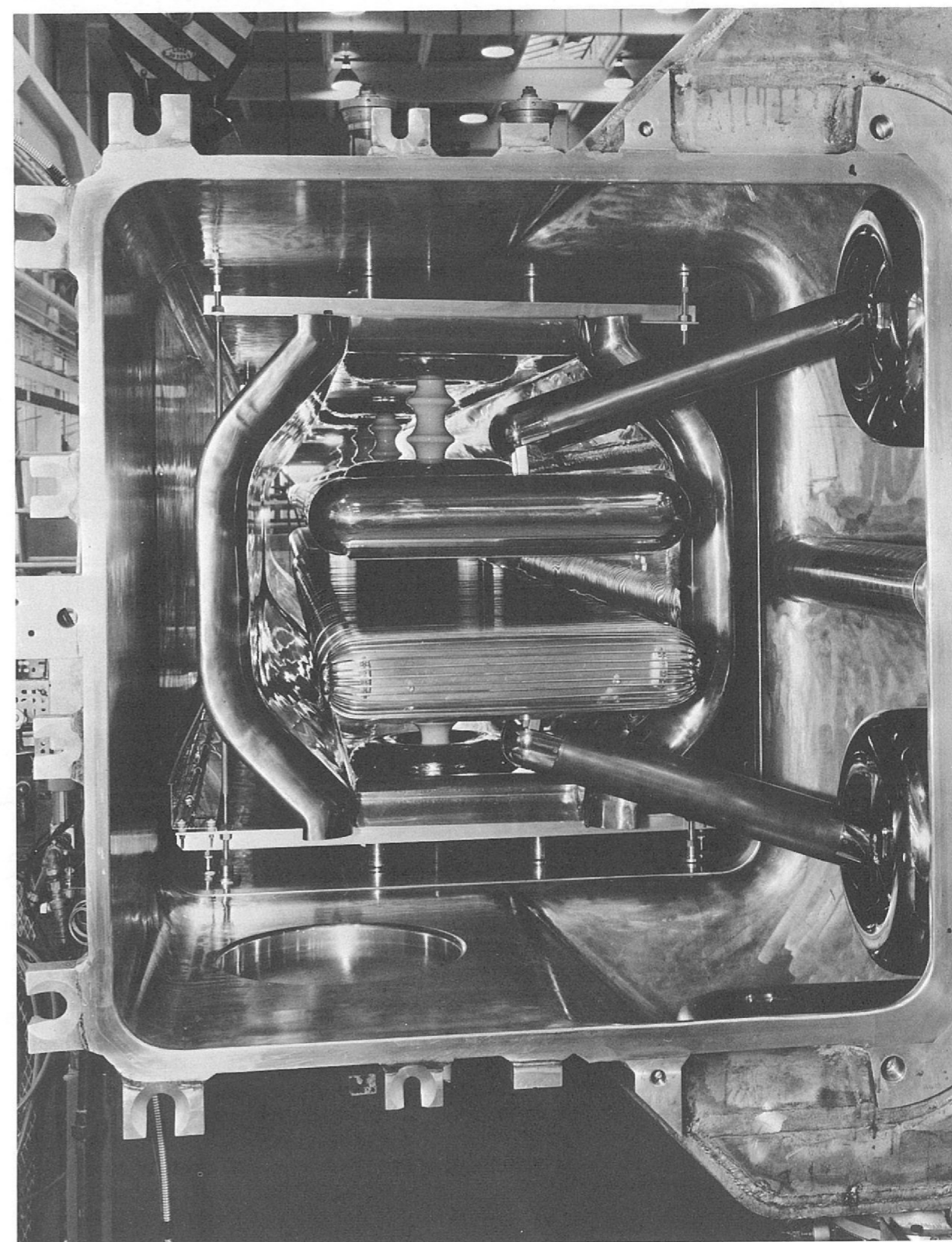
The AC3 pulsed dipole magnet, just after removal
from its liquid helium cryostat.

APPLIED
RESEARCH

Applied Research

Applied research at the Rutherford Laboratory has as its exclusive aim the development of new techniques to improve and extend the apparatus of high energy physics. A large part of the applied research programme continues, as in the past few years, to be devoted to the applications of superconductivity, a field in which the Rutherford Laboratory has gained an international reputation. The growing use of superconducting magnets for bubble chambers, spark chambers, polarized targets and beam handling magnets is a clearly discernible feature of present day experimental high energy physics, and this trend seems likely to develop further in the future and to encompass pulsed superconducting magnets for use in the accelerators themselves.

The full approval in early 1971 of the construction of the European 300 GeV accelerator adjacent to the present CERN site at Meyrin has already focussed attention on the long term possibilities of uprating this accelerator to 1000 GeV or more using high field superconducting magnets. The construction schedule laid down for the various stages of the 300 GeV project specifies several decision points at which superconducting magnets could be adopted for inclusion in the accelerator. The first of these is January 1974. If at that time it can be demonstrated that superconducting synchrotron magnets are both technically and economically feasible, then it seems likely they will be adopted for Stage B of the accelerator development programme to take the maximum energy of the machine from 200 GeV to 500 GeV or beyond.

The technical and economic evaluation of the superconducting synchrotron magnets has been made the responsibility of the GESSS Collaboration (Group for European Superconducting Synchrotron Studies), a collaboration involving the Rutherford Laboratory and the IEKP/Karlsruhe and CEN/Saclay laboratories. In close consultation with CERN, a programme of magnet development and also a design study on the superconducting synchrotron itself has been undertaken by the GESSS Collaboration with a view to providing the necessary information on which the January 1974 decision can be based. A significant milestone in this programme was the successful testing of the first prototype superconducting synchrotron magnet of representative aperture and magnetic field at the Rutherford Laboratory in September 1971. Details of the performance of this magnet are given.

A further type of superconducting device, namely a superconducting r.f. separator, is under development at the Rutherford Laboratory. The results obtained to date are presented. Such devices will provide separation of secondary particle beams into their constituent types with high resolution and low r.f. power.

As a counterpoise to the longer term development work described above, the applied research programme also involves the construction of advanced cryogenic apparatus for more immediate use in specific high energy physics experiments. A polarized target of the frozen spin type is nearing completion of construction and a further similar target is under consideration. A small rapid cycling hydrogen bubble chamber is proposed, the design to be based on experimental results which will be obtained from a test rig now nearing completion.

SUPERCONDUCTING MAGNET STUDIES

An extensive programme of development work is directed towards the evolution of reliable and economic superconducting magnets for possible applications in proton synchrotrons, storage rings, particle beam transport elements, and energy storage for synchrotron power supplies. *(ref. 121)*

The problems associated with pulsed synchrotron magnets have occupied the major part of the effort during the past year. The work falls essentially into two categories (1) the development of a suitable conductor, and (2) the construction of pulsed magnet prototypes. *(ref. 142, 143, 157, 227)*

Beginning with the conductor, work has continued on the development of a high current density transposed cable capable of carrying a current of several thousand amperes. Using the cabling research facilities now available at the Laboratory, a wide variety of compacted cable configurations have been attempted. These experiments have shown that high density compaction without breakage is difficult to achieve reliably with large numbers of fine strands, and the present preference is for configurations containing fewer separate wires of larger diameter. This in turn implies more superconducting filaments in each wire, and Figure 99 shows a cross-section of a sample filamentary composite containing up to 8,000 filaments, produced this year by Imperial Metals Industries under a research contract from this Laboratory. Further practical studies of the stability and loss properties of such composites have been carried out to assess their suitability for pulsed magnet applications. *Superconducting Cable (ref. 164, 165)*

Figure 99. Cross-section (enlarged) of a composite superconducting cable.
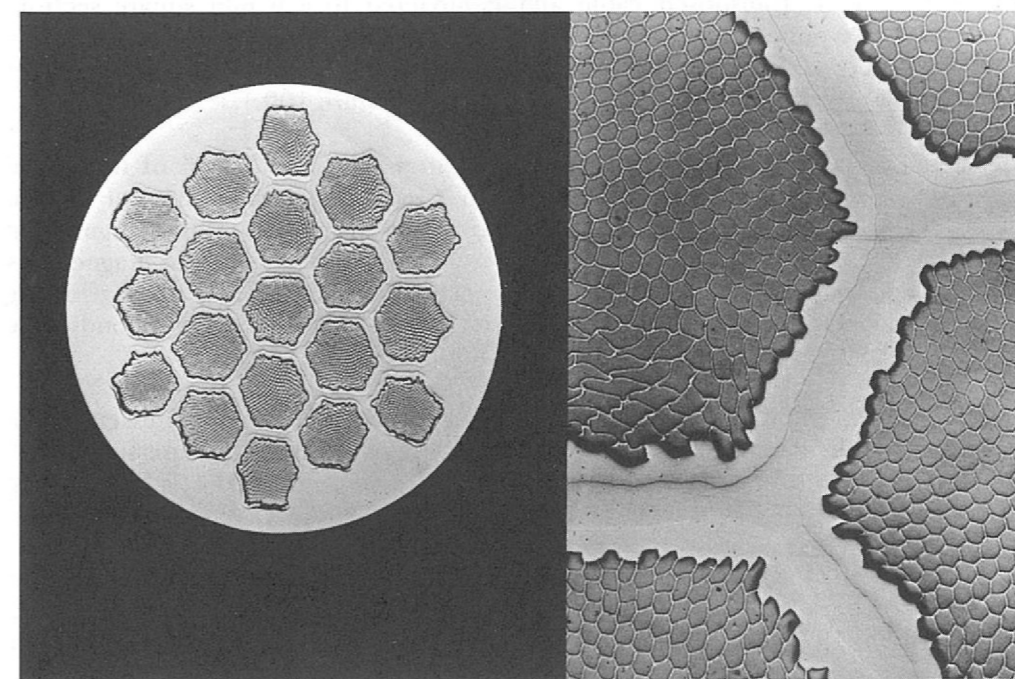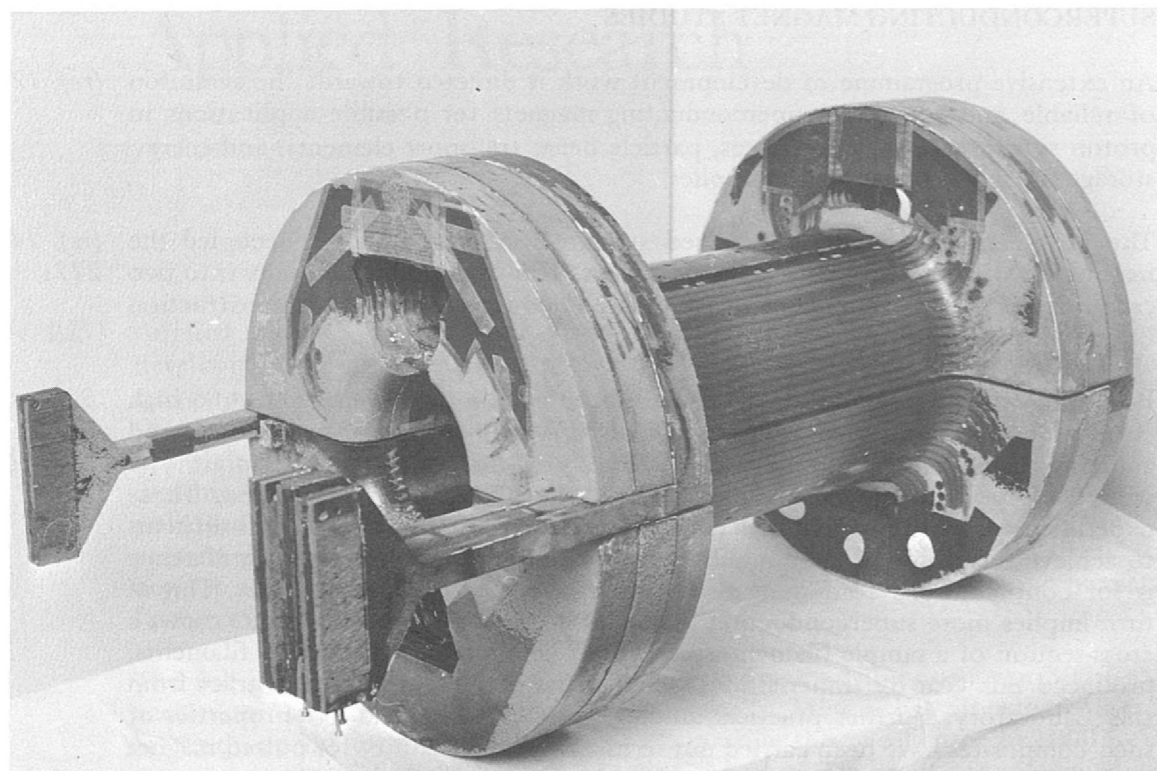
Figure 100. The AC3 pulsed dipole magnet.

AC3 Pulsed Dipole Magnet Although a number of details of conductor and cable manufacture are still to be resolved, an increasing scale of effort is now being devoted to the magnet design and engineering problems, in the construction of a series of pulsed dipole prototypes. The first of these, known as AC3, was successfully completed and tested during 1971. The basic conductor used was a 0·4 mm diameter composite manufactured by IMI and containing 1045 filaments of 8 μm dia. It was formed into a 90 strand transposed cable and compacted to a 5 mm square section. The coil was wound in six concentric layers, and fully impregnated with epoxy resin. Mats of copper wire were sandwiched between the winding layers to conduct the a.c. heat out of the coil to the liquid helium. (Figure 100.)

In its first tests the magnet was pulsed continuously at about 90% of its critical current (5,400 A), with rise times down to 1 second. The peak central field in these tests was about 4 T, (which in an actual synchrotron would be augmented to between 4·5 and 5·0 T by the addition of an iron shield). The magnet was given several thousand pulses, and also quenched many times, without affecting its performance. The measured a.c. loss was about 10 watts at a 4 second cycle time, close to the predicted value for the conductor used.

This dipole was about 40 cm long with a 10 cm bore, and, although essentially a research magnet, it represents the first pulsed dipole which has an aperture, field, operating current and cycle time comparable to the requirements of a high energy superconducting synchrotron.

AC4 and AC5 Pulsed Dipole Magnets Also during 1971 detailed design work was initiated on the next two dipole magnets: AC5, a realistic and accurately wound horizontal prototype to be completed in 1973 and its smaller trial predecessor, AC4, to be completed in 1972.

The design of AC4 and AC5 differs from that of the already tested AC3 in several significant respects. Both AC4 and AC5 will have iron shields since at the required magnetic field level of 4·5 T the iron itself contributes about one-third of the total field and in so doing significantly reduces the amount of super-conductor required and the stored energy in the magnetic field. A further advantage of an iron shield is that in principle it improves the field quality up to the point when untoward saturation effects dominate. Detailed computer studies have shown that, by shaping the inner boundary of the steel, saturation effects can be controlled sufficiently well to preserve the field uniformity for central fields up to at least 4·5 T. (AC3 has no iron shield.) Both AC4 and AC5 will aim at a uniformity of magnetic field of 1 part in 10^3 or better across the working aperture of the magnet. (AC3 was not designed with maximum field uniformity in mind). AC4 and particularly AC5 will be fully engineered magnets using in their construction only those techniques which lend themselves to the quantity production of magnets that would be required for a superconducting synchrotron. (AC3, being a first prototype, was not designed with this objective in mind.)

Construction of AC4 is well in hand and testing is programmed to start in May 1972. The superconducting cable for this magnet is to be made of 25 wires each of 0·85 mm diameter, each wire to contain 2035 filaments of niobium-titanium. The individual wires are insulated from one another by copper oxide and the overall cable is insulated with a woven Terylene braid after compaction to a rectangular cross-section of 5·85 mm x 3·85 mm. A model of a section through the mid-plane of the magnet is shown in Figure 101.

Figure 101. Model of a section through the mid-plane of the AC4 magnet.
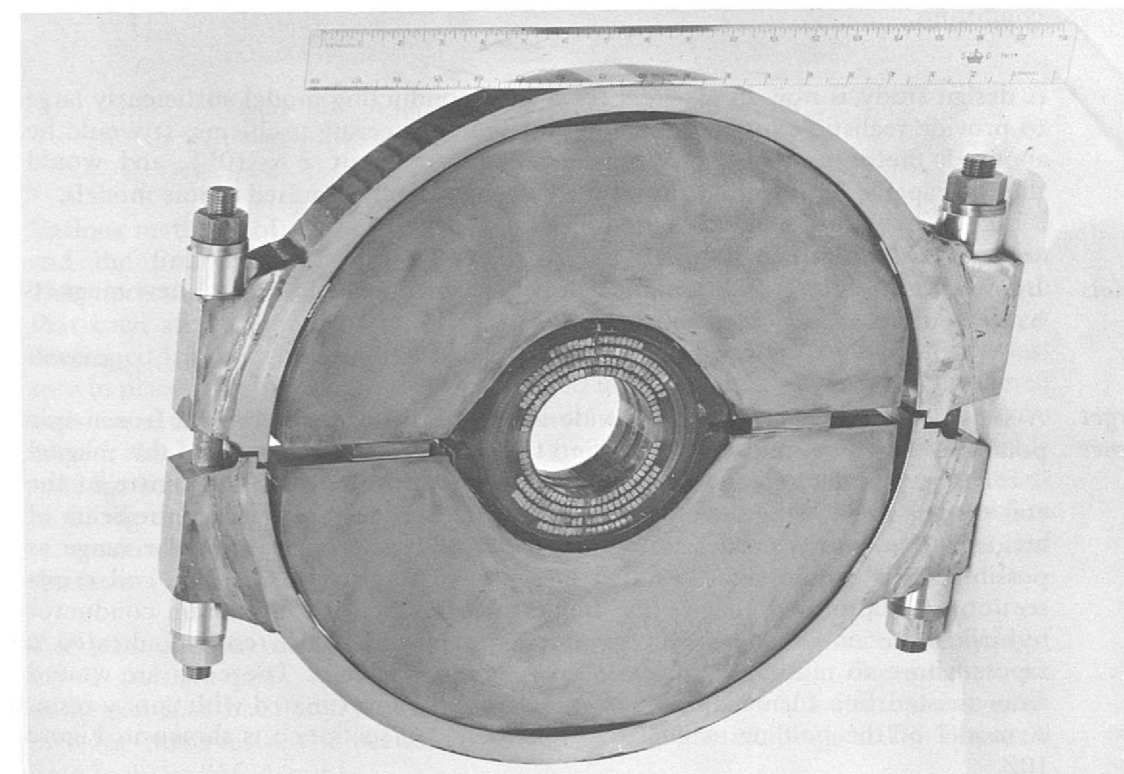
Winding trials have been carried out, to develop techniques of positioning the individual turns to the required accuracy. The method adopted involves winding onto the outside of a mandrel with high tension in the cable and around accurately positioned spacer pieces made from epoxy glass laminate. The cooling channels are moulded between each coil layer by winding in polythene strips which are then removed after impregnation of the coils with an epoxy resin. The high thermal contraction of resins compared with the conductor materials generates internal stresses in the coils on cooling to 4·2 K. Filled resins using such additives as silica, alumina and zirconium silicate are being considered to reduce the overall thermal contraction and usefully increase the thermal conductivity. Tests are in progress to find the optimum filler concentration since heavily filled mixtures are very viscous and unsuitable for vacuum potting.

Since the laminated iron shielding is positioned close to the coils, it has to operate at temperatures near to 4·2 K and at these temperatures iron can be very brittle. The main magnetic force in the coils is radially outwards and has to be counteracted by the iron. In AC4 the iron is split vertically to allow the coils to be dismantled easily thus allowing the forces to be transferred to an external stainless steel clamp. Experiments are in progress to confirm that this force restraining structure is adequate.

Superconducting Energy Transfer System for a Superconducting Synchrotron (ref. 141, 271, 280) In connection with the work towards a superconducting synchrotron, a novel rotating energy transfer system for powering the magnets of the synchrotron has been under study for some time. Further theoretical work on this totally superconducting system has been carried out and shows that the required coupling law can be achieved with a high degree of precision using realistic practical coil geometries to approximate to the idealised spherical distribution. In addition, theoretical work on dynamic fault behaviour, on a.c. losses, and control problems has been carried out. Practical confirmation of some of the theoretical predictions has been demonstrated by means of a room temperature analogue model which uses electronic techniques to imitate the constant flux property of each superconducting circuit. This model has been used for demonstration of the basic principles, for accurate coupling measurements, and for simulation of fault conditions.

A design study is now in progress for a superconducting model sufficiently large to provide realistic experience in some of the engineering problems. It would be about 1 metre in diameter, transferring up to about 2×10^5 J, and would thus be capable of powering any of the currently planned pulsed dipole models.

D.C. Magnets Interest in d.c. superconducting magnets has continued and several new magnets have been successfully tested during 1971.

Polarized Target Magnet A superconducting magnet to provide a holding field of 2·8 T for a frozen spin polarized target was required (see page 113). The basic requirement of this magnet is for large annular access to the polarized target positioned at the centre of the coil system so allowing secondary particles produced at the target by the beam of incident elementary particles to be detected over as large an angular range as possible. This requirement resulted in a coil of unusual shape. The coil cross-section was optimised to give the highest central field for minimum conductor by using the on-line computer graphics system and these results indicated a tapered bore to minimise the peak field within the coils. The coils are wound from twisted fine filament conductor and are fully impregnated with epoxy resin. A model of the holding magnet with one half coil sectioned is shown in Figure 102.
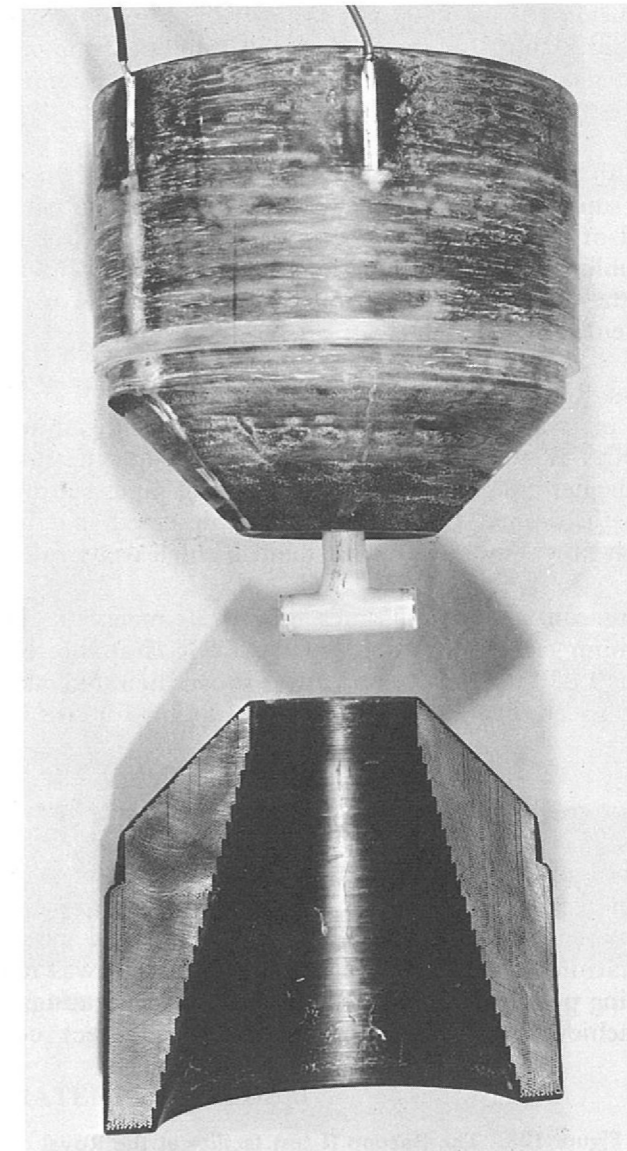
Figure 102. A model of the holding magnet, for the polarized target, with one half coil sectioned.

Various methods of winding coils with this unusual cross-section were examined and the final method adopted was to wind them as continuous layer coils. This necessitated producing a stepped former out of epoxy glass laminate such that each step catered for two layers of winding. The 45° slope on the coil was developed by reducing the number of turns in each layer and by holding the last turn in place with loops of glass fibre trapped under the next layer. The completed coils were closely wrapped with glass cloth on the outer surfaces, clamped in a mould, then impregnated with epoxy resin. Tests were made on the most suitable resin for impregnation and operation at liquid helium temperatures. Also, methods of filling the resin rich areas within the coils were examined to avoid the problem of cracking due to differential thermal contraction between the conductor and the resin.

The pair of coils has been successfully operated, producing a central field of 2·8 T (with a peak field at the conductor of almost 8 T). The magnet was immersed in a bath of liquid helium boiling at 2·2 K at a sub-atmospheric pressure for these tests. The overall current density in the windings at 2·8 T central field is about 250 A/mm².

Racoon II Magnet Further testing during 1971 of the RACOON II superconducting magnet built as part of the feasibility study for the High Field Bubble Chamber has been carried out. Construction details and results of the initial tests of the coils are given in the 1970 Annual Report.

The second stage of the RACOON II test programme was designed to demonstrate that the selected superconducting strip would carry its rated current of 7,500 A in a magnet field of 8·4 T, this being the peak field encountered in the coils of the proposed bubble chamber. For this test RACOON II in its own cryostat was mounted within the bore of a conventional 5 T water-cooled magnet at the Royal Radar Establishment, (RRE), Malvern.

The test facility at RRE (Figure 103) shows the RACOON II cryostat installed in the conventional magnet. Also shown are the large overhead busbars supplying current to RACOON II, the horizontal busbars supplying the required 17,500 A to the backing magnet and the two large horizontal pipes supplying the cooling water to the plastic domed headers especially designed and manufactured in epoxy resin carbon fibre laminate to withstand the high water pressures.

The magnets were run up several times to various magnetic field and current levels. The maximum current achieved in RACOON II at the required magnetic field of 8·4 T was 9,800 A. This value is well above the rated current of the conductor, 7,500 A, so confirming the conductor design for use in the proposed application.

The use of indirect cooling of d.c. superconducting magnets has also been studied further during 1971. Commissioning of a horizontal cryostat using pumped supercritical or two phase helium as the coolant (illustrated in the 1970 Annual Report) was completed, and tests were made using a fully impregnated quadrupole system cooled indirectly by means of a system of parallel tubes around its circumference. Operation at or very close to critical current was reliably achieved, with rapid recooling possible after a quench, thus demonstrating that reliable coil performance is achievable without the necessity of direct contact with the coolant.

Figure 103. The Racoon II test facility at the Royal Radar Establishment, Malvern (Photo RRE).
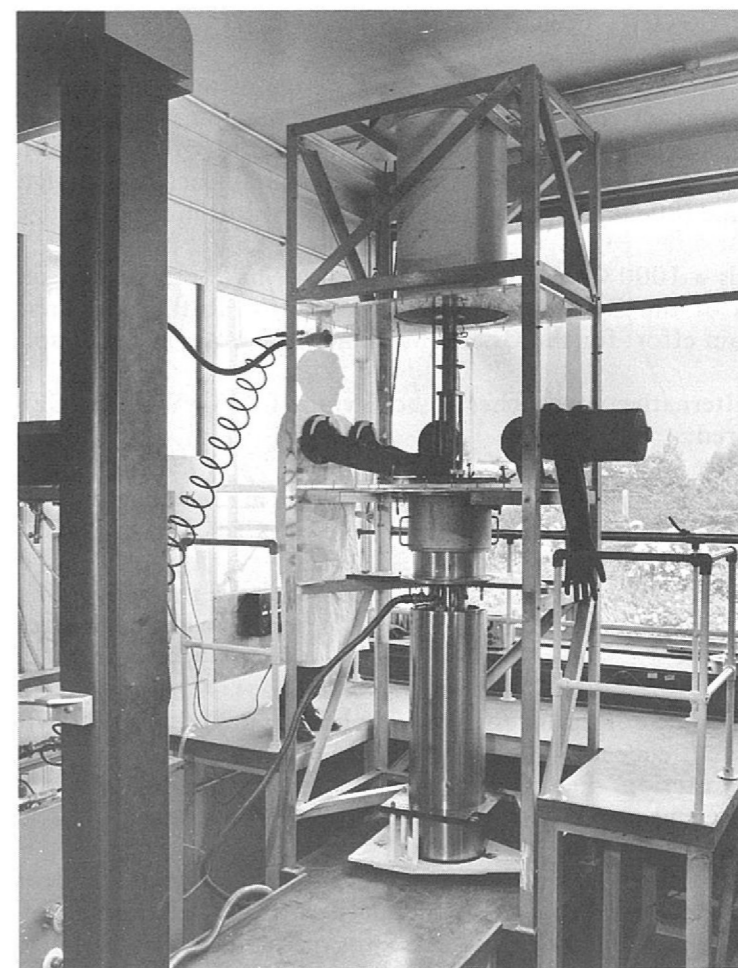
Figure 104. The low temperature testing facility.

CRYOGENIC MATERIALS STUDIES

Testing of epoxy resin systems for impregnation of superconducting windings has been continued. A year's operating experience has been obtained on the improved Instron low temperature testing facility (see Figure 104). This has shown that the anticipation of a saving of liquid helium has been fully realized, approximately 5 litres are required per test, as compared with 12 litres formerly. Furthermore gas recovery figures have improved from approximately 60% to better than 80% recovery. *(ref. 198)*

A better understanding of the effect of particulate fillers on resin performance has been gained, and some useful new resins have been developed and are now being evaluated. It is clear that no one resin system is suitable for all types of winding, and that resin and magnet construction must be chosen to be mutually suitable.

A reliable method of measuring crack resistance of resins would be of much assistance. Attempts are being made to measure fracture toughness at liquid helium temperature: the task is difficult.

An experimental programme on thermal conductivity of particulate filled resins is being conducted on our behalf by the Clarendon Laboratory, Oxford. It has been found that thermal conductivity is much affected by boundary resistances between particles and resin, particularly when the filler particles are very small, or the acoustic match between them and the resin is poor.

SUPERCONDUCTING SYNCHROTRON DESIGN STUDIES

(ref. 54, 105, 156, 229, 238, 248, 252, 261, 262, 263) A large part of our theoretical accelerator design effort is devoted to studies of proton synchrotrons to exploit the new superconducting technology. During 1971 this was directed towards the possible uprating of the new European SPS accelerator to 1000 GeV. A subsidiary interest has been the design of a lower energy machine (80 GeV) appropriate to an accelerator in the UK.

(ref. 222, 283 to 294) Work towards a 1000 GeV European accelerator has been carried out as part of the activities of the GESSS collaboration, with the Rutherford Laboratory providing the main effort for the GESSS Machine Design Working Group.

Two major alternative approaches to achieving 1000 GeV on the CERN site have been considered:

(i) Conventional 300 GeV magnets replaced (in two stages if desirable) by superconducting magnets. Injection from the CERN PS at 28 GeV.

(ii) New superconducting magnet ring installed above the conventional 300 GeV ring in the same tunnel. Injection from the conventional machine at, say, 200 GeV.

Various lattices have been investigated for both types of solution, with minimum dipole aperture (hence minimum stored energy and minimum cost) as the principal comparative criterion. Figure 105 indicates the approximate relation between dipole aperture and stored energy for a 1000 GeV machine.

The aperture requirements of resonant slow ejection have been identified as the most critical design factor. With standard lattices and ejection systems, the apertures required in the two types of solution are not markedly different: typical dipoles range from 30 mm to 55 mm inner coil radius, with stored energies in the range 500-700 MJ.

Figure 105. Stored energy vs. Dipole aperture for 1000 GeV, using 4·5 T dipoles with unsaturated iron shielding.
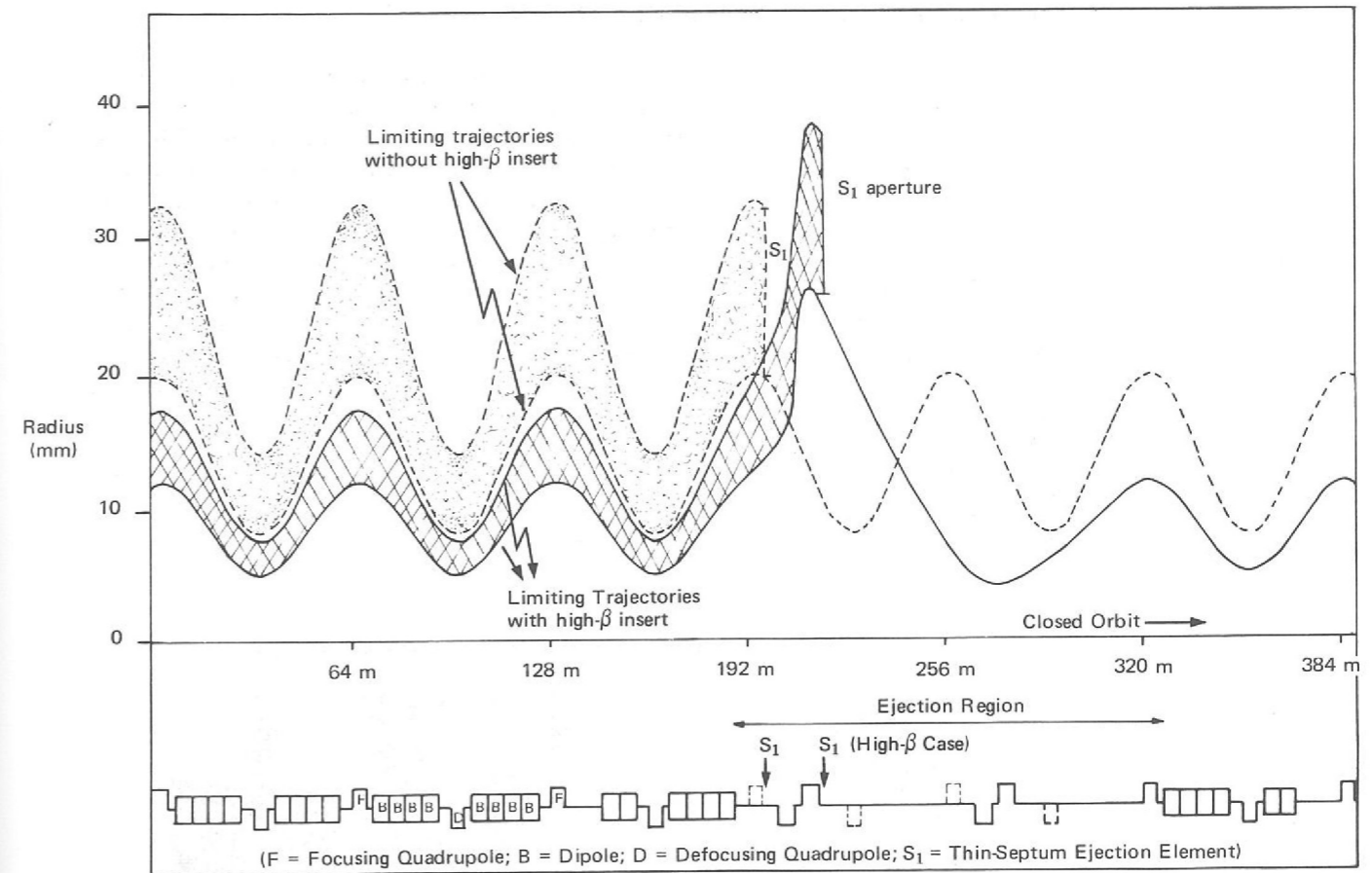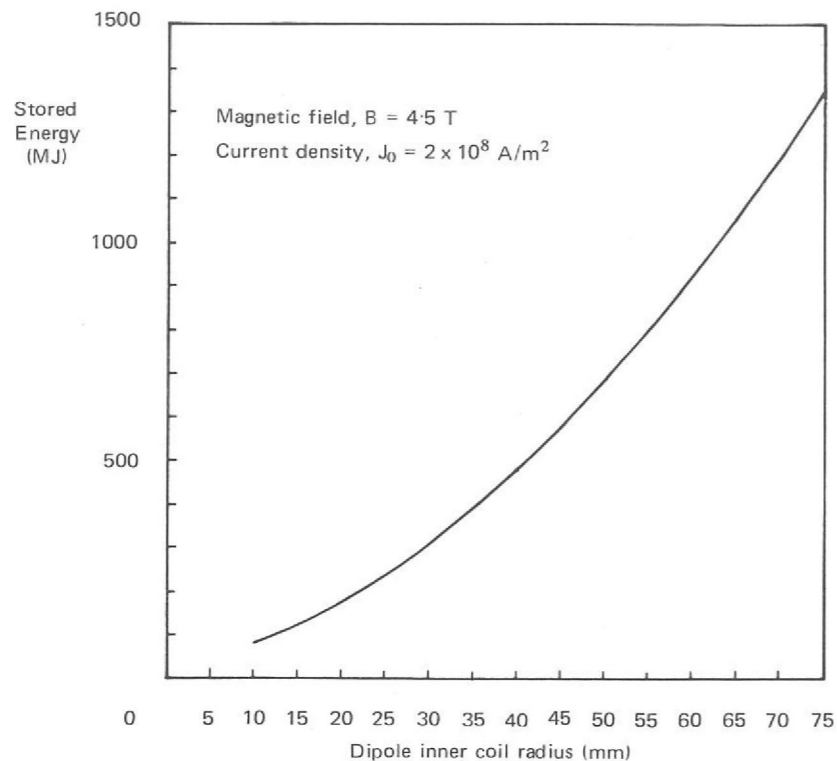
Figure 106. Effect of high-β insertion on aperture required for slow ejection from a 1000 GeV superconducting synchrotron.

Lattice is the FODO type chosen for the CERN 300 GeV machine.

'Limiting trajectories' refer to: (i) those making maximum excursion into the aperture of the first thin-septum element S_1; and (ii), those just scraping the S_1 septum. They are illustrated for the normal 300 GeV lattice with FODO insertion (broken lines), and for the same lattice with a high-β insertion (solid lines).

To calculate dipole magnet apertures, about 18.5 mm must be added to the trajectory radius in both cases, — consisting of about 5 mm residual closed orbit distortion, 3.5 mm sagitta, and 10 mm 'bad field' allowance.

Methods of overcoming this difficulty have been under intensive study during the last quarter of the year, and high β insertions is now advocated as a vital feature of 1000 GeV lattices to achieve small apertures and stored energies: typically, Type (ii) machines may be contemplated with dipole inner coil radii of 30-35 mm, and corresponding stored energies of 300-350 MJ. Type (i) machines are not capable of such great improvement, being limited by their lower injected beam size.

Briefly, the effect of a high-β insertion is to expand the beam profile in the region of the ejection straight section, whilst minimising it elsewhere in the machine: conversely, the extra aperture required at the ejection straight is de-magnified into the rest of the machine where the dipoles are located. Figure 106 illustrates the principle schematically for a FODO lattice of the type chosen for the 300 GeV conventional machine.

SUPERCONDUCTING R.F. SEPARATORS

Conventional electrostatic separators used in conjection with magnets for separation of beams of secondary charged particles suffer limitations at high particle momenta. Radio-frequency cavities may be used to extend the momentum range where unwanted particles are deflected into a stopper whilst the wanted particles are collected by a magnetic focusing system. At room temperature, the radio-frequency power dissipation (of the order of 1 MW/m) is such as to limit operation to short pulses which are suitable for particle beams for bubble chambers but are not sufficiently long ($\sim$ 0·5 s) for experiments using electronic detection techniques. Superconducting radio-frequency cavities operating at about 1·85 K offer the hope of reducing the power levels to the level of tens of watts which would then permit operation for electronic experiments at Nimrod and at high energy machines.

Two possible materials which are superconducting at radio-frequencies are niobium and lead. The Rutherford Laboratory has a programme for developing cavities with pure lead electro-deposited on a copper substrate.

Figure 107. The model r.f. separator cavity being prepared for the high field tests.

High Field Tests (ref. 138)
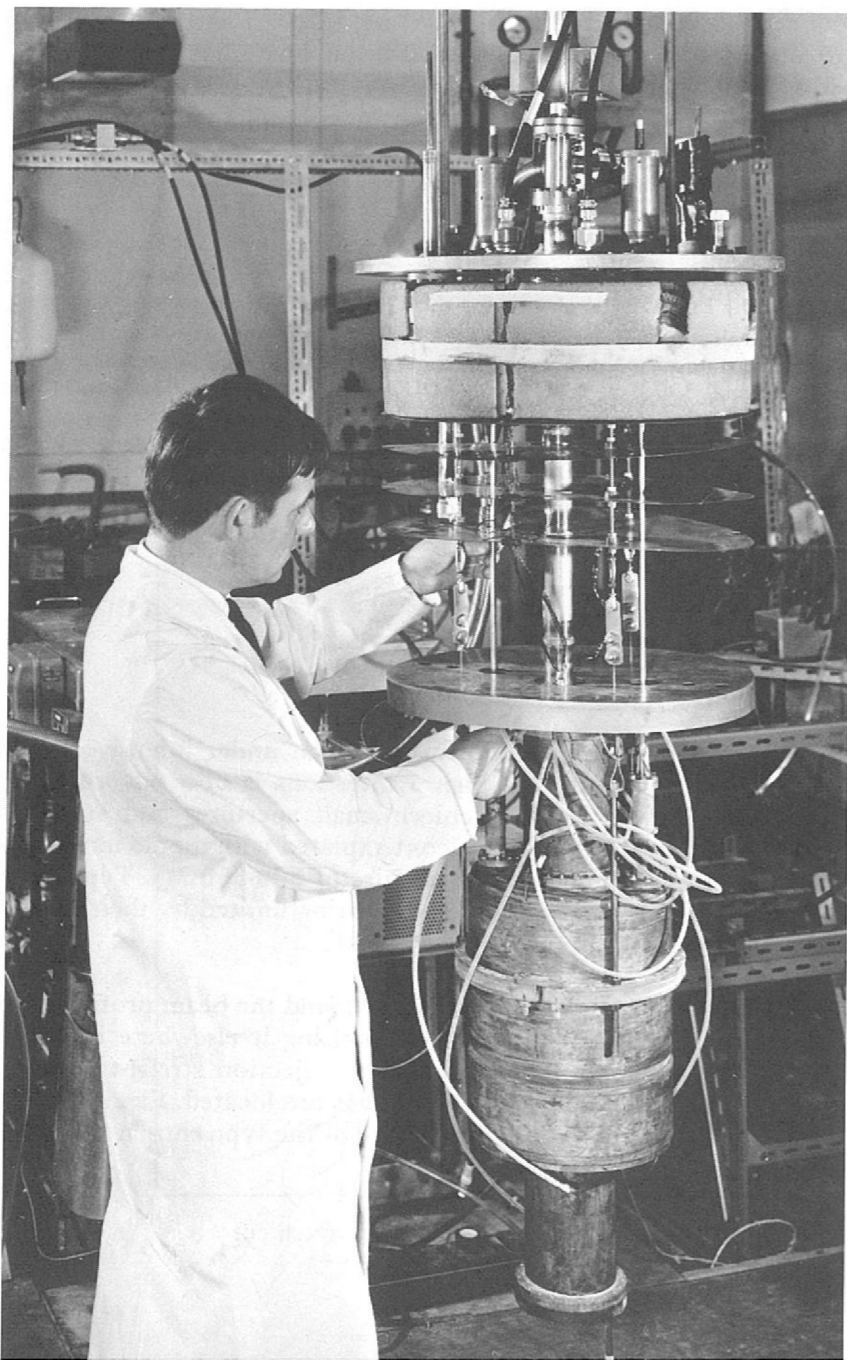
This year there has been good progress; a two-cell model of an r.f. separator cavity at the full scale frequency 1·3 GHz has been tested to show that the superconducting lead on its copper substrate can sustain the high electric and magnetic fields required for deflection. The model substrate was made in one piece from electro-formed copper to avoid the problem of r.f. joints, and consists of two cells, plus two end-sections with short lengths of beam pipe to simulate a realistic section of deflecting structure. The model cavity in its cryogenic rig is shown in Figure 107. The end-sections allow for reactive loading due to the beam pipes, and their combined effect reduces the Q-value by some 10% and increases the centre cell deflecting field by 6·7%. Elaborate precautions were taken to clean the copper prior to lead plating. The anodes themselves were made of "6 N's Lead", i.e. 99·9999% pure, and bagged in fine-weave Crimplene to avoid sedimentation. Three anodes per cell were used, a total of nine in all. After plating great care was taken to dry the lead free of stains by the use of de-oxygenated water, acetone and final vacuum drying. Several attempts were required to produce each successful plating, due largely to the peculiar geometry of the electro-formed model. These problems should be avoided in the future operational structures, and with the new proposed plating system described briefly later. After testing, the plating was analysed and found to contain impurities of copper, iron and zinc to a total of some 0·5%. Again, these difficulties should be avoided with the new plating system.

The assembled structure was baked-out at 100-110°C for some 48 hrs, prior to cooling down slowly firstly with nitrogen gas, then with helium gas to 4·2 K Care was taken to minimise the temperature gradient across the model at the critical temperature of lead, and typically temperature differences across the cavity a little less than 0·1 K were obtained.

Figure 108. Combined results: unloaded Q and peak surface magnetic field against cavity power.
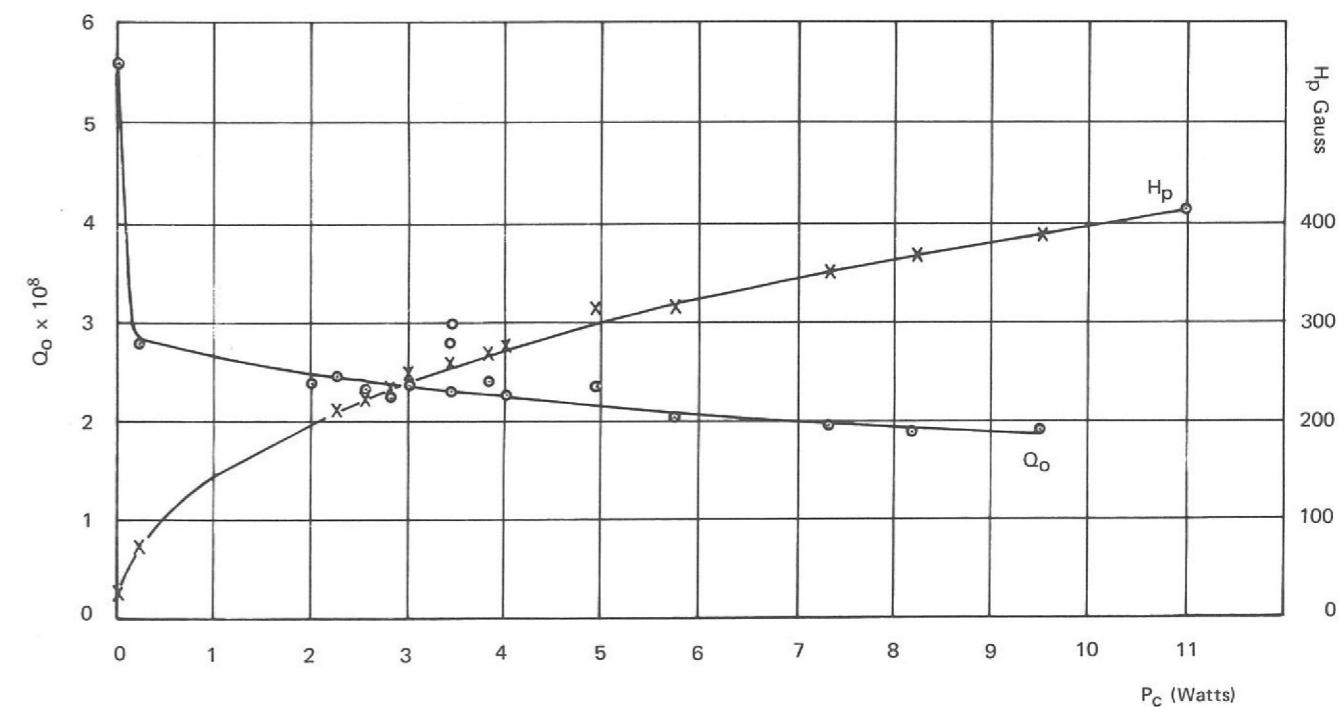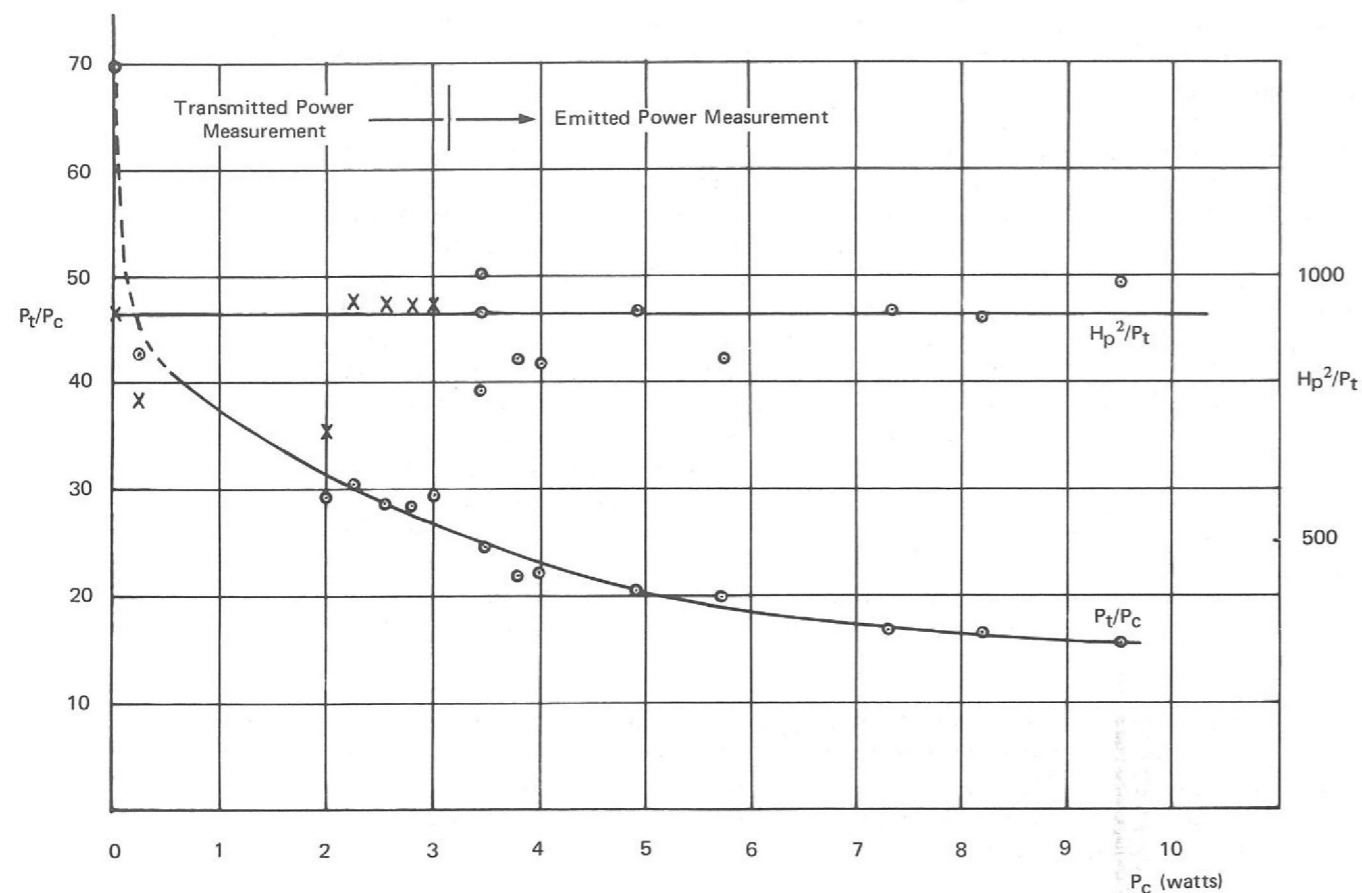
Figure 109. Combined results: H_p^2/P_t and P_t/P_c against cavity power.

Several tests were performed. In all tests the Q_o—values were similar, but in earlier ones instrumental and vacuum difficulties limited high field operation to a level where the magnetic field at the lead surface was about 200 gauss. The graphs, Figures 108 and 109, contain results of the last tests. At 4·2 K the low power unloaded Q-value was $1·64 \times 10^8$, i.e. 84% of theoretical Q. On cooldown to 2·05 K (the temperature limited by vacuum difficulties), the low power Q-value improved to $5·6 \times 10^8$ (an increase of 3·4 rather than the theoretical 37·5) falling to about 2×10^8 at the highest power levels. The limitation on Q improvement is due partly to the impurities, which can be avoided. The highest fields seen were $H_p = 410$ gauss, with $E_p = 9·92$ MV/m. This should be compared with the critical field of lead of about 750 gauss. The achieved fields correspond to an equivalent deflecting field 2·12 MV/m in the model cavity and would yield 2·74 MV/m on an operational deflecting structure. The value was limited by instrumentation difficulties and by the onset of field emission producing clamping. Corresponding X-ray emission was in the range 0-6 mR/hr. With these test figures, an operational system for Nimrod would have a performance only a little less than originally proposed. The results are sufficiently encouraging to warrant proceeding to a full-scale 10-cell separator cavity, whose parameters were described in the 1970 Annual Report, for testing in the Laboratory in 1972.

The full-scale 10-cell separator cavity will be built in two 3-cell sections, plus one 4-cell section, the whole assembly requiring two dry r.f. joints. An r.f. joint separating the functions of vacuum seal and r.f. joint was described in the 1970 Annual Report. An E_{010}-E_{011} cavity has been made to test this joint. The cavity is 16·26 cm long by 17·63 cm diameter to give the E_{010} frequency 1·3 GHz, the operational frequency in the separators. The joint is in the mid-plane of the cavity, so with the E_{010} mode r.f. current crosses the joint, and with the E_{011} mode no current crosses it. Two tests have been made so far. In the second test the unloaded Q-value was found to be 50% of theoretical value at 4·2 K, and with frequency scaling there was no difference in the effective surface resistivity between the modes. At the same time the joint has worked perfectly as a vacuum seal. A further test is to be done to confirm the performance of the joint at high field levels. *R.F. Joint Tester Model*

Despite the precautions taken, four attempts on average were required to produce each successful plating on the high field test model. The major difficulty was due to the peculiar geometry of that model, but contamination (particularly of copper) was also present in undesirably high amounts. The plating system used the open bath technique, where the cavity was immersed completely in the electrolyte in which the lead anodes rotated inside the cavity, or the cavity rotated about the anodes. This system has certain disadvantages: *New Plating System for R.F. Cavities*

(i) The successive cleaning operations prior to plating involving degreasing, rinsing, pickling, rinsing, etc. involve a considerable amount of onerous handling.

(ii) The outside of the cavity has to be covered to prevent contamination of the plating electrolyte.

(iii) There is a possibility of contamination of the plated surface from either the atmosphere or dust during transfer operations.

To overcome these disadvantages a closed circuit plating system has been devised and is being constructed. The system allows for all the cleaning and plating to be carried out by the operation of valves which control the movement of the various fluids into and out of the cavity. An inert gas (argon) is used to provide the pressure necessary to move the fluids. Only the internal surfaces of the cavity are involved so that elaborate covers for the unplated surfaces are no longer required.

The design of most of the cryostat components has been completed and manufacture has begun. The method of brazing the individual cavity sections together is still being developed, to find the precise quantity of brazing metal to leave no spillage. The lead joint has been designed as already described. The machining of the cavity sections to the very tight tolerances required is proceeding satisfactorily. This involves diamond machining in a temperature controlled room. *Cryostat and Cavity Manufacture*

A study has been made of methods to use liquid helium at 4·2 K from dewars to cool the superconducting r.f. cavity down to 1·85 K. The temperature of the cryostat containing the cavity must be maintained at 1·85 K ± 0·01 K, in order to maintain the pressure at 15 torr within a tolerance of ± ·02 torr. Similarly the level of the liquid helium in the cryostat has to be maintained within ± 1 mm, to avoid dimensional changes in the cavity. *Refrigeration for Laboratory Tests*

The normal evaporation refrigeration used to produce 1·85 K liquid from 4·2 K has many limitations such as:

(i) Low 1·85 K liquid yield.

(ii) Long cool down times.

(iii) Breakdown of test conditions during dewar changes and the necessary re-cooldown period.

(iv) Variable liquid level.

(v) Possibility of choking the system with contamination during dewar change.

A system is now being constructed which will use a heat exchanger to cool the incoming 4·2 K liquid before passing through a Joule-Thomson valve, which will considerably increase the liquid yield. The system also includes a device for enabling the dewar change-over to take place without interrupting the refrigeration of the cryostat.

The whole of the cryostat, cavity, and refrigeration equipment is due to be assembled and commissioned in the Laboratory in August 1972.

THE FAST CYCLING BUBBLE CHAMBER TEST RIG

(ref. 166, 167, 275) A fast cycling test rig has been designed to investigate factors affecting the performance of fast cycling bubble chambers, and to test further glass-reinforced plastic components under operating conditions.

Figure 110. Sectional view through the chamber of the fast cycling bubble chamber test rig.
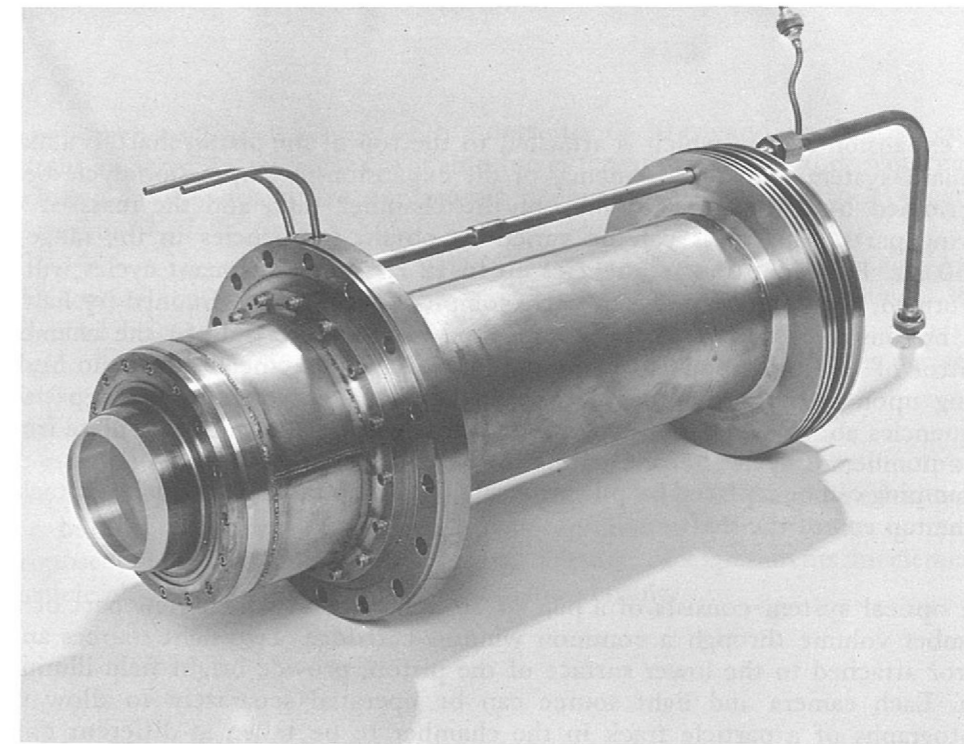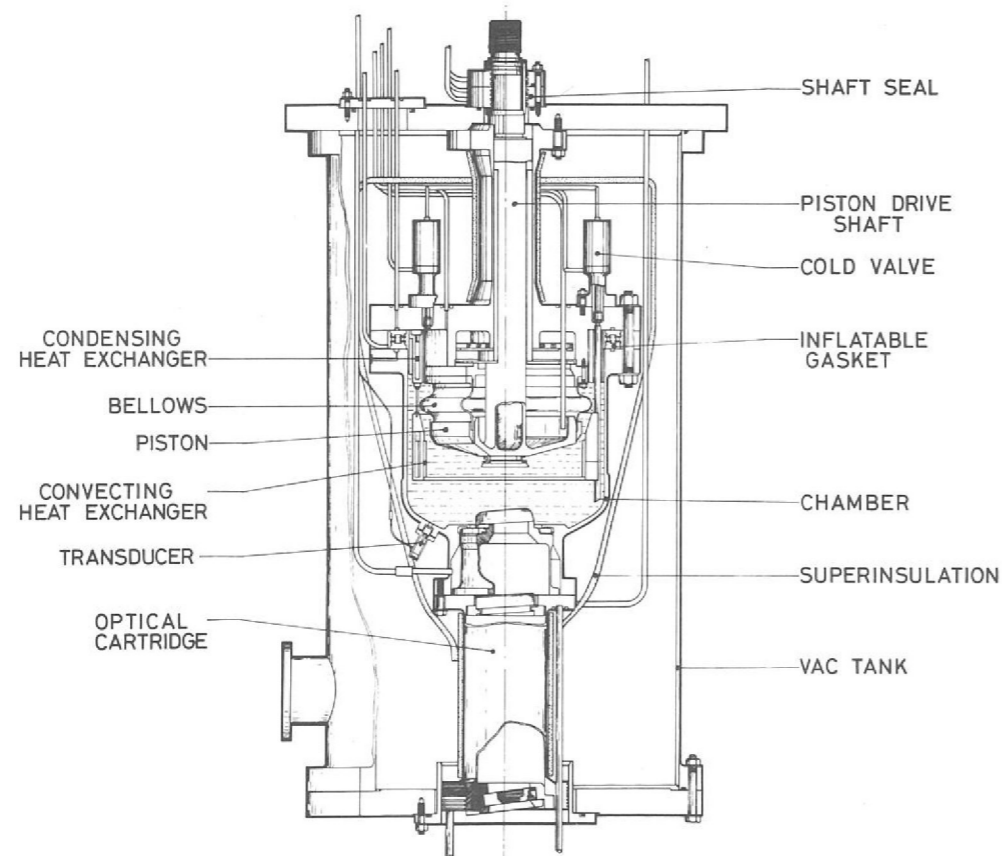
Figure 111. The optical cartridge for the fast cycling bubble chamber test rig.

The stainless steel chamber is 40 cm in diameter and holds 21 litres of hydrogen or deuterium. A sectional view is shown in Figure 110. It is supported by a single tube from the vacuum tank top plate, and has a 10 cm diameter window in the base through which part of the liquid can be viewed through an optical cartridge shown in Figure 111. To reduce the heat input to the chamber the optical cartridge contains three windows in series, the centre one being cooled by hydrogen to reduce heat radiated from room temperature; a heat exchanger is attached to the support tube, and the whole chamber assembly is surrounded by superinsulation. These features are designed to limit the heat flux into the fluid to less than 1 mW/cm² which should eliminate boiling at the walls of the chamber. Two annular heat exchangers inside the chamber are designed to remove the dynamic heat load by condensation and convection respectively.

The fluid is superheated by allowing a piston, situated at the top of the chamber, to move rapidly under the influence of the fluid pressure. The piston and the bellows which seal it to the chamber top plate, are of glass-reinforced plastic. This is one of the more important design and development features. (See Figure 112.)

Figure 112. The piston for the fast cycling bubble chamber test rig.
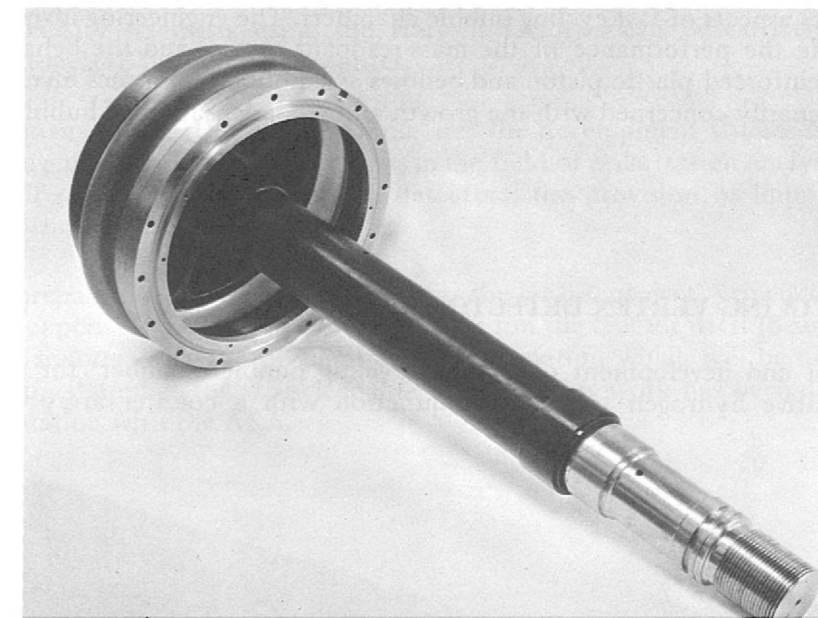
The expansion system which is attached to the top of the piston shaft, is a mass-resonant system with the frequency of the expansion-recompression cycle being determined by the compressibility of the chamber fluid and the mass of the moving parts. This mass can be varied to obtain frequencies in the range of 20-50 Hz. For repetition frequencies up to 12 Hz, single resonant cycles will be performed, the interval between each complete cycle being obtained by halting and holding the system at the compressed state of the fluid in the chamber. Control of this operation is by the application of high speed hydraulic brakes acting upon an extension of the expansion system drive shaft. For repetition frequencies above 12 Hz the expansion system will be allowed to oscillate freely for a number of cycles before halting in the compressed state. Energy losses due to damping can be replaced by pulsing a small hydraulic actuator which is attached to the top end of the shaft.

The optical system consists of a pair of 70 mm cameras which view part of the chamber volume through a common window cartridge. Two light sources and a mirror attached to the lower surface of the piston, provide bright field illumination. Each camera and light source can be operated separately to allow two photographs of a particle track in the chamber to be taken at different times. The camera lenses are Schneider Repro-Claron with 240 mm focal length, and with their apertures set at f/11 the resolution and demagnification will be such as to allow bubbles of diameter $> 100\mu m$ to be measured with an accuracy of better than 10%. Optical tests have been performed to optimise the parameters of the system including the choice of film which will be a high resolution micro film. To ensure good contrast the spaces between the windows of the optical cartridge are evacuated to $< 10^{-8}$ torr using vac-ion pumps.

The total static and dynamic heat loads are expected to be about 150 W and a Linde cycle hydrogen refrigerator capable of removing 200 W at 25 K has been constructed. The refrigerator is built as an integral unit with the valve vessel which contains the low temperature valves controlling the flow of liquid hydrogen through the chamber heat exchangers. The two hydrogen compressors which are used to supply this system are of the diaphragm type to reduce the problems of contamination.

The experimental investigation of bubble growth in the chamber will be performed by injecting γ rays from a Cobalt source into the chamber. This source is incorporated in a pulsed system. It is attached to a wheel rotating at 36 Hz and when the source comes into angular coincidence with a fixed slit in a lead shield and a slit in a rotating lead shield, a γ pulse is injected into the chamber. The pulse length is 0·5 milli-seconds and occurs once every 2 seconds.

The programme of investigation will be wide in range covering both engineering and physics aspects of fast cycling bubble chambers. The engineering investigation will include the performance of the mass-resonant system and the behaviour of the glass-reinforced plastic piston and bellows assembly. The physics investigation will be primarily concerned with the growth and recondensation of bubbles in the hydrogen.

RAPID CYCLING VERTEX DETECTOR

The design and development of a 'rapid cycling bubble chamber' for use as a track sensitive hydrogen target in conjunction with a counter array is being pursued.

It will have a sensitive volume with a diameter of 30 cm and depth of 15 cm and a solid angle of 3π steradians available for external counters. Other requirements included in the design are continuous operation at 60 Hz with hydrogen or deuterium.

The optical system of the chamber will give a resolution of $100\mu m$. Retro-directive bright field illumination will be employed. The cameras with a stereo angle of $8°$ will use 35 mm film and operate at a rate of 10 pictures per second for 0·5 seconds, repeated every 2 seconds.

Results to be obtained shortly from the fast cycling test rig will be incorporated into the final design of this new vertex detector. By combining the advantages of the bubble chamber and electronic counters into a hybrid system in the way proposed, it will be possible to perform a range of experiments in elementary particle physics which hitherto have been inaccessible.

NEUTRON BEAM RESEARCH

In April the Science Research Council considered the proposals prepared by the Rutherford Laboratory for the detailed design phase of the HFBR and decided it wished to proceed with the design in the expectation that construction would follow in about two years. Government approval has been sought but no decision has been announced. At the same time Council decided to seek access for UK scientists to the high flux beam reactor nearing completion at the Franco-German Institute Max von Laue-Paul Langevin (ILL), Grenoble, so that some high flux work could be carried out during construction of the UK facility. Discussions to this end are taking place between the SRC and the ILL. *The High Flux Beam Reactor*

As a further step in providing for an expanding neutron beam programme, Council also decided to set up a Neutron Beam Research Unit at the Rutherford Laboratory. This is being built up now and the number of staff is expected to reach a strength of 20 during 1972/73, or 30 if the HFBR goes ahead. The purpose of the Unit is to provide SRC Laboratory support for university scientists in this field in a manner similar to that in nuclear physics. Besides giving support to the current research programme the Unit will be particularly concerned with long-term development of instruments, techniques and sources for neutron beam research. It will work in close collaboration with university scientists and with the support teams at AERE Harwell and AWRE Aldermaston. *Neutron Beam Research Unit*

During 1971 the staff of the Unit have begun work on providing a computer link between AERE and the Rutherford Laboratory so that reduction of data obtained by university scientists using the Harwell facilities can be carried out on the Laboratory's IBM 360/195 computer.

Other items on the Unit's programme are: the development studies in the use of neutron guide tubes; feasibility studies in the field of polarization analysis; development of position-sensitive neutron detectors; the provision of improved monochromating crystals.

Some preparatory work has continued for the HFBR project, principally a review of the experimental facilities to be provided in the reactor itself (beam tubes and special sources) and the preparation of information which will be needed when the Council applies for a Nuclear Site Licence. This work has been done in close collaboration with the AEA.

ASTROPHYSICS RESEARCH UNIT, CULHAM
ATLAS COMPUTING LABORATORY, CHILTON
DEPARTMENT OF MATHEMATICS, MONS
INSTITUTE OF ASTROPHYSICS, LIEGE
ROYAL OBSERVATORY, EDINBURGH
RUTHERFORD LABORATORY

An SRC project team based at the Rutherford Laboratory has been active for the last two or three years in implementing apparatus for the S2/68 Experiment for the European Space Research Organisation (ESRO) TD1 Project. This experiment, conceived jointly by the Royal Observatory, Edinburgh and the Institute of Astrophysics, Liege, is the largest of seven experiments to be mounted on the TD1 satellite. The satellite is scheduled to be launched in 1972 by a Thor-Delta rocket at the Goddard Space Flight Centre, USA.

During the six-month lifetime of TD1, this particular experiment will produce the first complete ultra-violet scan of space with one instrument, identifying stellar sources and measuring photon fluxes of stars down to the 9th magnitude. This self-consistent set of measurements will be particularly useful for the study of inter-stellar ultra-violet absorption and its distribution.

In principle, the apparatus is a spectrometer measuring the intensity of ultra-violet light over the wavelength range 1330 Å to 2600 Å with a resolution of 35 Å covered by three detector channels; a fourth channel has a passband centred at 2800 Å with a half-width of 400 Å. A more detailed description can be found in the 1970 Annual Report. The measurements have to be correlated with the orientation of the satellite, to identify the sources of ultra-violet radiation.

A high level of activity has been maintained during the year, leading to the production of the flight model of the apparatus (preceded by several prototypes). The SRC project team has supervised the contract with Hawker Siddeley Dynamics for the construction of the models: other activities have included design, construction and calibration of equipment to test the functioning of the spectrometer, e.g. provision of a calibrated U-V source.

At the time of writing, problems due to contamination of mirror surfaces and electrical breakdown in the high voltage leads to the photomultiplier detectors have been satisfactorily solved and the acceptance tests on the flight model have been completed. Figure 113 shows the flight model. A successful launch of the satellite in 1972, followed by reliable functioning of the apparatus in orbit will be the rewarding culmination of three years of intensive effort and the realisation of an experiment conceived nearly ten years ago.

Figure 113. Testing the flight model for the S2/68 Experiment on the TD1 satellite.

INFRA-RED RADIOMETERS FOR ATMOSPHERIC TEMPERATURE SOUNDING

HERIOT-WATT UNIVERSITY
UNIVERSITY OF OXFORD
RUTHERFORD LABORATORY

Selective Chopper Radiometer

A Selective Chopper Radiometer will be carried as one of several experiments on the Nimbus-E satellite scheduled to be launched in late 1972 by NASA, USA.

This infra-red radiometer is designed to view the earth's atmosphere vertically below the satellite, so that a vertical temperature profile of the atmosphere from the ground to a height of 50 km can be reconstructed. It will also be possible to derive information on cloud height, density and ice particle size in cirrus clouds. Details of the system were given in the 1970 Annual Report. Measurement of the intensity of radiation in different spectral intervals uses the absorption property of carbon dioxide for infra-red radiation.

Work on the engineering model was completed during the year and it has since completed acceptance tests both here and at NASA headquarters. Calibrated radiation sources at ambient temperature and liquid nitrogen temperature have been provided as part of the test equipment, together with electronic and power circuits to simulate the satellite command system. The flight model and telemetry system are being manufactured by Marconi.

Some of the development units have been up-graded for use in a joint Oxford University — National Environmental Satellite Service experiment, as a further check under true atmospheric conditions, in a balloon flight during the summer of 1972.

Pressure Modulated Radiometer

As a follow-up to the Nimbus-E experiment, a pressure modulated radiometer will be flown on Nimbus-F satellite, scheduled for launch in 1974. This radiometer will make measurements of atmospheric temperature in the region 40 to 85 km above the earth compared to 0 to 50 km of the Nimbus-E radiometer. This measurement has only become possible following the development of the pressure modulated radiometer concept at the University of Oxford. In this device spectral selection is achieved by a single carbon dioxide cell, whose pressure is modulated by a piston driven electro-magnetically.

Supporting engineering work and tests are being carried out at the Rutherford Laboratory under a Project Manager, and similar services as for the Nimbus-E project are being provided. The manufacture of the engineering model will be done commercially. The projected lifetime for the radiometer in orbit is two years.
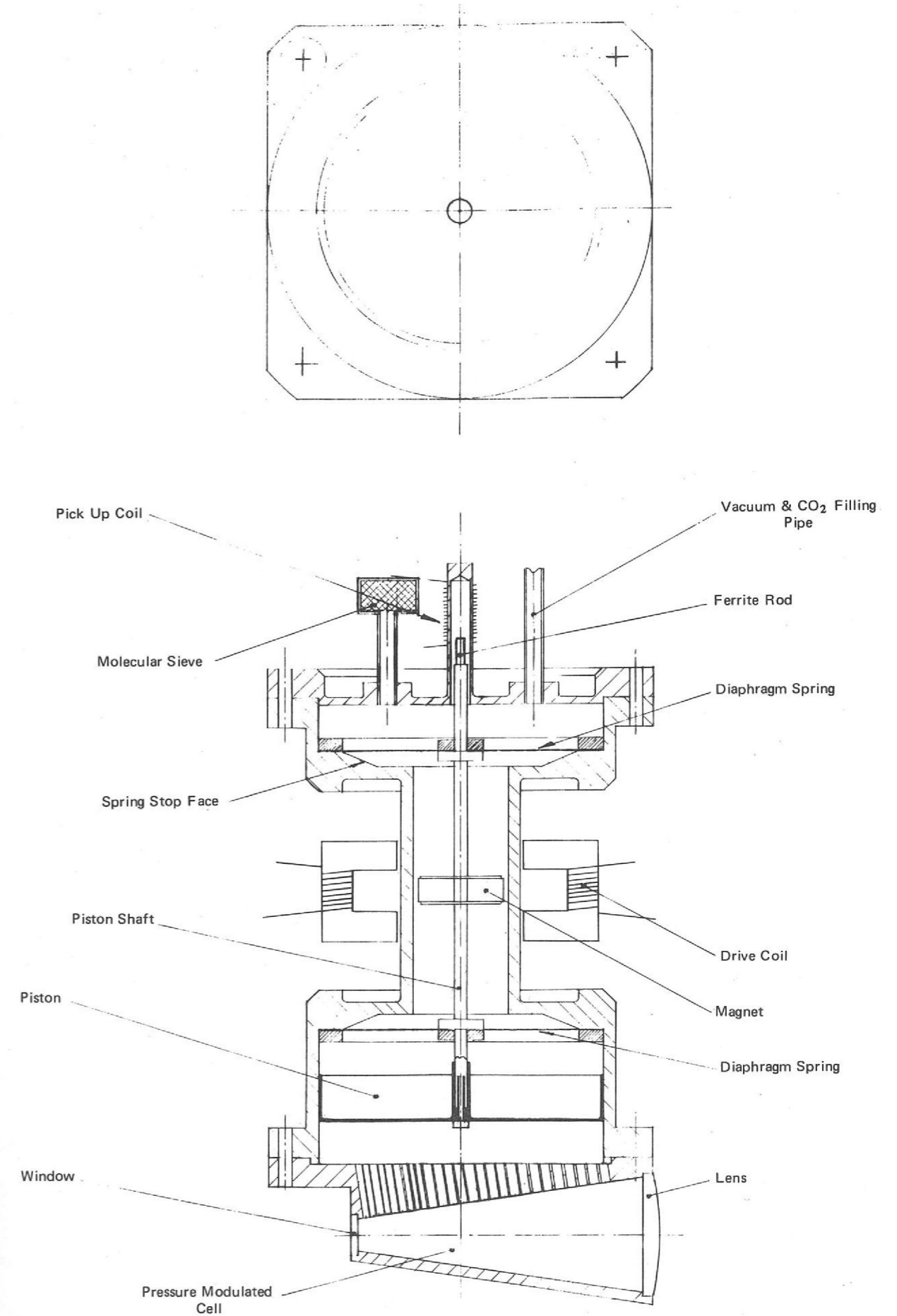
Figure 114. Details of the pressure modulator for the carbon dioxide cell (Nimbus F satellite experiment).

Control console for the
System 360/195 Central Computer

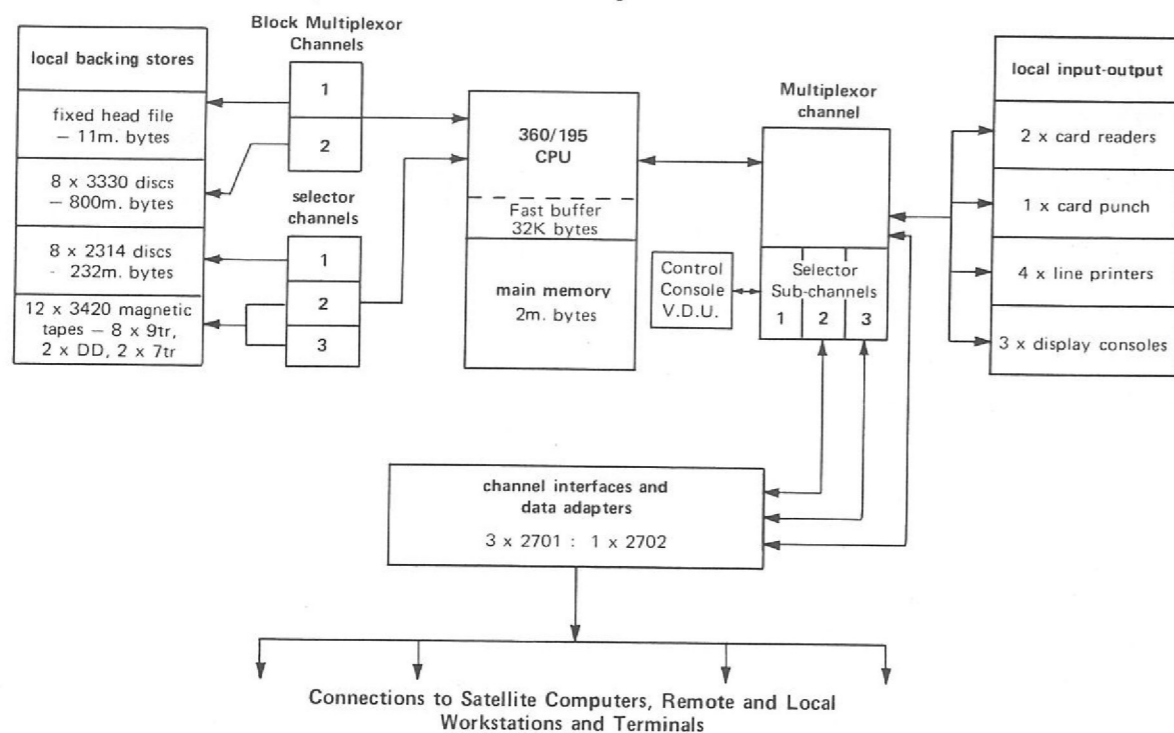**COMPUTER SYSTEMS
AND APPLICATIONS**

Computer Systems
And Applications

On 10th November 1970 approval was given for the purchase of a new central computer, an IBM Model 360/195, at a total cost of £3·6 million. Preparation for the installation went on throughout the year, and the machine was accepted on 15th November 1971 (six weeks ahead of the original schedule). To maintain an uninterrupted computing service the IBM 360/75 was kept in use (though with reduced peripheral equipment) during the transition period. Some batch work was immediately transferred to the new machine on its acceptance, tests with on-line equipment began, and HPDI was brought back into service on the evening of 15th November, after a break of 137 hours.

Other on-line developments, previously reported on, have reached fruition during the year. Some have accordingly been designated as public services, and become the responsibility of the Computer Manager. In this category are the terminal IBM 1130 (situated in Hall 3), the Remote Job Entry work-stations operating under HASP at Birmingham, London (Institute of Computer Science) and Oxford, the six IBM 2741 typewriters (situated in Building R1), the Computek visual display system (in R1) and the ELECTRIC software stytem. The Computek system in Building R25 (like the IDI display with light pen) has reached a similar state but is a private group facility, while other terminals are still under development.

The Computing Centre extends its service on 1st January 1972 to all members of the Nuclear Physics community (Counter, Film Analysis, Nuclear Structure and Theory) and to research workers in other fields selected by the ATLAS Laboratory. The fraction of time allocated to each category will be reviewed regularly by the Advisory Committee.

Figure 115. System 360/195 Central Computer.

Connections to Satellite Computers, Remote and Local
Workstations and Terminals

CENTRAL COMPUTER SYSTEM DEVELOPMENT

During the year several changes were made to the operating system under which the model 75 ran, in order to cope with the heavy load of production work, to allow for the attachment of new devices, and to prepare for the installation of the model 195 as a replacement machine.

MVT System

Since first installed, the model 75 had run under the MFT option of the Operating System (Multiprogramming with a Fixed number of Tasks). In many ways this was well suited to the Laboratory's work: there were many very long-lived jobs (the control programs of on-line devices) which had to operate in defined regions of memory, and MFT was the only variant of the system which allowed exploiting of the Large Core Store of 8 μs memory.

With Release 19 of the Operating System early in 1971, MVT (Multiprogramming with a Variable number of Tasks) became capable of controlling the LCS, but there still remained the problem of causing long-lived programs to be loaded into chosen locations. This was solved by writing code (collectively known as FENCE) which caused part of the machine to have dedicated partitions (as with MFT) while the remainder of memory was administered by MVT.

Thus we combined the benefits of MFT for very long jobs with the advantages of MVT for processing the batch-stream. It was expected that small quick jobs would benefit from MVT, and that MVT would be the preferred version of the Operating System for the model 195.

Diagnostics

Unlike MFT, the MVT option did not supply the programmer with an indicative dump in the event of abnormal job-end, so a substitute (but optional) routine PITFAL was written to give substantially equivalent facilities. Conventions also had to be designed for ensuring that logically interdependent jobs be run in the correct time-order.

By modifying a component of the Fortran library it was found possible to mitigate the consequences to programmers of one of the features of the 195 central processor, viz overlapped execution of several instructions ("imprecise interrupts").

Accounting

MVT entailed the abandonment of IBM(UK)'s MUSIC method (Machine Utilization Statistical Information Collector) of recording use of machine resources. Instead the IBM System Management Facility (SMF) had to be introduced and exploited in such a way as to produce the same statistical reports as before.

O/S 360 Release 20 and HASP

It was known that release 20 of the Operating System would be the first to support the model 195; also that the revision of HASP (Houston Automatic SPOOLing Program; SPOOL: Simultaneous Peripheral Operations On-Line) known as HASP2 Version 3 contained many good features, especially for the attachment of remote work-stations.

To provide early experience, Release 20 was implemented on the model 75 towards the end of its life here. This version gave a great deal of trouble for a few weeks but eventually corrections were found which restored reliability. During the year the practice was introduced of using new systems for a few short periods before establishing them as new standards, with the objects of familiarizing both operators and users with any new features, and of detecting any faults not revealed by the standard batch of test programs.

Figure 116. On-line Organisation.

To System 360/195

channel interfaces and data adapters (Op)

3 x 2701 : 1 x 2702

satellite computers

1 DDP 224 (Op)

2 DDP 516 (D)

3 DDP 516 (D)

4 IBM 1130 (Op)

5 IBM 1130 (Op)

local terminals

(10 Op / 2 D)

12 x typewriters

(Op)

6 x IBM 2741 typewriters

remote terminals (D)

6 x GPO lines on switched public network

Scanning Control (Op)

GRAPHICS (D)

HPD 2 (D)

HPD 1 CYCLOPS IDI 3 storage displays 2 computeks (Op)

local work station (Op)

7tr magnetic tape card reader line printer keyboard printer

remote work stations

Oxford University Nuclear Physics IBM 2780

Birmingham University Nuclear Physics IBM 360/44

Atlas Laboratory Chilton IBM 1130

Inst. of Computer Science London PDP 9

170

Figure 117. DD9 224 On-line Organisation.

To 360/195

Film measuring machines (Op)

HPD 1

cyclops

Point plotting displays (Op)

IDI

Tektronic 611 storage display

DDP 224 Computer (Op)

Graphics storage displays (Op)

Computek   Computek

For film measuring machines

For point plotting displays

For graphics storage displays

DDP 224 Console

General in-house use

Typewriters
(ELECTRIC facilities available from all typewriters)

(10 Op / 2 D)

171

Release 20·0 was used for the model 195 acceptance tests on November 15th. Trials of the test-batch were completed by about 1600 hours, and the on-line system became operational during the evening.

In December yet another version of the operating system was introduced, release 20·1; this supports the Block Multiplexor Channel which will connect the central processor with the new Fixed-Head File and the large-capacity disks which are expected to be available in January 1972. This version gave no trouble.

Throughout the year we have retained as standard the Fortran compilers and library associated with release 18·6. The Fortran components of release 20 are however available if wanted, and may become standard early in 1972.

TSO System Long-term studies have been initiated of a new optional feature of the Operating System known as TSO — the Time-Sharing Option — which would enable terminal users to create and edit stored files, and to initiate programs which would either run interactively with the terminal, or join the standard queues of jobs for the batch-stream.

(ref. 242) Our objective is to establish methods of benefitting from the time-shared method of using the machine without losing the advantages of the locally developed ELECTRIC subsystem of interactive file-handling, and the well-established MAST/DAEDALUS programs which support ELECTRIC as well as the on-line devices HPD I, HPD II, Cyclops and the interactive IDI display.

Extensions have been made to MAST so the ELECTRIC (and MAST) facilities are available at terminals (IBM 2741's and other manufacturers' equipment) which are connected directly to the central machine via an IBM 2702 teleprocessing controller (instead of through the satellite computers which were the original basis of MAST).

Scheduling In order to improve job turn-round, to increase operational efficiency, and to monitor use of the machine more dynamically, much work has been done on methods of scheduling jobs which require magnetic tapes or private disk-packs to be mounted ("set-up jobs"), and of relating (should need arise) the priorities of jobs to allocations of machine-time. These additions to the system have not yet been implemented.

COMPUTER OPERATIONS

Figure 118(a) and 118(b) show the weekly totals of batch jobs processed and the averages (per week) for central computer efficiency i.e. $\frac{\text{scheduled-down time}}{\text{scheduled time}}$ and CPU utilisation i.e. $\frac{\text{CPU time used}}{\text{Scheduled-down time}}$. The totals of batch jobs processed were 145,000 on the 360/75 (from 1/1/71 to 17/11/71) and 20,000 on the 360/195 (from 15/11/71 to 1/12/71).

Little or no change was required in most user programs when the 360/195 came into operation: the upwards compatibility of the 360 series paid off well. Commissioning of the new central computer, and of the remote and local on-line facilities, was quick and virtually trouble-free. The CPU time used by programs fell by a factor of ≈ 5 from the 360/75. In the short time it has been here, the reliability and operation of the 360/195 have been very encouraging.

Work Stations During the year three remote work-stations have become fully operational. They are at Birmingham University (IBM 360/44), Oxford University (IBM 2780) and the Institute of Computer Science in London (PDP9). Job entry and output retrieval is possible at each station. At Oxford, the station is used for some 35 hours and 400 jobs per week. The London group, running jobs with an average of about 5000 lines of output, are sometimes limited by the link speed, and average 30 jobs in 12½ hours/week.
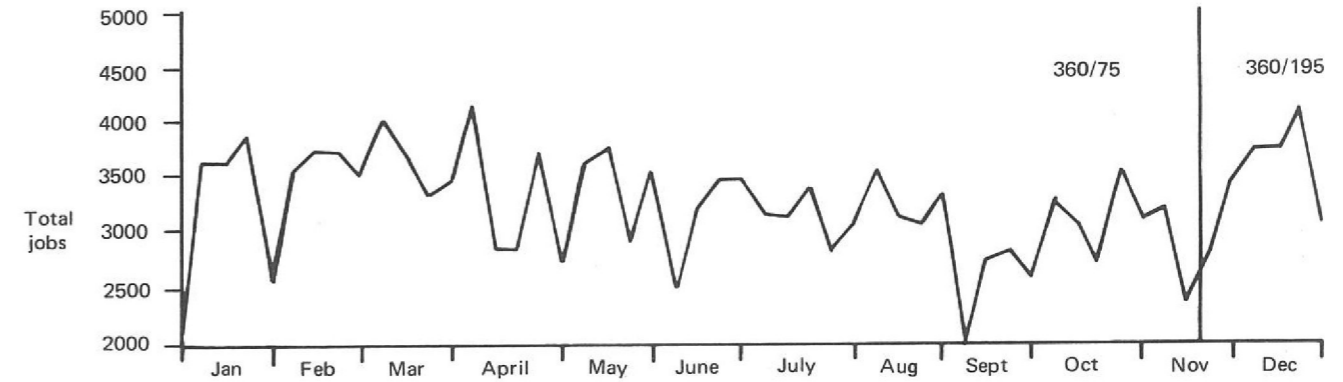
Figure 118(a). Total number of jobs run each week on the Central Computer during 1971.

Figure 118(b). Central Computer machine statistics for each week during 1971.
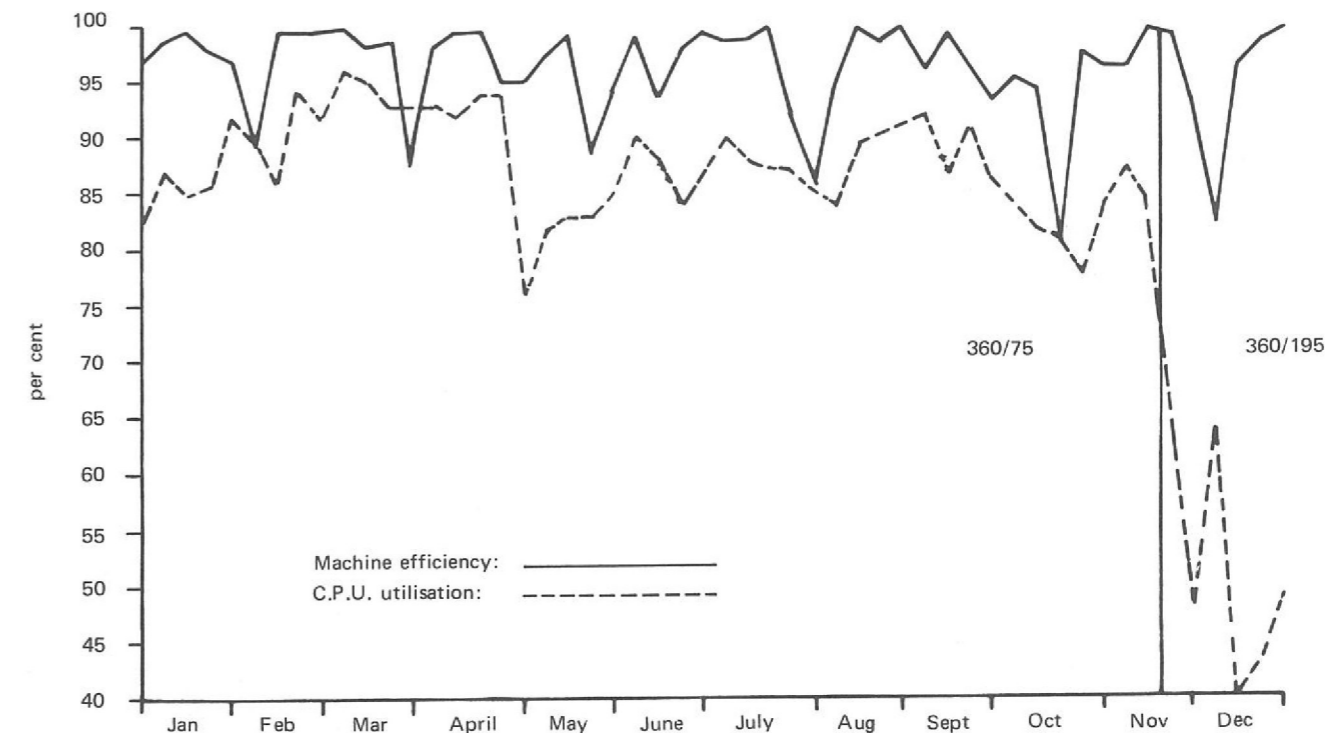
ELECTRIC System   The ELECTRIC job submission and file-handling system has come into full use, as a public service, during the year. About 60 programmers actively used the system, and 15-20% of all jobs are now submitted from terminals. Some statistics of ELECTRIC use appear in Figure 119. There are in the Laboratory six public keyboard terminals (IBM type 2741) available for using ELECTRIC and nearly a dozen others (mainly IBM type 735 'golfball' typewriters) which are not all publicly available. Developments under way will allow external users similar facilities via GPO telephone lines, including use of remote displays.
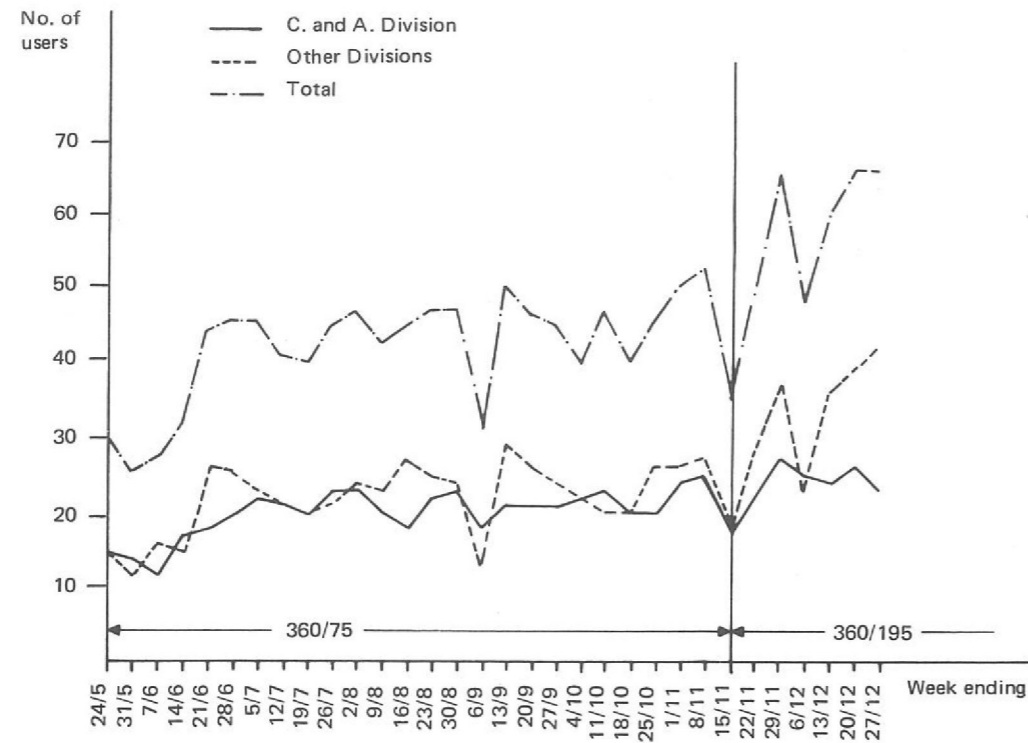
Figure 119(a). Number of users of ELECTRIC terminals for each week during the period 24.5.71—27.12.71.

Figure 119(b). Total CPU time of jobs submitted to the batch from ELECTRIC per week.
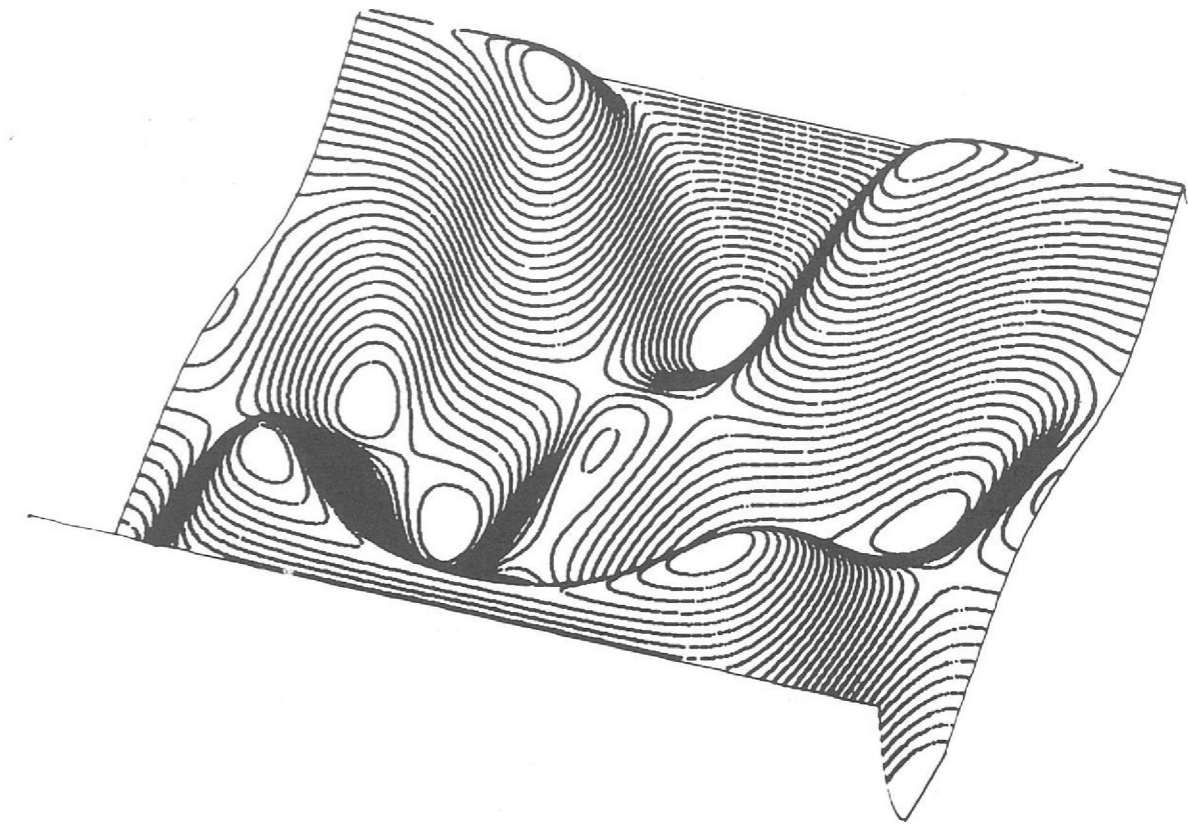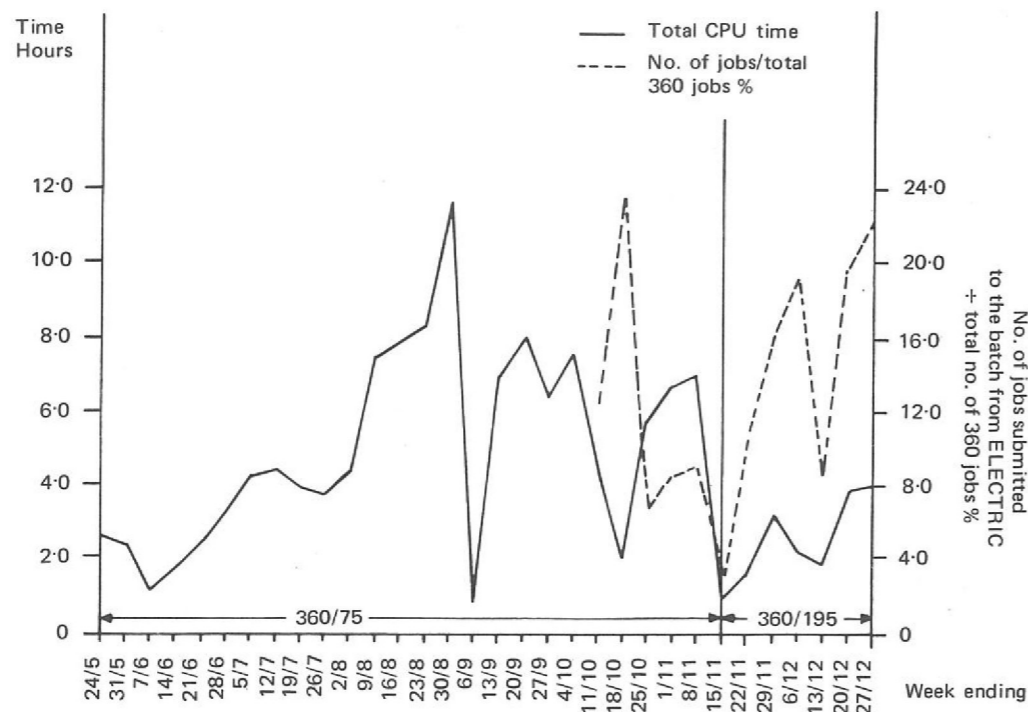
Figure 120. An example of a three-dimensional plot using the graphic facilities in ELECTRIC.

Graphics Facilities   The graphics file retrieval facilities in ELECTRIC have some 60 users, of whom
(ref. 209, 210, 267)   about 20 are normally active in any week. Edited line printer output from batch jobs can be filed, allowing remote selective examination on any typewriter, Visual Display Unit or other display attached to the system. About 30 of the 180 graphics files held at the year-end are of this type. The graphics software has been extended to include drawing of histograms, logarithmic and three-dimensional plots (see Figure 120). Rarely used files may now be 'archived' to tape.

A second Computek 400, stationed in Building R25, has been attached to the system. It is used by the Applied Physics Division both for line-printer and graphics file retrieval, and interactively for magnet design.

Terminal IBM 1130   The 'Terminal' IBM 1130 is situated in Hall 3 and provides experimenters in the area with a direct link to the Central Computer. Users can submit jobs or data (on cards or 7 track magnetic tape) and receive output on an 80 lines/minute line printer. It is also possible to communicate with ELECTRIC via the console typewriter. Communication between the two computers is via an 880 kbit/sec serial link. Further developments (described later) will allow another sixteen devices to be linked to the terminal computer.

USER SUPPORT

As already mentioned, the IBM 360/195 will be available to many users outside the Rutherford Laboratory from 1 January 1972. Some 20 University Nuclear Physics groups have requested computing time. To assist this increased number to utilise the computing system effectively, a User Support section has been set up. Some of its functions during the year are described below, while new and extended activities are expected next year, particularly in education, technical assistance and program library facilities.

Program Advice and Technical Assistance   Program advisers have been available daily from late September, to deal with queries regarding Job Control Language, Fortran and Assembler coding. Towards the year end, the main task was to introduce new (external) users to the system. Detailed technical assistance was provided for several projects, in particular for the Queen Mary College/Liverpool/Daresbury/Rutherford experiment (S99) and to the Finance section of the Laboratory.

Liaison   The User Support section intends to provide effective liaison between each user and the central computer organisation. For this purpose each user group has been asked to appoint a representative who has an overall idea of the computing work within the group. This will ensure that every user has at least a formal line of communication to the central organisation.

Accounting   A watch has been kept on the weekly accounts of computer usage. The User Support section was involved in the "voluntary restraint" introduced for a very busy period in early summer, and will participate actively in the new accounting system to be introduced next year.

Documentation, Education and Information   Assistance was given in producing the second issue of CIGAR (Computer Introductory Guide And Reference), the Computing and Automation Division's Quarterly Reports, the "Introduction to Central Computer Facilities" and numerous bulletins and reports.

A fortnightly series "Seminars on Computing" was arranged, concentrating during 1971 on on-line computing. Two courses of lectures were organised, one on 'ASSEMBLER' language, the other on the 'ELECTRIC' system. Each course was attended by about 50 persons. The program libraries have been extended during the year, and a full list appears in 'CIGAR'.

Figure 121. Average weekly totals of events measured on HPD I during 1971. (1970 statistics are shown dotted).
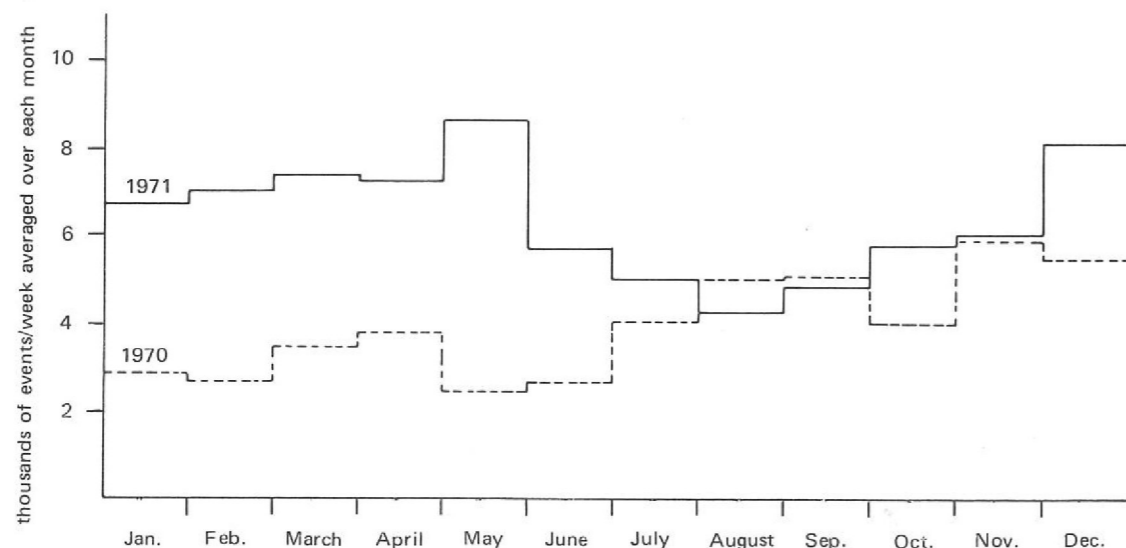
On-Line Computer Applications

AUTOMATIC FILM MEASUREMENT

During 1971 one-third of a million events (one million stereo-views) were measured on HPD I. This total covered three experiments undertaken by the Bubble Chamber Research Group, involving film exposed at the CERN 2m chamber. Numbers for each experiment were:— *HPD I*

Experiment	Events
K^-p (14 GeV/c)	92,000
K^-p (1·0-1·4 GeV/c)	216,000
π^+d (4 GeV/c)	28,000
Total	336,000

These figures include re-measurements of events which have failed Geometry tests; and in the case of the 14 GeV/c K^-p experiment, nearly 2000 beam tracks. None of the experiments has been finished during the year, but the bulk of the measuring for the two experiments on K meson interactions has been done. A group from Durham University is collaborating in the πd experiment and the first film pre-digitised at Durham, where there are no fast measuring facilities comparable with an HPD, will be measured here early in 1972.

The average measuring rate has been over 50% greater than last year's, but suffered from unavailability of pre-digitised film (especially during the summer), a total of some 1200 hours being lost during the year from this cause. The weekly average for each month of 1971 is shown in Figure 121, which includes figures from 1970 for comparison. The peak reached for any week was 13,556 events: but this included 1690 beam tracks, and the equivalent estimated total for 'normal' events is about 12,500.

Various minor improvements in both hardware and software have been consolidated during the year. Additionally, there have been the change of computer and changes to the system software already described. Excluding time spent on maintenance, breakdowns and errors, the actual time for which the HPD has been measuring is some 3700 hours or 45% of the year.

The change-over to operation with the 360/195 computer went very smoothly. The measuring rate, which is governed to a very large extent by the HPD hardware, was hardly affected. Central Processor usage by the on-line control program fell to about 2½% of measuring time. No significant changes of operating technique have been made, though the new computer and new peripherals due shortly will make changes possible; in particular, further development of the Minimum Guidance measuring mode.

Work has continued throughout the year to prepare the machine for production measurement of 70 mm spark chamber film early in 1972. *HPD II (ref. 146)*

Major hardware changes have been made, primarily to allow 70 mm film to be measured. Optical modifications were necessary to cover the full 70 mm width; a new film gate was designed and constructed for more rapid clamping of sprocketed or unsprocketed film, and work continues on changes to the film transport system, which will make it able to handle the new standard 300 metre spools of film and *Hardware Development (ref. 47, 206, 207)*

to position individual frames with reference to sprocket holes or Brenner marks on the film. Development continued on the laser system and a detailed analysis of the new optics was carried out, to determine the effects of degradation of the measuring spot. Although there is still some concern about lens performance, line widths below 5 μm are detectable, which is encouraging for measurement of BEBC film. Laser systems modelled on HPD II were adopted by four other laboratories during the year. In addition, the hydraulic ram control has been improved, allowing stage speeds of over 200 mm/sec, and hydraulically operated brakes have been installed to prevent possible stage creep. Electronic changes include provision of a track width measurement facility, essential for some spark chamber film.

Software Development

Software development has reached a position where test film in different formats (derived from bubble- or spark-chambers) can be measured. The new control program resident in the 360/195 has been successfully tested with both HPD I and HPD II. It is the first version of a program which will be used for both HPDs in the future, and occupies 136 k-bytes of memory, a saving of 50 k-bytes over the previous version for the 360/195. On-line diagnostic facilities have been provided and (for HPD II) extensive use made of the Tektronix 611 graphics equipment. The command structure for HPD II has been somewhat modified from that used for some time on HPD I, and data output is in a standard form for both bubble chamber and spark chamber film. Detailed changes to the DDP-516 programs have been made, including changes to the control program arising from an altered command structure and others arising from investigations of the DDP-516 interaction with MAST.

Transfer from the 360/75 to 360/195 went without incident, the HPD II-DDP combination functioning immediately it was re-connected. The main effect was a three-fold increase in the maximum HPD data rate acceptable to the central computer.

In the present configuration, HPD II can transmit data at rates as high as 30 k-words/second successfully, compared with 10 k-words/second for the 360/75. This should be adequate for HPD II running at 6000 rpm.

Tests

An important achievement late in the year was the successful calibration of HPD II, using a version of the old calibration program with some improvements and modifications to make results available on the Tektronix 611 display. This successful result is important because it confirms the mechanical, optical and electronic quality of the machine.

In preparation for the first film to be measured, from the two spark chamber experiments at CERN (S104 at the PS and 18 at the ISR) a number of individual frames have been digitised and written to tape for off-line examination. The frames were taken from experiment S104 film, from some cosmic ray events photographed with the ISR experiment apparatus, and from some simulated film (displaying fiducials, etc.) for the latter. Data on the tape was displayed at the HEP Graphics Terminal and looked satisfactory. Some work has been done to evaluate the photographic techniques required to produce spark chamber film of optimum density and contrast for an HPD.

CYCLOPS
(ref. 260)

Against expectations at the beginning of the year, the film measuring load on CYCLOPS during 1971 has been far below the machine's capacity. This situation was caused by delays in running experiments, and in consequence no tight scheduling was necessary. Film from two experiments was measured in production running. Some 23,000 frames from the Cambridge University/Rutherford Laboratory experiment [$\Delta S = \Delta Q$ rule, **Experiment 20**] were measured, completing automatic measuring of this experiment.

152,000 events (on 76000 frames) from a Glasgow University/Sheffield University/ Daresbury Laboratory experiment on π° photo-production were measured, all during the first quarter of the year. This experiment was also completed. Measuring tests were carried out on film from Oxford University (K10S) and Rutherford Laboratory (K13C) as it became available, but no production measuring has been done so far.

Limited hardware developments included a new Brenner mark detector, capable of handling a wide variety of shapes of marks, and an overhaul of the optics. On the software side, the on-line control program was changed to detect some types of machine faults immediately, allowing the operator to take corrective action. Off-line analysis of measurements was made as soon as possible after measuring: this feed-back of information gave early indications of faulty operation, which had not always been so in the past.

Work continued on the measurement and analysis of film portraying action *(ref. 239)* potential in nerve cells. After the program had been 'tuned' for one good sample of film, its results agreed very nearly with those from visual observations and measurement of the film. Subsequent samples differed considerably: they will require re-tuning of the program, which has not been completed. In December, it was decided to avoid some of the problems by using a new film format. No samples have yet been exposed in the new format.

The IDI display and light pen system was in use throughout the year for "patching-up" track measurements from HPD which failed various quality criteria. There were no significant changes to the system during this period, either in design or operation. It was used for up to 50 hours per week, processing about 1000 events weekly, and some 65% of these events were successfully treated, subsequently satisfying the set criteria.

IDI Display and Light Pen

ON-LINE DEVELOPMENTS

During the year a new multiplexor was commissioned on the DDP-224 satellite *Hardware* computer. This allows up to sixteen slow-speed devices to communicate simul- *(ref. 228)* taneously with the central computer via the MAST-DAEDALUS system. There are at present ten devices connected to the multiplexor, via eight 'golfball' IBM typewriters and two Tektronix graphics storage tubes.

A similar multiplexor to that used with the DDP-224 has been commissioned for the terminal IBM 1130 computer, allowing sixteen devices to be linked to the computer. Some of these links will go to experiment local control rooms, while others may be used for connecting terminals adjacent to the IBM 1130. This system is not yet fully operational and cannot be made so until an extra 8k core storage module has been installed on the terminal computer.

Some trials have been carried out to assess the problems of connecting slow-speed terminals via the switched public network supplied by the GPO. The tests have been completed and most of the operational problems resolved. However, the system cannot be made generally available until further equipment, to allow the automatic answering of Datel calls, is obtained from the GPO. The present system is limited to speeds of 110 baud, i.e. to devices such as teletypes whose speed does not exceed 10 characters/second.

In preparation for public use of the ELECTRIC system, program facilities were *Software* provided for accounting (see Figure 122) for controlling the space taken by a user *(ref. 259)* (so that it should not exceed the amount allocated), and to enable some operational intervention by the central computer staff (e.g. to transfer a user to a good
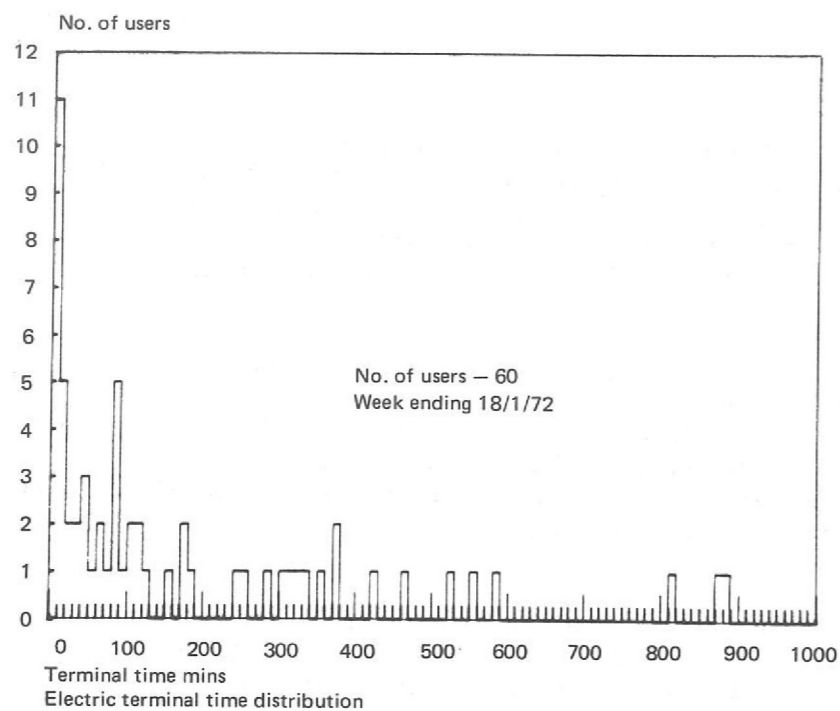
Figure 122. Example of accounting statistics for ELECTRIC users.

terminal from one which has just developed a fault). In addition, many detailed changes have been made which extend the facilities available to the user. It is expected that some future graphics users will choose other types of display from those currently used here. Interpreter programs have therefore been written and tested which will allow the present graphics software to be used with other displays attached (Tektronix 4002 and 4010). A user may have a display attached via the GPO switched public network.

DATA ANALYSIS SOFTWARE

Bubble Chambers: Road Guidance In the 'Road Guidance' production measuring system, work has concentrated on improving the pass rate (through GEOMETRY) and reducing the computer time per event. The pass rate for the low energy K⁻ experiment is now over 90% and the computer CPU time (on the 360/195) for the filtering and matching chain is about 0·6 s event. A detailed mathematical investigation of the paths of slow particles suffering significant energy loss in the chamber liquid showed that very few faulty track reconstructions could be attributed to any deficiencies in the approximations currently used.

Minimum Guidance (ref. 224) Little work has been done on the Minimum Guidance system this year. It was impracticable to use it in production with the 360/75 computer, because each event took about 10 seconds CPU time. And the increased number of digitisings which have to be stored for every frame makes its large scale use difficult. Samples of events have, however, been passed through the complete MG chain of programs, and a geometry pass rate of over 75% achieved after 'rescuing' failures on the IDI display and light pen.

Computing time is available on the 360/195 for production use of the MG system, and extra storage space will be available in 1972. Tests have accordingly continued, with attention concentrated on reducing the quantity of digitisings per frame (e.g. by a preliminary measurement of the vertex region, which may enable approximate track directions there to be found by on-line filtering) and improving the rescue system, which is unsatisfactory at present.

Large Chambers Some preliminary software changes are being made for processing data from the new generation of large bubble chambers. The CERN program LBCG, for geometrical reconstruction of tracks in large chambers, is being integrated into the Rutherford Laboratory processing chain.

A version of the fiducial and track finding program was modified to process data from the Daresbury/Glasgow/Sheffield photoproduction experiment. About 30% of the processing was done at the Laboratory, and the program then taken to Daresbury, where processing was completed. *Spark Chambers*

The CYCLOPS control program has been modified for measurement of film from the Oxford K10S and Rutherford Laboratory K13C experiments, including the measurement of grid film.

The work on momentum determination in terms of entry and exit parameters for trajectories through a non-uniform magnetic field has been completed and fully utilised in the analysis of Experiment 21 (π8).

DATA HANDLING FOR SPARK CHAMBER AND COUNTER EXPERIMENTS

The growing complexity of spark chamber and counter experiments has been accompanied by the increased use of computer generated visual displays. Events which cause problems to automatic analysis programs may be displayed pictorially on a television-like display screen. The experimenter can examine these pictures and supply guidance information to assist his analysis program or estimate the incidence of a particular class of event by scanning a sample of his data.

The group has implemented such a system which uses a 16K Honeywell DDP516 computer and two display consoles. So far, events from the data collected in Nimrod Experiments 1,9,21 and 22 and CERN experiment S70 have been displayed and on example is shown in Figure 123.

A supervising program has been written to allow the concurrent operation of four programs. A number of utility routines written for this system have been made available for other DDP 516 users,

A fast data link to the Laboratory's central IBM 360/195 computer has been successfully commissioned and will eliminate the use of magnetic tapes in transferring data between the two machines. Overall event processing time will thus be significantly reduced. During the coming year it is planned to connect three film measuring machines and two more display consoles to the system to satisfy the requirements of new experiments.

As reported elsewhere, interpretive techniques have been applied to the computer control of the K9 beamline. The Data Handling Group has started a similar project for DDP516 computers in local control rooms. This will enable users to communicate easily by CAMAC interfaces in order to monitor a wide range of experimental apparatus including beamline components and particle detectors.

Figure 123. Example of a spark chamber event from a visual display system.
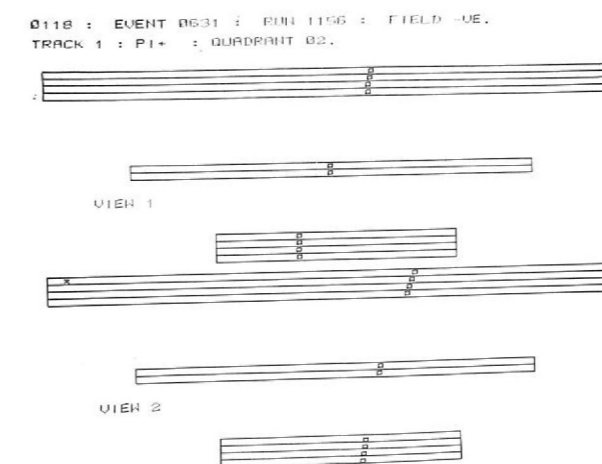
The Restaurant

TECHNICAL AND
ADMINISTRATIVE SERVICES

Technical and Administrative Services

RADIATION PROTECTION

Personal Dosimetry (ref. 245, 246) The response of a two element dosimeter (neutron track film plus slow neutron TLD), developed at the Laboratory to overcome the highly neutron spectrum dependent response of the track film alone, has been further investigated for various types of track films and for various irradiation conditions. The calibration factors chosen originally have been found to be still valid for all the conditions examined.

At November 1971 regular dosimeter issues were as follows:

Beta-gamma films (monthly issue)	400
Beta-gamma TLD (6 monthly issue)	240
Fast neutron films plus slow neutron TLD (monthly issue)	270
Beta-gamma TLD plus slow neutron TLD (6 monthly issue)	140

The total number of persons at the Laboratory issued regularly with some kind of personal dosimeter has remained sensibly constant (780 in 1971 compared with 700 in 1970).

As in previous years the personnel engaged in the maintenance and repair of Nimrod continue to be the most heavily exposed group at the Laboratory but none, however, is expected to exceed the yearly permitted dose although this may be approached in one or two cases.

Environmental Health Physics There have been no new problems associated with the operation of Nimrod; the long standing problem of the "leaking" X2 extracted beam blockhouse was resolved by the dismantling of the K14 and K11 beam lines and subsequent tidying-up of the blockhouse. There has been no significant change in the pattern of induced activity either in or near the machine or the extracted proton beams.

There have been no requirements during the year to handle work involving significant amounts of loose contamination in the Radiation Workshop (R52). Only infrequent use is made of the unsealed source facilities in the Radiochemistry Wing of R34.

Research (ref. 79, 115, 247) Topics under active consideration include:
Comparisons between measured and theoretically predicted levels of induced activity in and around Nimrod.
The calibration of contamination monitors for the nuclides found in accelerator environments.
The dosimetry of secondary beams.
The attenuation of dose-equivalent in labyrinths and tunnels in extracted proton beam blockhouses.

Radiation Physics (ref. 161, 273) Measurement, made during the previous year, of the angular distribution of the lower energy secondary particles emitted from targets in extracted proton beams have now been examined in detail. Preliminary results were presented at the International Congress on Protection against Accelerator and Space Radiation, and an edited record of all the experimental data has been prepared to facilitate independent further analysis. The results and conclusions drawn from detailed analysis are presented in a paper to be published in Particle Accelerators.

(ref. 116) The analysis of data on the transmission of radiation in a tunnel penetrating the X3 blockhouse has been completed.

The Group has continued to provide gamma spectrometry services, including the identification and quantification of gamma-ray emitting radio-isotopes encountered in routine radiation protection work. A calibrated gamma spectrometer is now used routinely for the assay of sodium-24 in the aluminium foils used to measure the intensity of internal and external Nimrod beams. Auto-radiography of these foils has also been carried out to provide information on the shape of the beam at several points of interest along its path.

Radiobiological Pion Irradiation Facility (ref. 162) Negative pions are of particular interest to radiobiologists who are investigating radiations which may be of value in the treatment of cancer. Several accelerator establishments already have plans for medical pion beam facilities which will have much more intense beams than are now available. Existing beams, however, such as $\pi 11$ on the Nimrod X3 extracted beam, can provide dose rates sufficiently high to allow a number of relevant biological experiments to be carried out. The performance of $\pi 11$ has now been optimised for radiobiological use and the properties of the beam have been studied, particularly the dose distribution when the pions are brought to rest in tissue equivalent materials.

A preliminary series of radiobiological experiments has been successfully carried out in collaboration with St Bartholomew's Hospital Medical College, The Churchill Hospital, AERE, and the Christie Hospital. For these experiments a mean pion range of 16 g cm^{-2} in tissue equivalent material was used (beam momentum 160 ± 10 MeV/c). The dose rates at the end-of-range ionisation peak were 15-30 rad/h over a useful field of about 2 cm diameter. It was shown that, under special Nimrod operating conditions, dose rates of 100 rad/h could be achieved.

SAFETY AT THE LABORATORY

The major function of the Safety Group is to encourage effective participation by all employees in accident prevention. This presents a continuing challenge to change people's attitude to safety from the optimistic "it won't happen to me" to the more realistic "it will — if I don't do something about it".

During the year, in addition to the Group's regular surveillance and inspection of potentially hazardous situations and apparatus, an increasing number of requests for advice were received. This is most satisfying as only by continuing to encourage communication and consultation will accidents be prevented.

Publicity displays of new and existing hazards were again exhibited at various points in the Laboratory, and several "Safety News" dealing with various topics were issued to stimulate interest in accident prevention.

As in previous years Safety Group organised Safety Tours which inspect all areas of the Laboratory. The touring parties consist of Safety Professionals augmented by a member of the Safety Committee and as a result of observations made by the touring party many recommendations were implemented to improve potentially unsafe conditions.

To complement the existing practical safety training programme, theoretical training by means of lectures, films and pre-recorded slide programmes were introduced during the year. Ten sessions were given in the Lecture Theatre to a total of 665 employees.

The number of items registered for periodic inspection continued to increase during 1971 to a total of 4,628. The rate of increase during 1971 was slightly below 5% as against the 1970 increase of 13%. The service introduced in 1970 to periodically test and set safety valves was used to an increasing extent and 239 safety valves were registered at the end of the year. The total of registered items is as follows with the 1970 total in brackets:— Lifting Tackle — 2,508 (2341), Pressure Vessels — 892 (872), High Voltage Equipment — 408 (408), Lifting Machines — 387 (392), Safety Valves — 239 (103), Breathing Apparatus and Safety Equipment — 147 (139) and Fire Prevention — 51 (49).

The total number of inspections of registered items carried out during 1971 was 8,091 (1970 total 7,780).

During 1971 (1970 figures in brackets) a total of 107 (126) injuries involving Laboratory Staff were reported, 10 (11) of these resulting in lost time, the average absence of the latter being 43·8 (18·8) days. The causes of the accidents were:—

Handling goods	23
Stepping on or striking against objects	17
Falls of persons	20
Use of hand tools	17
Machinery	5
Falls of objects	2
Electric shock	0
Miscellaneous	23

A nationally used method of representing injury incidence is to compute the Injury Frequency Rate which is defined as (numbers of injuries x 100,000)/ (number of man-hours worked). The figure of 100,000 is the number of working hours in an average man's career. The Laboratory's Injury Frequency Rate fell from 4·6 to 3·9 and the Lost Time Frequency Rate fell from 0·40 to 0·36.

ENGINEERING SUPPORT SERVICES

Electrical Services The main manufacturing effort has continued to be on magnet development, winding and potting techniques and superconducting joints. Six pancakes comprising magnet AC3 were completed, assembled and as noted elsewhere pulsed satisfactorily. A smooth ended uniform field magnet was developed with winding techniques suitable for super-conducting use. This model incorporating copper conductors for evaluation of the field distribution was completed with coils wound and potted in a mould. Cast-in-concrete magnets were further developed and a small superconducting magnet of this type was made.

A 5000 A d.c. variable voltage supply was constructed and installed for super-conducting magnet testing and a second harmonic bias supply for the Nimrod r.f. system was also constructed and installed. A comprehensive alarm system to monitor plant serviced by the Engineering Services Department (including the Atlas Laboratory) was installed and commissioned with alarm panels giving indications of faulty operation in the Mechanical and Electrical Workshops and also to the security wardens at the Main Entrance.

Plant services work in conjunction with other sections include:

(i) In the Rutherford Laboratory; a chilled water facility for air conditioning plant, IBM 360/195 computer power supplies, air conditioning plant and controls, a fire detection system for Building R1, plant for a new helium recovery system, a 900kW rectifier installation in the magnet room.

(ii) At the Atlas Laboratory; design and supervision of installation of ICL 1906A computer and installation of Sigma II interface switchboard designed and constructed by electronics section.

(iii) At the RSRS, Slough; project engineering and services for a new photographic block.

Electronic Services 102 different printed circuit boards were designed resulting in over 380 new drawings. There was a marked increase in complexity in many designs particularly those associated with the CAMAC Modular System. The more complex designs (some 25% of total) were done at the Laboratory. Manufacture of electronic units to the value of about £150,000 was undertaken including component costs which in the case of semi-conductors have reduced markedly during the year. Of this total about 50% was done outside and the remainder in the Laboratory's prototype shop (351 different jobs ranging from ½ man-day to ½ man-year) and the small production shop (172 separate jobs mostly assembling printed circuit boards).

Included in the above total is £18,000 for printed circuit boards including large flexible circuits for spark chambers and termination boards for wire chambers both manufactured to extreme accuracy. During the year over 2,500 instruments were checked and repaired by the Electronic and Instrument Section.

Track Analysis Machine Section The work of this section has continued to expand and during the year a further two digitisers had been installed and commissioned for 'on-line' rough measurement of bubble chamber films bringing the total to 12 connected to the IBM 1130 computer. During the year three Vanguard measuring machines were installed and commissioned initially for use 'off-line' and preparation is in hand for connection of other digitisers to the DDP516 computer for 'on-line' use in the measurement of spark chamber film. This section has also undertaken responsibility for maintenance, operation and performance checks of the automatic measuring machine HPD 1 now used as a production machine.

Buildings and Mechanical Services The major project undertaken during this year has been the extension to Building R1 to house the IBM 360/195 Computer and its associated chilled water and air conditioning plants. The installation and commissioning of plant was complicated by the requirement to maintain air conditioning to the existing IBM 360/75 Computer whilst removal of its air conditioning plant was underway and the replacement plant was being installed.

The R9 Workshop and Outside Manufacturing Sections have been giving support to the many experimental projects both within the Laboratory and at CERN. Support work to Groups employed on satellite projects has occupied a substantial portion of the work load.

Figure 124. View of Building R1 showing the recent extension to accommodate the 360/195 computer.

Helium Recovery Helium recovery demands have necessitated additional low and high pressure gas storage and compressing capacity. The existing compressing plant has been relocated in Building R7 and a further compressor included in a fully automated collecting, compressing and high pressure charging plant.

ADMINISTRATION

Housing The number of staff at CERN has continued to increase during 1971. This has caused problems with housing and with the same situation developing at Daresbury it was agreed that Rutherford's General Administration Group would look after the housing needs for both Laboratories and their University visitors. A total of 38 furnished apartments were occupied at the end of the year and more accommodation on long term leases was being sought.

At home the demand for different types of rented accommodation has remained at a very high level. Private furnished accommodation has been obtained for an increased number of short-term visitors and another furnished house in Abingdon will be made available in 1972 for visitors.

Office Services The re-organisation of the Section in 1970 has shown increased results in 1971 with a saving of about £4,000 over the previous year's expenditure on outside printing. Pre-prints are an example of the increased volume and calibre of work undertaken internally. Of 62 pre-prints submitted for printing only one was completed externally.

Finance In the financial year 1971/72, the total Laboratory expenditure was £10·5 million, of which £3·7 million was for capital items (including the new IBM 360/195 computer) and £6·8 million was recurrent. Corresponding figures for 1970/71 were £8·05 M, £1·1 M and £6·95 M. The total expenditure is conventionally subdivided in the table below, with corresponding figures for the previous year shown in brackets.

	£ million
Staff expenditure (salaries and wages, insurance, superannuation, travel, etc.)	3·26 (2·91)
Research and Development (see below)	3·80 (4·40)
Plant and equipment (major components and including a single item of £3·0 M for a computer)	3·30 (0·71)
Building works	0·14 (0·03)
Totals	10·50 (8·05)

A proportional representation of the breakdown of the £3·80 million R and D expenditure into divisional and other main components is shown in the pie chart. (Figure 125).
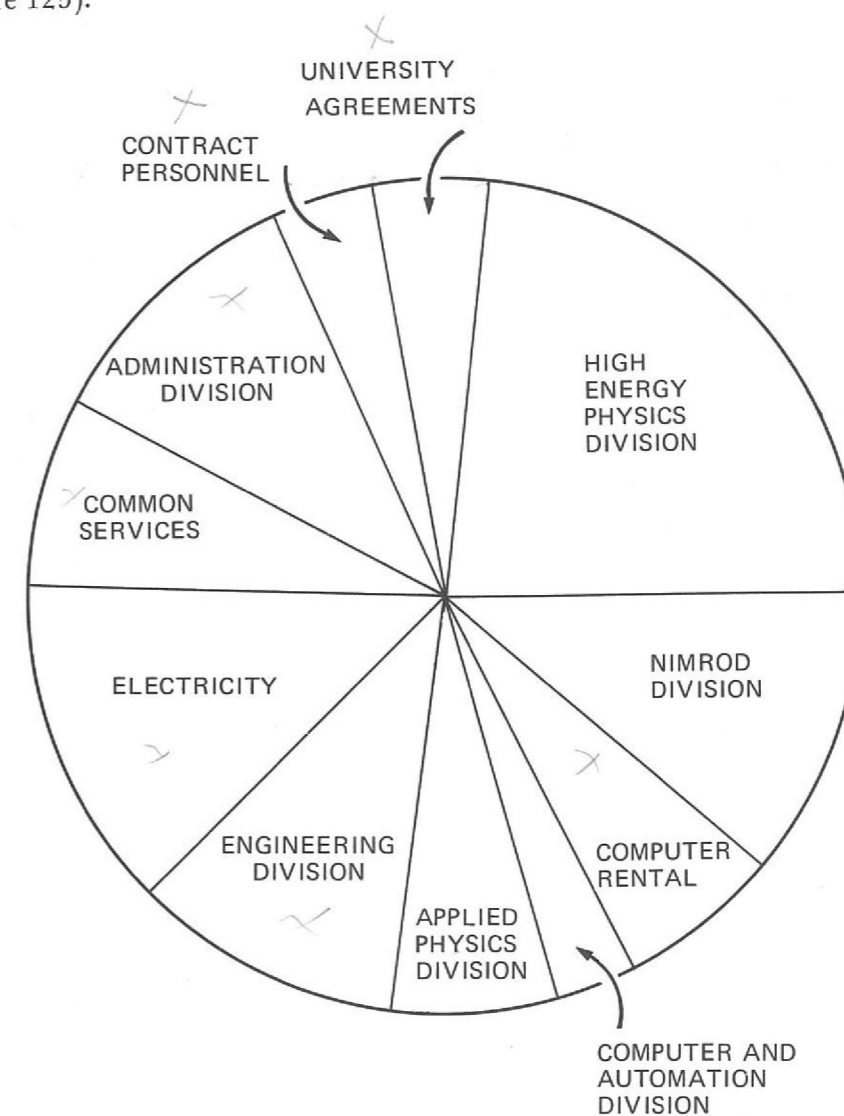

Figure 125. Breakdown of the £3·8 million R and D expenditure.

Table 13

Staff Numbers 1971 The staff position at the beginning and end of the year.

	Opening Strength 1.1.71	Changes during 1971		Closing Strength 31.12.71
		Gains	Losses	
PROFESSIONAL				
Senior and Banded Staff	24	3	2	25
*SO class	74	6·5	6	74·5
Research Associates	49	28	21	56
*Exp. O. class	118	6	2	122
Engineers I, II, III	107	3	6	104
ADE	4	0	0	4
Total Professional	376	46·5	37	385·5
ANCILLARY				
*SA and SSA	46·5	4·5	5	46
Draughtsmen	43	0	1	42
Technical class	193	3	7	189
Non-Techs. and Stores	42	0	0	42
Administrative	30	2	3	29
Librarian	1	0	0	1
Clerical	49	2	7	44
Secretarial and Typing	32·5	3	7	28·5
Photographers	4	0	0	4
Photoprinters	5	0	0	5
Machine Operators	69	10·5	17	62·5
Hostel Manageress	1	1	0	2
Telephone Operators	2	2	2	2
Total Ancillary	518	28	49	497
INDUSTRIAL				
Craft	188·5	2	9	181·5
Non-craft	139·5	7	18·5	128
Apprentices	30	5	6	29
Total Industrial	358	14	33·5	338·5
GRAND TOTALS	1,252	88·5	119·5	1,221

The figures listed under "changes" include new entrants, resignations and promotions. Staff on sandwich courses, and those working part-time are counted as half.

Staff Structure As from the beginning of the year, the Scientific, Experimental and Scientific Assistant Classes were merged into the Science Group. For comparison purposes they are shown, asterisked, under their former titles in the above table.

Staff Relations The local Joint Consultative Committee and the Joint Consultative Productivity Committee continued to meet regularly during the year. Subjects discussed included productivity and methods of wage payment.

Changes in membership of the local Whitley Committee, coupled with cuts in expenditure resulting in the withdrawal of certain facilities, have made this year a busy and difficult one. The full Committee met on four occasions, the Director taking the Chair at the Annual Meeting in June; in addition there have been several smaller meetings to discuss specific issues as they arose. The wide variety of topics discussed covered both the future of the Laboratory and policy decisions affecting working conditions.

The Committees dealing with Safety, Shift Working and Suggestions Awards have worked well, to safeguard and advance the interests of both management and staff in their respective fields of activity. Inflationary trends in commodity and labour costs have forced the Restaurant Committee to raise the prices of mid-day meals, and discussions are in progress on possible ways of reducing prices, or at least minimising future increases.

Training The overall pattern of training in the Rutherford Laboratory during the academic year 1970/71 was generally that to be expected in an establishment with a low recruitment rate. Both day-release training concessions and external short course attendances declined in numbers to some extent, but full-time training remained at its highest level during the Laboratory's history because students were completing courses started several years ago.

The total number of part-time concessions awarded was 137, about 11% of the total staff of the Laboratory compared with 13% last year. The 121 students who sat examinations achieved an overall pass-rate of 77%, slightly lower than last year's figure of 79% but still well above the national average for this kind of course.

Three full-time students from the Laboratory graduated from University this year, all with degrees in Applied Physics. One student was awarded First Class Honours at Brunel University, one obtained Upper Second Class Honours at the University of Aston and the third student obtained Third Class Honours at the City University. The Laboratory's other three full-time students are making satisfactory progress on their courses, two on the HND course in Mechanical Engineering at Oxford Polytechnic and one on the CNAA Electrical Engineering Honours Degree Course at Lanchester Polytechnic (Rugby). Five of these six students held Laboratory Awards and the sixth received unpaid leave. The three final-year students required no industrial training but the other three students returned to the Laboratory for this purpose.

Once again the principal source of external short courses, on both technical and management topics, has been the AERE Education and Training Department — to the extent of about 75% of the total number of participants. Laboratory staff also participated in some of the scientific and technical courses on the teaching side. The Laboratory took up its full allocation of places on SRC management courses and staff attended other short courses run by a wide range of organisations including Universities, Polytechnics and Technical Colleges, the Cranfield School of Management Studies, PERA, the Industrial Society, the Welding Institute and a number of firms in the computer, electronic, photographic, cryogenic and high vacuum equipment industries.

Three members of the staff of the Laboratory are registered research students, one with the University of London, one with the University of Surrey and one with the Council for National Academic Awards. One research student is about to submit his thesis and the others have not yet reached that point in their work.

In addition to training concessions awarded to permanent staff nearly 30 Craft Apprentices and Student Engineers received training in the Apprentice Training Scheme run jointly with AERE. Five apprentices completed their "time" during the year and two Student Engineers graduated from University, one with Lower Second Class Honours in Engineering-with-Social-Studies from the University of Sussex and the other with Lower Second Class Honours in Mechanical Engineering from the City University. It is now 10 years since the Rutherford Laboratory started to participate in the AERE Apprentice Training Scheme and during that term 80 apprentices were recruited for the Laboratory, 52 completed their training and 33 took appointments with the Laboratory on completion of training.

The Rutherford Laboratory acted as host establishment for two SRC Central Induction Courses held in December 1971. This has become an annual event, timed to enable visitors from other SRC establishments to see Nimrod during the winter shut-down.

The Laboratory provided industrial training during the academic year for a record number of college-based sandwich students, 49 in all, bringing the total of such students trained in the Laboratory over the last 11 years to 315. The increase was largely due to the increased demand from colleges for industrial training places for Applied Mathematics and Computer Science students and the realisation that these students could be employed, to the Laboratory's advantage as well as their own, on data-handling and programming work in experimental groups as well as on more obviously theoretically-orientated projects. However the majority of students were studying Applied Physics, a few Electronics, and several Applied Chemistry students were placed in the Chemical Technology Group.

Schools Liaison   Contact with individual schools has continued throughout the year: there have been no major developments. One such contact with Abingdon School has been very successful: boys have studied various physical properties such as thermal expansion and Young's Modulus of resin samples as a function of temperature. These samples were supplied by the Laboratory. The study was supplementary to the Laboratory programme in searching for resins suitable for superconducting magnets. Different groups of boys adopted different methods of measurement and compared and contrasted the results obtained. The project has been described in an article for publication.

In addition, two boys from Leighton Park School visited in February: they were attached to the Bubble Chamber Group, and conducted a small study in optics.

Exhibitions   The Laboratory showed five pieces of equipment at the Physics Exhibition in London, 19–22 April. The widespread use of spark chambers in high energy physics was reflected by two of the exhibits — foil stretching technology and a gas purification rig. The electron monochromator on display is used for calibrating various types of electronic particle detector. Liquid hydrogen target technology was represented by a cryogenic heat pipe, and there was a demonstration of a television camera specially shielded against the effects of pulsating magnetic fields such as are encountered close to Nimrod's main magnet ring.

At the Exhibition staged in conjunction with the United Nations 4th International Conference on the Peaceful Uses of Atomic Energy in Geneva, 6–12 September, the Laboratory contributed an exhibit describing a Superconducting Energy Transfer System.

Bulletin   During the year a new style of Rutherford Laboratory Bulletin was introduced. More space is available for news items, and the layout of the forthcoming week's events has been improved.

Conferences   The annual Theoretical High Energy Physics gathering took place from 4 to 6 January, and from 6 to 24 September the first British Vacation School in Theoretical Elementary Particle Physics was held. For the latter event, the formal sessions in the Laboratory's Lecture Theatre were supplemented by evening tutorials and informal discussions at The Cosener's House, Abingdon, where the participants were accommodated.

The Laboratory was host to two one-day Institute of Physics Conferences on specialist subjects connected with the research programme, namely Ultrasonic Bubble Chambers (18 March) and Stabilising Superconductors (23 April).

Visitors   On 29 October, as part of the Royal Society's celebrations of the centenary of Lord Rutherford's birth, the Laboratory was visited by a group of 30 eminent scientists representing a wide range of overseas learned societies, universities and other institutions. Many of the visitors had been associated with Rutherford at the Cavendish Laboratory. They were shown Nimrod, the K12A kaon-nucleon scattering experiment, and a display of modern instrumentation for particle physics experiments.

In addition, the Laboratory provided guided tours for parties totalling just over one thousand persons. They covered the usual wide spectrum of scientific attainment; an innovation this year was the inclusion of three parties of participants in courses at the Civil Service College.

Figure 126. Professor Amaldi and Dr. Stafford, examining with interest one of the exhibits (a section through a trial winding of the polarized proton target 'holding magnet') during the visit of the Royal Society.
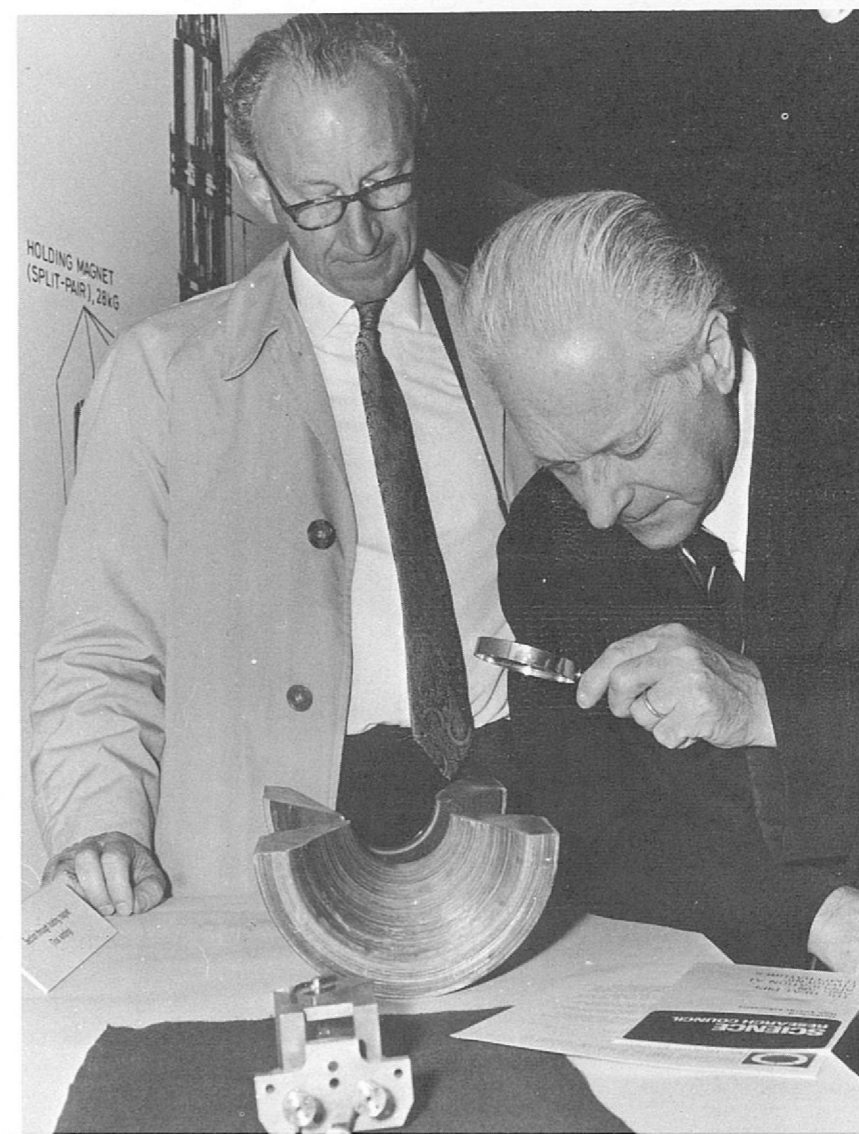
The Lecture Theatre

PUBLICATIONS
AND LECTURES

List of Publications

JOURNAL ARTICLES

1 ADAMS C. J., DAVIES J. D., DOWELL J. D., GRAYER G. H., HATTERSLEY P. M., HOWELLS R. J., McLEOD C., McMAHON T. J., VAN DER RAAY H. B., ROB L., DAMERELL C. J. S., HOMER R. J., HOTCHKISS M. J.
   K^+p elastic scattering between 432 and 939 MeV/c.
   Phys. Rev., D4 (9) 2637 (November 1971), preprinted as RPP/H75.

2 ALLEN W. D.
   The search for gravitational radiation.
   Reseach (Reading University Physics Department) April 1971.

3 ALPIN P. S., COWAN I. M., GIBSON W. M., GILMORE R. S., GREEN K., MALOS J., SMITH V. J., WARD D. L., KEMP M. A. R., LEA A. T., McKENZIE R., OADES G. C.
   DCS for π^-p elastic scattering from 1·2 to 3·0 GeV/c and phase shift analysis.
   Nucl. Phys., B32 (2) 253 (September 1971), preprinted as RPP/H67.

4 AOI H., BOOTH N. E., CAVERZASIO C., DICK L., GONIDEC A., JANOUT Z., KURODA K., MICHALOWICZ A., POULET M., SILLOU D., SPENCER C. M., WILLIAMS W. S. C.
   Polarization in backward π^+p elastic scattering at 6 GeV/c.
   Phys. Lett., 35B (1) 90 (April 1971).

5 BACON T. C., BUTTERWORTH I., MILLER R. J., PHELAN J. J., DONALD R. A., EDWARDS D. N., HOWARD D. C., MOORE R.S.
   Non-annihilation channels in $\bar{p}p$ interactions near centre of mass energy 2200 MeV.
   Nucl. Phys., B32 (1) 66 (August 1971), preprinted as RPP/H72.

6 BAIRSTOW R., BRANDSTETTER A., HUNT J.
   A simple ionisation measuring device for bubble chamber pictures.
   Nucl. Instrum. Meth., 99 (2) 345 (March 1972), preprinted as RPP/H81.

7 BAKER S. L., DORNAN P. J., GOPAL G. P., WEBSTER G. J., BULL V. A., MARCH P. V., TAYLER V., TOWNSEND D. W.
   A constrained phase shift analysis of π^+p data in the mass range 1600 to 1700 MeV.
   Nucl. Phys., B30 (1) 116 (July 1971).

8 BARGER V., GEER K., PHILLIPS R. J. N.
   Asymptotic pp elastic scattering.
   Phys. Lett., 36B (4) 343 (September 1971).

9 BARGER V., GEER K., PHILLIPS R. J. N.
   Extrapolation of pp diffraction slope to infinity.
   Phys. Lett., 36B (4) 350 (September 1971).

10 BARGER V., PHILLIPS R. J. N.
   Complex Regge poles.
   Nucl. Phys., B33 (1) 200 (October 1971), preprinted as RPP/C9.

11 BARGER V., PHILLIPS R. J. N.
   Deductions from new $\pi^-p \to \pi^\circ n$ data at large momentum transfer.
   Nucl. Phys., B33 (1) 22 (October 1971).

12 BARGER V., PHILLIPS R. J. N.
   Phenomenology of total cross-sections and forward scattering at high energy.
   Nucl. Phys., B32 (2) 93 (August 1971).

13 BARLOUTAUD R., BORG A., LOUDEC C., PIERRE F., SPIRO M., MILLER R. J., PHELAN J. J., SHAH T. P., CHAURAND B., DREVIL-LON B., LABROSSE G., LINGLIN D., SALMERON R. A.
   Energy dependence of the reactions $K^\pm p \to K^{*\pm}$ (890)p and $K^\pm$ $p \to K^{*\pm}$ (1420)p.
   Phys. Lett., 38B (4) 257 (February 1972).

14 BATTY C. J.
   The nucleon-nucleus spin-spin interaction.
   Nucl. Phys., A178 (1) 17 (December 1971), preprinted as RPP/NS 4.

15 BATTY C. J., FRIEDMAN E.
   Nuclear mass distributions from the elastic scattering of low-energy α-particles.
   Phys. Lett., 34B (1) 7 (January 1971).

16 BATTY C. J., FRIEDMAN E.
   Nuclear sizes derived from high-energy reaction cross-sections.
   Nucl. Phys., A179 (3) 701 (February 1972), preprinted as RPP/NS 5.

17 BATTY C. J., FRIEDMAN E., JACKSON D. F.
   The effective α-nucleon interaction in nuclei.
   Nucl. Phys., A175 (1) (November 1971), preprinted as RPP/NS 3.

18 BATTY C. J., KILVINGTON A. I., MARINOV A.
   Velocity measurements of recoil nuclei from α-decay and the determination of their mass.
   Nucl. Instrum. Meth., 99 (2) 179 (March 1972), preprinted as RPP/NS 6.

19 DE BELLEFON A., BERTHON A., RANGAN L. K., VRANA J., BACON T. C., BRANDSTETTER A., BUTTERWORTH I., DEEN S. M., FISHER C. M., LITCHFIELD P. J., MILLER R. J., SMITH J. R., BURGUN G., MEYER J., PAULI E., POULARD G., TALLINI B., WOJCIK W., ZATZ J., STRUB R.
   Channel cross-sections of K^-p reactions from 1·26-1·98 GeV/c.
   Nuovo Cim., 7A (3) 567 (February 1972).

20 BENNETT J. R. J.
   Stripping in cyclotrons to obtain high-energy heavy ions.
   Particle Accel., 3 (1) 43 (January 1972).

21 BINNIE D. M., CAMILLERI L., DUANE A., FARUQI A. R., GARBUTT D. A., JONES W. G., KAY M. E., LEWIS M., NICHOLSON P. J., SIOTIS J., UPADHYAY P. N., WILSON J. G., BURTON I. F., FRANK S. G., GEORGE R., HAQUE M., McEWAN J. G.
   A_2^- production in the channel $\pi^+\pi^-\pi^-$ near threshold.
   Phys. Lett., 36B (3) 257 (September 1971), preprinted as RPP/H78.

22 BINNIE D. M., CAMILLERI L., DUANE A., GARBUTT D. A. HOLMES J. R., JONES W. G., KEYNE J., LEWIS M., SIOTIS I., UPADHYAY P. N., BURTON I. F., GEORGE R. McEWAN J. G.
   A_2^- production in the channel π^- + neutrals near threshold.
   Phys. Lett., 36B (5) 537 (October 1971), preprinted as RPP/H82.

23 BRUNET J. M., NARJOUX J. L., DANYSZ J. A., GOLDSACK S. J., PENNEY B. K., STEWART B. C., THOMPSON G., JACOBS N. J. D., LEWIS P. H., MARCH P. V.
Resonance production in the reactions $K^+p \to KN\pi$ in the intermediate energy range.
Nucl. Phys., B37 (1) 114 (February 1972), preprinted as RPP/H76.

24 BRUNET J. M., NARJOUX J. L., DANYSZ J. A., SPIRO M., VERGLAS A., BAKER S. L., ORR R. S., PENNEY B. K., STEWARD B. C., THOMPSON G., ALLEN J. E., JACOBS N. J. D., LEWIS P. H., MARCH P. V.
K^+p cross-sections between 2·1 and 2·7 GeV/c.
Nucl. Phys., B36 (1) 45 (January 1972), preprinted as RPP/H74.

25 BUGG D. V., BUSSEY P. J., DANCE D. R., SMITH A. R., CARTER A. A., WILLIAMS J. R.
The $\pi^-p \to \pi^\circ n$ charge exchange cross-sections between 90 MeV and 290 MeV.
Nucl. Phys., B26 (3) 588 (March 1971).

26 CARTER A. A., WILLIAMS J. R., BUGG D. V., BUSSEY P. J., DANCE D. R.
The total cross-sections for pion-proton scattering between 70 MeV and 290 MeV.
Nucl. Phys., B26 (3) 445 (March 1971), preprinted as RPP/H70.

27 CHAURAND B., DREVILLON B., LABROSSE G., LINGLIN D., SALMERON R. A., BARLOUTAUD R., BORG A., LOUEDEC C., PIERRE F., SPIRO M., MILLER R. J., PHELAN J. J., SHAH T. P.
The reactions $K^-p \to K^{*\bar{o}}(890)N$ and $K^-p \to K^{*\bar{o}}(1420)N$ at 14·3 GeV/c.
Phys. Lett., 38B (4) 253 (February 1972).

28 CLARKE N. M.
Energy spread in thin absorbers.
Nucl. Instrum. Meth., 96 (4) 497 (November 1971).

29 CLARKE N. M.
A polarization analyser for medium energy ^{3}He particles.
Nucl. Instrum. Meth., 97 (2) 399 (December 1971).

30 CLARKE N. M.
Triple scattering parameters in optical model analyses.
Nucl. Phys., A178 (2) 513 (January 1972).

31 COHEN-TANNOUDJI G., KANE G., QUIGG C.
How much of diffraction dissociation cross-section is diffractive?
Nucl. Phys., B37 (1) 77 (February 1972), preprinted as RPP/C27.

32 COLLEY D. C., COX G. F., EASTWOOD D., FRY J. R., HEATH-COTE F. R., ISLAM G. S., SAFDER A., CANDLIN D. J., COLVINE J. G. COPLEY G., FANCEY N. E., MUIR J., ANGUS W., CAMPBELL J. R., MORTON W. T., NEGUS P. J., ALI S. S., BUTTERWORTH I., FUCHS F., GOYAL D. P., MILLER D. B., PEARCE D., SCHWARZSCHILD B.
Resonance production in K^- neutron interactions at K^- momenta of 1·45 and 1·65 GeV/c.
Nucl. Phys., B31 (1) 61 (August 1971).

33 DASS G. V., KABIR P. K., KENNY B. G.
The tests of TCP invariance in neutral kaon decays.
Proc. Roy. Soc., 325A (1560) 101 (October 1971), preprinted as RPP/C13.

34 EASTWOOD D., FRY J. R., HEATHCOTE F. R., ISLAM G. S., CANDLIN D. J., COPLEY G., EVANS G. R., CAMPBELL J. R., MORTON W. T., NEGUS P. J., COUNIHAN M. J., GOYAL D. P., MILLER D. B., SCHWARZSCHILD B.
The 2130 MeV $\Lambda^\circ p$ mass enhancement in the reaction $K^-d \to \Lambda^\circ p\pi^-$ at 1·45 and 1·65 GeV/c.
Phys. Rev., D3 (11) 2603 (June 1971).

35 EBEL G., MULLENSIEFEN A., PILKUHN H., STEINER F., WEGENER D., GOURDIN M., MICHAEL C., PETERSEN J. L., ROOS M., MARTIN B. R., OADES G. C., DE SWART J. J.
Compilation of coupling constants and low-energy parameters.
Nucl. Phys., B33 (2) 317 (November 1971).

36 FRIEDMAN E.
Coulomb energies and the anomaly in nuclear matter radii.
Phys. Lett., 35B (7) 543 (July 1971).

37 FRIEDMAN E.
Neutron distributions from a hydrodynamical model.
Nucl. Phys., A170 (1) 214 (July 1971), preprinted as RPP/NS2.

38 GOPAL G. P., MIGNERON R., ROTHERY A.
Resonance structure of the Veneziano model for $\bar{p}n \to 3\pi$ at rest.
Phys. Rev., D4 (7) 2169 (October 1971), preprinted as RPP/H73.

39 GUNION J., ROBERTS R. G.
Analysis of meson-baryon scattering processes related by SU(3) in a unitarized Veneziano model.
Nucl. Phys., B28 (1) 210 (May 1971).

40 GUNION J. F., ROBERTS R. G.
Redemption of the dual description of production processes by unitarity. The relevance of the eikonal model.
Nucl. Phys., B28 (1) 189 (May 1971).

41 GUNION J. F., ROBERTS R. G.
A multiparticle eikonal model with high-energy S-channel helicity conservation.
Nucl. Phys., B28 (1) 205 (May 1971).

42 HANNA A. M., GRIFFITHS R. J., CLARKE N. M., SQUIER G. T. A.
A study of the reactions $^{16}O(p,2p)^{15}N$ and $^{12}C(p,2p)^{11}B$ at 50 MeV.
Phys. Lett., B37 (4) 361 (December 1971).

43 INGRAM C. H. Q., TANNER N. W., DOMINGO J. J., ROHLIN J.
Pion production and bound nuclei.
Nucl. Phys., B31 (2) 331 (September 1971).

44 KAMAL A. N., WONG N. N.
Radiative corrections to $K\ell_3$ Dalitz plot.
Nucl. Phys., B31 (1) 48 (August 1971).

45 KABIR P. K., KAMAL A. N.
Muon flux deep underground and the question of strong W interactions.
Lett. Nuovo Cim., 1 (1) 1 (January 1971), preprinted as RPP/C6.

46 KWIECINSKI J.
Possible new threshold sum rules implied by unitarity.
Lett. Nuovo Cim., 1 (4) 146 (January 1971), preprinted as RPP/C5.

47 LAWES R. A., WELFORD W. T.
   An illumination system of improved power and resolution for the Hough Powell Device.
   Nucl. Instrum. Meth., 96 (3) 383 (October 1971).

48 LAWSON J. D.
   Collective and coherent methods of particle acceleration.
   Particle Accel., 3 (1) 21 (January 1972).

49 LAWSON J. D.
   On the rest mass of the photon.
   Amer. J. Phys., 39 (11) 1411 (November 1971).

50 LEA A. T., MARTIN B. R., THOMPSON G. D.
   K^+p partial wave amplitudes below 2 GeV/c.
   Nucl. Phys., B26 (2) 413 (February 1971), preprinted as RPP/C2.

51 LITCHFIELD, P. J., BACON T. C., BUTTERWORTH I, SMITH J. R., LESQUOY E., STRUB R., BERTHON A., VRANA J., MEYER J., PAULI E., TALLINI B., ZATZ J.
   K^-p elastic and charge exchange scattering in the c.m. energy range 1915-2168 MeV.
   Nucl. Phys., B30 (1) 125 (July 1971), preprinted as RPP/H71.

52 LOVE A., ROSS G. G.
   Duality and nonlinear SU_3.
   Phys. Lett., 36B (2) 118 (August 1971), preprinted as RPP/C17.

53 LOVE A., ROSS G. G.
   Nonlinear unitary symmetry.
   Phys. Lett., 35B (3) 231 (May 1971), preprinted as RPP/C7.

54 MAIDMENT J. R., PLANNER C. W.
   An analytic method for closed orbit correction in high energy synchrotrons.
   Nucl. Instrum. Meth., 98 (2) 279 (January 1972), preprinted as RPP/N24.

55 MARINOV A., BATTY C. J., KILVINGTON A. I., NEWTON G. W. A., HEMINGWAY J. D.
   Evidence for the possible existence of a superheavy element with atomic number 112.
   Nature, 229 (5285) 464 (February 1971), preprinted as RPP/NS1.

56 MARINOV A., BATTY C. J., KILVINGTON A. I., WEIL J. L., FRIEDMAN A. M., NEWTON G. W. A., ROBINSON V. J., HEMINGWAY J. D., MATHER D. S.
   On the spontaneous fission previously observed in a mercury source.
   Nature, 234 (5326) 212 (November 1971), preprinted as RPP/NS 7.

57 MARTIN A. D., MARTIN B. R., ROSS G. G.
   Models of Y_0^* (1405) and low-energy $\bar{K}N$ interactions.
   Phys. Lett., 35B (1) 62 (April 1971), preprinted as RPP/C10.

58 MILLER R. J., PHELAN J. J., SMITH J. R., BARLOUTAUD R., LOUEDEC C., PIERRE F., PORTE J. P. SPIRO M., DREVILLON B., LINGLIN D., SALMERON R. A.
   K^-p elastic scattering at 14.25 GeV/c.
   Phys. Lett., 34B (3) 230 (February 1971).

59 NEWPORT R. W.
   Applications of cryogenics to nuclear physics — low temperature bubble chambers.
   Advanced Cryogenics, Bailey C. A. (ed.), Plenum Press 1971.

60 NIELSEN H.
   Pion-nucleon phase shifts below 270 MeV.
   Nucl. Phys., B30 (2) 317 (July 1971).

61 NIELSEN H.
   The invariant amplitudes of πN scattering in the unphysical region for $t \leqslant 4\mu^2$ and helicity amplitudes.
   Nucl. Phys., B33 (1) 152 (October 1971).

62 OADES G. C., RASCHE G.
   Coulomb and mass difference corrections to K^-p scattering.
   Phys. Rev., D4 (7) 2153 (October 1971), preprinted as RPP/C18.

63 OADES G. C., RASCHE G.
   Coulomb corrections to low-energy elastic and charge exchange πN scattering.
   Helv. Phys. Acta., 44 (1) 5 (February 1971).

64 OADES G. C., RASCHE G.
   Mass differences as additional electromagnetic corrections in low-energy elastic and charge exchange πN scattering.
   Helv. Phys. Acta., 44 (2) 160 (April 1971).

65 OADES G. C., RASCHE G., ZIMMERMANN H.
   Remarks on $\pi \pm {}^4$He scattering and the electromagnetic radius of the charged π mesons.
   Nuovo Cim., 2A (2) 438 (March 1971).

66 PHILLIPS R. J. N., RINGLAND G. A.
   Polarization tests of absorptive cut models.
   Nucl. Phys., B32 (1) 131 (August 1971), preprinted as RPP/C8.

67 RINGLAND G. A., ROY D. P.
   Real part of the nonflip amplitude in πN charge exchange scattering.
   Phys. Lett., 36B (2) 110 (August 1971).

68 ROBERTS R. G.
   How is the A_1 produced?
   Phys. Lett., 35B (6) 525 (July 1971), preprinted as RPP/C19.

69 ROBERTS R., ROY D. P.
   Limiting fragment distribution of inclusive reactions.
   Nucl. Phys., B38 (2) 587 (March 1972), preprinted as RPP/C21.

70 ROHLIN J., ROHLIN S., ALLARDYCE B. W., DOMINGO J. J., INGRAM C. H. Q., TANNER N. W., RIMMER E. M., GIRADEAU-MONTAUT J. P.
   Elastic and inelastic scattering of 385 MeV/c pions by ^{16}O.
   Nucl. Phys., B37 (2) 461 (February 1972).

71 ROSS G. G.
   Data representation and modified dispersion.
   Nucl. Phys. B31 (1) 113 (August 1971), preprinted as RPP/C12.

72 ROSS G. G.
   Optimised integral continuation methods.
   Nucl. Phys., B., (in the press).

73 ROY D. P.
   Planar versus local duality.
   Lett. Nuovo Cim., 2 (11) 545 (September 1971), preprinted as RPP/C15.

74 ROY D. P., KWIECINSKI J., DESAI B. R., ZACHARIASEN F.
   Complex Regge poles and line reversed reactions.
   Phys. Lett., 34B (6) 512 (March 1971).

75 RUSH A. A., BURGE E. J., SMITH D. A.
Elastic and inelastic scattering of 30 and 50 MeV polarized and un-polarized protons by ^{40}Ar and ^{14}N.
Nucl. Phys., A166 (2) 378 (May 1971).

76 SINHA B. C., EDWARDS V. R. W.
Evidence for a real Saxon-Woods derivative term in the proton optical potential.
Phys. Lett., 35B (5) 391 (June 1971).

77 SQUIER G. T. A., JOHNSTON A. R., MEGAW J. H. P. C., GRIFFITHS R. J., KINGSTON F. G.
Asymmetry measurements for the reaction ^{10}B(p, d)^{9}B, induced by polarized protons.
Nucl. Phys., A167 (3) 465 (June 1971).

78 SQUIER G. T. A., JOHNSTON A. R., SPIERS E. W., HARBISON S. A., STEWART N. M.
Cross-section measurements for the reaction ^{10}B(p, ^{3}He)^{8}Be.
Nucl. Phys., A160 (3) 602 (January 1971).

79 STAPLETON G. B., THOMAS R. H.
The production of ^{7}Be by 7GeV proton interactions with oxygen.
Nucl. Phys., A175 (1) 124 (November 1971).

80 STEWART N. M., GIBSON W. M., KINGSTON F. G.
Depolarization measurements in the elastic scattering of protons by deuterons.
Nucl. Phys., A171 (2) 225 (August 1971).

81 STEWART N. M., GIBSON W. R., MEGAW J. H. P. C.
A measurement of the rotation parameter R in proton-deuteron scattering.
Nucl. Phys., A174 (2) 338 (October 1971).

82 THOMAS G. L., BURGE E. J., SMITH D. A.
Proton elastic scattering from ^{63}Cu and ^{65}Cu at 30 and 50 MeV (I Differential cross-sections and polarization measurements).
Nucl. Phys., A171 (1) 165 (August 1971).

83 THOMAS G. L.
Proton elastic scattering from ^{63}Cu and ^{65}Cu at 30 and 50 MeV (II Optical and model analysis)
Nucl. Phys., A171 (1) 177 (August 1971).

84 THOMAS G. L., SINHA B. C.
Optical model for proton scattering from ^{40}Ca.
Phys. Rev. Lett., 26 (6) 325 (February 1971).

85 ULEHLA I.
A solution of the reaction matrix equation in nuclear matter.
Nucl. Phys., A181 (1) 262 (February 1972), preprinted as RPP/C20.

86 WOOLLAM P. B., GRIFFITHS R. J.
A comment on the momentum mismatch in the ^{144}Sm (^{3}He, α)^{143}Sm reaction.
Phys. Lett., 37B (1) 13 (November 1971).

UNPUBLISHED PREPRINTS

87 BAKER S. L., DORNAN P. J., GOPAL G. P., STARK J., WEBSTER G. J., BUCKLEY T. S., BULL V. A., TAYLER V., TOWNSEND D. W., WHITE A.
Single pion production in π^+p interactions at 895, 945, 995 and 1040 MeV/c.
Imperial College preprint (un-numbered).

88 BARGER V., PHILLIPS R. J. N.
Rival models for total cross-sections.
Madison preprint (un-numbered).

89 BENNETT J. R. J., GAVIN B.
A high power penning source for multiply charged heavy ions.
RPP/A84.

90 BENTLEY K. R., DAVIES J. D., DOWELL J. D., McLEOD C., McMAHON T. J., VAN DER RAAY H. B., RHOADES T. G., WICKENS F. J., DAMERELL C. J. S., HOMER R. J., HOTCHKISS M. J.
An automatic spark chamber system with sonic and magnetostrictive readout.
RPP/H84.

91 BENTLEY K. R., DAVIES J. D., DOWELL J. D., McLEOD C., McMAHON T. J., VAN DER RAAY H. D., RHOADES T. G., WICKENS F. J., DAMERELL C. J. S., HOMER R. J., HOTCHKISS M. J.
Time of flight calibration for the Birmingham/RHEL K±n experiment (K12A).
University of Birmingham Physics Department Paper 71/18.

92 BRANDSTETTER A., BUTTERWORTH I., DEEN S. M., LITCHFIELD P. J., BERTHON A., VRANA J., ZATZ J., WOJCIK W., MEYER J., TALLINI B.
The reaction K$^-$p$\rightarrow\omega\Lambda$ in the c.m. energy range 1915-2168 MeV.
RPP/H80.

93 COHEN-TANNOUDJI G., LACAZE R., KANE G., HENYEY F., ZAKRZEWSKI W., RICHARDS D.
Unitarity, absorption and duality — a general discussion and a specific model.
Saclay preprint D Ph—T/72—6.

94 DRUMMOND I, KANE G.
On the interest of polarization in multiparticle reactions.
Cambridge preprint, DAMTP 72/2.

95 ELLIS R. J., BLAIR I. M., TAYLOR A. E., ASTBURY A., AXEN D., KALMUS P. I. P., SHERMAN H. J., WILLIAMS D. T., GIBSON W. R., BLOODWORTH I., GOUANERE M., MEYER S. L., EFREMENKO J.
Measurement of the electron asymmetry parameter in the decay of polarised Σ^- hyperons.
RPP/H79.

96 ELVEKJAER F., NIELSEN H.
Can present information on pion-nucleon elastic scattering solve the UP-DOWN ambiguity for the pion-pion isospin zero s-wave?
RPP/C22.

97 GABATHULER K., ROHLIN J., DOMINGO J. J., TANNER N. W.
Pion production in the reactions ^{3}He(p, π^+)^{4}He and ^{4}He(p,π^+)^{5}He.
CERN preprint MSC-71-10.

98 HARTLEY B., KANE G.
Interpretation of πN high energy scattering amplitudes.
Imperial college preprint ICTP/71/18.

99 HENYEY F., KANE G.
Selection rule for Regge-Regge cut.
Michigan preprint (un-numbered).

100 HUMBLE S., VAUGHN M. H., ZIA R.
A dual model for πN scattering without parity doublets.
RPP/C11.

101 KAMAL A. N.
A calculation of the charge radius of the π meson.
RPP/C32.

102 KAMAL A. N.
Impact parameter representations.
RPP/C28.

103 KUGLER M., LYONS L., ROBERTS R.
Exclusive estimates of inclusive reactions.
Weizmann preprint WIS 71/50 Ph.

104 KUGLER M.
Transverse momentum correlations in multiparticle production.
RPP/C26.

105 MAIDMENT J. R., PLANNER C. W.
Practical high-β insertions with application to a 1000 GeV superconducting extension of the European Accelerator.
RPP/N25.

106 MARTIN A., MICHAEL C., PHILLIPS R. J. N.
Polarization relations in charge and hypercharge exchange reactions.
CERN preprint TH 1436.

107 MIETTINEN H. I.
Factorization and exchange degeneracy of secondary trajectories in inclusive reactions.
RPP/C35.

108 MORGAN D., SHAW G.
Low energy pion-pion scattering from current algebra — unitarity corrections.
DNPL/P77.

109 NIELSEN H., OADES G. C.
K$^+$p backward dispersion relations.
RPP/C31.

110 PENNEY B. K., STEWART B. C., THOMPSON G., DANYSZ J. A.,
BRUNET J. L., NARJOUX J. L., JACOBS N. J. D., LEWIS P. H., MARCH P. V.
K$^+$p elastic scattering between 2·11 and 2·72 GeV/c.
RPP/H83.

111 PHILLIPS R. J. N.
Notes on Regge phenomenology; Lectures at the University of Riverside, California.
Riverside preprint UCR-34-P107-131.

112 RANFT G.
The shapes of inclusive single particle spectra in the fragmentation and pionisation regions.
RPP/C34.

113 ROBERTS R. G.
Exchange degeneracy breaking for hypercharge exchange reactions.
RPP/C14.

114 ROSS G. G.
Optimised integral continuation methods.
RPP/C29.

115 STAPLETON G. B., THOMAS R. H.
Estimation of the induced radioactivity of the ground water system in the neighbourhood of a proposed 300 GeV high energy accelerator situated on a chalk site.
RPP/A83.

116 STEVENSON G. R., SQUIER D. M.
An experimental study of the attenuation of radiation in tunnels penetrating the shield of an extracted beam of the 7 GeV proton synchrotron Nimrod.
RPP/R10.

117 WILLIAMS D. T., BLOODWORTH I. J. EISENHANDLER E., GIBSON
W. R., KALMUS P. I. P., LEE CHI KWONG L. C. Y., ARNISON G. J. T.,
ASTBURY A., GJESDAL S., LILLETHUN E., STAVE B., ULLALAND
O., WATKINS I. L.
Wide angle proton-proton elastic scattering from 1·3 to 3·0 GeV/c.
RPP/H77.

CONFERENCE PAPERS (alphabetically by conference title, then by author).

118 RUTHERFORD/SACLAY/ECOLE POLYTECHNIQUE COLLABORATION.
The (K*)$^-$ spectrum from 14 GeV/c K$^-$ proton interactions.
American Physical Society Spring Meeting, Washington, 26-29 April 1971.

119 RUTHERFORD/SACLAY/ECOLE POLYTECHNIQUE COLLABORATION
Kπ nucleon final states in K$^-$ proton interactions at 14 GeV/c.
Ibid.

120 BROWN J. K., ETHERIDGE D. M., WILLIAMS W. G.
The ESR study of a Cr(V) species.
Chemical Society Annual Meeting, York, 27-30 September 1971.

121 WILSON M. N.
Superconducting magnets.
Cryogenics, University Seminar on, Southampton 12 February 1971.

122 EASTWOOD A. W.
Electrical safety on the 1·4 m heavy liquid bubble chamber.
Electrical Safety in Hazardous Environments. IEE Conference on, London 16-18 March 1971. Proceedings (IEE Publicaiton No. 74) p136.

123 BROWN R. M., DUKE P. J., GROVES E. S., HILL R. E., HOLLEY W. R., JONES D. P., MARTIN J. F., SLEEMAN J. C., THRESHER J. J.
 The scattering of π^+ mesons in the momentum range 0·62-2·65 GeV/c from a polarized target.
 Elementary Particle Physics, IOP Conference on, Lancaster, 5-7 April 1971.

124 THOMAS D. B.
 Uses of super conductivity in elementary particle physics.
 Ibid.

125 ADAMS C. J., DAVIES J. D., DOWELL J. D., GRAYER G. H., HATTERSLEY P. M., HOWELLS R. J., McLEOD C., McMAHON T. J., HOTCHKISS M. J.
 K^+p elastic scattering between 432 and 939 MeV/c.
 Elementary Particles, International Conference on, Amsterdam, 30 June — 6 July 1971.

126 ADAMS C. J., DAVIES J. D., DOWELL J. D., CRAYER G. H., HATTERSLEY P. M., HOWELLS R. J., McLEOD C., McMAHON T. J., VAN DER RAAY H. B., ROB L., DAMERELL C. J. S., HOMER R. J., HOTCHKISS M. J.
 Measurement of Coulomb interference in K^+p elastic scattering at 432 MeV/c.
 Ibid.

127 AOI H, ASCHMAN D., BOOTH N. E., CAVERZASIO C., DICK L., GONIDEC A., GREEN K., JANOUT Z., JURODA K., MICHALOWICZ A., POULET M., SPENCER C. M.
 Polarization measurements in $\pi\pm p$ backward scattering at 6 GeV/c.
 Ibid.

128 BAXTER D. F., BUCKINGHAM I., CORBETT I. F., EMMERSON J. McL., GARVEY J., HUGHES G., MAYBURY R., SCHEID J., SEGAR A. M., QUIRK T. W., DUNN P. A., HART F.
 A study of $\Lambda\pi^\circ$ and $\Sigma^\circ\pi^\circ$ final states from K^-p interactions in the range 685 to 805 MeV/c.
 Ibid.

129 BINNIE D. M., CAMILLERI L., DUANE A., FARUQI A. R., GARBUTT D. A., JONES W. G., KAY M. E., LEWIS M., NICHOLSON P. J., SIOTIS J., UPADHYAY P. N., WILSON J. G., BURTON I. F., FRANK S. G., GEORGE R., HAQUE M., McEWAN J. G.
 A_2^- production in the channel $\pi^+\pi^-\pi^-$ near threshold.
 Ibid.

130 BINNIE D. M., CAMILLERI L., DUANE A., FARUQI A. R., GARBUTT D. A., JONES W. G., KAY M. E., LEWIS M., NICHOLSON P. J., SIOTIS J., UPADHYAY P. N. WILSON J. G., BURTON I. F., FRANK S. G., GEORGE R., HAQUE M., McEWAN J. G.
 High resolution measurements on the ω_o meson.
 Ibid.

131 BINNIE D. M., CAMILLERI L., DUANE A., GARBUTT D. A., HOLMES J. R., JONES W. G., KEYNE J., LEWIS M., SIOTIS I., UPADHYAY P. N., BURTON I. F., GEORGE R., McEWAN J. G.
 A_2^- production in the channel π^-+ neutrals near threshold.
 Ibid.

132 BRANDSTETTER A., BUTTERWORTH I., DEEN S. M., LITCHFIELD P. J., BERTHON A., VRANA J., ZATZ J., WOJCIK W., MEYER J., TALLINI B.,
 Partial wave analysis of the reaction $K^-p \rightarrow \Lambda\omega$ in the c.m. energy range 1915 to 2168 MeV.
 Ibid.

133 BROWN R. M., DUKE P. J., GROVES E. S., HILL R. E., HOLLEY W. R., JONES D. P., MARTIN J. F., SLEEMAN J. C., THRESHER J. J.
 The scattering of π^+ mesons in the momentum range 0·62-2·65 GeV/c. from a polarized target.
 Ibid.

134 MORGAN D.
 Low energy $\pi\pi$ scattering — on shell theory (Mini-rapporteur talk).
 Ibid, preprinted as RPP/C30.

135 PHILLIPS R. J. N.
 Regge cuts and related topics (Rapporteur talk).
 Ibid, preprinted as RPP/C24.

136 RUTHERFORD/SACLAY/ECOLE POLYTECHNIQUE COLLABORATION
 The cross-section for the reaction $K^-p \rightarrow K^{*-}(890)p$ at 14·3 GeV/c.
 Ibid.

137 ADAMS P., MORGAN R. H. C., SMITH W. A., ATCHISON F., KERR J. C.,
 Initial experience of the use of interpretive software for beamline control.
 High Energy Accelerators, 8th International Conference on, CERN, 20-24 September 1971. Proceedings (Blewett M. H., ed.) p437, preprinted as Nimrod (PD) 71-10.

138 CARNE A., BENDALL R. G., BRADY B. G., SIDLOW R., KUSTOM R. L.
 High field tests in a model superconducting r.f. separator at 1·3 GHz.
 Ibid., p 248, preprinted as Nimrod (PD) 71-23.

139 HYMAN J. T.
 Computer controls: state of the art and future developments.
 Ibid., p 415, preprinted as RPP/A85.

140 LANE H., MOIR J., MORGAN R. H. C., MOTT E. M., NEVITT J., SMITH J. V., TURNER J.
 Hardware for a computer control system for the 1·5 m bubble chamber beamline at Nimrod.
 Ibid., p 435, preprinted as Nimrod (PD) 71-22.

141 SMITH P. F.
 Multi-stage energy transfer schemes.
 Ibid., p 213.

142 SMITH P. F.
 Superconducting synchrotron magnets-present status.
 Ibid., p 35.

143 THOMAS D. B.
 Superconducting pulsed magnets for a 1000 GeV synchrotron.
 Ibid., p 190, preprinted as RPP/A87.

144 ROY D. P.
Complex conjugate Regge Poles.
High Energy Interactions, 6th Moriond Meeting on, Meribel-les-Allues, 7-19 March 1971. Proceedings ("High Energy Phenomenology", Tran Thanh Van J., ed.) p 309, preprinted as RPP/C16.

145 ROHLIN J., DOMINGO J. J.
$\pi\pm$ production.
High Energy Physics and Nuclear Structure, 4th International Conference on, Dubna, 7-12 September 1971.

146 LAWES R. A.
HPD 2 development at the Rutherford Laboratory.
HPD Collaboration Meeting, CERN, September 1971.

147 LAWSON J. D.
Diversity and unity in sources and beams.
Ion Sources and the Formation of Ion Beams, Conference on, Brookhaven, 19-21 October 1971. Proceedings (BNL 50301) p1.

148 BELL A. G., LAWES R. A.
Use of a computer as a data concentrator.
Micro and Mini Computer Seminars, Brunel University, September 1971 and the Hague, December 1971.

149 BENNETT J. R. J.
A review of PIG sources for multiply charged heavy ions.
Multiply Charged Heavy Ion Sources and Accelerating Systems, International Conference on, Gatlinburg, October 1971.

150 AOI H., ASCHMAN D., BOOTH N. E., CAVERZASIO C., DICK L., GONIDEC A., GREEN K., JANOUT Z., JURODA K., MICHALOWICZ A., POULET M., SPENCER C. M.
Polarization measurements in $\pi\pm$p backward elastic scattering at 6 GeV/c.
Nuclear and Particle Physics, IOP Conference on, Oxford, 22-24 September, 1971.

151 BATTY C. J., FRIEDMAN E., JACKSON D. F.
The effective α - nucleon interaction in nuclei.
Ibid.

152 EDGINGTON J. A., HOWARD V. J., DAS GUPTA S. S., BRADY F. P., BLAIR I. M., BAKER C. A., BONNER B. E., McNAUGHTON M. W.
Measurements of n-p bremsstrahlung near 130 MeV.
Ibid.

153 EDWARDS V. R. W., SINHA B. C.
Critique of the collective model of inelastic scattering.
Ibid.

154 McNAUGHTON M. W., GRIFFITHS R. J., EDGINGTON J. A., BONNER B. E., BLAIR I. M.
A kinematically complete experiment on the d(n,np)n reaction.
Nuclear Three Body Problem, International Conference on, Budapest, 8-11 July 1971.

155 BENNETT J. R. J.
High charge state heavy ion sources.
Particle Accelerator Conference, Chicago, 1-3 March 1971. Proceedings (IEEE Trans. Nucl. Sci., NS-18 (3) (June 1971)) p55.

156 DONALD M. H. R., HAROLD M. R., KING N. M., LOACH B. G., MAIDMENT J. R. M., PLANNER C. W., REES G. H., TROTMAN J. V.
A superconducting synchrotron design study at the Rutherford Laboratory.
Ibid., p 703, preprinted as RPP/N23.

157 SMITH P. F.
Superconducting synchrotron development: Notes on recent work at the Rutherford Laboratory.
Ibid., p 641.

158 BERGER E. L., FOX G., QUIGG C., RINGLAND G. A.
Useful hadronic experiments at intermediate energies.
Particle Physics Workshop, Pasadena, 29-30 March 1971. Proceedings (UCRL-20655, Field RD ed.) p 453b.

159 BUGG D. V.
πp elastic scattering, 0-300 MeV.
Pion Interactions at Low and Medium Energies, SIN-CERN Spring School on, Zuoz, 29 March-8 April 1971. Proceedings (CERN 71-14) p 379.

160 RUSSELL F. M.
Present and future prospects for separated function frozen targets.
Polarized Targets, 2nd International Conference on, Berkeley, 30 August-2 September 1971 Proceedings (LBL 500, Shapiro G. (ed.)) p 89, preprinted as RPP/A86.

161 LEVINE G. S., SQUIER D. M., STAPLETON G. B., STEVENSON G. R., GOEBEL L., RANFT J.
The distribution of dose and induced activity around external proton beam targets.
Protection against Accelerator and Space Radiation, International Congress on, CERN, 26-30 April 1971. Proceedings (CERN 71-16, Baarli J., Dutrannois J. (eds.) 2,798, preprinted as RPP/R9.

162 PERRY D. R., HYNES M. A.
A pion beam for radiobiological and dosimetric studies, using a proton synchrotron external target.
Ibid., 1,220, preprinted as RPP/R8.

163 ADAMS P.
Interpretive software for computer control.
Real Time Programming, European Seminar on, Harwell, April 1971, preprinted as Nimrod (PD) 71-11.

164 SMITH P. F.
The performance of coils wound with filamentary conductors.
Stabilising Superconductors, IOP Low Temperature Group Meeting on, RHEL, 23 April 1971.

165 WILSON M. N.
Twisting and transposition of composites and cables.
Ibid.

166 FISHER C. M.
High energy physics considerations in the design of fast cycling bubble chambers.
Ultrasonic Bubble Chambers, IOP Acoustic Group Meeting on, RHEL, 18 March 1971.

167 TURNER L.
Prediction of bubble growth and recompression during a bubble chamber cycle.
Ibid.

THESES FOR HIGHER DEGREES

(i) **D.Sc.**

168 BATTY C. J. (University of Birmingham).
Published work.

(ii) **Ph.D. and D.Phil.**

169 BAXTER D. F. (University of Oxford).
A study of resonances in the Kp system.

170 BUSSEY P. J. (University of Cambridge).
The interaction of pions on protons between 70 and 300 MeV.
Reprinted as HEP/T/23.

171 CHARLES B. J. (University of Bristol).
Differential cross-sections for positive kaon-proton elastic scattering.
Reprinted as HEP/T/26.

172 CHARLESWORTH J. A. (University of Cambridge).
Strange particle production in neutron-proton interactions.
Reprinted as HEP/T/24.

173 CRAWFORD J. F. (Westfield College, University of London).
On the non-leptonic decay of the Σ^+ hyperon.
Reprinted as HEP/T/19.

174 FUCHS F. D. (Imperial College, University of London).
Kaon-nucleon interactions in the T = 1 state at 1·6 GeV/c incident momentum.
Reprinted as HEP/T/18.

175 GUY J. V. (University College, University of London).
A study of hyperons produced by 2·2 GeV/c K$^-$ mesons.
Reprinted as HEP/T/21.

176 HOWARD D. C. (University of Liverpool).
An anti proton-proton formation experiment in search of the T meson.

177 HOWELLS R. J. W. (University of Birmingham).
Kaon-nucleon elastic scattering below 1 GeV/c.

178 HUGHES G. (University of Oxford).
The formation and decay of neutral baryon resonances in K$^-$p interactions.

179 INGRAM C. H. Q. (University of Oxford).
Pions from capture of 600 MeV protons.

180 JONES C. M. S. (University of Oxford).
The formation of neutral baryon resonances of strangeness minus one.

181 MARCHESE C. J. (King's College, University of London).
Study of the interaction of helions with Iron isotopes.

182 MAYBURY R. (University of Oxford).
A study of baryon resonances of hypercharge zero.

183 PENNEY B. K. (Imperial College, University of London).
An automatic measuring machine for bubble chamber film and its use for a K$^+$p experiment.
Reprinted as HEP/T/20.

184 SIOTIS I. (Imperial College, University of London).
A_2^- meson production at low momentum transfer.

185 TAIT W. H. (King's College, University of London).
A study of proton scattering from the isotopes of Zinc.

186 TAYLER V. (Westfield College, University of London).
A study of π^+p interactions around 1 GeV/c and a partial wave analysis of a three body channel.
Reprinted as HEP/T/16.

187 THOMPSON G. (Imperial College, University of London).
Single pion production in intermediate energy range K$^+$p reactions.
Reprinted as HEP/T/13.

188 TOWNSEND D. W. (Westfield College, University of London).
π^+p elastic and inelastic interactions around 1 GeV/c.
Reprinted as HEP/T/17.

189 UPADHYAY P. N. (Imperial College, University of London).
A search of the δ (962) meson.

190 WINSBORROW L. A. (King's College, University of London).
A study of nuclei in the Z = 50 region.

191 WOOLLAM P. B. (King's College, University of London).
Nuclear structure study of the Samarium isotopes.

(iii) **M.Sc.**

192 BENTLEY K. R. (University of Birmingham).
An experiment to measure the elastic scattering of kaons from neutrons.

REPORTS

193 ATCHISON F., FISHER C. M.
Study of the homogeneity and stopping power of neon-hydrogen mixtures in the 1·5 metre bubble chamber.
RHEL/R 218.

194 BRANDSTETTER A., DEEN S. M., LITCHFIELD P. J.
Coefficients for partial wave analysis of the reaction
$0^- + \frac{1}{2}^+ \rightarrow 1^- + \frac{1}{2}^+$.
RHEL/R 224

195 GRAGG D. A.
The evolution of the pumping groups used on the Rutherford Laboratory helium-3 refrigerator.
RHEL/R 208.

196 CULLIFORD D. R.
A precision shunt with small temperature coefficient.
RHEL/R 234.

197 DAVIES K. H.
An international survey of the operation of DC electrostatic particle separators.
RHEL/R 222.

198 EVANS D., MORGAN J. T., STAPLETON G. B.
The effect of ionising radiation on synthetic resins at very low temperature — An initial study.
RHEL/R 220.

199 GOPAL G. P.
Calibration of image-plane digitizers.
RHEL/R 223.

200 GRAY D. E. (Ed.)
Nimrod operation and development quarterly report — October 1 to December 31 1970.
RHEL/R 211.

201 GRAY D. E. (Ed.)
Nimrod operation and development quarterly report — January 1 to March 31, 1971.
RHEL/R 219

202 GRAY D. E. (Ed.)
Nimrod operation and development quarterly report — April 1 to June 30 1971.
RHEL/R 227.

203 GRAY D. E. (Ed.)
Nimrod operation and development quarterly report — July 1 to September 30 1971.
RHEL/R 233.

204 HYMAN J. T.
Use of interpretive software in high energy physics experiments.
RHEL/R/221.

205 LARBALESTIER D. C., KING H. W.
Non magnetic stainless steels for cryogenic purposes.
RHEL/R 217

206 LAWES R. A.
The interface network for the HPD 2 computer.
RHEL/R 228.

207 LAWES R. A., WELFORD W. T.
A laser illumination system for a Hough-Powell device.
RHEL/R 212.

208 MOORE D. R.
Some engineering aspects of the Nimrod thin septum extraction systems and components.
RHEL/R 209.

209 ROSE I. H., SCOTT D. B.
MUGWUMP — An off-line graphics filing system.
RHEL/R 231.

210 ROSE I. H., SCOTT D. B.
The graphics file retrieval and archiving facilities in the ELECTRIC terminal system.
RHEL/R 232.

211 RUSSELL F. M.
Operation and performance of the frozen target and possible improvements.
RHEL/R 225.

212 SALTER D. C.
Information on the Nimrod experimental programme.
RHEL/R 214.

213 SMITH J. R., TELLING F. M. (Eds.)
The work of the Rutherford Laboratory in 1970.
RHEL/R 215.

214 SMITH W. T.
Continuous refrigeration at $1 \cdot 8°K$ in laboratory cryostats using a $4 \cdot 2°K$ liquid helium dewar supply.
RHEL/R 236.

215 WILLIAMS W. G., THOMAS J. L.
Dynamic polarization measurements in polyhydric alcohols doped with their chromium V complexes at approx. $1°K$ and at 3kG magnetic fields.
RHEL/R 213.

216 WROE H., FOWLER R. G.
A 500 kV, medium gradient preinjector.
RHEL/R 226.

MEMORANDA

217 ATCHISON F.
A low momentum separated beam for use with the $1 \cdot 5m$ bubble chamber.
RHEL/M/NIM 9.

218 ATCHISON F.
Target yields at Nimrod.
RHEL/M/NIM 10.

219 ATCHISON F., FISHER C. M., SMITH W. A.
Antiproton fluxes for the British National Hydrogen Bubble Chamber.
RHEL/M/NIM 7.

220 ARMSTRONG A. G. A. M.
Rounding errors in TRIM: applications to synchrotron dipole magnets.
RHEL/M/A 14.

221 BRANDSTETTER A.
On scan efficiencies in bubble chamber picture analysis.
RHEL/M/H 4.

222 BROOKS H. C.
The use of rotating plant for energy storage.
SCS/POWER SUPPLY/2.

223 BROWN R. M., BUTTERWORTH I., CORBETT I. F., DAMERELL C. J. S., DUKE P. J., FISHER C. M.
An experimental programme for the Nimrod accelerator.
RHEL/M/H 7.

224 BRYDEN A. D.
Current status of HPD minimum guidance at RHEL and other laboratories.
RHEL/M/C 9.

225 CARNE A., FOX J. A., GARVEY J., LAWES R. A., NEWPORT R. W., RUSSELL F. M., SMITH P. F., THOMAS D. B., TROWBRIDGE C. W., WILLIAMS P. R.
The applied physics support programme for high energy physics at the Rutherford Laboratory.
RHEL/M/A11 (revised).

226 COLLINS D. N.
Development of a control system for bubble chamber magnet power supplies.
Nimrod (EF) 71-15.

227 COLYER B.
The natural circulation of liquid helium in pulsed superconducting magnet channels.
RHEL/M/A15.

228 CURTIS M. M., HEMMINGS P. J., MAYHOOK A. R.
Daedalus Version 2-360 Users' guide.
RHEL/M/C11.

229 DONALD M. H. R.
The Q_H-Q_V difference resonance in the SCS.
SCS/MACHINE/35

230 DONALD M. H. R.
Superconducting magnets as an aid to X-ray spectroscopy.
Nimrod (ABT) 71-17.

231 DUKE P. J.
Some comments on a stopping K beam for Nimrod.
RHEL/M/H6.

232 DUKE P. J.
Fundamental particles — an elementary introduction.
RHEL/M/H8.

233 EASTWOOD A. W.
A beam timing indicator.
Nimrod (EF) 71-6.

234 EVANS W. M., BAKER J. C.
A short investigation into the use of flash tubes as particle detectors.
RHEL/M/H5.

235 FAIL B, WORDINGHAM V.
Measurement of cyclic stress in Nimrod pole piece studs.
Nimrod (SME) 71-4.

236 FERGUSON N. W.
Analysis of vibration characteristics of some Rootes type vacuum pumps.
Nimrod (NDG) 71-2.

237 FERGUSON N. W.
Noise survey — K13A LCR.
Nimrod (NDG) 71-1.

238 FORTUNA L., MAIDMENT J. R.
Further studies of closed orbit control techniques in the SCS.
SCS/MACHINE/34.

239 FOSTER J. A., OXLEY A. J.
Measurement and analysis of nerve cell pulses.
RHEL/M/C16.

240 FOSTER J. H.
Failure of the target in the 1·5m cryogenic bubble chamber.
Nimrod (EF) 71-13.

241 FOSTER J. H.
Use of track sensitive targets.
Nimrod (EF) 71-18.

242 GIRARD P. M.
The HASP/ELECTRIC interface for line printer output.
RHEL/M/C12.

243 GOTTFELDT P.
Computer based operating facility on the 1·5 m hydrogen bubble chamber.
Nimrod (EF) 71-9.

244 GRIFFITHS P. A.
Procedure for the installation of the pole-face windings water cooled power supply.
Nimrod (DG) 71-26.

245 HACK R. C.
Radiation Protection Group (operations) — Progress report for 1970.
RHEL/M/R5.

246 HACK R. C.
Personal fast neutron dosimetry around Nimrod. A third note.
RHEL/M/R8.

247 HACK R. C., STEVENSON G. R.
Radiation protection in high energy accelerator environments.
RHEL/M/R6.

248 KING N. M., REES G. H.
A possible future high energy proton facility at the Rutherford Laboratory.
SCS/MACHINE/36.

249 LAWSON J. D.
A comparison of different models of the Bennett pinch.
RHEL/M/A3.

250 LAWSON J. D.
The equilibrium radius of a ring current in an external magnetic field: Comparison of published calculations.
RHEL/M/A4.

251 LEA A. T., HAMILTON J.
Effective range formulae for N_{33}.
RHEL/M/C10.

252 LEWIN J. D.
Rapid Q-shifting in a superconducting synchrotron.
RHEL/M/A8.

253 LEWIS R. S.
        Mini-monitor, a secondary disk monitor for the PDP-8.
     RHEL/M/NIM 6.

254 LOACH B. G.
        DUBACC: A Fortran program to survey quadrupole doublet lens
        systems.
     Nimrod (ABT) 71-16.

255 MADEN D.
        Further notes on the stopping K beam.
     Nimrod (ABT) 71-7.

256 MORGAN D., OADES G. C., PHILLIPS R. J. N., RINGLAND G. A.
        A case for medium-energy hadron physics.
     RHEL/M/C8.

257 MORTIMER A. R.
        The management of complex projects in a research establishment.
     Nimrod (NDG) 71-3.

258 MORTIMER A. R., GRESHAM A. T.
        Preliminary trials on a thin septum for magnets for particle accelera-
        tors.
     RHEL/M/NIM 8.

259 PETT T. G.
        GRADIS — The on-line GRAph DISplayer.
     RHEL/M/C6.

260 REDMAN A. J.
        CYCLOPS and its software environment.
     RHEL/M/C 15.

261 REES G. H.
        Estimates of beam size at ejection in the SCS.
     SCS/MACHINE/33.

262 REES G. H., TROTMAN J. V.
        Longitudinal space charge forces at injection in the SCS.
     SCS/MACHINE/32.

263 REES G. H., TROTMAN J. V.
        Beam size at transition in the SCS.
     SCS/MACHINE/31.

264 RUSSELL F. M.
        Feasibility of the frozen and deep-freeze polarized targets.
     RHEL/M/A6.

265 RUSSELL F. M.
        Some aspects of the cryogenic system of the frozen target.
     RHEL/M/A7.

266 RUSSELL F. M.
        Feasibility of a large volume polarized target.
     RHEL/M/A13.

267 SCOTT D. B.
        An interactive graphical package and direct access filing system for
        Computek displays.
     RHEL/M/C14.

268 SEAGER P.
        Engineering test of target in the 1·5 m cryogenic bubble chamber
        during July 1971.
     Nimrod (EF) 71-19.

269 SEAGER P.
        Stress in plexiglass walls of targets for 1·5 m cryogenic bubble
        chamber.
     Nimrod (EF) 71-20.

270 SIMKIN J., WEST N. D.
        Correction of magnet error fields by means of self-excited supercon-
        ducting windings.
     RHEL/M/A5.

271 SMITH P. F.
        Multi-stage energy transfer schemes.
     RHEL/M/A9.

272 SMITH W. T.
        Proposed joint seals for superfluid helium.
     Nimrod (NDG) 71-5.

273 STEVENSON G. R. SQUIER D. M., LEVINE G. S.
        Measurements of the angular dependence of dose and hadron yield
        from targets in 8 GeV/c and 24 GeV/c extracted proton beams.
     RHEL/M/R7.

274 STOKOE J. R., DENTON L. G.
        The type II LH$_2$ target operations manual.
     Nimrod (NDG) 71-12.

275 TURNER L. R.
        Growth and recondensation of bubble chamber bubbles: Numerical
        calculations.
     RHEL/M/A12.

276 WALKINSHAW W., LEA A. T. (Eds.)
        Computing and Automation Division quarterly report, January 1 —
        March 31 1971.
     RHEL/M/C5.

277 WALKINSHAW W., LEA A. T. (Eds.)
        Computing and Automation Division quarterly report April 1 — June
        30 1971.
     RHEL/M/C7.

278 WALKINSHAW W., HEMMINGS P. J. (Eds.)
        Computing and Automation Division quarterly report 1 July — 30
        September 1971.
     RHEL/M/C13.

279 WALKINSHAW W., LEA A. T. (Eds.)
        Computing and Automation Division quarterly report 1 October —
        31 December 1971.
     RHEL/M/C19.

280 WEST N. D.
        Practical coil configurations for superconducting energy transfer
        systems.
     RHEL/M/A16.

281 WILLIAMS P. R.
    Dynamic loads on the track sensitive target in the 1·5 m bubble
    chamber.
    Nimrod (EF) 71-14.

282 WILLIAMS W. G.
    The optimisation of the free radical dope concentration in a "frozen
    spin" polarized target.
    RHEL/M/A10.

GESSS PAPERS (Group for European Superconducting Synchrotron Studies
              Karlsruhe, Sacley, RHEL collaboration).

283 HAROLD M. R.
    On the minimum aperture required for resonant slow ejection at
    1000 GeV.
    GESS/MD/11.

284 HAROLD M. R.
    Progress on some 1000 GeV design topics.
    GESSS/MD/4.

285 HAROLD M. R., REES G. H.
    An insertion for lattice SC_1 : beam size estimates and extraction
    studies.
    GESSS/MD/13.

286 KING N. M.
    Some comments on 1000 GeV machine design problems.
    GESSS/MD/3.

287 KING N. M.
    Stored energy considerations for 1000 GeV superconducting
    sychrotrons.
    GESSS/MD/1.

288 KING N. M., MAIDMENT J. R.
    Apertures and stored energies for 1000 GeV.
    GESSS/MD/12.

289 MAIDMENT J. R., PLANNER C. W.
    On the provision of long straight sections to simplify extraction from
    the conventional European Accelerator.
    GESSS/MD/18.

290 MAIDMENT J. R., PLANNER C. W.
    Practical high-β insertions with application to a 1000 GeV super-
    conducting extension of the European Accelerator.
    GESSS/MD/15.

291 REES G. H.
    An alternative injection scheme for the 1000 GeV machine.
    GESSS/MD/17.

292 REES G. H.
    Choice of injection energy for a superconducting modification of the
    European machine.
    GESSS/MD/2.

293 REES G. H.
    Lattice SC_1.
    GESSS/MD/10.

294 REES G. H.
    One type of high $-\beta$ insertion for the S/C machine with 200 GeV
    injection.
    GESSS/MD/16.

Lectures

RUTHERFORD LABORATORY LECTURES

A series of lectures in which eminent people are invited to the Laboratory to
address the staff on subjects of general scientific importance.

JONES F. E. (Mullard Ltd., 4 February): A Scientist's view of industry.

AGIUS P. J. (Esso Ltd., 11 March): The role of industry in air quality conservation.

JELLEY J. V. (AERE, 22 April): The astronomy of rare events on short time
scales.

MITCHELL E. W. J. (Reading, 27 May): The use of neutrons in the study of
condensed matter.

ALLEN W. D. (RHEL, 15 July): Evidence of gravitational radiation.

STANNARD F. R. (Open University, 7 October): The Open University's approach
to science teaching.

WILKINS M. F. H. (KCL, 4 November): Social responsibility in science.

NIMROD LECTURES

A weekly series in which physicists active in high energy physics talk about their
research programmes, or on topics related to particle physics.

SCHECK F. (SIN, Zurich, 11 January): Nuclear and particle properties from exotic
atoms.

SALIN P. (Bordeaux, 18 January): Pomeron structure and low energy K^+p
scattering.

HYAMS B. (CERN, 25 January): Measurement of A_2 mass spectrum.

OADES G. C. (RHEL, 1 February): Why we need to understand Coulomb
corrections in order to interpret hadronic data.

WHITE D. H. (UCL, 8 February): Pion charge exchange in the backward direction
at high energies at BNL.

WAGNER F. (Munich, 15 February): Phase shift analysis of $\pi^-p \to K\Lambda$.

SATZ H. (Helsinki, 22 February): Aspects of diffraction disassociation.

ROSS M. (Michigan and WCL, 1 March): Understanding two-body reactions.

AMATI D. (CERN, 8 March): Building a hadron theory from duality.

DUKE P. J. (RHEL, 15 March): A search for charge asymmetric effects in the
decay modes $K^\pm \to \pi^\pm\pi^\circ\pi^\circ$ and $K^\pm \to \pi^\pm\pi^\circ\gamma$.

KRZYWICKI A. (Orsay and CERN, 22 March): Large angle scattering of hadrons.

GUISAN O. (CERN, 29 March): New and preliminary results about pion charge exchange polarization.

RINGLAND G. A. (RHEL, 19 April): Report on phenomenology conferences at Cal-Tech.

BRODY A. (CERN, 26 April): Partial wave analysis of the reactions $\pi^- p \rightarrow \Delta^- \pi^+$, $K^- p \rightarrow Y^* \pi$ up to 2 GeV.

GAILLARD M. (CERN, 3 May): Leptonic K decays.

FERRO LUZZI M. (CERN, 10 May): Recent activity in baryon resonances.

CHAN H. M. (CERN, 12 May): Predictions of Regge theory for inclusive reactions.

SHAW G. (DNPL, 17 May): Exotic EM current and CP violation.

PERKINS D. H. (Oxford, 24 May): Deep inelastic electron scattering.

ROBERTS R. G. (RHEL, 7 June): Report on Helsinki Conference.

MONTANET L. (CERN, 14 June): Recent progress in meson resonances as observed in p̄p annihilation.

STAUDE A. (CERN, 17 June): Recent results from the ISR.

LLEWELYN-SMITH C. (SLAC, 21 June): Neutrinos as a probe of hadron structure.

MERIO J. P. (Saclay, 24 June): Measurements of A and R parameters at high energies.

MORRISON D. R. O. (CERN, 12, 13 and 14 July): Review of strong interactions at high energy.

MICHAEL C. (CERN, 26 July): Two-body scattering at high energies.

ROSNER J. (Minnesota, 16 August): Resonance physics at very high energy.

von HOLTEY G. (Bonn, 6 September): Status of pion production in the first resonance region.

BUSZA W. (DESY, 10 September): ρ, ω interference in photoproduction.

DONNACHIE A. (DNPL, 27 September): Report on Cornell conference.

PEREZ MENDEZ V. (LRL, 30 September): Multiwire proportional chambers: read-outs and applications.

FIDECARO M. (CERN, 4 October): Pion scattering on a polarized target at 2 and 4 GeV/c.

DONOHUE J. T. (Nice, 5 October): Baryon spin determination using polarized targets.

FRENCH B. (CERN, 11 October): Problems of experimentation at 200 GeV.

FRANZINETTI C. (CERN, 18 October): Recent progress in neutrino physics.

SQUIRES E. J. (Durham, 25 October): Inclusive reactions and duality.

KANE G. (Michigan and RHEL, 1 November): A current review of Regge and dual model physics.

HOGAASEN H. (Orsay, 8 November): Regge cuts in two-body processes.

MANDELSTAM S. (Berkeley and IC, 15 November): Qualitative discussion of dual resonance models.

GIACOMELLI G. (Bologna, 22 November): High energy hadron physics.

OADES G. C. (RHEL) and MARTIN B. (UCL): Report on weekend KN discussion meeting.

RADICATI L. (Pisa and Oxford, 9 December): Electromagnetic and weak interaction symmetry breaking.

FETKOVITCH J. (RHEL, 13 December): Recent results on Λ β-decay.

STONE S. (Rochester, 20 December): Single and two particle inclusive reactions.


SEMINARS ON COMPUTING

The speakers are from the Rutherford Laboratory unless otherwise stated.

BURREN J. W. (15 January): ELECTRIC: Technical details.

ADAMS P. (29 January): A real time interpreter for beam line control.

TAYLOR R. (12 February): General information on the Rutherford Laboratory's 360/195.

McLATCHIE R. C. F. (AERE, 26 February): The HUW system at AERE.

BRYDEN A. D. (12 March): Data analysis in bubble chamber physics.

HURST H. (26 March): SHARE — the IBM Computer Users Association.

SHARP P. H. (23 April): A User's experience of CYCLOPS.

OXLEY A. J. (7 May): Experience with the Rutherford Laboratory's HPD's.

MacEWAN J. F. (24 May): Looking to the future of on-line hardware systems at the Rutherford Laboratory.

ROSNER R. A. (4 June): The use of small computers at the Rutherford Laboratory.

JANE M. R. (18 June): On-line computers for CERN's Ω project.

SCHWARTZ J. L. (MIT 2 July): Computer generated films in quantum mechanics and electrodynamics.

BRACHER B. H. (9 July): The on-line rough digitising system.

DANIELS T. (DNPL, 16 July): On-line computing and interactive graphics at the Daresbury Laboratory.

TURNILL M. (CERN, 6 August): The data processing problems associated with large bubble chambers.

GENERAL MEETING (8 October).

LAWES R. A. (22 October): The HPD flying spot digitiser.

TAYLOR R. (5 November): What is good programming?

LAWES R. A. (19 November): HPD2 developments at the Rutherford Laboratory.

BALDERSON C. (3 December): Making use of JCL.

MAYHOOK A. R. (17 December): TSO.

The two lecture courses held were:—

TAYLOR R. (8-12 March): Introduction to the IBM 360 ASSEMBLER language.

BURREN J., PETT T. and SCOTT D. B. (10-14 May): A User's introduction to the ELECTRIC and MUGWUMP Systems.

1.5m bubble chamber

HALL 1

K12A

K9

K13C

X2

X1

K10S

π7

HALL 2

π10

P71
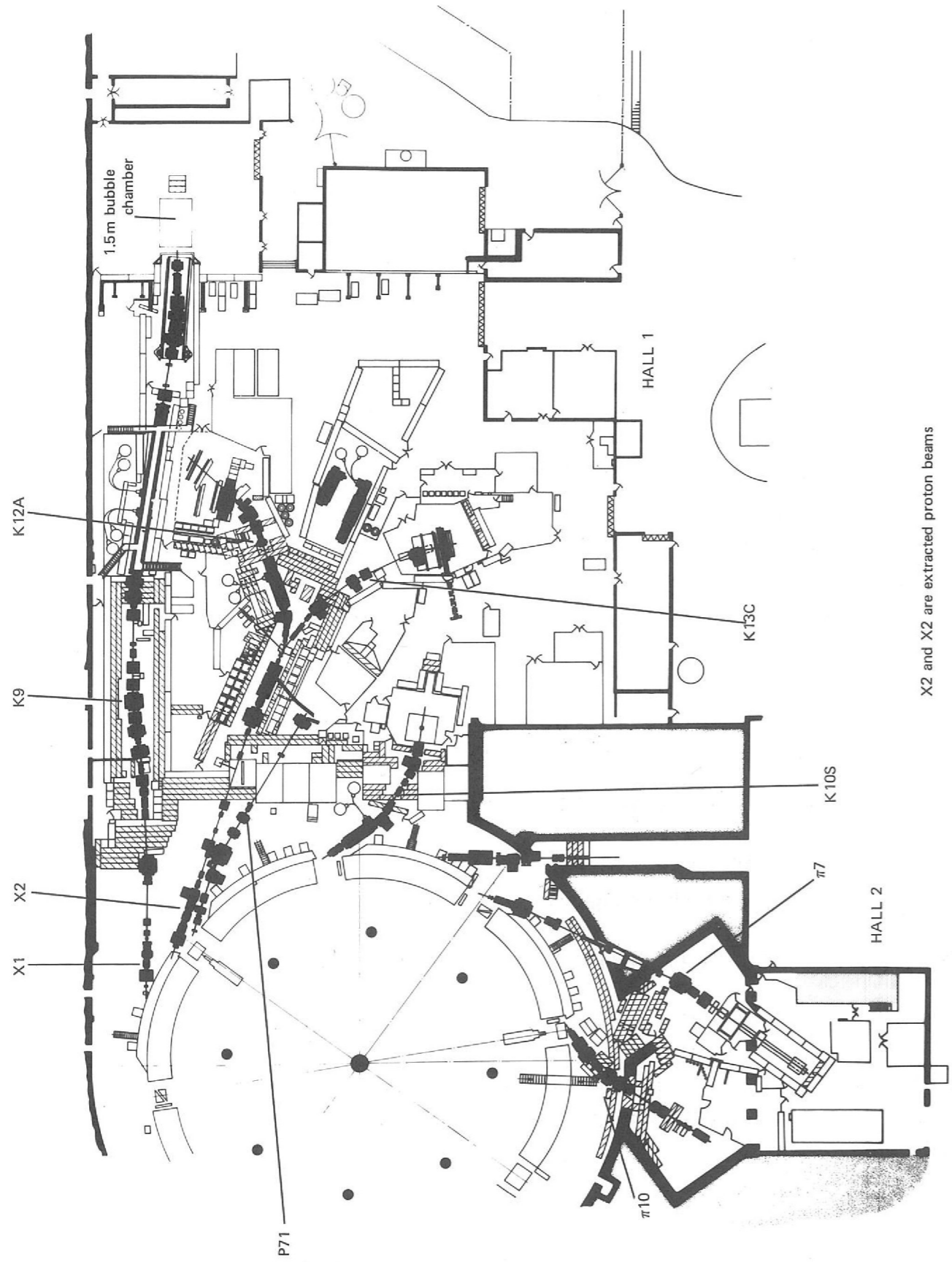
X2 and X2 are extracted proton beams

Figure 127. Beam lines in Experimental Hall 1 and Hall 2 (January 1972).

N4

K15

X3

π9

X3X

π8

π11
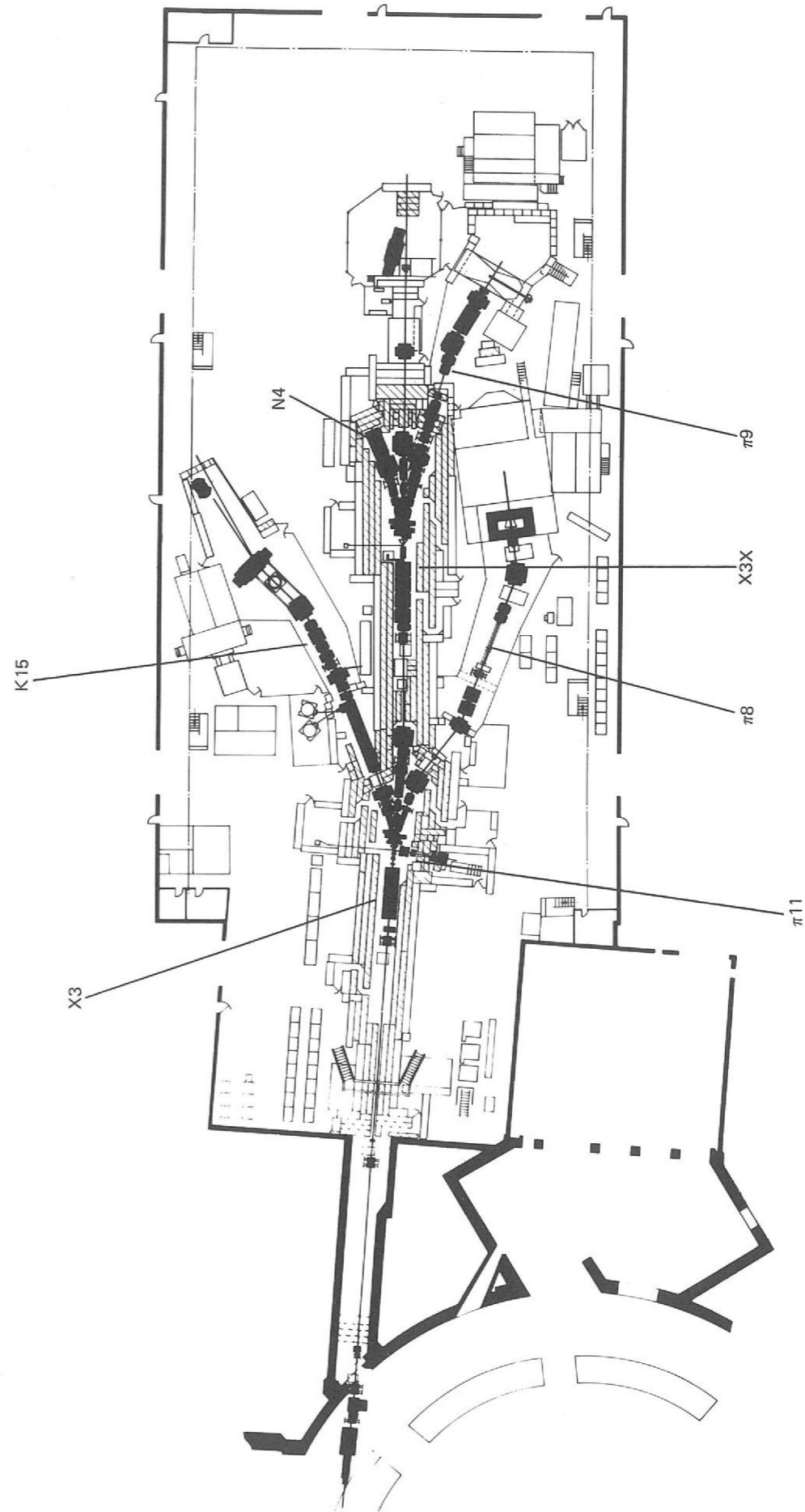
X3 is the extracted proton beam.
X3X is the extension of X3 to a second target station.

Figure 128. Beam lines in Experimental Hall 3 (January 1972).